EVALUATION OF ATMOSPHERIC IMPACTS OF SELECTED COATINGS VOC EMISSIONS

Final Report to the

California Air Resources Board
Contract No. 00-333

By

William P. L. Carter and Irina L. Malkina

March 21, 2005

Center for Environmental Research and Technology
College of Engineering
University of California
Riverside, California 92521

ABSTRACT

An experimental and modeling study was carried out to reduce uncertainties in atmospheric ozone impacts of architectural coatings VOCs. The focus of this project was Texanol® (isobutyrate monoesters of 2,2,4-trimethyl-1,3-pentanediol), which is widely used in water-based coatings, and various hydrocarbon solvents representative of those used in solvent-based coatings. The hydrocarbon "bin" reactivity assignments developed by the CARB for hydrocarbon solvents were evaluated using compositional data from 124 different solvents, and a new methodology was developed for deriving such assignments that can be used when reactivity scales are updated or modified. Progress was made towards developing a direct reactivity measurement method that does not require gas chromatographic analyses, but additional work is needed before data can be obtained for solvents of interest. Environmental chamber experiments were carried out to evaluate the abilities of mechanisms of Texanol® and six different types of hydrocarbon solvents to predict their atmospheric ozone impacts, and comparable experiments were carried out with m-xylene and n-octane for control and comparison purposes. Chamber data were also used to derive rate constants for the reactions of OH radials with the Texanol® isomers that are in excellent agreement with current estimates. The UCR EPA environmental chamber was employed, and the experiments were carried out at NO_x levels of 25-30 ppb and at ROG/NO_x ratios representing maximum incremental reactivity (MIR) and NO_x-limited conditions. The current SAPRC-99 mechanism was found to simulate the results of the experiments with Texanol® and the primarily alkane petroleum distillate solvents reasonably well, though uncertainties exist because of problems with the model simulating results of the MIR base case experiments. The mechanism also simulated the effects of Aromatic 100 on O_3 formation in the MIR experiments, but underpredicted the tendency for the aromatics to inhibit O_3 in NO_x -limited experiments and had other problems. The results of the experiments with the synthetic C_{10}-C_{12} isoparaffinic mixture were not well simulated by the model, and suggest that current mechanisms may underpredict their atmospheric reactivities by 25-75% depending on the source of the discrepancy. Recommended needs for additional research are discussed.

ACKNOWLEDGEMENTS AND DISCLAIMERS

This work was funded primarily by the California Air Resources Board (CARB) through contract number Contract 00-333, though some of the experiments discussed herein were funded by other projects. Some of the initial chamber effects evaluation experiments and the reactivity experiments for m-xylene and n-octane were funded by the United States EPA through cooperative agreement number CR 827331-01-0. A few experiments were also funded by the previous CARB contract number 01-304. The CO_2 analyzer used in the direct reactivity measurement project was purchased using gift funds from the American Chemistry Council. Additional support for this project was provided by the South Coast Air Quality Management District through contract no. 03468, though most of the data provided by that project will be discussed in a separate report that is in preparation.

The UCR EPA chamber experiments were carried out at the College of Engineering Center for Environmental Research and Technology primarily by Irina Malkina and Kurt Bumiller with the assistance of Chen Song and Bethany Warren. Valuable assistance in carrying out the experiments was also provided by Dennis Fitz, Charles Bufalino, John Pisano and Dr. David Cocker of CE-CERT. Mr. Dennis Fitz also provided valuable assistance in administering this project.

Helpful discussions with Dr. Dongmin Luo and other members of the CARB staff concerning the research directions for this project are gratefully acknowledged. We also gratefully acknowledge the American Chemistry Council (ACC) Hydrocarbon Panel, particularly Andrew Jaques of the ACC, Mr. Bob Hinrics of Citco, and Ms. Arlean Medeiros of ExxonMobil, for helpful discussions and providing much of the compositional data used for this project. We also thank Dr. Albert Censullo of California Polytechnic State University for providing data from his study prior to the completion of his final report, and thank Dr. David Morgott and Rodney Boatman of Eastman Kodak for helpful discussions regarding Texanol®.

Although this work was funded primarily by the CARB and in part by other agencies, it reflects only the opinions and conclusions of the primary author. Mention of trade names and commercial products does not constitute endorsement or recommendation for use.

TABLE OF CONTENTS

EXECUTIVE SUMMARY xi
Background xi
Investigation of Methods to Estimate Reactivities of Complex Hydrocarbon Solvents xii
Further Development of a Direct Reactivity Measurement Method xiii
Environmental Chamber Experiments for Mechanism Evaluation xiv
Recommendations xviii

INTRODUCTION 1
Background 1
Quantification of VOC Reactivity 1
Application to Architectural Coatings 2
Objectives and Overall Approach 2

ESTIMATION OF HYDROCARBON SOLVENT REACTIVITIES 5
Introduction and Background 5
Compositional Data Employed and Calculated Solvent Reactivity 5
Derivation of Reactivity Estimates with Limited Compositional Information 11
Derivation of Carbon Number Distributions from Boiling Point Data 11
Estimation of Compositions of Aromatic Fractions 15
Derivation of Reactivity Estimates 15
Comparison of Results with ARB Bin and Explicitly Calculated Reactivities 19

DIRECT REACTIVITY MEASUREMENT 23
Introduction 23
Approach 24
Modified flow system 24
Total carbon analysis 26
Data Analysis Method 26
Results 28

ENVIRONMENTAL CHAMBER EXPERIMENTS 32
Experimental Methods 34
Chamber Description 34
Analytical Instrumentation 36
Sampling methods 40
Characterization Methods 40
Experimental Procedures 41
Injection Tests 42
Texanol® 42
Hydrocarbon Solvents 44
Results 45
Characterization Results 45
Mechanism Evaluation Experiments 46
OH Radical Rate Constant Determination for the Texanol® isomers 50

MECHANISM EVALUATION 54
Modeling methods 54
Standard Chemical Mechanism 54

TABLE OF CONTENTS (continued)

Adjusted Mechanisms 55
Representation of Chamber Conditions 59
Atmospheric Reactivity Simulations 59
Simulations of Base Case Experiments 60
Effect of Mechanism Adjustments 60
Predicted Effects of Removing Formaldehyde Base ROG Surrogate 63
Simulations of Reactivity Results 65
m-Xylene 65
n-Octane 68
Texanol® 71
Hydrocarbon Solvent ASTM-1C 71
VMP Naphaha Solvent 73
Hydrocarbon Solvent ASTM-1B 76
Hydrocarbon Solvent ASTM-1A 76
Aromatic 100 Solvent 76
Synthetic Hydrocarbon Solvent ASTM-3C1 79

DISCUSSION AND CONCLUSIONS 84
Estimation of Hydrocarbon Solvent Compositions and Reactivity 85
Progress in Developing a Direct Reactivity Measurement Method 87
Environmental Chamber Reactivity Evaluations 87
Use of Chamber Data for Mechanism Evaluation 88
Evaluation Results for Texnaol® 91
Evaluation Results for Petroleum Distillate Hydrocarbon Samples 92
Evaluation Results for the Synthetic Branched Alkane Hydrocarbon Sample 93
Implications of Chamber Results on Maximum Incremental Reactivities 95
Recommendations 97

REFERENCES 101

APPENDIX A. LISTINGS AND TABULATIONS 105
Hydrocarbon Solvent Composition Data 105
Chamber Experiment Listing 123

LIST OF TABLES

Table E-1. Summary of solvents studied in the environmental chamber experiments and the overall conclusions from the evaluation results. xvi

Table 1. Summary of hydrocarbon solvents studied in environmental chamber experiments for this project 4

Table 2. Hydrocarbon solvent bins derived by Kwok et al (2000) for use in estimating solvent MIRs for the CARB aerosol coatings regulation. 6

Table 3. Summary of hydrocarbon solvents whose compositional information was used in this analysis of hydrocarbon solvent reactivity. 7

Table 4. Boiling points and carbon numbers for compounds used to derive carbon number from boiling point estimates 12

Table 5. List of C_8 - C_{11} aromatic compounds identified in the hydrocarbon solvents used in this study for aromatic fraction analysis, and average contributions of the compounds to the total aromatics with the same carbon number 16

Table 6. Input parameters and MIR values derived from the spreadsheet method compared to the CARB hydrocarbon bins. 21

Table 7. Summary and conditions and results of the HONO flow direct reactivity experiments carried out in the final configuration. 29

Table 8. Composition of base case reactive organic gas (ROG) surrogate employed in the initial incremental reactivity experiments for this project. 33

Table 9. List of analytical and characterization instrumentation for the UCR EPA chamber. 37

Table 10. Summary of initial concentrations and selected gas-phase results of the incremental reactivity and solvent - NO_x experiments. 47

Table 11. Information on the Texanol® isomers relevant to this project. 51

Table 12. Data used for OH radical rate constant determinations for the Texanol® isomers. 53

Table 13. Lumping method used when representing complex hydrocarbon mixtures in the model simulations for this project. 55

Table 14. Lumped molecule representations used when representing the complex mixture hydrocarbon solvents. 56

Table 15. Selected mechanistic parameters for the lumped ALK5 model species used to represent the ASTM-3C1 in the chamber and atmospheric reactivity simulations. 83

Table 16. Atmospheric MIR values calculated for the ASTM-3C1 sample using various assumed compositions and adjusted mechanisms. 95

Table 17. Current best estimate MIRs and uncertainty classification codes for the compounds or solvents studied for this project 98

LIST OF TABLES (continued)

Table A-1. SAPRC-99 detailed model species compositional assignments for the hydrocarbon solvents studied in environmental chamber experiments for this project. 105

Table A-2. SAPRC-99 detailed model species compositional assignments for the hydrocarbon solvents analyzed by Censullo et al (2002). 107

Table A-3. SAPRC-99 detailed model species compositional assignments for the hydrocarbon solvents whose analysis was provided by the ACC (Jaques, 2002). 116

Table A-4. Summary chamber experiments that are relevant to this project. 123

LIST OF FIGURES

Figure E-1. Comparison of experimental and calculated direct reactivity measurements normalized to the direct reactivity measurements for propane. xiv

Figure 1. Plots of differences between CARB bin MIRs and explicitly calculated SAPRC-99 MIRs for the hydrocarbon solvents for which compositional data were provided. 10

Figure 2. Plots of carbon numbers against boiling points for various alkanes and aromatic hydrocarbons. 13

Figure 3. Distributions of Calculated SAPRC-99 Maximum Incremental Reactivities for aromatic constituents with a given carbon number for the hydrocarbon solvents with aromatic speciation data and non-negligible aromatic constituents with those carbon numbers. 17

Figure 4. Plots of differences between spreadsheet and explicitly calculated SAPRC-99 MIR's and EBIR's for the hydrocarbon solvents for which compositional data were provided. 20

Figure 5. Plots of differences between spreadsheet calculated bin and explicitly calculated SAPRC-99 MIR's for the hydrocarbon solvents for which compositional data were provided. 22

Figure 6. Diagram of setup for plug flow reactor being evaluated for use with the total carbon analysis system. 25

Figure 7. Diagram of the HONO generation system. 25

Figure 8. Plots of experimental changes in Δ([O3]-[NO]) against the test VOC concentrations, derived from the CO_2 data, for the HONO flow direct reactivity experiments. 30

Figure 9. Comparison of experimental and calculated direct reactivity measurements normalized to the direct reactivity measurements for propane. Error bars show the range of variability for the experiments. 31

Figure 10. Schematic of the UCR EPA environmental chamber reactors and enclosure. 35

Figure 11. Spectrum of the argon arc light source used in the UCR EPA chamber. Blacklight and representative solar spectra, with relative intensities normalized to give the same NO_2 photolysis rate as that for the UCR EPA spectrum, are also shown. 35

Figure 12. Experimental and calculated Texanol carbon levels in the Texanol injection test experiment. 43

Figure 13. Plots of best fit HONO offgasing parameters against UCR EPA run number. (Data from Carter (2004a), with results of newer experiments for this project added.) 45

Figure 14. Plots of Equation (VIII) for the data from the Texanol® reactivity experiments. 52

Figure 15. Dependence of the Δ([O3]-[NO]) and IntOH model underprediction bias on initial ROG/NO_x ratio in the surrogate - NO_x experiments for the SAPRC-99 model calculations using the standard and adjusted aromatics mechanisms. 61

LIST OF FIGURES (continued)

Figure 16. Experimental and calculated Δ([O_3]-[NO]) and IntOH for selected base case experiments carried out for this project. 62

Figure 17. Effects of removing formaldehyde and increasing the base ROG concentrations by 10% on model simulations of the standard incremental reactivity base case experiments. 64

Figure 18. Comparisons of mechanistic reactivities calculated for all the SAPRC-99 detailed model species for simulated MIR or MOIR/2 incremental reactivity experiments using the standard ROG surrogate with those for the ROG surrogate with formaldehyde removed. 64

Figure 19. Experimental and calculated concentration-time plots for the m-xylene incremental reactivity experiments at the lower ROG/NO_x ratios. The mechanism for the added m-xylene was not adjusted for test case calculations. 66

Figure 20. Experimental and calculated concentration-time plots for the m-xylene incremental reactivity experiments at the higher ROG/NO_x ratios. The mechanism for the added m-xylene was not adjusted for test case calculations. 67

Figure 21. Experimental and calculated concentration-time plots for the n-octane incremental reactivity experiments at the lower ROG/NO_x ratios. 69

Figure 22. Experimental and calculated concentration-time plots for the n-octane incremental reactivity experiments at the higher ROG/NO_x ratios. 70

Figure 23. Experimental and calculated concentration-time plots for the Texanol® incremental reactivity experiments. 72

Figure 24. Experimental and calculated concentration-time plots for the ASTM-1C incremental reactivity experiments. 73

Figure 25. Experimental and calculated concentration-time plots for the VMP-Naphtha incremental reactivity experiments. Note that the effect of the naphtha on IntOH could not be determined because of interferences on the GC analysis for the tracer compounds. 74

Figure 26. Experimental and calculated concentration-time plots for the ASTM-1B incremental reactivity experiments. 75

Figure 27. Experimental and calculated concentration-time plots for the ASTM-1A incremental reactivity experiments. 77

Figure 28. Experimental and calculated concentration-time plots for the Aromatic-100 incremental reactivity experiments. 78

Figure 29. Experimental and calculated concentration-time plots for selected species for the Aromatic-100 - NO_x and Aromatic-100 - NO_x + CO experiments. 80

Figure 30. Experimental and calculated concentration-time plots for the ASTM-3C1 incremental reactivity experiments. 81

Figure 31. Effects of alternative representations and mechanisms on calculated effects of ASTM-3C1 addition on Δ([O_3]-[NO]) and IntOH. All calculations used the adjusted aromatics mechanism for the base ROG simulation. 83

LIST OF FIGURES (continued)

Figure 32. Comparisons of environmental chamber and atmospheric incremental reactivity simulations for equal relative additions of Texanol® or ASTM-1C solvent. 89

Figure 33. Experimental and calculated concentration-time plots for selected incremental reactivity experiments with ISOPAR-M®, carried out by Carter et al (2000). 96

EXECUTIVE SUMMARY

Background

Emissions from architectural coatings are an important component of the total emissions of volatile organic compounds (VOCs) into the atmosphere. When emitted into the atmosphere, VOCs react in sunlight in the presence of oxides of nitrogen (NO_x) emitted from other sources to contribute to the formation of ground-level ozone (O_3), an important air pollution problem in California. Because of this, the California Air Resources Board (CARB) is considering implementing additional controls for VOC emissions from architectural coatings.

One factor that needs to be considered when implementing new VOC controls is the fact that VOCs consist of many different chemical compounds, and because of differences in atmospheric reaction rates and mechanisms, these compounds can differ significantly in their effects on ozone. The possibility of taking these differences into account, referred to as "reactivity" in the subsequent discussion, is being considered because this can potentially make the new regulations more cost-effective and flexible. Because of this, reactivity considerations have already been implemented in regulations for mobile source (CARB, 1993) and aerosol coatings (CARB, 2000) emissions in California. These are based on use of the Maximum Incremental Reactivity (MIR) scale, which is designed to reflect differences in impacts of VOCs on O_3 formation in environments where O_3 is most sensitive to VOC emissions. However, the uncertainties in quantification of ozone impacts of coatings VOCs are a concern.

Because of the variety of types of coatings in use, a variety of types of VOCs can be emitted and need to have their reactivities quantified. An examination of the results of a recent survey of coatings VOCs carried out by the CARB indicates that there are several important types of coatings VOCs where additional reactivity research is needed. The first concerns Texanol®[1] (2,2,4-trimethyl-1,3-pentanediol isobutyrate, CAS number 25265-77-4), which is an additive in many coatings formulations. The second concerns the various types of hydrocarbon solvents, variously referred to as "Mineral Spirits", "Naphtha", "Stoddard Solvent", "Lactol Spirits," etc, that are used primarily in solvent-based coatings. These generally are highly complex mixtures of alkanes and (in some cases) aromatics and (less frequently) olefins in various boiling point ranges. The CARB staff developed a general method to estimate MIR values from boiling point ranges and other characteristics for hydrocarbon solvents for the California aerosol coatings regulation, but the performance of this method in deriving actual impacts has not been fully evaluated, and it would need to be re-derived when the regulatory reactivity scale is updated or modified due to advances in atmospheric chemistry or VOC reactivity assessment methods.

In view of this, the CARB funded the College of Engineering Center for Environmental Research and Technology (CE-CERT) to carry out a project to reduce uncertainties in ozone reactivity estimates for selected major types of coatings VOCs. Two types of uncertainty were addressed in this project, compositional uncertainty and chemical mechanism uncertainty. Compositional uncertainty is applicable to complex mixtures of compounds of differing reactivities that are not completely speciated, and in the context of coatings this is primarily applicable to hydrocarbon solvents such as petroleum distillates and synthetic hydrocarbon mixtures. Chemical mechanism uncertainty is applicable to all VOCs, and comes from the fact that the only practical way to obtain *quantitative* estimates of a VOCs impact in the

[1] Texanol is a registered trademark of Eastman Chemical Company. It is used throughout this report rather than the generic chemical name for simplicity.

atmosphere is to calculate them in computer airshed models. This is because it is not practical in the laboratory to experimentally duplicate all aspects that affect atmospheric reactivity. The approach that must be used is to develop models for the VOC's atmospheric reaction (its "chemical mechanism") and incorporate them in computer airshed models of the atmosphere to calculate the VOCs ozone impact. Since the results are no more reliable than the chemical mechanism used, experiments need to be carried out to test the predictive capabilities of the mechanisms used in the models. Different types of experiments are needed to test different aspects of the VOC's mechanisms that affect predictions of atmospheric reactivities under various atmospheric conditions. This uncertainty is the greatest for the VOCs that have not been previously studied, so experiments for this project focused on such VOCs.

The objectives, approaches, and results of the tasks that were designed to address these uncertainties are summarized below.

Investigation of Methods to Estimate Reactivities of Complex Hydrocarbon Solvents

The objective of this task was to develop and evaluate procedures for estimating reactivities for complex hydrocarbon mixtures for which detailed compositional data are limited. A new method was developed to estimate reactivities of hydrocarbon solvents in any reactivity scale, given boiling point ranges and type analysis results. The bin MIR assignments incorporated in the CARB aerosol coatings regulations were evaluated using detailed compositional data for 124 different solvents, representing 19 of the 24 CARB hydrocarbon bins. The sources of data included the American Chemistry Council, who provided compositions for a subset of those used by the CARB to evaluate their method, and the results of the CARB-funded study of Censullo et al (2002), which was carried out after the CARB bins were developed.

We found that the bin assignments developed by the CARB perform reasonably well in predicting MIRs for hydrocarbon solvents for which detailed compositional data are available for the most of the bins. The exceptions were for the light hydrocarbon bins 1 and 3-5, where the bin MIRs were 25-50% higher than derived for the solvents in those bins. This is due the fact that the number of solvents used in these bins in the evaluation in this work and by the CARB were relatively limited, and the CARB staff felt that for regulatory purposes the possibility that there may be more reactive solvents in these bins needs to be taken into account. The specific issue is whether cyclopentanes, which are somewhat more reactive than other hydrocarbons in this weight range, are present in significant levels in the lower boiling point solvents currently in use.

A general problem with the derivation of the CARB bin MIRs is that it is based on relating compositional categories and estimated carbon number distributions directly to MIRs, which makes it less straightforward to update or incorporate an alternative reactivity scale and makes analysis of compositional uncertainty more difficult. Therefore, for this project we developed a general procedure for estimating compositions of hydrocarbon solvents with limited compositional data, and these estimated compositions can then be used to derive reactivities in any given scale. The information it requires is the same as that required to make CARB bin assignments, though the more precise the information (e.g., specific boiling points or aromatic contents, rather than general ranges) the more precise the estimate. The new method was found to predict reactivities derived from detailed compositional data for the individual hydrocarbons to better than ±15% in most cases. It can be used to derive bin assignments that perform at least as well as the CARB assignments for the hydrocarbon solvents used in this evaluation, predicting the reactivities derived from the detailed compositional data to within ±25% for all the bins, including the low boiling point bins 1 and 3-5.

There are no data available to us to evaluate the performance of the CARB MIR assignments for bins 13, 18-20 and 24. However, given the performance of the method developed in this work in predicting reactivities derived from detailed compositional data for the other bins, it is reasonable to expect that its performance in predicting the reactivities of these other bins is also satisfactory. The predictions using the method developed gave reasonably good agreement with the CARB bin MIR assignments.

The new method for deriving hydrocarbon composition and reactivity estimates could be used as a basis for updating the bin reactivity assignments when reactivity scales are updated, or if use of a different reactivity scale is adopted. However, before it is used in a regulatory application it needs to be evaluated using the full distribution of solvents in use, including solvents in bins 1 or 3-5 that might possibly have higher cyclopentane content than predicted by this method.

These results suggest that uncertainty in reactivity assignments due to compositional uncertainty is approximately ±25% if unbiased bin assignments are used, and better than ±15% if the specific type distribution and boiling point data are taken into account. It is important to recognize that this does not take into account chemical mechanism uncertainty, which might be significantly greater, particularly for solvents high in aromatics or branched alkanes. The environmental chamber experiments, discussed below, provide the appropriate basis for assessing chemical mechanism uncertainty. For example, the results suggest that it is probably appropriate to put synthetic hydrocarbon mixtures of branched alkanes in separate bins with higher reactivity estimates than currently used for them.

Further Development of a Direct Reactivity Measurement Method

The impact of a VOC on ozone formation depends on various aspects of its atmospheric reaction mechanism, whose relative importance in terms of affecting ozone depends on environmental conditions. These include the amount of O_3 formed resulting directly from the reactions of the VOC itself or its major oxidation products, referred to as the “direct reactivity” of the VOC, and the effects of the reactions of the VOC on O_3 formation from all the VOCs present, which differ depending on the environmental conditions. All these aspects of reactivity are important and need to be appropriately represented to predict a VOC’s ozone impacts under the full variety of atmospheric conditions. Environmental chamber experiments can to some extent be used to test these different aspects, but results of such experiments can often be somewhat ambiguous, particularly in the evaluations of the direct reactivity. Because of this, if an experiment could be developed that provides a measurement that is primarily sensitive to direct reactivity effects, then a source of ambiguity in the evaluation of mechanisms would be removed. This would reduce uncertainties when applying chamber-derived mechanisms to model simulations of ozone formation in the atmosphere.

In a previous CARB project we developed a direct reactivity measurement method based on the photolysis of nitrous acid (HONO) in the presence of varying amounts of the VOC in a plug flow system, and measuring the effect of the VOC on NO oxidation and ozone formation (CARB contract no. 97-314, Carter and Malkina, 2002). The results were promising but were not practical for application to complex hydrocarbon solvents or low volatility materials because it depended on the use of gas chromatographic analyses to quantify the amount of VOC present in the flow reactor, and this is a problem for many types of solvents. Therefore, for this project we investigated the use of interfacing a total carbon analyzer interfaced to the flow system to continuously quantify the amount of VOC present. In order for the response to be independent of the nature of the VOC used, the analysis was based on use of a combustion catalyst to quantitatively convert the VOC to CO_2, then using a sensitive CO_2 analyzer to measure the amount of CO_2 formed. CO_2-free air was used in the flow system to permit the analysis.

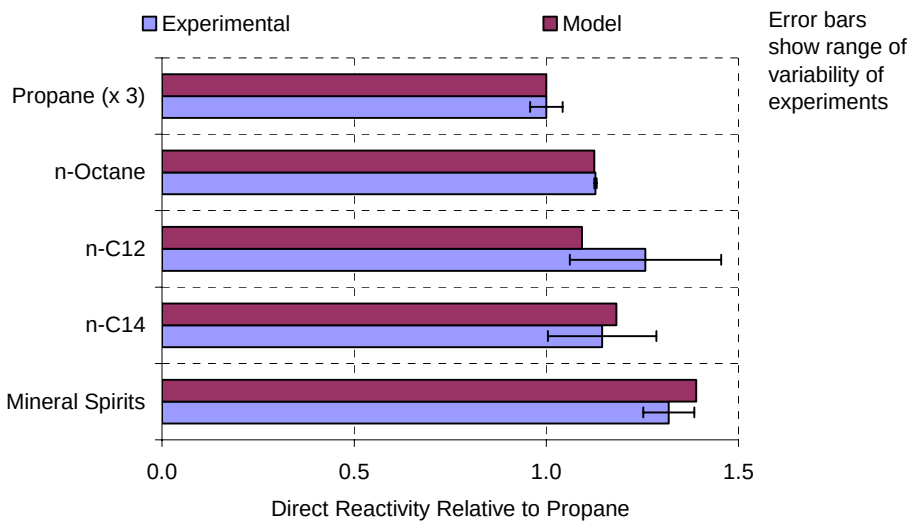

Figure E-1. Comparison of experimental and calculated direct reactivity measurements normalized to the direct reactivity measurements for propane.

Although progress was made towards the objective of this project, additional work is needed before we can obtain data of relevance to coatings VOC reactivity assessment. The addition of the total carbon analyzer based on a combustion catalyst and CO_2 monitoring was found to solve the problem of analyzing the amount of test compound added, and provided a useful method for monitoring how changes in the amount of added VOC affected the measurements. However, it was also found that this introduced a source of uncharacterized variability in the data, and the results of experiments with compounds with known direct reactivities were not well simulated by the model. On the other hand, if the direct reactivity results for a standard compound with a well characterized mechanism, such as propane or n-octane, are used to normalize the data, then the results are consistent with model predictions, even for compounds with as low a volatility as n-tetradecane. This is shown in Figure E-1 for the compounds and mixtures that were studied. It may be possible to obtain equally consistent measures of direct reactivity for materials with even lower volatility, but this has not been assessed. In any case, the results to date suggest that the method could be useful as a screening method for assessing direct reactivities of hydrocarbon solvents, especially in the volatility range used in architectural coatings, if used in a relative sense.

Unfortunately, the time and resources allocated to this task were expended before we could investigate or improve this method further and apply it more widely to other compounds and hydrocarbon solvents. Although normalizing the direct reactivity results to those for a known compound appear to yield satisfactory results, it obviously would be better if the conditions of the experiments that affect the results were better characterized and the sources of uncharacterized variability were removed. In any case, additional funding would be required to develop and apply this method further. Direct reactivity measurements for the synthetic branched alkanes solvent would have been particularly useful in this regard, as discussed below.

Environmental Chamber Experiments for Mechanism Evaluation

The major task in this project was to conduct environmental chamber experiments to evaluate the ability of chemical mechanisms to predict atmospheric ozone impacts of the water-based coatings solvent

Texanol® and representatives of different six different types of hydrocarbon solvents used in coatings. The chamber experiments were carried out in the new UCR EPA chamber that was developed under EPA funding for more precise mechanism evaluation at lower and more atmospherically representative pollutant levels than previously possible. The type of experiments carried out were "incremental reactivity" experiments, which involved determining the effect of adding the solvent to standard reactive organic gas (ROG) surrogate - NO_x experiments designed to simulate the chemical conditions of polluted urban atmospheres. Experiments at two different ROG and NO_x levels were employed to represent different conditions of NO_x availability, to provide a more comprehensive test of the mechanisms under differing chemical conditions that affect reactivity. The total NO_x levels employed were in the 25-30 ppb range, which is designed to be representative of those in urban areas in California and which are lower than employed in previous reactivity chamber studies. Comparable reactivity experiments with m-xylene and n-octane were also carried out for control and comparison purposes.

The solvents studied in the environmental chamber experiments for this project are summarized in Table E-1. The experiments were used to evaluate the reactivity predictions of the SAPRC-99 mechanism (Carter, 2000a), which is the mechanism used to derive the current version of the MIR scale used in California, and represents the current state of the art in this regard. The results of the evaluation against this mechanism are also summarized in Table E-1, and are discussed further below.

It is important to recognize that the evaluation results are somewhat uncertain because, as discussed in a previous report to the CARB (Contract 01-305, Carter, 2004a), the SAPRC-99 mechanism tends to underpredict rates of O_3 formation in the experiments that represent MIR conditions. We believe that this is due to problems with the aromatics mechanisms that have not yet been addressed. In order to remove or at least assess this potential source of bias in the evaluation, evaluation calculations were also carried out with an adjusted version of the aromatics mechanism where the tendency to underpredict O_3 in the MIR simulation experiments was removed. It is important to recognize that this is not a "better" aromatics mechanism, because it still has problems and its predictions are not consistent with results of experiments used to develop the current mechanism.

The results of the evaluations of the mechanisms for the solvents listed on Table E-1 were found not to be significantly different when the adjusted mechanism was used, suggesting that they may also be applicable when the mechanism is updated. However, this cannot be assured since the source of the problem with the aromatics is unknown, and correcting this problem may have effects on the evaluation that are different than those of the adjustments examined in this work. Therefore, the conclusions concerning the mechanism evaluation results, summarized on Table E-1, must in some regards be considered to be preliminary, and need to be re-evaluated when the mechanism is updated.

The results of the experiments with Texanol® tended to validate the existing mechanism assignments that were made for its constituents that were based on applications of various estimation methods (Carter, 2000a). Despite our concerns about being able to obtain quality data for such a low volatility material, tests indicated that our ability to quantitatively inject and analyze the Texanol® isomers in the gas phase was entirely satisfactory. Indeed, the gas-phase analysis of the isomers was sufficiently precise that we were able to use relative rate technique to measure their OH radical rate constants. The rate constants obtained were 1.62 and 1.29 x 10^{-11} cm^3 $molec^{-1}$ s^{-1} for 3-hydroxy-2,2,4-trimethylpentyl-1-isobutyrate and 1-hydroxy-2,2,4-trimethylpentyl-3-isobutyrate, respectively. These were within 5% of the estimated values incorporated in the present mechanism. These results, indicate that there is no need to revise the current mechanisms used for the Texanol® isomers, or revise the current estimates for their atmospheric reactivities.

However, it was also found that the ratio of the two trimethylpentanediol isobutyrate isomers were different when measured in the gas phase than when measured in the liquid, presumably due to a

Table E-1. Summary of solvents studied in the environmental chamber experiments and the overall conclusions from the evaluation results.

Solvent [a]	Description	Evaluation Results [b]	MIR [c]	
			This work [d]	Previous value [e]
Texanol® [f]	Isobutyrate monoesters of 2,2,4-trimethyl-1,3-pentanediol	Experimental results generally consistent with chamber data. The OH radical rate constants found to be in good agreement with values used in the mechanism.	0.88	0.88
VMP Naphtha	Petroleum Distillate derived. Primarily C_7-C_9 mixed alkane. CARB Bin 6 [g]	Experimental results generally consistent with chamber data.	1.35	1.41
Dearomatized Mixed Alkanes (ASTM-1C)	Petroleum Distillate derived. Primarily C_{10}-C_{12} mixed alkanes. CARB bin 11	Experimental results generally consistent with chamber data.	0.96	0.91
Reduced Aromatics Mineral Spirits (ASTM-1B)	Petroleum Distillate derived. Primarily C_{10}-C_{12} mixed alkanes with 6% aromatics. CARB bin 14	Experimental results generally consistent with chamber data.	1.26	1.21
Regular mineral spirits (ASTM-1A)	Petroleum Distillate derived. Primarily C_{10}-C_{12} mixed alkanes with 19% aromatics. CARB bin 15	Experimental results generally consistent with chamber data.	1.97	1.82
Aromatic 100	Petroleum Distillate derived. Primarily C_9-C_{10} alkylbenzenes. CARB bin 22	Experimental results representing MIR conditions generally consistent with model predictions. But model underpredicted O_3 inhibition in low NO_x conditions and has other problems.	7.70	7.51
Synthetic isoparaffinic alkanes (ASTM-3C1)	Synthetic mixture of primarily C_{10}-C_{12} branched alkanes. CARB bin 12	Data not well simulated by the model. Model probably underpredicts atmospheric ozone formation by 25-75%, depending on the cause of the discrepancy.	1.1 - 1.5 [h]	0.81

[a] ASTM designations based on the D 235-02 specification (ASTM, 2003).

[b] Evaluation results applicable to the SAPRC-99 mechanism (Carter, 2000a).

[c] Maximum incremental reactivity in gm O_3 per gm VOC.

[d] Best estimate MIRs based on the results of the current study. Except for the synthetic isoparaffinic alkanes (ASTM-3C1) the results of this study do not indicate any need to change the MIR derived by

Table E-1 (continued)

the current SAPRC-99 mechanism. The change in MIR that may result when the mechanism is updated is unknown.

[e] MIR values incorporated in CARB regulations. The value for Texanol® is was calculated using the existing SAPRC-99 mechanism (Carter, 2000a), which was not changed as a result of this work. The values for the hydrocarbon solvents were derived using the CARB Bin assignments developed by Kwok et al (2000).

[f] Texanol is a registered trademark of Eastman Chemical Company.

[g] CARB hydrocarbon bin used to assign MIR in the aerosol coatings regulation

[h] Range of MIRs for alternative mechanisms adjusted to fit the chamber data. The available data are inadequate to distinguish between these mechanisms.

relatively facile interconversion of the isomers. This indicates that the ratio of the two isomers used when calculating the atmospheric reactivity of the whole solvent needs to be modified when the reactivity scale is updated or modified. However, this change has only a minimal effect on the predicted MIRs in the current scale.

The results of the chamber experiments petroleum-distillate-derived primarily alkane hydrocarbon solvents were generally consistent with model predictions, and generally were comparable to the evaluation results for n-octane, whose mechanism is considered to be reasonably well established, and whose reactivity characteristics are similar. Therefore, although there are uncertainties due to problems with the base mechanism, the data obtained tend to validate our existing estimates for the reactivities of these types of solvents, and do not indicate a need to change the atmospheric reactivity estimates for them at the present time.

Despite the fact that over half of the mass of the Aromatic 100 mixture were compounds whose mechanisms were based on uncertain extrapolations, the model tended to simulate the results of the experiments with this mixture as well as it could simulate experiments with m-xylene, an aromatic compound that has been extensively studied. As with m-xylene, the model gives reasonably good simulations of the impacts of Aromatic 100 on the results of the MIR experiments and during the first period of the lower NO_x incremental reactivity runs, and also gives reasonably good simulations of O_3 formation in aromatics - NO_x experiments without the added base ROG surrogate. Therefore, the mechanistic estimates and lumped-molecule assignments made when deriving mechanisms for the Aromatic 100 constituents for which no data are available appear to be validated at least to some extent, at least for purposes of deriving a MIR scale. However, it is possible (indeed likely) that assignments that underestimate the reactivities of some of the components in the complex mixture are being cancelled out by assignments that overestimate reactivities of other constituents. It may be that the more complex the mixture the less uncertain the reactivity estimate.

The results of the evaluation for Aromatic 100 are also similar to those for other aromatics in indicating problems with the mechanisms for aromatics in general. The model did not correctly predict the extent to which the added solvent inhibited final O_3 levels under NO_x-limited conditions, and had other problems simulating other aspects of the data. Therefore, all the aromatic mechanism problems that apply to the more well-studied aromatics are applicable to Aromatic 100 as well. Better model performance in simulating Aromatic 100 reactivity would be expected if the base mechanism is improved, but this would need to be evaluated.

The most unexpected result of this project was the relatively poor model performance in simulating the environmental chamber experiments with the synthetic mixture of predominantly C_{10}-C_{12}

branched alkanes. The model consistently predicted a tendency of this mixture to inhibit O_3 formation in the experiments that was greater than was observed experimentally. Using different representation of the unspeciated branched alkanes based on assuming more highly branched compounds only marginally improved the model performance, even though it caused almost a 50% increase in the calculated atmospheric MIR for the mixture. The source of this discrepancy is unknown, but it is presumably due to either the wrong compounds being used to represent the unspeciated branched alkanes or those compounds having much higher reactivities than predicted in current mechanisms for C_{10}-C_{12} branched alkanes. Depending on how the mechanisms are adjusted to fit the data, the discrepancy could result in anywhere between a 25% and a 75% increase in the calculated MIR for this solvent. The source of this discrepancy should be determined so the appropriate adjustment can be made, and the actual impact on the atmospheric reactivity can be determined. As it is, the bin MIR assignment for these compounds may be low by anywhere between ~30% and a factor of 2.

Recommendations

The recommendations regarding reducing uncertainties in O_3 impacts of architectural coatings VOCs and VOCs in general can be summarized as follows. Some of these are being addressed to some extent by projects that are underway, but additional work is needed in all cases.

- Improve the mechanisms for the aromatics and (if applicable) other compounds so that the model gives better simulations of how O_3 formation is affected by changes in ROG and NO_x levels, and so that results of other types of experiments are consistent with available data. We are attempting to address this in our current SAPRC mechanism update project for the CARB (Contract 03-318), but progress to date is insufficient and additional work is needed.
- Obtain information needed to determine why the reactivities of synthetic branched alkane mixtures are so different than current model predictions. Carry out reactivity evaluation studies using other such mixtures currently in use to determine if the results obtained in this study are typical.
- Conduct experimental reactivity studies of complex mixtures of higher aromatics, such as Aromatics 150 and Aromatic 200, where the extrapolations based on mechanisms of previously studied compounds to those in the solvents are much more uncertain than is the case for Aromatic 100. Obtain reactivity data for representatives of higher molecular weight aromatics.
- Evaluate and if necessary update the mixture used to represent the reactive organic gases present in ambient air to use in incremental reactivity experiments for future environmental chamber studies of VOC reactivity.
- Provide the relatively limited additional funding needed to apply the direct reactivity measurement method to hydrocarbon solvents of interest. Direct reactivity data for the synthetic branched alkane mixtures would be particularly useful and could have significant impacts on estimated reactivities of these poorly characterized mixtures.
- Conduct a survey of the cyclopentane content of the lower boiling point hydrocarbon solvents to determine appropriate reactivity ranges for solvents in those bins. Cyclopentanes are more reactive than other hydrocarbons in this boiling point range and differing assumptions about cyclopentane contents caused discrepancies in the evaluations of the current bins.
- The hydrocarbon bin assignments will need to be revised when the regulatory reactivity scale is updated or if a new regulatory reactivity scale is adopted. The updated bin reactivities should based on methodologies that derive compositions for the purposes of deriving reactivities, not deriving reactivities from hydrocarbon type and carbon number estimates directly. The approach needs to be peer reviewed and should include protocols for estimating upper limit, lower limit,

and “best estimate” reactivities for regulatory applications. Separate bins will probably be needed for synthetic branched alkane mixtures.

Impacts on ground level ozone formation are not the only potential areas of concern for architectural coatings VOCs. The reactions of higher molecular weight solvents may affect formation of secondary particulate matter (PM), which is another area of regulatory concern. We have obtained funding from the South Coast Air Quality Management District to make PM measurements of during the course of the experiments carried out for this project, and some funding for this purpose was also included with this project, and the results will be discussed in a subsequent report which is in preparation. However, the data obtained to date represent only a beginning in the work needed to develop and evaluate predictive models for the effects of VOCs on secondary PM formation, and considerably more work in this area is required before we can have any confidence in model predictions of impacts of VOCs on secondary PM formation.

INTRODUCTION

Background

Quantification of VOC Reactivity

Many different types of volatile organic compounds (VOCs) are emitted into the atmosphere, where they can affect photochemical ozone formation and other measures of air quality. Because VOCs can react in the atmospheres at different rates and with different mechanisms, the different types of VOCs can differ significantly in their effects on air quality. Therefore, VOC control strategies that take these "reactivity" differences into account can potentially achieve ozone reductions and other air quality benefits in a more cost-effective manner than strategies that treat all non-exempt VOCs equally. Reactivity-based control strategies have already been implemented in the California Clean Fuel/Low Emissions Vehicle (CF/LEV) regulations (CARB, 1993), aerosol coatings regulations (CARB, 2000), and are being considered for other stationary source applications. Since California has been successful in implementing reactivity-based regulations as a cost-effective way to reduce ozone, it is reasonable to expect that this approach will be adopted in other jurisdictions as well.

Implementation of reactivity-based controls requires some means to measure and quantify relative ozone impacts of different VOCs. This is not a simple problem, because the ozone impact of a VOC depends on the environment where the VOC is emitted as well as the nature of the VOC (e.g., see Carter and Atkinson, 1989). The effect of a VOC on ozone formation in a particular environment can be measured by its "incremental reactivity", which is defined as the amount of additional ozone formed when a small amount of the VOC is added to the environment, divided by the amount added. Although this can be measured in environmental chamber experiments, such experiment cannot be assumed to be the same as incremental reactivities in the atmosphere (Carter and Atkinson, 1989; Carter et al., 1995a). This is because it is not currently practical to duplicate in an experiment all the environmental factors that affect relative reactivities; and, even if it were, the results would only be applicable to a single type of environment. The only practical means to assess atmospheric reactivity, and how it varies among different environments, is to estimate its atmospheric ozone impacts using airshed models. However, such model calculations are no more reliable than the chemical mechanisms upon which they are based. While the initial atmospheric reaction rates for most VOCs are reasonably well known or at least can be estimated, for most VOCs the subsequent reactions of the radicals formed are complex and have uncertainties that can significantly affect predictions of atmospheric impacts. Laboratory studies can reduce these uncertainties, but for most VOCs they will not provide the needed information in the time frame required for current regulatory applications. For this reason, environmental chamber experiments and other experimental measurements of reactivity are necessary to test and verify the predictive capabilities of the chemical mechanisms used to calculate atmospheric reactivities.

Therefore, experimental measurements of reactivity play an essential role in reactivity quantification. They provide the only means to assess as a whole all the many mechanistic factors that might affect reactivity, including the role of products or processes that cannot be studied directly using currently available techniques. Because of this, the ARB and others have funded programs of environmental chamber studies to provide data needed to reduce uncertainties in reactivity assessments of the major classes of VOCs present in emissions, and the data obtained were used in the development of the most recent mechanism for deriving ozone reactivity scales (see Carter, 2000a and references therein). Although there has been significant progress, environmental chamber data are not available to test reactivity predictions for all of the compounds that are important in emissions inventories.

Application to Architectural Coatings

Emissions from architectural coatings are an important component of the stationary source VOC inventory. Because of this, the California Air Resources Board (CARB) is considering implementing additional controls for VOC emissions from architectural coatings. The possibility of taking reactivity into account in these new regulations is being considered because this can potentially make the new regulations more cost-effective and flexible. However, the uncertainties in quantification of ozone impacts of coatings VOCs are a concern. Because of the variety of types of coatings in use, a variety of types of VOCs can be emitted and need to have their reactivities quantified.

Reactivity estimates are currently available for a wide variety of VOCs (Carter, 2000a), which includes many of those that are emitted from architectural coatings. These are based on the current version of the SAPRC-99 mechanism, which incorporates results of environmental chamber and laboratory studies of a variety of representative compounds (Carter, 2000a, and references therein). However, an examination of the results of a recent survey of coatings VOCs carried out by the CARB indicates that there are at several important types of coatings VOCs where additional reactivity research is needed. These are briefly discussed below.

The first concerns Texanol®[2] (2,2,4-trimethyl-1,3-pentanediol isobutyrate, CAS number 25265-77-4), which is an additive in many coatings formulations. It is actually a mixture of two isomers that rapidly interconvert (Morgott, Eastman Kodak Co, private communication). Although methods exist to estimate the mechanism and reactivities of these glycol esters (Carter, 2000a), they are based on data for much lower molecular weight and much higher volatility compounds. Until this project, no environmental chamber or mechanistic data are available to evaluate the estimated mechanism for this compound.

The second type of coatings VOC where research is needed concerns various types of hydrocarbon solvents, variously referred to as “Mineral Spirits”, “Naphtha”, “Stoddard Solvent”, “Lactol Spirits,” etc. These generally are highly complex mixtures of alkanes and (in some cases) aromatics and (less frequently) olefins in various boiling point ranges. Experimental data and reactivity estimates are available concerning the reactivities of several such mixtures (Carter et al, 1997, 2000, 2002), though their applicability to other types of hydrocarbon solvents is uncertain. The reactivity estimates depend on the types of alkane and aromatics present, which in many cases are uncertain. The CARB staff developed a general method to estimate Maximum Incremental Reactivity (MIR) values for hydrocarbon solvents based on boiling point ranges and other known characteristics (Kwok et al, 2000), but the performance of this method in deriving actual impacts measured experimentally has not been fully evaluated. In addition, reactivity estimates for the aromatic components of the higher molecular weight fractions are uncertain because they are represented in the model by lower molecular weight aromatics that may have significantly different reactivities.

Objectives and Overall Approach

The major objective of the project described in this report is to carry out, at least in part, research most needed to reduce uncertainties in ozone reactivity estimates for selected major types of coatings VOCs. After discussion with the CARB staff and an advisory group representing the coatings and solvents industries, it was decided to focus on Texaonl® and representative hydrocarbon solvents. The specific tasks that were carried out included the following:

---

[2] Texanol is a registered trademark of Eastman Chemical Company. This trade name is used throughout this report rather than the generic chemical name for simplicity.

- Develop and evaluate procedures for estimating reactivities for complex hydrocarbon mixtures for which detailed compositional data are limited. This includes an evaluation of the hydrocarbon "bin" MIR assignments incorporated in the CARB aerosol coatings regulations (Kwok et al, 2000), and developing an alternative procedure to make such estimates that can be used for other reactivity scales.
- Further develop and evaluate the "direct reactivity" measurement method initially developed for previous CARB project (Carter and Malkina, 2002) for application to coatings solvents reactivity evaluation. As discussed previously (Carter and Malkina, 2002) this method showed promise as a lower cost alternative to chamber experiments for reactivity screening and chemical mechanism evaluation, but additional development work was required before it could be useful for coatings solvents.
- Conduct environmental chamber experiments to test current model predictions of the atmospheric ozone and other impacts of Texanol®, the most important constituent of water-based coatings for which environmental chamber data have not been available. Because Texanol® has lower volatility than compounds we have studied previously, part of this project included an evaluation of methods to quantitatively inject and analyze this material in the gas phase. The Texanol® sample used for study was provided by Eastman Chemical Company.
- Conduct environmental chamber experiments to test model predictions of the atmospheric ozone and other impacts of representative hydrocarbon solvents used in architectural coatings. After discussions with the CARB staff, representatives of the coatings industry, and the American Chemistry Council (ACC)'s Hydrocarbon Panel, six different representative hydrocarbon solvents were chosen for study. The major characteristics of these solvents are listed in Table 1. The samples used were provided by members of the ACC's Hydrocarbon Panel.
- Conduct model simulations of the experiments using the current version of the SAPRC-99 chemical mechanism (Carter, 2000a) to evaluate its ability to estimate atmospheric ozone impacts of the compounds studied in the chamber experiments. This is the version of the mechanism that was used to derive the MIR scale for the CARB's aerosol coatings regulation and is sill the most current and extensively evaluated mechanism useful for detailed reactivity assessment.
- Evaluate the implications of the results as to the accuracy and uncertainties of current reactivity estimates for architectural coatings solvents and make recommendations for additional research that may be needed.

The chamber experiments were carried out in the new UCR EPA chamber, which was developed under EPA funding for more precise mechanism evaluation at lower and more atmospherically representative pollutant levels than previously possible (Carter, 2002a). Results of initial experiments carried out in this chamber, including characterization results that are applicable to this study, are given in a previous report to the CARB Carter (2004a).

The methods of procedure and results of these various tasks, and the conclusions that can be drawn from them are discussed in the various sections in the remainder of this report. Additional experiments related to atmospheric impacts architectural coatings solvents, including experiments on glycols and other solvents and data on the PM formation potentials of these materials, were carried out primarily under funding from the California Air Quality Management District. These will be discussed in a separate report that is in preparation.

Table 1. Summary of hydrocarbon solvents studied in environmental chamber experiments for this project

Designation [a]	Description	Dist Range (F)	Avg C's	Type Summary (%)			
				N-Alk	Iso-Alk	Cyc-Alk	Arom.
VMP-NAPH	VMP Naphtha	240-304	8.7	13	44	42	~0
ASTM-1C [b]	Dearomatized Alkanes, mixed, predominately C_{10}-C_{12}	315-390	10.8	14	30	56	-
ASTM-3C1	Synthetic isoparaffinic alkane mixture, predominately C_{10}-C_{12}	354-369	11.0	-	96	4	-
ASTM-1B	Reduced Aromatics Mineral Spirits	315-397	10.8	14	31	49	6
ASTM-1A	Regular mineral spirits	315-394	10.7	15	32	34	19
AROM-100	Aromatic 100	322-341	9.1	-	-	-	100

[a] Designations for these solvent samples that is used throughout this report. Note that solvents of these types from other sources may have somewhat different compositions.

[b] The ASTM designations used throughout this report are based on the D 235-02 specification (ASTM, 2003).

ESTIMATION OF HYDROCARBON SOLVENT REACTIVITIES

Introduction and Background

Hydrocarbon solvents used in coatings and other applications (e.g., “mineral spirits”, “naphtha”, etc.) are generally complex mixtures of alkanes and in some cases aromatics. We have previously shown that reactivity estimates for complex hydrocarbon mixtures can be made provided that information is available concerning the carbon number distribution, the distributions of normal, branched, and cyclic alkanes, and the amounts and types of aromatics that may be present (Carter et al, 1997, 2000, 2002). Although problems were encountered using earlier versions of the SAPRC mechanism (Carter et al, 1997), the SAPRC-99 mechanism (Carter, 2000a) was found to usually give predictions that are reasonably consistent with environmental chamber data for most of the types of complex hydrocarbon solvents that have been studied to date (Carter et al, 2000a,b; see also the “Mechanism Evaluation” section of this report). However, the type of compositional analysis required for a comprehensive reactivity evaluation requires extensive analytical information that is expensive to obtain and is not generally available for many if not most hydrocarbon solvent products.

Because of the need to derive reactivity estimates for such materials in its aerosol coatings regulations (CARB, 2000), the California Air Resources Board developed a general “Binning” procedure to estimating MIRs for hydrocarbon solvents based on their boiling point ranges, aromatic fractions, and (if available) type of alkane primarily present (Kwok et al, 2000). The bin specifications and their corresponding MIR assignments are shown on Table 2. This is an important contribution towards reducing uncertainties in reactivity estimates for these important types of VOCs. Unfortunately, the speciation data used by Kwok et al (2000) to evaluate the MIR assignments for the bins was not provided because the data used were proprietary, and the available documentation does not provide information necessary to revise the estimates should the underlying reactivity scale be modified or updated.

As part of this project we carried out an analysis of the available compositional data and other relevant information for representatives of various types of hydrocarbon solvents, and used the results to develop and evaluate a methods to estimate reactivities for hydrocarbon solvents with limited compositional information. As part of this effort we developed an alternative general method for estimating hydrocarbon solvent reactivities applicable to any incremental reactivity scale, and compare the results with the binning method developed by Kwok et al (2000). The data used, procedures, and results are described in this section.

Compositional Data Employed and Calculated Solvent Reactivity

Although the composition data used by Kwok et al (2000) to evaluate the CARB hydrocarbon bin MIR assignments on Table 2 are not available due to confidentiality concerns, we were able to obtain detailed composition analysis of a variety of hydrocarbon solvent types for use in this study. An important source was from the study of Censullo et al (2002), who conduced a detailed compositional analysis of 42 different hydrocarbon solvents, representing 19 of the 24 solvent bins on Table 2. These data were not available at the time the Kwok et al (2000) work was carried out. Another source was the hydrocarbon panel of the American Chemistry Council (Jaques, 2002), who provided carbon number distribution and hydrocarbon type information for 77 types of solvents. This is a subset of the solvents used in the Kwok et al (2000) study. In addition, the American Chemistry Council provided compositional information needed for reactivity assessment for the six hydrocarbon solvents studied in the chamber experiments for this project (Jaques, 2003, 2004; Medeiros, 2004). The solvents whose data were used in this study are

Table 2. Hydrocarbon solvent bins derived by Kwok et al (2000) for use in estimating solvent MIRs for the CARB aerosol coatings regulation.

Bin	Average Boiling Point [a] (Deg F)	Criteria	MIR
1	80-205	Alkanes (< 2% Aromatics)	2.08
2	80-205	N- & Iso-Alkanes (≥ 90% and < 2% Aromatics)	1.59
3	80-205	Cyclo-Alkanes (≥ 90% and < 2% Aromatics)	2.52
4	80-205	Alkanes (2 to < 8% Aromatics)	2.24
5	80-205	Alkanes (8 to 22% Aromatics)	2.56
6	>205-340	Alkanes (< 2% Aromatics)	1.41
7	>205-340	N- & Iso-Alkanes (≥ 90% and < 2% Aromatics)	1.17
8	>205-340	Cyclo-Alkanes (≥ 90% and < 2% Aromatics)	1.65
9	>205-340	Alkanes (2 to < 8% Aromatics)	1.62
10	>205-340	Alkanes (8 to 22% Aromatics)	2.03
11	>340-460	Alkanes (< 2% Aromatics)	0.91
12	>340-460	N- & Iso-Alkanes (≥ 90% and < 2% Aromatics)	0.81
13	>340-460	Cyclo-Alkanes (≥ 90% and < 2% Aromatics)	1.01
14	>340-460	Alkanes (2 to < 8% Aromatics)	1.21
15	>340-460	Alkanes (8 to 22% Aromatics)	1.82
16	>460-580	Alkanes (< 2% Aromatics)	0.57
17	>460-580	N- & Iso-Alkanes (≥ 90% and < 2% Aromatics)	0.51
18	>460-580	Cyclo-Alkanes (≥ 90% and < 2% Aromatics)	0.63
19	>460-580	Alkanes (2 to < 8% Aromatics)	0.88
20	>460-580	Alkanes (8 to 22% Aromatics)	1.49
21	280-290	Aromatic Content (≥98%)	7.37
22	320-350	Aromatic Content (≥98%)	7.51
23	355-420	Aromatic Content (≥98%)	8.07
24	450-535	Aromatic Content (≥98%)	5.00

[a] Average boiling point = (Initial boiling point + dry point) / 2

listed on Table 3, and the detailed speciated information [in terms of SAPRC-99 detailed model species (Carter, 2000a)] are given in Table A-1 through Table A-3 in Appendix A. The methods used to assign detailed model species from the available compositional information are discussed below.

In the cases of the solvents analyzed by Censullo et al (2002), the compositional data were given in terms of individual compounds that could be distinguished by the GC methods they employed, and for other compounds as unspeciated branched, cyclic, or unknown alkanes of given carbon numbers and unspeciated aromatics of given carbon numbers. The latter were assigned compounds as used in the speciation database that was developed for processing speciation data in emissions profiles (Carter, 2004b), and these compounds were then assigned SAPRC-99 detailed model species using the assignments incorporated in the speciation database (Carter, 2004a).

For the other solvents, the alkane fractions were given in terms of distributions of carbon numbers and distributions of alkane types (normal, branched, or cyclic). In those cases, we assumed the type

Table 3. Summary of hydrocarbon solvents whose compositional information was used in this analysis of hydrocarbon solvent reactivity.

ID	Description [a]	Source [b]	Dist Range (F)	Avg C's	Type Summary (%) N-Alk	Iso-Alk	Cyc-Alk	Arom.	MIR [c]
			CARB Bin 1						2.08
1-A	Bin 1 solvent “A”	A	151-157	6.0	64	23	13	-	1.45
1-B	Bin 1 solvent “B”	A	148-185	6.2	32	49	19	-	1.51
1-C	Bin 1 solvent “C”	A	172-210	6.6	24	28	48	-	1.61
			CARB Bin 2						1.69
2-O	Bin 2 solvent “O”	A	148-201	6.3	25	68	6	1	1.51
2-D	Bin 2 solvent “D”	A	194-206	7.0	19	73	8	0	1.58
2-A	Bin 2 solvent “A”	A	150-159	6.0	50	49	1	-	1.48
2-B	Bin 2 solvent “B”	A	200-210	7.1	30	63	7	-	1.53
2-C	Bin 2 solvent “C”	A	142-170	6.1	29	62	9	-	1.50
2-E	Bin 2 solvent “E”	A	82-97	5.0	80	20	-	-	1.56
2-F	Bin 2 solvent “F”	A	95-140	5.2	73	26	1	-	1.55
2-G	Bin 2 solvent “G”	A	123-150	6.0	1	99	-	-	1.52
2-H	Bin 2 solvent “H”	A	151-157	6.0	83	8	9	-	1.44
2-I	Bin 2 solvent “I”	A	133-155	6.0	45	55	-	-	1.48
2-J	Bin 2 solvent “J”	A	190-210	7.0	7	91	2	-	1.60
2-K	Bin 2 solvent “K”	A	190-218	7.7	-	100	-	-	1.57
2-L	Bin 2 solvent “L”	A	140-145	6.0	4	95	1	-	1.52
2-M	Bin 2 solvent “M”	A	151-156	6.1	52	47	1	-	1.47
2-N	Bin 2 solvent “N”	A	151-156	6.0	48	45	7	-	1.47
			CARB Bin 3						2.52
3-B	Bin 3 solvent “B”	A	209-237	7.0	5	2	93	0	1.92
3-A	Bin 3 solvent “A”	A	174-180	6.2	-	13	87	-	1.51
			CARB Bin 4						2.24
4-A	Bin 4 solvent “A”	A	195-210	7.0	26	69	2	3	1.60
CP05	Lactol Spirits	B	185-220	7.3	8	29	56	7	1.85
			CARB Bin 5						2.56
5-A	Bin 5 solvent “A”	A	151-218	6.5	-	88	2	10	1.62
			CARB Bin 6						1.41
6-G	Bin 6 solvent “G”	A	247-282	8.3	14	20	65	1	1.54
6-F	Bin 6 solvent “F”	A	209-230	7.3	20	16	64	0	1.72
6-A	Bin 6 solvent “A”	A	317-347	10.1	-	47	53	0	1.14
6-B	Bin 6 solvent “B”	A	312-356	9.8	17	25	58	-	1.17
6-C	Bin 6 solvent “C”	A	265-290	8.6	19	18	63	-	1.45
6-D	Bin 6 solvent “D”	A	241-292	8.2	18	27	55	-	1.50
6-E	Bin 6 solvent “E”	A	317-351	10.3	19	30	51	-	1.04
CP04	VM&P naphtha HT	B	240-285	8.3	19	34	47	-	1.39
CP14	VM&P Naphtha	B	244-287	8.3	20	32	47	1	1.46
CP23	VM&P Naphtha	B	260-288	8.5	9	25	66	1	1.53
CP24	VM&P Naphtha	B	244-287	8.4	9	24	66	1	1.54
CP29	aliphatic petroleum distillates	B	285-335	9.3	18	34	47	0	1.26
CP43	Mineral spirits	B	300-365	10.0	27	47	26	-	1.03
VMP-NAPH	VMP Naphtha	C	240-304	8.7	13	44	42	0	1.38
			CARB Bin 7						1.17
7-A	Bin 7 solvent “A”	A	201-210	7.1	35	62	3	-	1.49

Table 3 (continued)

ID	Description [a]	Source [b]	Dist Range (F)	Avg C's	Type Summary (%) N-Alk	Iso-Alk	Cyc-Alk	Arom.	MIR [c]
7-B	Bin 7 solvent “B”	A	320-349	10.2	-	97	3	-	1.02
7-C	Bin 7 solvent “C”	A	250-320	9.2	-	100	-	-	1.20
7-D	Bin 7 solvent “D”	A	320-332	10.0	-	100	-	-	1.06
7-E	Bin 7 solvent “E”	A	204-218	8.0	-	100	-	-	1.55
CP38	isoparaffinic hydrocarbon	B	320-351	10.7	-	100	-	-	[d]
			CARB Bin 8						1.65
8-A	Bin 8 solvent “A”	A	280-328	9.1	-	-	100	-	1.49
			CARB Bin 9						1.62
CP28	light naphtha solvent	B	195-225	7.5	23	40	35	2	1.59
9-A	Bin 9 solvent “A”	A	240-250	8.0	27	33	37	3	1.58
9-B	Bin 9 solvent “B”	A	158-270	6.7	28	41	28	3	1.53
CP12	Mineral Spirits	B	300-365	10.0	24	33	40	3	1.28
CP11	Mineral Spirits	B	300-365	9.9	20	30	47	3	1.29
CP30	VM&P naphtha	B	240-285	8.5	22	43	28	6	1.72
			CARB Bin 10						2.03
10-B	Bin 10 solvent “B”	A	207-242	7.3	17	28	47	8	1.81
CP35	VM&P naphtha	B	247-282	8.4	17	29	45	10	2.01
10-A	Bin 10 solvent “A”	A	202-222	7.1	20	27	38	15	1.98
10-C	Bin 10 solvent “C”	A	316-350	9.3	18	31	33	18	2.14
CP01	VM&P naphtha	B	240-305	8.4	37	28	13	23	2.70
			CARB Bin 11						0.91
11-B	Bin 11 solvent “B”	A	374-405	11.5	22	21	57	0	0.85
11-I	Bin 11 solvent “I”	A	370-485	12.0	2	43	55	0	0.86
11-K	Bin 11 solvent “K”	A	395-445	11.8	2	43	55	0	0.88
11-L	Bin 11 solvent “L”	A	415-450	12.6	2	58	40	0	0.76
11-J	Bin 11 solvent “J”	A	380-410	10.9	2	28	70	0	1.00
11-A	Bin 11 solvent “A”	A	380-410	10.9	24	12	64	-	0.94
11-C	Bin 11 solvent “C”	A	315-390	9.9	18	24	58	-	1.16
11-D	Bin 11 solvent “D”	A	324-394	10.8	14	29	57	-	0.98
11-E	Bin 11 solvent “E”	A	370-408	11.9	20	29	51	-	0.80
11-F	Bin 11 solvent “F”	A	383-419	11.9	22	24	54	-	0.80
11-G	Bin 11 solvent “G”	A	408-453	12.7	22	32	46	-	0.73
11-H	Bin 11 solvent “H”	A	370-405	11.5	-	89	11	-	0.82
CP16	aliphatic petroleum distillates	B	351-415	11.3	31	42	27	-	0.85
CP18	aliphatic petroleum distillates	B	312-387	11.3	30	43	27	-	0.85
CP33	Mineral Spirits	B	324-402	10.4	24	42	34	1	1.06
ASTM-1C	Low aromatic mineral spirits	D	315-390	10.8	14	30	56	-	0.98
			CARB Bin 12						0.81
12-A	Bin 12 solvent “A”	A	357-408	11.5	-	100	-	-	0.81
12-B	Bin 12 solvent “B”	A	388-459	12.2	-	100	-	-	0.76
12-C	Bin 12 solvent “C”	A	434-472	13.3	-	100	-	-	0.68
12-D	Bin 12 solvent “D”	A	355-400	11.8	-	100	-	-	0.79
12-E	Bin 12 solvent “E”	A	352-370	11.0	-	96	4	-	0.87
12-F	Bin 12 solvent “F”	A	354-385	11.5	-	97	3	-	0.82
12-G	Bin 12 solvent “G”	A	372-426	11.5	99	1	-	-	0.69
12-H	Bin 12 solvent “H”	A	432-469	13.2	99	1	-	-	0.59
ASTM-3C1	Synthetic isoparaffinic hydrocarbon	D	354-369	11.0	-	96	4	-	0.87

Table 3 (continued)

ID	Description [a]	Source [b]	Dist Range (F)	Avg C's	Type Summary (%) N-Alk	Iso-Alk	Cyc-Alk	Arom.	MIR [c]
		CARB Bin 14							1.21
CP03	Light HC solvent	B	379-405	11.6	4	54	40	2	0.94
14-C	Bin 14 solvent “C”	A	370-408	11.6	23	26	46	5	1.17
15-F	“Bin 15” solvent “F” [e]	A	320-396	10.4	19	30	46	5	1.40
15-D	“Bin 15” solvent “D” [e]	A	320-398	10.8	15	30	49	6	1.40
ASTM-1B	Mineral Spirits 75	D,E	315-397	10.8	14	31	49	6	1.31
14-A	Bin 14 solvent “A”	A	315-400	10.1	34	19	40	7	1.42
		CARB Bin 15							1.82
CP06	Mineral Spirits	B	324-402	10.2	10	33	47	10	1.71
CP20	Stoddard Solvent	B	312-387	10.1	10	31	49	10	1.77
CP25	Mineral Spirits	B	318-380	10.2	11	32	47	11	1.80
CP10	Mineral Spirits	B	307-389	10.1	9	31	49	11	1.80
15-G	Bin 15 solvent “G”	A	370-510	12.0	2	43	42	13	1.70
CP26	Mineral Spirits	B	307-389	10.1	10	26	48	15	1.98
CP15	aliphatic petroleum distillates	B	351-415	10.1	13	27	44	15	1.92
15-A	Bin 15 solvent “A”	A	315-410	10.4	31	18	35	16	1.88
15-E	Bin 15 solvent “E”	A	370-406	11.6	23	25	36	16	1.90
14-B	“Bin 14” solvent “B” [e]	A	316-399	9.4	20	29	34	17	2.37
CP02	300-66 solvent, Mineral Spirits 66	B	310-400	9.9	21	32	30	17	2.20
CP39	paraffinic petroleum distillate	B	315-397	9.9	21	29	32	18	2.18
15-C	Bin 15 solvent “C”	A	316-399	10.7	16	31	34	19	2.32
ASTM-1A	Regular mineral spirits	D,E	315-394	10.7	15	32	34	19	2.03
		CARB Bin 16							0.57
16-A	Bin 16 solvent “A”	A	482-514	14.8	21	33	45	1	0.66
16-D	Bin 16 solvent “D”	A	460-525	14.4	2	63	35	0	0.65
16-E	Bin 16 solvent “E”	A	465-530	14.4	22	50	28	0	0.62
16-B	Bin 16 solvent “B”	A	540-593	17.1	18	21	61	-	0.52
16-C	Bin 16 solvent “C”	A	522-592	16.8	-	54	46	-	0.53
		CARB Bin 17							0.51
17-A	Bin 17 solvent “A”	A	451-536	14.0	-	100	-	-	0.64
17-B	Bin 17 solvent “B”	A	480-525	14.9	99	1	-	-	0.53
17-C	Bin 17 solvent “C”	A	489-541	14.5	97	2	2	-	0.55
		CARB Bin 21							7.37
CP19	Xylene	B	280-286	0.1	-	-	-	100	7.51
CP27	Xylene	B	280-286	0.0	-	-	-	100	7.48
CP34	Xylene	B	280-286	0.0	-	-	-	100	7.55
CP40	Xylene	B	280-286	8.0	-	-	-	100	7.50
CP41	Xylene	B	280-286	0.1	-	-	-	100	7.34
		CARB Bin 22							7.51
CP07	Aromatic 100	B	320-348	9.1	-	-	-	100	7.61
CP13	Aromatic 100	B	320-348	9.1	0	0	0	100	7.55
CP21	Aromatic 100	B	320-348	9.1	-	0	-	100	7.48
CP31	Aromatic 100	B	320-348	9.0	-	-	-	100	7.53
CP36	Aromatic 100	B	320-348	9.1	-	-	-	100	7.62
CP42	Aromatic 100	B	320-348	9.1	-	-	-	100	7.70
AROM-100	Aromatic 100	C	322-341	9.1	-	-	-	100	7.45

Table 3 (continued)

ID	Description [a]	Source [b]	Dist Range (F)	Avg C's	Type Summary (%) N-Alk	Iso-Alk	Cyc-Alk	Arom.	MIR [c]
			CARB Bin 23						8.07
CP08	Aromatic 150	B	343-407	10.0	-	-	-	100	7.16
CP17	Aromatic 150	B	343-407	10.1	-	-	0	100	7.67
CP22	Aromatic 150	B	343-407	10.0	-	-	-	100	7.62
CP32	Aromatic 150	B	343-407	10.0	-	0	-	100	7.17
CP37	Aromatic 150	B	343-407	10.1	-	-	-	100	7.33

[a] Description that was provided with the solvent or (for ASTM-3C1) from its MSDS sheet. Entries that are underlined are solvents that were studied in chamber experiments for this project.

[b] Source codes for compositional information are as follows: (A) Jaques (2002); (B) Censullo et al (2002); (C) Jaques (2003); (D) Jaques (2004); (E) aromatic fraction composition provided by Medeiros (2004). For solvents with codes "D" the boiling point ranges were taken from the MSDS sheet provided with the samples, and are considered to be approximate.

[c] Incremental reactivity in the SAPRC-99 MIR scale, in units of grams O_3 per gram solvent, calculated using the available compositional data or assigned to the bin (Table 2)

[d] The detailed compositional information was not included in Censullo et al (2002) report, so its MIR could not be calculated using available compositional information.

[e] The bin assignment indicated in the ACC designation was not consistent with the reported aromatic content. The bin assignment was modified to be consistent with Table 1.

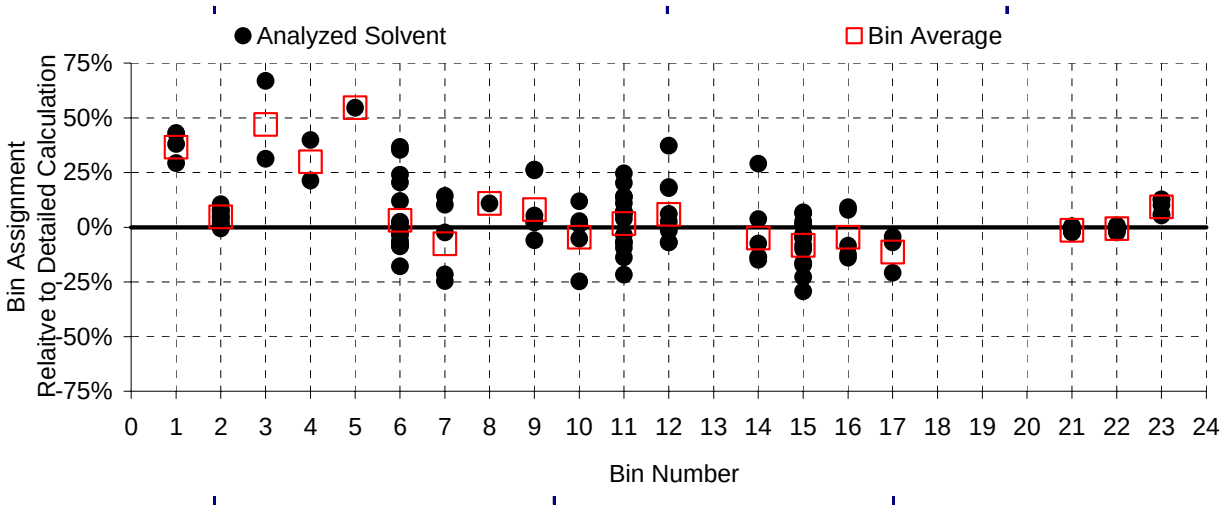

Figure 1. Plots of differences between CARB bin MIRs and explicitly calculated SAPRC-99 MIRs for the hydrocarbon solvents for which compositional data were provided.

distributions were the same for each carbon number, allowing us to assign the alkane fractions to distributions of detailed model species such as N-Cn, BR-Cn, CYC-Cn, for normal, branched, and cyclic alkanes of carbon number "n". The generic branched and cyclic alkane model species are represented in the model using mechanism of individual compounds chosen to be representative of the categories, as indicated in Table 14 in the "Modeling Methods" section, below.

The level of detail for which aromatic compositional information was available was not the same for all the solvents in this dataset. The greatest detail was available for the solvents analyzed by Censullo et al (2002) and the Aromatic-100, VMP Naphtha (Jaques, 2003) and ASTM-1A (Medeiros, 2004) solvents studied in our experiments. Therefore, these solvents were used as the basis for estimating compositions of aromatics fractions, as described in the following sections. These were assigned detailed model species for the individual compounds. The unspeciated aromatics (which had relatively minor contributions in the case of these solvents) were assigned model species using the speciation database assignments (Carter, 2004b) for the solvents studied by Censullo et al (2002) or using the generic aromatic model species listed in Table 14, below, for the other sol vents.

In the cases of the solvents whose compositions were provided by Jaques (2002), the detailed speciated information for the aromatics was not provided, but the totals were given for mono-, di-, and tri+- substituted benzenes, for the various carbon numbers. These were assigned SAPRC-99 detailed model species representing the various types of compounds, which in turn are represented by individual by individual compounds as indicated on Table 14 in the "Modeling Methods" section, below.

Table 3 also gives the incremental reactivities in the SAPRC-99 MIR scale (Carter, 2000a, 2003a) calculated from the compositional data provided with the solvents and the tabulated MIR's of the constituents (Carter, 2000a), and Figure 1 shows the relative differences between these calculated MIR's and those derived from the bin assignments on Table 2. It can be seen that the bin assignments of Kwok et al (2000) perform reasonably well for the primarily alkane solvent bins 2 and 6-17 and for the aromatic bins 21-23, predicting most to within ±25% and all to within ±50%, and having relatively little overall bias. On the other hand, the CARB bin assignments for the lighter hydrocarbon bins 1 and 3-5, tend to be higher than the calculated results by ~25-50%, due to assumption regarding hydrocarbon solvents with higher content of more reactive cycloalkanes. There are no data available to evaluate the CARB MIR assignments for bins 13, 18-20 and 24.

Derivation of Reactivity Estimates with Limited Compositional Information

In the following sections, we will discuss an alternative method to derive reactivity estimates for hydrocarbon solvents for which the only information available is that needed to make the bin assignments as shown on Table 2. This can serve as an additional evaluation of the existing bin assignments, and provide a means to make bin assignments for other or updated reactivity scales. The general procedure involves (1) deriving carbon number distributions from boiling point data; (2) deriving estimated aromatic compositions given the aromatic carbon number distributions, and (3) applying a standard general methodology for reactivity estimates, as discussed in the following sections. Following a discussion of the procedures and the data used to derive them, we give a comparison of how the results of this method compare with the reactivities derived using the detailed compositional data for the solvents listed on Table 3, and with the CARB bin MIR assignments shown on Table 2.

Derivation of Carbon Number Distributions from Boiling Point Data

In order to derive reactivity estimates from boiling point information, it is necessary to first to derive estimates of carbon number distributions from the boiling point ranges. For this purpose, we

Table 4. Boiling points and carbon numbers for compounds used to derive carbon number from boiling point estimates.

Compound	nC	Bp (C)	Compound	nC	Bp (C)
n-Alkanes			Cycloalkanes		
n-Pentane	5	36.0	Cyclohexane	6	80.7
n-Hexane	6	68.7	Isopropyl Cyclopropane	6	58.3
n-Heptane	7	98.5	Methylcyclopentane	6	71.8
n-Octane	8	125.6	Ethyl Cyclopentane	7	103.5
n-Nonane	9	150.8	Methylcyclohexane	7	100.9
n-Decane	10	174.1	1,3-Dimethyl Cyclohexane	8	122.5
n-Undecane	11	195.9	Ethylcyclohexane	8	131.9
n-Dodecane	12	216.3	Propyl Cyclopentane	8	131.0
n-Tridecane	13	235.4	1,1,3-Trimethyl Cyclohexane	9	136.6
n-Tetradecane	14	253.5	Propyl Cyclohexane	9	156.7
n-Pentadecane	15	270.6	1-Methyl-3-Isopropyl Cyclohexane	10	166.5
n-C16	16	286.8	Butyl Cyclohexane	10	180.9
n-C17	17	302.0	Pentyl Cyclohexane	11	203.7
n-C18	18	316.3	Hexyl Cyclohexane	12	224.0
n-C19	19	329.9	Heptyl Cyclohexane	13	244.0
n-C20	20	343.0	Octyl Cyclohexane	14	264.0
n-C21	21	356.5	Nonyl Cyclohexane	15	282.0
n-C22	22	368.6	Decyl Cyclohexane	16	299.0
Branched Alkanes			Aromatics (≤ 3 Constituents)		
2,2-Dimethyl Butane	6	49.7	Benzene	6	80.1
2,3-Dimethyl Butane	6	57.9	Toluene	7	110.6
2-Methyl Pentane	6	60.2	Ethyl Benzene	8	136.2
3-Methylpentane	6	63.2	Isopropyl Benzene (cumene)	9	151.0
2,2,3-Trimethyl Butane	7	80.8	n-Propyl Benzene	9	159.0
2,2-Dimethyl Pentane	7	79.2	tert-Butylbenzene	10	169.0
2,3-Dimethyl Pentane	7	89.7	Isobutylbenzene	10	173.0
2,4-Dimethyl Pentane	7	80.4	s-Butyl Benzene	10	173.0
2-Methyl Hexane	7	90.0	butyl benzene	10	183.0
3,3-Dimethyl Pentane	7	86.0	n-Butyl Benzene	10	183.0
3-Methyl Hexane	7	91.0	n-Hexylbenzene	12	226.0
2,2,3,3-Tetramethyl Butane	8	106.4	p-Xylene	8	138.3
2,2,4-Trimethyl Pentane	8	99.2	m-Xylene	8	139.1
2,2-Dimethyl Hexane	8	106.8	o-Xylene	8	144.0
2,3,4-Trimethyl Pentane	8	113.5	4-Ethyltoluene	9	162.0
2,3-Dimethyl Hexane	8	115.6	2-Ethyltoluene	9	164.5
2,4-Dimethyl Hexane	8	109.5	Cymene	10	177.0
2,5-Dimethyl Hexane	8	109.1	o-Cymene	10	178.0
2-Methyl Heptane	8	117.6	m-Diethyl benzene	10	181.0
3-Methyl Heptane	8	118.0	1-Methyl-3-propylbenzene	10	182.0
4-Methyl Heptane	8	117.7	p-Diethylbenzene	10	184.0
2,2,5-Trimethyl Hexane	9	124.0	p-tert-butyl toluene	11	192.8
2,3,5-Trimethyl Hexane	9	131.4	1-Ethyl-3-propylbenzene	11	201.0
2,4-Dimethyl Heptane	9	132.9	1-Ethyl-2-propylbenzene	11	203.0
2-Methyl Octane	9	143.2	1-Methyl-3-butylbenzene	11	205.0

Table 4 (continued)

Compound	nC	Bp (C)	Compound	nC	Bp (C)
Branched Alkanes (continued)			Aromatics (≤ 3 Constituents) (continued)		
3,3-Diethyl Pentane	9	146.3	Pentyl Benzene	11	205.0
3,5-Dimethyl Heptane	9	136.0	1,3-Di-iso-propylbenzene	12	203.0
4-Ethyl Heptane	9	141.2	1,3,5-Trimethyl Benzene	9	165.0
4-Methyl Octane	9	142.4	1,2,4-Trimethyl Benzene	9	169.0
2,4-Dimethyl Octane	10	156.0	1,2,3-Trimethyl Benzene	9	175.0
2,6-Dimethyl Octane	10	160.4	1,2-Dimethyl-3-isopropylbenzene	11	203.0
2-Methyl Nonane	10	167.1	tert-butyl-m-xylene	12	205.5
3,4-Diethyl Hexane	10	163.9	Triethylbenzenes	12	217.0
3-Methyl Nonane	10	167.9			
4-Methyl Nonane	10	165.7	Aromatics (4+ Substituents)		
4-Propyl Heptane	10	157.5	1,2,4,5-Tetramethylbenzene	10	134.2
2,4,6-Trimethyl Heptane	10	147.6	1,2,3,5-Tetramethylbenzene	10	134.2
3-Methyl Decane	11	188.1	1,2,3,4-Tetramethylbenzene	10	134.2
4-Methyl Decane	11	187.0	Pentamethylbenzene	11	148.2
			hexamethylbenzene	12	162.3

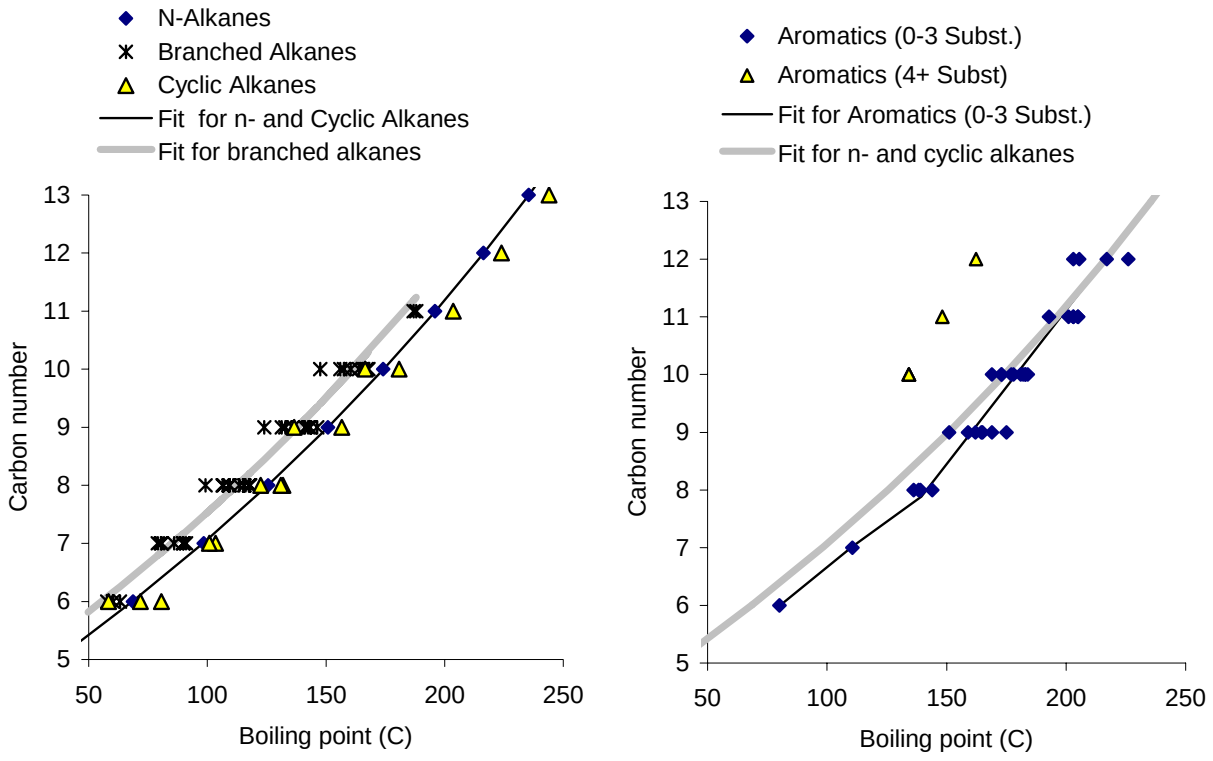

Figure 2. Plots of carbon numbers against boiling points for various alkanes and aromatic hydrocarbons.

assume that the relationship between boiling points and carbon numbers for mixtures can be approximate by those for pure compounds. Although this is not strictly speaking valid, we assume that the error introduced by making this approximation is not large compared to the other uncertainties in making reactivity estimates for unspeciated aromatics. However, we have not evaluated the magnitude of possible errors or biases introduced into the reactivity estimates resulting from use of this approximation.

Table 4 lists the compounds that were used as the basis for the carbon number-from-boiling point estimates derived in this work. Most of the data for the alkanes were taken from the physical properties data available at the Syracuse Research Corporation website (at http://www.syrres.com/esc/physdemo .htm), while most of the data for the aromatics were taken from the ChemFinder website at http://chemfinder.cambridgesoft.com. The carbon numbers are plotted against boiling points on Figure 2.

As might be expected, the data for the normal alkanes all fall on a smooth curve, which is well fit by the equation:

$$nC\ (\text{normal alkanes}) = 3.95 + 2.81\ (Bp/100) + 0.21\ (Bp/100)^2 + 0.096\ (Bp/100)^3 \qquad \text{(I)}$$

where nC is the carbon number and Bp is the boiling point in ^oC. The data for the branched alkanes are more scattered, but can be approximately fit by Equation (I) if the boiling point is increased by 13^oC, i.e,

$$nC\ (\text{branched alkanes}) = 3.95 + 2.81\ [(Bp+13)/100] + 0.21\ [(Bp+13)/100]^2 + 0.096\ [(Bp+13)/100]^3 \qquad \text{(II)}$$

The cycloalkane data are also scattered, but in this case there does not appear to be a consistent tendency to be higher or lower than n-alkanes. Therefore, for the purpose of our estimates, we also use Equation (I) to estimate carbon numbers from boiling points for cycloalkanes. The carbon numbers predicted using this method are shown on Figure 2.

In the case of the aromatics, the boiling points for the benzene and the alkylbenzenes with 1-3 substituents are not greatly different from the trends predicted for the n-alkanes, but the data for the alkylbenzenes with more substituents are quite different. However, most of the alkylbenzenes in the hydrocarbon mixtures whose data we use in this study have 3 or fewer substituents, so the data for these compounds are used for estimation purposes. Although Equation (I) would not do a bad job of estimating carbon numbers for these compounds, somewhat better fits are obtained using:

$$\begin{aligned} nC\ (\text{aromatics}) &= 3.3 + 0.03372\ Bp\ (\text{for } Bp \le 144.85^oC) \\ &= 0.4 + 0.05337\ Bp\ (\text{for } Bp > 144.85^oC) \end{aligned} \qquad \text{(III)}$$

where nC is the carbon number and Bp is the boiling point in ^oC. The carbon numbers predicted using this method are shown on Figure 2, where the fit using Equation (I) is shown for comparison.

Of course, the above equations would usually predict non-integer carbon numbers for a given boiling point. This is obviously possible when considering mixtures of compounds with different carbon numbers, and would correspond to the average carbon number of the mixture. For estimation purposes, we treat this as a mixture of compounds with the two carbon numbers surrounding the average, with relative weights derived to correspond to the average. Thus if the carbon number derived by the above equations is nC_{avg}, and if nC_1 is the largest integer $\le nC_{avg}$, and if $nC_2=nC_1+1$, then the assumed carbon number distribution corresponding to nC_{avg} is given by

$$\begin{aligned} \text{Fraction } (nC_1) &= 1 - (nC_{avg}-nC_1) \\ \text{Fraction } (nC_2) &= nC_{avg}-nC_1 \end{aligned} \qquad \text{(IV)}$$

Actual mixtures may in general have wider distributions of carbon numbers than predicted using Equation (IV). However, for estimation purposes the effects of broader distributions of carbon numbers is taken

into account by varying the boiling point temperature used to derive the carbon numbers, as described in the “Derivation of Reactivity Estimates” section, below.

Estimation of Compositions of Aromatic Fractions

Aromatics are highly reactive constituents of many types of hydrocarbon solvents, and, as indicated on Table 2, even relatively small fractions of aromatics can significantly affect estimated reactivities. Reactivities of aromatic compounds vary considerably from compound to compound, depending not only the number of substituents around the aromatic ring, but also on the varying from isomer to isomer (Carter, 2000a, and references therein). Therefore, it is important to assume an appropriate composition for the aromatic fraction of hydrocarbon solvents with non-negligible aromatic content in order to appropriately estimate their reactivities. The best approach is obviously to use a speciated analysis of the aromatics for reactivity estimation purposes. Because this analysis is usually not available, in this section we discuss the derivation of a “typical” aromatic composition for the purpose of reactivity estimates. The level of uncertainty in such estimates will depend on the degree of variability of reactivities of aromatic fractions of hydrocarbon solvents in general, which is also discussed below.

Table 5 lists the aromatic compounds identified in the hydrocarbon solvents that had non-negligible aromatic content and speciated aromatic information, and gives the average contributions of each to aromatics with the same carbon number. The current SAPRC-99 MIR values (Carter, 2000a, 2003a) for these compounds are also given on the table, indicating the variability of the reactivities of the compounds. Figure 3 shows the distributions of MIR's for the aromatic fractions for the various carbon numbers, and also indicates the solvents used to derive the distributions shown on the figure and the averages on Table 5. (The detailed speciated data for the various solvents used are given in Table A-1 and Table A-2 in Appendix A.) The standard deviations of the averages on Table 5 indicate that there is relatively wide variability in the compositions, but Figure 3 shows that the variabilities of the MIRs of the aromatics with the given carbon numbers are relatively small.

The relatively small variability in the calculated MIR's for the aromatic fractions with the various carbon numbers suggests that reactivity estimates based on the average compositions shown on Table 5 may give reasonably good approximations to those derived from detailed speciated information. In this case, the only information required is the total aromatic content and the carbon number distributions of the aromatic fractions. The latter can be estimated from the boiling point ranges of the solvents as discussed in the following section.

Derivation of Reactivity Estimates

In this section, we describe the general procedures for deriving reactivity estimates for hydrocarbon solvents given only the information required to make the CARB bin assignments as indicated on Table 2. This is implemented in a spreadsheet HCcalc.xls, which is distributed with this report (Carter and Malkina, 2005), and is discussed further in this section. The specific input requirements are as follows:

- The designation of the reactivity scale. The current version of HCcalc.xls has data needed to calculate reactivities in the SAPRC-99 MIR, MOIR, and EBIR scales (Carter, 2000a, 2003a), but data for other reactivity scales can be added as discussed below.
- The weight fractions of normal, branched, and cyclic alkanes and the weight fraction of aromatics. The current procedure does not support mixtures with significant quantities of other types of compounds. These fractions must be normalized to 100%, so if there are other types of compounds or unknowns these need to be distributed among the four supported categories as

Table 5. List of C_8 - C_{11} aromatic compounds identified in the hydrocarbon solvents used in this study for aromatic fraction analysis, and average contributions of the compounds to the total aromatics with the same carbon number.

Description	Detailed Model Species	nC	Contribution to carbon number		MIR
			Average	StDev	
o-Xylene	O-XYLENE	8	41.8%	31.7%	7.48
m-Xylene	M-XYLENE	8	34.5%	19.1%	10.61
p-Xylene	P-XYLENE	8	13.0%	7.2%	4.24
Ethyl Benzene	C2-BENZ	8	10.7%	6.9%	2.79
1,2,4-Trimethyl Benzene	124-TMB	9	29.5%	11.3%	7.18
1,2,3-Trimethyl Benzene	123-TMB	9	16.3%	8.9%	11.25
m-Ethyl Toluene	M-ET-TOL	9	14.7%	6.2%	9.37
1,3,5-Trimethyl Benzene	135-TMB	9	10.3%	3.8%	11.22
p-Ethyl Toluene	P-ET-TOL	9	7.7%	3.2%	3.75
o-Ethyl Toluene	O-ET-TOL	9	7.6%	8.7%	6.61
n-Propyl Benzene	N-C3-BEN	9	5.5%	3.4%	2.20
Indan	INDAN	9	5.0%	5.7%	3.16
Isopropyl Benzene	I-C3-BEN	9	3.5%	4.7%	2.32
C10 Trisubstituted Benzenes	C10-BEN3	10	35.4%	7.5%	8.86
C10 Disubstituted Benzenes	C10-BEN2	10	23.4%	11.3%	5.92
C10 Tetrasubstituted Benzenes	C10-BEN4	10	9.0%	5.1%	8.86
Methyl Indans	ME-INDAN	10	7.3%	5.9%	2.83
1,2,3,5 Tetramethyl Benzene	1235MBEN	10	6.9%	5.0%	8.25
m-Diethyl Benzene	M-DE-BEN	10	4.6%	2.4%	8.39
C10 Monosubstituted Benzenes	C10-BEN1	10	3.3%	2.8%	1.97
p-Diethyl Benzene	P-DE-BEN	10	2.8%	3.7%	3.36
n-Butyl Benzene	N-C4-BEN	10	2.7%	3.5%	1.97
Naphthalene	NAPHTHAL	10	2.7%	2.9%	3.26
o-Diethyl Benzene	O-DE-BEN	10	1.4%	2.6%	5.92
Tetralin	TETRALIN	10	0.2%	0.3%	2.83
s-Butyl Benzene	S-C4-BEN	10	0.2%	0.5%	1.97
C11 Trisubstituted Benzenes	C11-BEN3	11	47.5%	3.8%	8.02
C11 Tetrasubstituted Benzenes	C11-BEN4	11	23.9%	1.2%	8.02
C11 Tetralin or Indane	C11-TET	11	9.6%	2.6%	2.55
C11 Disubstituted Benzenes	C11-BEN2	11	7.3%	1.2%	5.35
2-Methyl Naphthalene	2ME-NAPH	11	4.5%	1.0%	4.61
C11 Pentasubstituted Benzenes	C11-BEN5	11	3.8%	1.7%	8.02
C11 Monosubstituted Benzenes	C11-BEN1	11	2.5%	0.5%	1.78
1-Methyl Naphthalene	1ME-NAPH	11	1.0%	0.3%	4.61

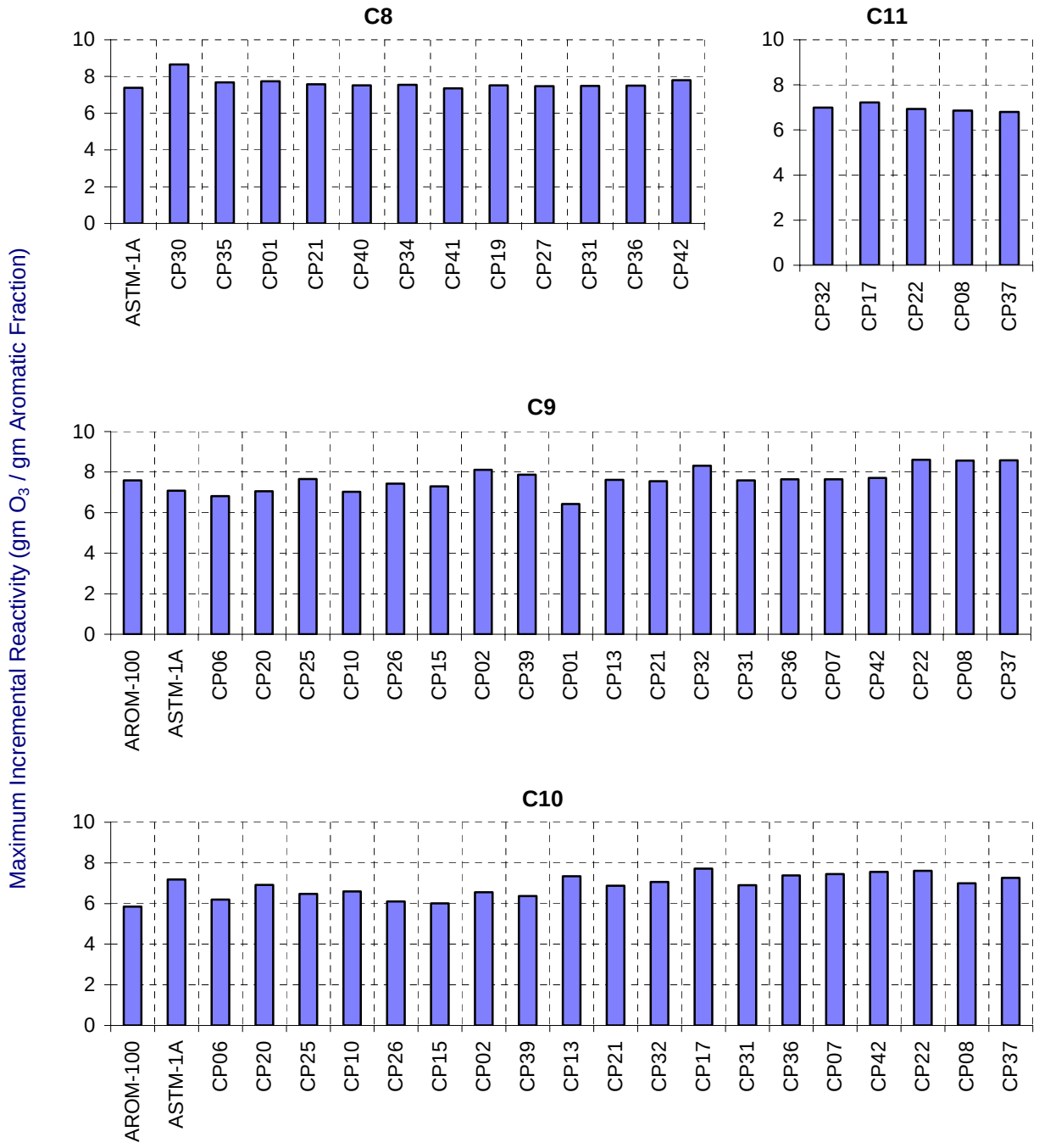

Figure 3. Distributions of Calculated SAPRC-99 Maximum Incremental Reactivities for aromatic constituents with a given carbon number for the hydrocarbon solvents with aromatic speciation data and non-negligible aromatic constituents with those carbon numbers.

appropriate. (For example, if small amounts of olefins are present it is probably best to lump these with the aromatics, whose reactivities are closer to olefins than alkanes.)

- The minimum and maximum boiling point range and the average or main boiling point, in ^{o}C or ^{o}F. The "average" could either be the average of the minimum and maximum (as it is in the examples shown in this work) or it could be chosen to be representative of the central temperature where most of the material boils.

The boiling point range is used to derive the carbon number distributions for normal, branched, and cyclic alkanes and for aromatics using Equations (I), (II), (I), or (III), respectively, with fractional carbon numbers apportioned distributions of integer carbon numbers as indicated in Equation (IV), above. The width of the carbon number distribution is approximated as follows

$$\text{Fraction in solvent with carbon number n} = 0.5 \times \text{Fraction with carbon number n calculated for } T_{avg} + 0.25 \times \text{Fraction with carbon number n calculated for } (T_{avg}+T_{max})/2 + 0.25 \times \text{Fraction with carbon number n calculated for } (T_{avg}+T_{min})/2 \qquad \text{(V)}$$

where Tavg, Tmax, and Tmin are the average, minimum, and maximum for the boiling point range, and the fractions with the given carbon number are calculated separately for normal, branched, and cyclic alkanes and for aromatics using the appropriate equation as indicated above.

For low boiling point aromatic solvents it is assumed that the minimum aromatic carbon number is 6.5, which corresponds to a mixture of equal mass fractions of benzene and toluene. This tends to give predictions that are more consistent with the limited available compositional analysis of the solvents of this type. For alkanes, it is assumed that the minimum carbon number is 5, since this approach is not designed for gaseous or very low boiling point hydrocarbon mixtures.

This procedure, combined with the given total weight fractions for the various constituent types, gives derived compositions of the mixtures in terms of normal, branched, and cyclic alkanes and aromatics for each carbon number. These various types of constituents are assigned to SAPRC detailed model species as follows:

- Normal alkanes with a given carbon number refer to a single compound, such as n-hexane (N-C6), etc.
- Branched alkanes or cyclic alkanes with a given carbon number are represented by the generic branched or cyclic alkane model species BR-Cn, or CYC-Cn, where n is the carbon number. The only exception is cycloalkanes with 5 carbons, which are represented by cyclopentane (CYCC5) explicitly. The specific compounds used to calculate the reactivities of these generic model species are shown in Table 14 in the "Modeling Methods" section of this report.
- C_6 and C_7 aromatics are assigned to benzene and toluene, respectively. C_9-C_{11} aromatics are assigned to the mixture of compounds given for the corresponding carbon number on Table 5, based on the analysis of aromatic constituents in the analyzed hydrocarbon solvents samples as discussed above. C_{12+} aromatics are assumed to have the same per-molecule reactivity as assigned for C_{11} aromatics, i.e., their reactivities are derived from those of the C_{11} aromatic mixture on Table 5 times the molecular weight for C_{11} alkylbenzenes, divided by that for the C_{12+} alkylbenzenes.

The Excel spreadsheet HCcalc.xls implements these procedures as discussed below. The sheet "React'y Calc" is the main sheet where the calculations are carried out, with the cells in red font containing the input data (scale designation, weight fractions of the hydrocarbon types, and average,

minimum, and maximum boiling point ranges in ^{o}C), and the cell labeled "AlkRct" having the calculated reactivity value. The formulas in that sheet can be examined to determine the specifics of how the mixture reactivity is calculated. (Blue font is used to indicate cells with formulas.) The sheet "Reactivity Scales" has the incremental reactivity data for all the detailed model species used for the SAPRC-99 MIR, MOIR, and EBIR reactivity scales (Carter, 2000a, 2003a). Additional columns can be added to give reactivity data for other scales, to permit calculations of hydrocarbon reactivities using those scales. The data for the MIR and other scales can be updated as scales are updated and modified.

The sheet "Calculation Summary" and macros included in the workbook can be used to readily calculate reactivities of various solvents given the required input data. (Note that the macros only copy input data to the "React'y Calc" sheet and copy the results back; they do not do any calculations other than converting temperature units if needed.) The first column gives an ID code for the solvent, which is ignored by the macros, and the next 9 columns give the input data that are needed to calculate the reactivities. These input data are copied to the appropriate cells in the "React'y calc" sheet when the macro is executed, and the macro then copies the reactivity result from the "React'y calc" sheet to the 10th column in the appropriate row in the "Calculation Summary" sheet. One macro can be used to calculate the reactivity for a solvent whose data are in a selected row, and the other can be used to calculate the reactivity for that solvent and rows below it, until a blank row is encountered.

Comparison of Results with ARB Bin and Explicitly Calculated Reactivities

Figure 4 shows the relative differences between the MIR's calculated using the spreadsheet method described above and the MIR's calculated using the detailed composition data for the analyzed solvents listed in Table 3. It can be seen that this method performs somewhat better than the ARB bin assignments in predicting the detailed calculated MIR's of the solvents, with the average biases being within ~5% for almost all bins, and the errors being no greater than ±20% and in most cases less than ±10%. (Note that Figure 4 has a smaller scale for the deviations than is the case for Figure 1, with the maximum deviation in this case being ±20%, compared with ±75% in Figure 1). Figure 4 also shows the relative differences for the low NO_x EBIR scale, where the performance of the method is equally good (The results for the MOIR scale, not shown, are similar.) Therefore, this method provides reasonably good approximations to reactivities calculated based on detailed composition data.

When evaluating the ARB bin assignments it should be noted that compositional data were not available for all the solvents that may be in use. The relatively high MIR assignments for Bins 1 and 3-5 reflected the possibility that solvents in these bins may contain non-negligible amounts of cyclopentane and methyl cyclopentane, which have relatively high MIRs (2.7 and 2.4 gm O_3 /gm VOC, respectively) compared to other alkanes in this molecular weight range. Note that cycloalkanes are not present in bin 2 solvents, so the high cyclopentane reactivities did not affect the assignment for this bin.

In addition, one would expect the spreadsheet method to perform better than the bin method in predicting reactivities derived from detailed composition data because the spreadsheet method uses the type distribution and boiling point data for the individual solvents for which this information is available, while the bin assignments applies to a range of solvents for which compositional data may be more limited. The spreadsheet method has the advantage that it takes into account the differences among solvents within a bin. On the other hand, the binning method has the advantage that it does not require as precise a knowledge of the type distributions and boiling point ranges in order to classify and derive reactivity estimates for the solvents.

The spreadsheet method could be evaluated against the existing binning approach to determine which is more appropriate for regulatory purposes the next time the regulatory reactivity scale needs to be updated. It could also be used for deriving or evaluating bin assignments for other reactivity scales. In

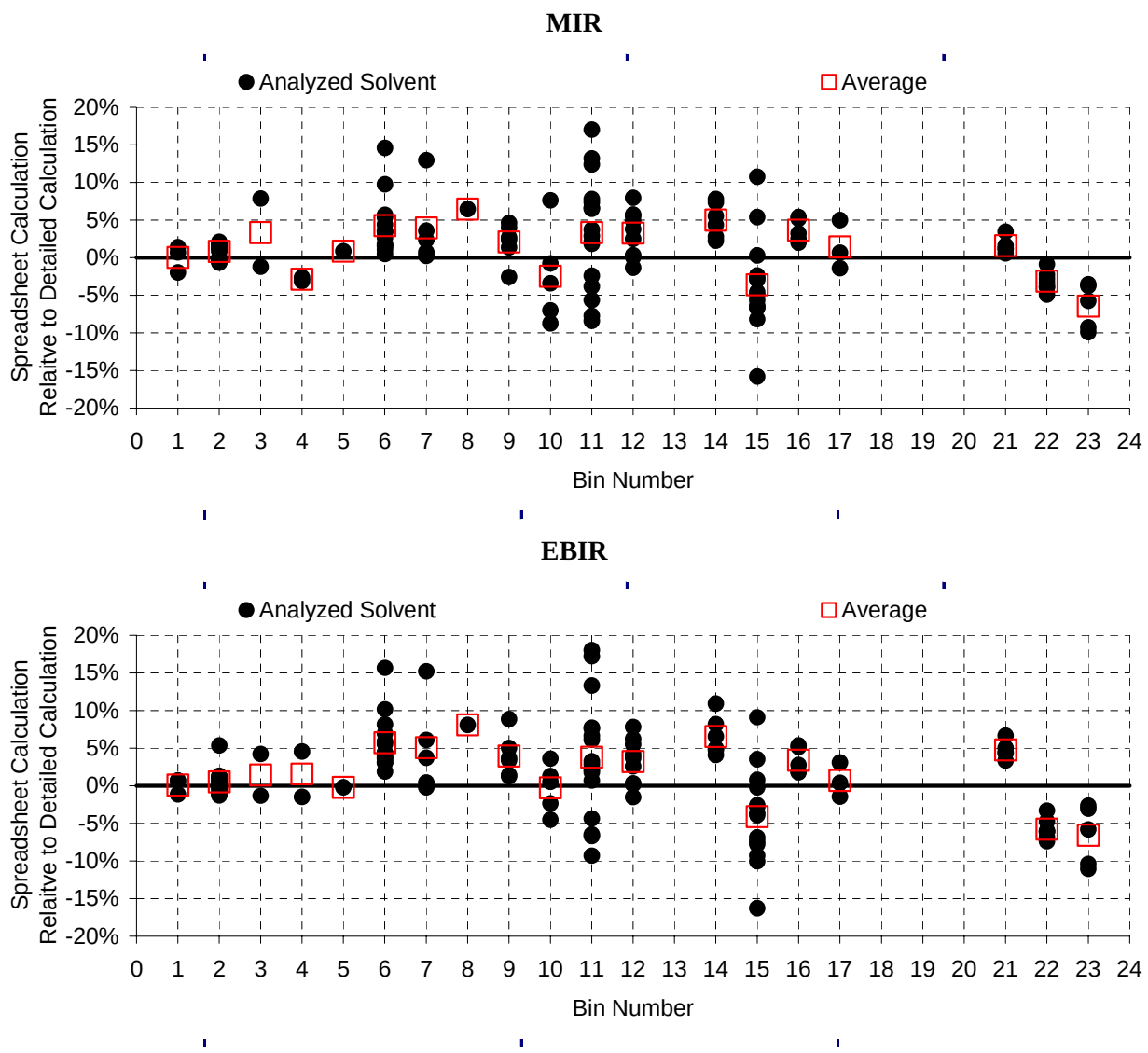

Figure 4. Plots of differences between spreadsheet and explicitly calculated SAPRC-99 MIR's and EBIR's for the hydrocarbon solvents for which compositional data were provided.

order to do this, is necessary to specify specific type distributions and boiling point ranges that are representative of the bin. In order to use the spreadsheet method for deriving an MIR estimate for a bin, it is necessary to assume hydrocarbon type distributions and boiling point ranges that are representative of that bin. Obviously actual hydrocarbon compositions and boiling point ranges would vary within a bin, so no assumed distributions or ranges would fit all solvents. In order to make assignments with the objective of representing the midpoint of the distribution in terms of predicted reactivity, we assume equal distributions of the alkane types associated with the bins, and use the minimum and maximum boiling points associated with the bins, and derive the average as the average of the minimum and maximum. Note that these boiling point ranges are used for calculation purposes only, and do not represent how the bin assignments are made (which is based on the average temperature of the boiling point range).

Table 6. Input parameters and MIR values derived from the spreadsheet method compared to the CARB hydrocarbon bins.

Bin	Type distribution				Boiling Range (^oF) [a]			MIR [b]			Other Scales [c]	
	n-Alk.	Iso-Alk.	Cyc-Alk	Arom.	Avg	Min	Max	Calc.	CARB	Diff	MOIR	EBIR
1	33%	33%	33%	-	143	80	205	1.62	2.08	28%	0.98	0.65
2	50%	50%	-	-	143	80	205	1.51	1.59	6%	0.92	0.61
3	-	-	100%	-	143	80	205	1.86	2.52	35%	1.10	0.71
4	32%	32%	32%	5%	143	80	205	1.66	2.24	35%	0.97	0.63
5	28%	28%	28%	15%	143	80	205	1.74	2.56	47%	0.94	0.59
6	33%	33%	33%	-	273	205	340	1.33	1.41	6%	0.79	0.47
7	50%	50%	-	-	273	205	340	1.17	1.17	0%	0.72	0.42
8	-	-	100%	-	273	205	340	1.66	1.65	0%	0.93	0.56
9	32%	32%	32%	5%	273	205	340	1.59	1.62	2%	0.85	0.49
10	28%	28%	28%	15%	273	205	340	2.11	2.03	-4%	0.97	0.53
11	33%	33%	33%	-	400	340	460	0.80	0.91	14%	0.50	0.26
12	50%	50%	-	-	400	340	460	0.73	0.81	11%	0.47	0.24
13	-	-	100%	-	400	340	460	0.93	1.01	8%	0.55	0.30
14	32%	32%	32%	5%	400	340	460	1.08	1.21	12%	0.57	0.30
15	28%	28%	28%	15%	400	340	460	1.65	1.82	10%	0.72	0.37
16	33%	33%	33%	-	520	460	580	0.57	0.57	0%	0.37	0.19
17	50%	50%	-	-	520	460	580	0.53	0.51	-4%	0.35	0.18
18	-	-	100%	-	520	460	580	0.64	0.63	-2%	0.40	0.21
19	32%	32%	32%	5%	520	460	580	0.78	0.88	13%	0.42	0.22
20	28%	28%	28%	15%	520	460	580	1.21	1.49	24%	0.54	0.27
21	-	-	-	100%	285	280	290	7.62	7.37	-3%	2.41	1.16
22	-	-	-	100%	335	320	350	7.31	7.51	3%	2.26	1.10
23	-	-	-	100%	388	355	420	6.84	8.07	18%	2.09	1.02
24	-	-	-	100%	443	350	535	5.83	5.00	-14%	1.79	0.87

[a] These are the ranges that were used for calculation purposes and do not directly relate to how the CARB bin assignments are applied. The assignment of compounds to the CARB bins is based on the average boiling point only (see Table 2). Actual boiling point ranges for compounds in those bins would vary.

[b] SAPRC-99 maximum incremental reactivity (MIR) in gm O_3/ gm solvent. “Calc” is value calculated using the spreadsheet method as discussed in the text. “CARB” is the standard bin MIR value derived by Kwok et al (2000).

[c] SAPRC-99 maximum ozone incremental reactivities (MOIR) and equal benefit incremental reactivities (EBIR) calculated using the spreadsheet method as described in the text

Table 6 shows the type distributions and boiling point range assignments associated with the bins for this purpose, and the SAPRC-99 MIR's calculated from those data. The bin MIR's given by Kwok et al (2000) are also given on the table for comparison, along with the relative differences between the values. Reactivities for the SAPRC-99 MOIR and EBIR scales are also shown on the table.

It can be seen that the bin MIR's calculated using this method agree with the values of Kwok et al (2000) to within ±15% in most cases, but there are some bins, such as 1 and 3-5 where the discrepancy is greater. These are the four bins where the greatest biases are seen when comparing the bin MIRs with the MIRs calculated using the detailed composition data, as shown on Figure 1. As discussed above, this is because the CARB Bin MIRs were derived on the basis that these solvents may contain higher amounts of cyclopentanes than the solvents used in this evaluation, and than predicted using the spreadsheet method.

Plots of differences between the bin MIRs derived using the spreadsheet method and the explicitly calculated values are shown on Figure 5. This can be compared with the plots on Figure 1,which show the results for the standard CARB bin assignments. It can be seen that the bias is removed for bins 1 and 3-5, but the biases and scatter for the other bins is only slightly less than the prediction using the CARB bin MIRs. In general, the MIR values derived from the spreadsheet method predict the explicitly calculated values to with ±25% in most cases.

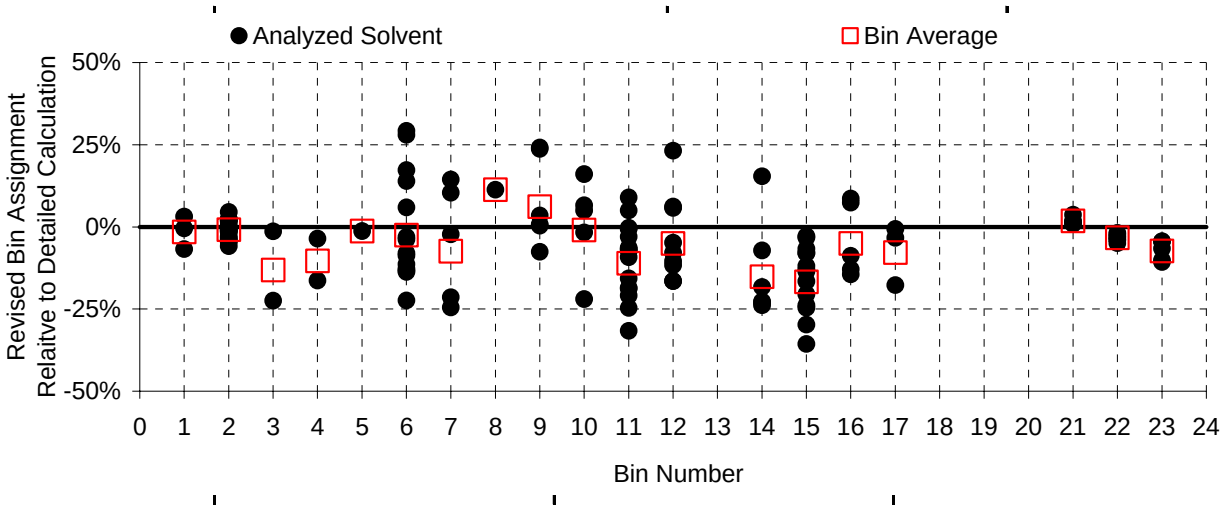

Figure 5. Plots of differences between spreadsheet calculated bin and explicitly calculated SAPRC-99 MIR's for the hydrocarbon solvents for which compositional data were provided.

DIRECT REACTIVITY MEASUREMENT

Introduction

Although environmental chamber experiments provide the best method for evaluating the overall performance of the mechanisms for predicting reactivity under atmospheric conditions, they are expensive and also they do not provide an unambiguous evaluation of all the important components of the mechanism. The direct reactivity of a VOC, which is the rate at which the VOC reacts and converts NO to NO_2, is an important component of VOC reactivity that is difficult to test unambiguously using environmental chamber experiments because other mechanistic factors, such as the effects of the VOCs on radical levels and NO_x sinks, are also very important in affecting the results. Direct reactivity reflects not only how rapidly the VOC reacts in the atmosphere, but also the amount of ozone formation that can be directly attributed to its reactions[3]. If it is uncertain whether the model has a correct representation of this important component of reactivity for a VOC, it cannot be relied upon to give accurate predictions of its effect on ozone formation in the atmosphere.

Measurements of direct reactivity not only provide useful data for more unambiguous evaluation of this component of the mechanism, if it can be carried out more easily and inexpensively than chamber studies, it can also provide a potentially valuable reactivity screening tool. Direct reactivity measurements are particularly useful for VOCs whose atmospheric reaction rate constants are unknown and difficult to measure, or for complex mixtures of VOCs that may have varying rate constants or mechanisms. Thus, they would be particularly useful for the many types of coatings VOCs of interest. In the case of petroleum distillates and other complex hydrocarbon solvents, the large number of components means that at best the chemical compositions can only be determined approximately and generally in terms of representative or "generic" species, and in most cases the distribution of components is uncertain. This results in a corresponding uncertainty in the representation of the mechanism and the rate constant in the model.

Initial work in the development of a direct reactivity method was carried out in a previous project for the CARB, and the results are described by Carter and Malkina (2002). The direct reactivity measurement method developed for that project involves use of a test VOC continuously injected into a HONO-air flow, with the mixture is irradiated in a plug flow system. The amount of NO consumed and O_3 formed compared to when the HONO flow is irradiated in the absence of the test VOC provides a measure of the rate at which the reactions of the VOC converts NO to NO_2, which is the process responsible for ozone formation. This method was successfully employed to measure the direct reactivities of a number of representative organics with sufficient volatility that they were not absorbed on surfaces and which could be quantitatively analyzed by gas chromatography (Carter and Malkina, 2002).

The main limitation to the method as described by Carter and Malkina (2002) is the need to measure the amount of VOC injected to assure that it agrees with the amount calculated from the liquid and gas flows.

---

[3] On the other hand, the indirect reactivity is the change in ozone formation caused by the effect of the VOC's reactions on the reactions of the other VOCs that are present. For example, if the VOC's reactions cause radical levels to increase because of radical initiation processes, it would have a high indirect reactivity because it causes more of the other VOCs present to react and form ozone than would otherwise be the case. Incremental reactivities of VOCs are affected by both these compositions of reactivity, but their relative importance tends to depend significantly on environmental conditions.

This is particularly important for low volatility compounds because absorption on surfaces may mean that the gas-phase concentration is less than the concentration calculated from the flows. Unfortunately, low volatility compounds are also the most difficult to analyze reliably. In addition, the chromatographic measurements are also the most expensive and time-consuming aspect of carrying out experiments using the method as currently employed.

To address this limitation, for this program we investigated use of a total carbon analysis system to measure the amount of VOC compound or mixture injected into the gas phase flow reactor, and investigated the use of this method with several test compounds and a representative hydrocarbon solvent sample. The work in this task, and the results obtained, are described in this section.

Approach

Modified flow system

A schematic of the modified HONO flow system for direct reactivity measurement that was evaluated for this project is shown in Figure 6. Except for the total carbon analyzer developed for this project, the system is essentially the same as the quartz tube plug flow system described by Carter and Malkina (2002). Its major components are summarized below.

The HONO generation system is based on the method developed by Febo et al (1995) to generate nearly pure HONO from the reactions of dilute HCl gas in humidified air passing through stirred $NaNO_2$ salt. A schematic of the system employed is shown on Figure 7. The reaction occurred in a temperature-controlled oven held at ~40°C. With a total HONO source and dilution air flow of ~5 liters per minute (as s shown on Figure 6), measured HONO concentrations (as obtained from the "NO_2" channel of a commercial NO - NO_x analyzer) was typically 1.5 - 1.75 ppm. Additional details of the system are given by Carter and Malkina (2002).

The gaseous or liquid VOC samples were introduced into the flow system into heated Pyrex® tubing as shown on Figure 6. The injection lines were generally heated to ~90°C. The only gaseous test compound used in the flow experiments for this project was propane, which was prepared in a tank at a high concentration and metered into the flow system at the appropriate flow to achieve the desired concentration. Liquid reactants were injected into the heated line using a syringe pump system as described by Carter and Malkina (2002).

The reactor employed in this project was a 1.25" x 35" quartz tube reactor inside an air-cooled 57" x 16" x 17.5" enclosure fitted with blacklights. The ends of the reactor were covered, with the irradiated portion being ~32" with a measured volume of 263 ml. The light intensity inside the irradiated enclosure was measured using the quartz tube method of Zafonte et al (1977) modified as described by Carter et al (1995b), using the same quartz tube reactor for the actinometry as employed in the direct reactivity experiment. The measured NO_2 photolysis rate was 0.674 min^{-1}.

The outlet of the reactor was diluted as shown in Figure 6 in order to provide sufficient flow for the analyzers without having excessive flow, and the resulting short residence times, in the reactor. Ozone was monitored using a Dasibi 1003-AH UV photometric ozone analyzer. NO and species converted to NO using heated Molybdenum catalysts (e.g., HONO and NO_2) were monitored using a Teco model 42 chemiluminescent NO - NO_x analyzer fitted with a NaCl filter to remove interferences from HNO_3. All flows were measured as accurately as possible so the concentrations exiting the reactor prior to dilution, and the residence times of the reactants in the reactor (required to model the reactivity measurement) could be accurately determined.

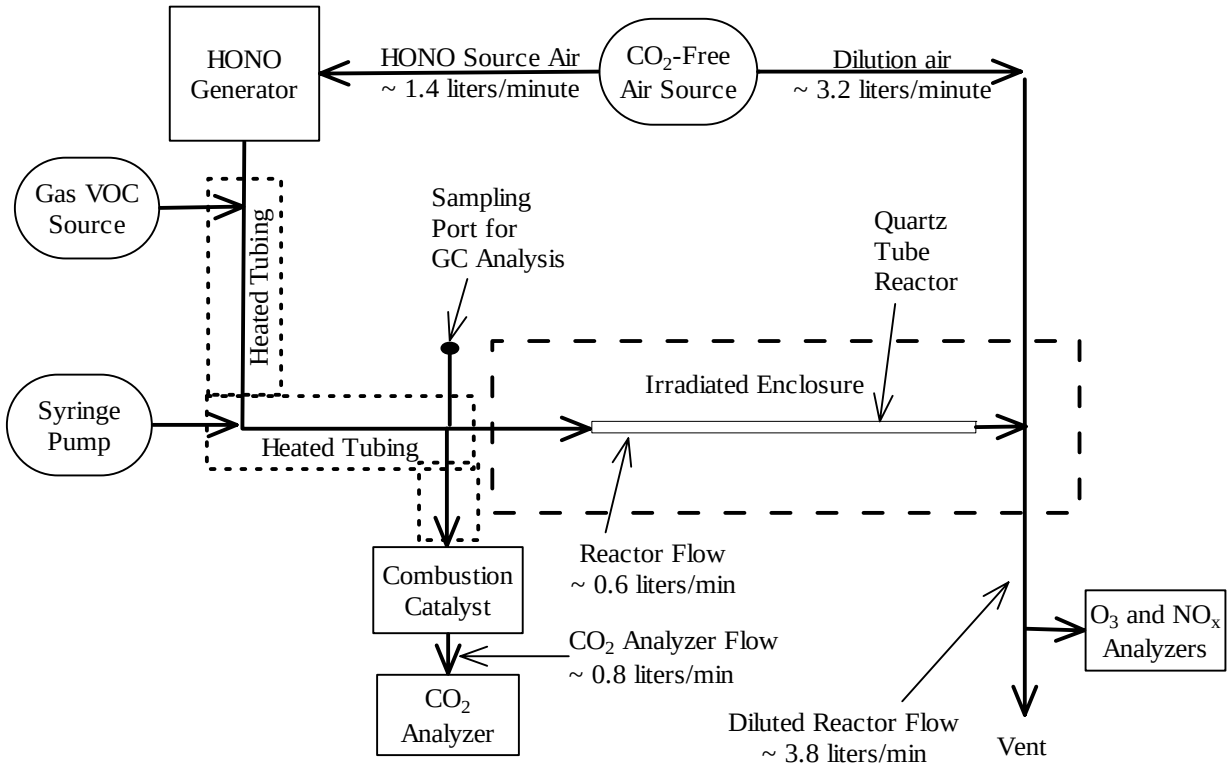

Figure 6. Diagram of setup for plug flow reactor being evaluated for use with the total carbon analysis system.

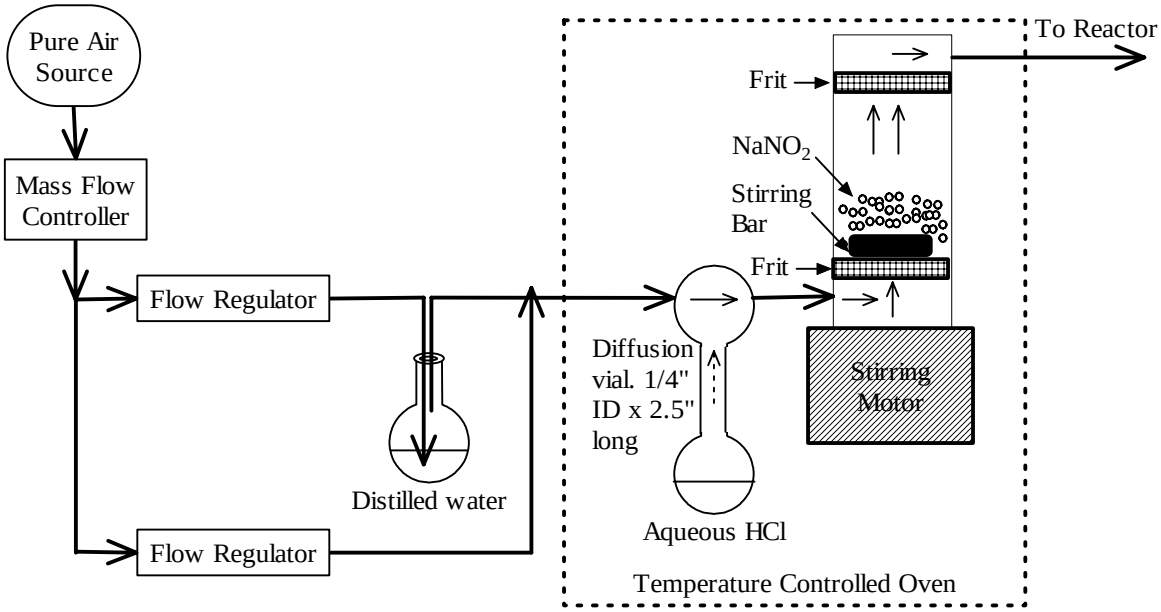

Figure 7. Diagram of the HONO generation system.

Total carbon analysis

The major modification to the system for this project was to interface a total carbon analysis system to the flow system as a means to determine the amount of gas-phase VOC introduced into the reactor. In order to provide a reliable total carbon measurement without the need for GC analysis or assumptions of complete injection it is necessary that the carbon response of the system be independent of the compound or mixture being analyzed, which rules out use of FID. Therefore, the approach chosen was to use a combustion catalyst to quantitatively convert the gas-phase VOCs to CO_2, then use a sensitive CO_2 analyzer to measure the total carbon. This required the use of nearly CO_2-free air as the pure air source in order to bring the background CO_2 to a sufficiently low level for a sensitive VOC measurement.

An API Model 360U ultra high sensitivity CO_2 analyzer was purchased for this project using remaining gift funds previously provided by the ACC for the purpose of expediting work on the direct reactivity measurement method. Several different combustion catalysts and combustion temperatures were tested for this project, but the most satisfactory results were obtained using Hopcalite catalyst (a manganese dioxide - copper oxide mixture), mesh size 8-14, heated to ~550°C. Use of lower temperatures for the catalyst was found to result memory effects in the analysis, presumably due to hang-up of partially combusted material.

Two different geometries were used for the combustion catalyst system for the experiments discussed in this report. In the first set of experiments the tube containing the catalyst was straight, while in the second set the tube was bent at a right angle during the preheat area in order to minimize space taken up by the system. None of the flows or other conditions that should affect the results of the experiments were changed, and no impact on the results were expected to be caused by this change. However, as discussed below some differences in the data were observed when this configuration was changed, so this change is noted here.

The total carbon analysis system was calibrated using CO_2 (diluted from a calibration standard tank) and propane (analyzed by gas chromatography) and found to give a linear response for concentrations below ~30 ppm. A slight curvature in the response was observed at higher concentrations, so only data below ~30 ppm was used in our data analysis. The pure air source had a background CO_2 levels ranging from about 1-4 ppm, depending on the source and other factors. This was subtracted off the CO_2 measurement prior to applying calibration factors or any other analyses. Although variable over time, it was sufficiently constant during experiments that it did not significantly affect the data. The background CO_2 levels were determined prior to and after experiments and subtracted from the data.

A comparison between GC measurements and total carbon analysis using this method for compounds that could be precisely analyzed by GC (e.g., propane and n-octane) indicated that the total carbon analysis was not a significant source of uncertainty in this system, at least for volatile compounds. Since the inlet to the system was heated it is assumed that the analysis should be equally valid for the lower volatility compounds or mixtures that were studied, where GC analysis was suitable for quantification.

Data Analysis Method

The photolysis of HONO in the absence of added VOC resulted in measured formation of NO caused by its photolysis (Carter and Malkina, 2002). (NO_2 is also formed but could not be distinguished from HONO with the NO_x analyzer employed.) The addition of the reactant VOC caused a reduction in the formation of NO and eventually, if sufficient VOC is added, the formation of ozone. This is due to the NO to NO_2 conversions caused by the reactions of the VOC, which is the quantity of interest. Therefore,

the direct reactivity response is measured by $\Delta([O_3]\text{-}[NO])$, or $([O_3]\text{-}[NO])^{\text{added VOC}} - ([O_3]\text{-}[NO])^{\text{HONO only}}$. The quantity $([O_3]\text{-}[NO])^{\text{HONO only}}$ was determined prior to and after the injection of the VOC. In some experiments changed slightly during the course of the run, and this was corrected for by assuming a linear change with time, to interpolate the $([O_3]\text{-}[NO])^{\text{HONO only}}$ during the periods the VOC was injected. The amount of added VOC was varied during the experiment from low levels that barely caused the formation of NO to change to sufficiently high levels that $([O_3]\text{-}[NO])^{\text{added VOC}}$ no longer changed significantly when the VOC increased. The amount of VOC added was monitored with the total carbon analyzer, calibrated as discussed above.

As discussed by Carter and Malkina (2002), the $\Delta([O_3]\text{-}[NO])$ response increased approximately linearly with added VOC for low amounts of VOC added but eventually leveled off to a constant value, designated R_{max}. The initial slope at the low VOC limit, designated R_0, is the actual direct reactivity measure of interest, being directly related to the rate that the VOC reacts with OH radicals and converts NO to NO_2 (Carter and Malkina, 2002). The dependence of $\Delta([O_3]\text{-}[NO])$ on added VOC are well fit by the following empirical relationship, which was the means used to derive R_0, the direct reactivity measure of interest, from the data

$$\Delta([O_3]\text{-}[NO]) = R_{max}\,(1 - e^{-([VOC]-C_0)\,R_0/R_{max}}). \qquad \text{(VI)}$$

where R_0, R_{max}, and C_0 were adjusted using a nonlinear least squares optimization method to fit the data for each experiment. This is the same as the empirical fit used by Carter and Malkina (2002) except that an additional adjustable parameter, C0, was added to account for variability in the background for the CO_2 measurement that is used to determine [VOC].

Some scatter in the $\Delta([O_3]\text{-}[NO])$ vs. [VOC] data was observed when the VOC concentrations were changed rapidly and not yet stabilized. These outlier points were obvious and removed from the dataset prior to adjusting the parameters to fit Equation (VI).

The direct reactivity response is expected to increase approximately linearly with residence time, t_R and the light intensity in the reactor, which is measured by k_1, the NO_2 photolysis rate. In order to provide a unitless measure of direct reactivity that is less dependent on these experimental variables, the reported direct reactivity measures are given as $R_0/(t_R \times k_1)$ in the subsequent discussion. The residence time is calculated from the irradiated volume of the reactor (0.263 liters in this case) and the flow rate through the reactor, and was typically ~18 seconds. The NO_2 photolysis rate was assumed to be 0.674 min^{-1} in all the experiments reported here, based on the results of the actinometry measurements discussed above.

Model simulations of the experiments were also carried out, using the same approach and assumptions as discussed by Carter and Malkina (2002) when modeling the plug flow experiments. The SAPRC-99 detailed mechanism (Carter, 2000a) was used without modifications. The plug flow system was represented in the model as a static irradiation for the period of the residence time, and the wall effects model, whose parameters had negligible effects on the calculated direct reactivity results, was the same as used by Carter and Malkina (2002) for the quartz tube runs. The HONO and other photolysis rates were calculated using the absorption cross sections and quantum yields in the mechanism, the measured NO_2 photolysis rate, and the blacklight spectral distribution given by Carter et al (1995b). The results were analyzed to obtain R_0 and R_{max} in Equation (VI) as discussed above for the experimental data, except that experimental zero offset parameter, C_0, was set at zero.

Results

A large number of experiments and tests were carried out when developing and testing the system, but for brevity we will discuss only the experiments with the system in the final two configurations. Tests were conducted using propane, n-octane, n-tetradecane, n-dodecane, and the Mineral Spirits Sample "B" used for the Safety-Kleen study (Carter et al, 1997). The latter is an all-alkane petroleum distillate mixture with carbon numbers in the 9-15 range, centered at C_{12}-C_{13}, and provides a test of the ability of the system to assess reactivities of petroleum distillates. The composition given by Carter et al (1997) was used in modeling the experiments with this mixture.

The conditions and selected results of the experiments with the final configurations are summarized on Table 7. Plots of $\Delta([O_3]-[NO])$ against added VOC, as measured by the total carbon analyzer, are shown on Figure 8. Fits to the data using Equation (VI) are shown for selected propane runs and all the runs with the other VOCs. Results of model calculations for representative conditions, discussed below, are also shown on Table 7.

It can be seen that reasonably consistent results for the direct reactivity measure, $R_0/(t_R \times k_1)$, are obtained in experiments with the same test compound, but the limiting high concentration $\Delta([O_3]-[NO])$, R_{max}, changed significantly when the geometry of the combustion catalyst system was changed. The change was not consistent; it increased in the propane runs, decreased in the n-octane and n-tetradecane runs, and did not change significantly in the runs with n-dodecane. There is no known reason why changing the geometry of the preheat area of the combustion catalyst could affect the results, and none of the flows or other parameters changed significantly between the two sets of runs. It may be that the source of variability is something other than the combustion catalyst geometry and the association of the geometry change with the variable results may be coincidental.

The results of these experiments were also not well simulated by the model, with the model overpredicting both the direct reactivity measure and the high concentration limit $\Delta([O_3]-[NO])$. The model could also not simulate the run-to-run variability in R_{max}, even if the run-to-run variabilities in the flows and initial reactant concentrations are taken into account. This is despite the fact that the results of the quartz tube plug flow experiments of Carter and Malkina (2002), which employed essentially the same setup except without the total carbon analyzer, could be reasonably well simulated by the model for these compounds. Apparently the sampling by the total carbon analyzer is causing a perturbation and source of variability that is not adequately understood.

However, the relatively consistent results for the direct reactivity measures for a given compound indicate that the uncharacterized variability in the experimental conditions appears to significantly affect only the results at the higher added VOC concentrations, and not at the low concentration limit that are relevant to the direct reactivity measure. In addition, the model bias appears to be consistent, suggesting that it can be corrected for by using the reactivity results for a compound with a well-characterized mechanism to normalize the data.

The effect of normalizing the experimental and calculated direct reactivity results to those for propane are shown on Figure 9. It can be seen that this normalization results in the data being consistent with the model predictions within the experimental variability for the n-octane through n-tetradecane, and almost to within the experimental variability for the mineral spirits.

Table 7. Summary and conditions and results of the HONO flow direct reactivity experiments carried out in the final configuration.

Run No.	Set [a]	Initial Conc (ppm) HONO	NO	Flows (liter/min) Reactor	Total	100 x R_o /(t_R x k_1) [b]	R_{max} (ppb) [b]
				Propane			
Model [c]						3.57	119
19	1	1.75	0.009	0.93	4.71	2.37	45
20	1	1.85	0.015	1.03	4.75	2.11	47
25	2	1.62	0.012	0.82	4.75	2.09	104
26	2	1.65	0.013	0.82	4.80	2.35	92
				n-Octane			
Model						12.04	133
21	1	1.67	0.031	0.84	4.82	7.56	117
28	2	1.75	0.012	0.93	4.83	7.54	64
				n-Dodecane			
Model						11.70	131
13	1	1.65	0.026	0.84	4.58	7.76	89
32	2	1.74	0.042	0.90	4.65	9.08	84
				n-Tetradecane			
Model						12.66	131
14	1	1.65	0.031	0.84	4.66	7.19	88
29	2	1.74	0.013	0.89	4.78	8.14	62
				Mineral Spirits "B"			
Model [d]						14.89	136
30	2	1.73	0.025	0.88	4.75	8.60	87
31	2	1.73	0.035	0.92	4.71	9.05	91

[a] Set 1 experiments were carried out before the combustion catalyst geometry was changed and Set 2 experiments were carried out afterwards. No conditions were changed that would significantly affect model simulations.

[b] R_0 and R_{max} are respectively the direct reactivity and the high concentration limit Δ([O3]-[NO]) parameters in Equation (VI) that best fit the data, t_R is the residence time and k_1 is the NO_2 photolysis rate.

[c] SAPRC-99 model calculation for the averaged conditions of the experiments.

[d] Model used the Mineral Spirits "B" composition given by Carter et al (1997).

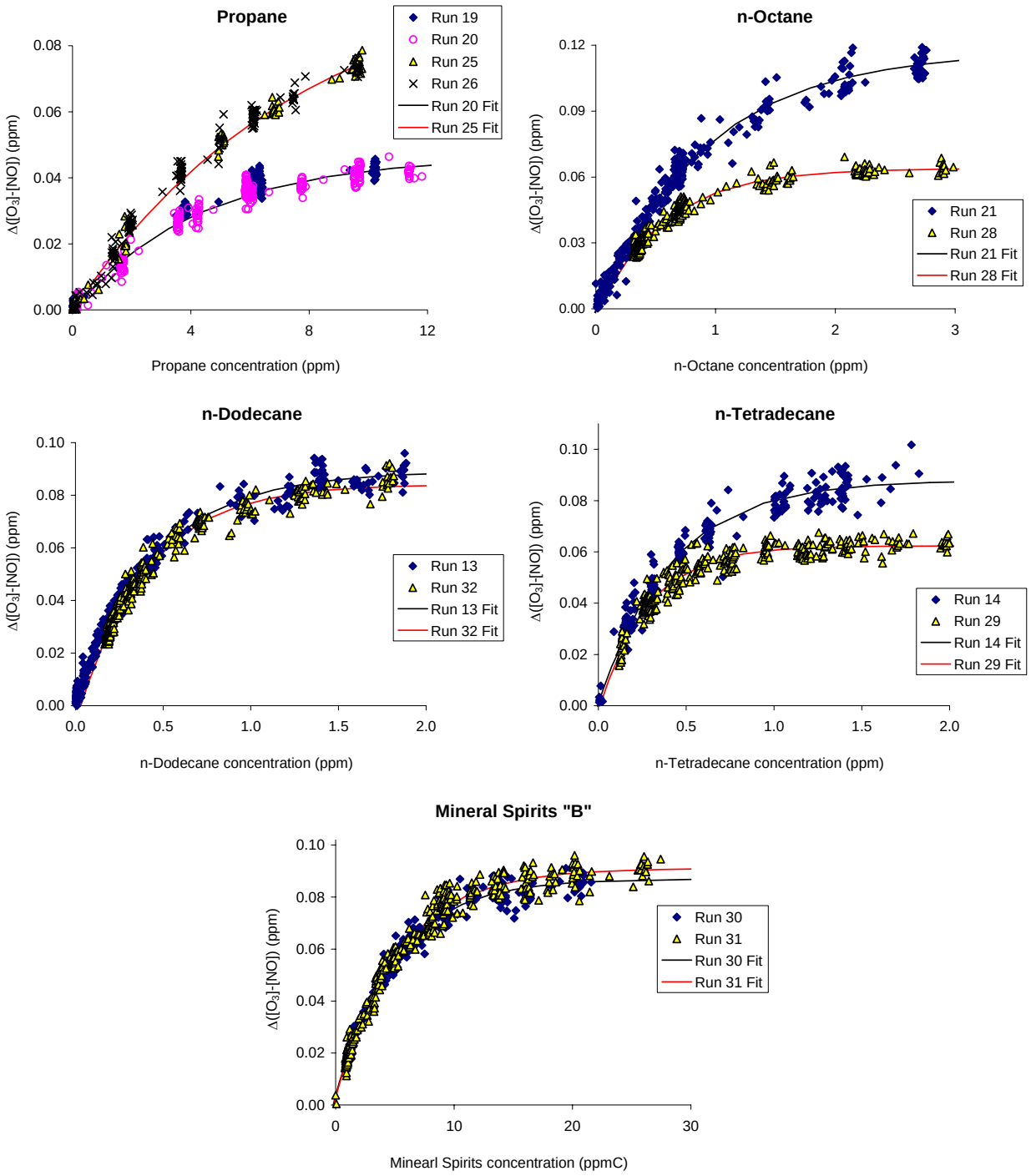

Figure 8. Plots of experimental changes in Δ([O3]-[NO]) against the test VOC concentrations, derived from the CO_2 data, for the HONO flow direct reactivity experiments.

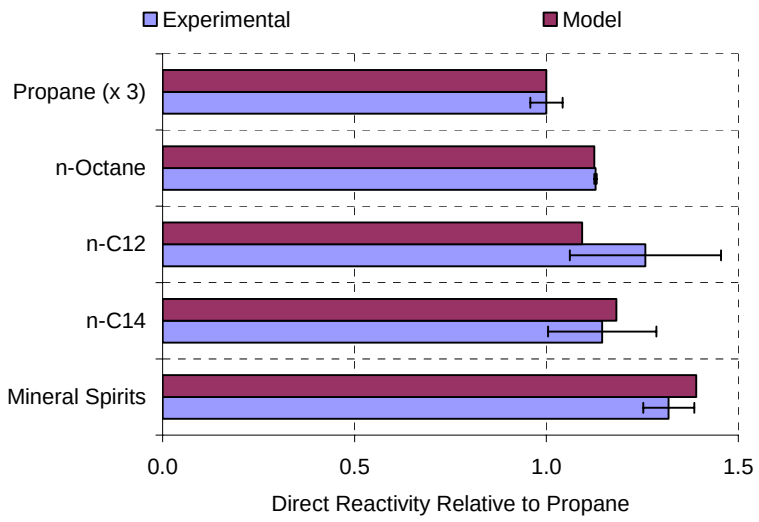

Figure 9. Comparison of experimental and calculated direct reactivity measurements normalized to the direct reactivity measurements for propane. Error bars show the range of variability for the experiments.

ENVIRONMENTAL CHAMBER EXPERIMENTS

The major effort of this project consisted of conducting environmental chamber experiments, using the state-of-the-art UCR EPA chamber (Carter et al 2002a; Carter, 2004a), for selected architectural coatings solvents. After discussions with the California Air Resources Board staff and representatives of the solvents and coatings industries, the materials selected for study were the water-based coatings solvent Texanol® and six representative hydrocarbon solvents used in solvent-based coatings. The primary objective of these experiments was not to directly measure atmospheric reactivity, but to provide data to test the ability of chemical mechanisms used in models to predict their impacts in the atmosphere. This is because atmospheric conditions that affect VOC reactivity are highly variable, and it is not practical to duplicate in an environmental chamber all of the physical conditions that will affect quantitative measures of atmospheric reactivity. Even if it were, the results would only be representative of the conditions of the particular experiments that were carried out. Instead the objective of the experiments is simulate, under well characterized conditions, representative *chemical* environments in which the VOCs react, and use the results to test the abilities of the chemical mechanisms used in models to predict the impacts of the VOCs on ozone formation and other measures of reactivity in these environments. If the mechanism can be shown to adequately simulate the relevant impacts of the VOC in a range of chemical conditions representative of the atmosphere, one has increased confidence in the predictive capabilities of the model when applied to atmospheric scenarios. If the mechanism performance in simulating well-characterized experiments is less than satisfactory, then the need to improve the mechanism is indicated, and one has decreased confidence in its predictions of atmospheric reactivity.

The most realistic chemical environment in this regard is one where the test compounds or mixtures react in the presence of the other pollutants present in the atmosphere. Therefore, most of the environmental chamber experiments for this program consisted of measurements of "incremental reactivity" of the subject compounds or solvents under various conditions. These involve two types of irradiations of model photochemical smog mixtures. The first is a "base case" experiment where a mixture of reactive organic gases (ROGs) representing those present in polluted atmospheres (the "ROG surrogate") is irradiated in the presence of oxides of nitrogen (NO_x) in air. The second is the "test" experiment that consists of duplicating the base case irradiation except that the VOC whose reactivity is being assessed is added. The differences between the results of these experiments provide a measure of the atmospheric impact of the test compound, and can be used as a basis to test a chemical mechanism's to predict these atmospheric impacts under the chemical conditions of the experiment.

Base case experiments to simulate ambient chemical environments require choice of an appropriate reactive organic gas (ROG) surrogate mixture to represent the reactive organics that are important in affecting ozone formation in the urban atmospheres. For this project, we continued to use the 8-component "full surrogate" that was employed in our previous reactivity studies for the initial reactivity studies for this project. This is because as discussed previously (Carter et al, 1995a) this gives a reasonably good representation of ambient anthropogenic VOC emissions as represented in current models, and use of more detailed mixtures would not give significantly different reactivity results. However, because of experimental problems, for some experiments for this project the formaldehyde was removed from the surrogate and the initial concentrations of the other ROG components were increased by 10% to make up for the reactivity. Model calculations, discussed later in this report, indicate that this surrogate modification should not have measurable effects on experimental incremental reactivity results. The target and average measured compositions of the ROG surrogates for the reactivity experiments for this project, given as ppm of component per ppmC of nominal ROG surrogate, are given in Table 8.

Table 8. Composition of base case reactive organic gas (ROG) surrogate employed in the initial incremental reactivity experiments for this project.

Compound	Relative amounts (ppb/ppmC)		
	Target	Average Measured	
		Initial	After 11/03
Ethene	16.3	15.6	16.4
Propene	13.6	14.4	15.3
trans-2-Butene	13.6	12.8	15.9
n-Butane	89.8	90.1	88.8
n-Octane	23.1	22.0	22.6
Toluene	20.7	21.0	21.5
m-Xylene	20.6	20.9	21.4
Formaldehyde	18.3	23.2	-

In order to provide data to test mechanism impacts of the test compounds or mixtures under differing atmospheric conditions, the incremental reactivity experiments were carried out using two different standard conditions of NO_x availability relevant to VOC reactivity assessment. Probably the most relevant for CARB regulatory applications is "maximum incremental reactivity" (MIR) conditions, which are relatively high NO_x conditions where ozone formation is most sensitive to VOC emissions. However, it is also necessary to provide data to test mechanism predictions under lower NO_x conditions, since different aspects of the mechanisms are important when NO_x is limited. The NO_x levels that define the boundary line between VOC-sensitive, MIR-like conditions and NO_x-limited (and therefore NO_x-sensitive) conditions is the NO_x level that yields the maximum ozone concentrations for the given level of ROGs, or the conditions of the "maximum ozone incremental reactivity" (MOIR) scale. Therefore, experiments with NO_x levels that are approximately half that for MOIR conditions might provide an appropriate test of the mechanism under NO_x-limited conditions. This is referred to as "MOIR/2" conditions in the subsequent discussion. If NO_x levels are reduced significantly below this, the experiment becomes less sensitive to VOC levels and thus less relevant to VOC reactivity assessment.

The conditions of NO_x availability are determined by the ROG/NO_x ratios in the base case incremental reactivity experiments. In order to completely fix the conditions of these experiments, it is also necessary to specify a desired absolute NO_x level. In order to determine this, we sought input from the CARB staff concerning the NO_x levels they would consider to be appropriate to use for reactivity studies in the new chamber. The guidance we obtained in this regard was as follows:

> "For the CMAQ runs in South Coast in 2000, the NOx levels of 1, 50, and 500 ppb are the low end, typical, and high end. The focus of future experiments should be in the range of 1-50 ppb since runs with higher NOx levels are available from other investigators (TVA and CSIRO)." (Luo, CARB research division, personal communication, 2003)

Based on this, we decided that 25-30 ppb NO_x probably would be appropriate for the incremental reactivity experiments for this project. Model calculations, using the SAPRC-99 mechanism (Carter, 2000a) and the chamber characterization model developed for this chamber by Carter (2004a), were carried out to determine the base ROG levels that would yield either MIR or MOIR/2 conditions. Based on the results, it was determined that the nominal initial concentrations of the MIR base case experiment

would consist of ~30 ppb NO_x and ~0.5 ppmC ROG surrogate, and the MOIR/2 experiment would consist of ~25 ppb NO_x and ~1 ppmC ROG surrogate. These were therefore the two standard base cases for all the incremental reactivity experiments discussed in this report.

In order to provide additional mechanism evaluation data for the aromatics-100 mixture, we also carried out an experiment where this mixture was irradiated in the presence of NO_x without any added base ROGs. Such experiments are not useful for alkanes or alkane-like materials such as Texanol® that do not have large internal radical sources because the results are highly sensitive to chamber effects (Carter et al, 1982, Carter and Lurmann, 1991). However, they can provide data for highly reactive materials such as aromatics and olefins. An additional experiment was carried out where CO was added to the aromatic-100 - NO_x irradiation, since experiments with other aromatics indicated problems with model predictions of the effects of CO on aromatic - NO_x irradiations (Carter, 2004a).

For comparison purposes and as part of our initial evaluation of use of the new chamber and base case conditions for incremental reactivity experiments, we also carried out incremental reactivity experiments using n-octane and m-xylene as the test compound. These serve as useful control experiments that are relevant to this project because both compounds have been extensively studied previously (Carter, 2000a, and references therein), and serve as simplified model compounds for the alkanes and aromatics present in complex hydrocarbon solvents. These experiments were carried out at a variety of base case ROG and NO_x levels in addition to those for the standard MIR and MOIR/2 experiments discussed above.

A number of other control and characterization experiments were also carried out in conjunction with the incremental reactivity experiments in order to adequately characterize the conditions of the chamber for mechanism evaluation. These experiments are discussed where applicable in the results and modeling methods sections.

Experimental Methods

Chamber Description

All of the environmental chamber experiments for this project were carried out using the UCR EPA chamber. This chamber was constructed under EPA funding to address the needs for an improved environmental chamber database for mechanism evaluation (Carter, 2002a). The objectives, design, construction, and results of the initial evaluation of this chamber facility are described in more detail elsewhere (Carter, 2002a, b; Carter, 2004a). A description of the chamber is also given below.

The UCR EPA chamber consists of two ~85,000-liter Teflon® reactors located inside a 16,000 cubic ft temperature-controlled “clean room” that is continuously flushed with purified air. The clean room design is employed in order to minimize background contaminants into the reactor due to permeation or leaks. The primary light source consists of a 200 KW argon arc lamp with specially designed UV filters that give a UV and visible spectrum similar to sunlight. This light source was used for almost all of the experiments discussed in this report. Banks of blacklights are also present to serve as a backup light source for experiments where blacklight irradiation is sufficient. The interior of the enclosure is covered with reflective aluminum panels in order to maximize the available light intensity and to attain sufficient light uniformity, which is estimated to be ±10% or better in the portion of the enclosure where the reactors are located (Carter, 2002a). A diagram of the enclosure and reactors is shown on Figure 10, and the spectrum of the light source is shown on Figure 11.

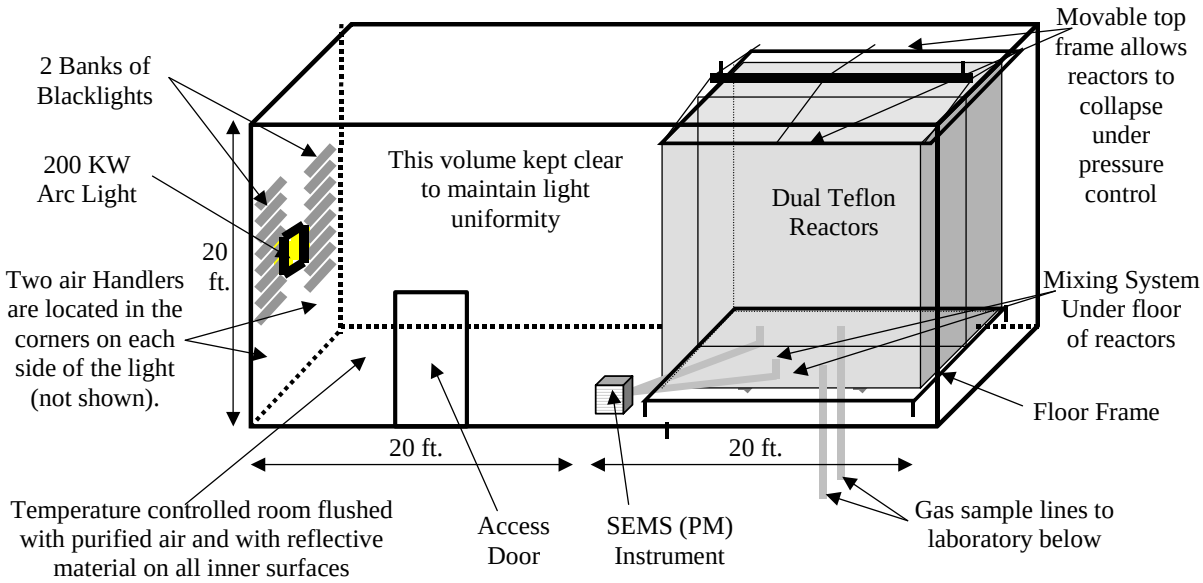

Figure 10. Schematic of the UCR EPA environmental chamber reactors and enclosure.

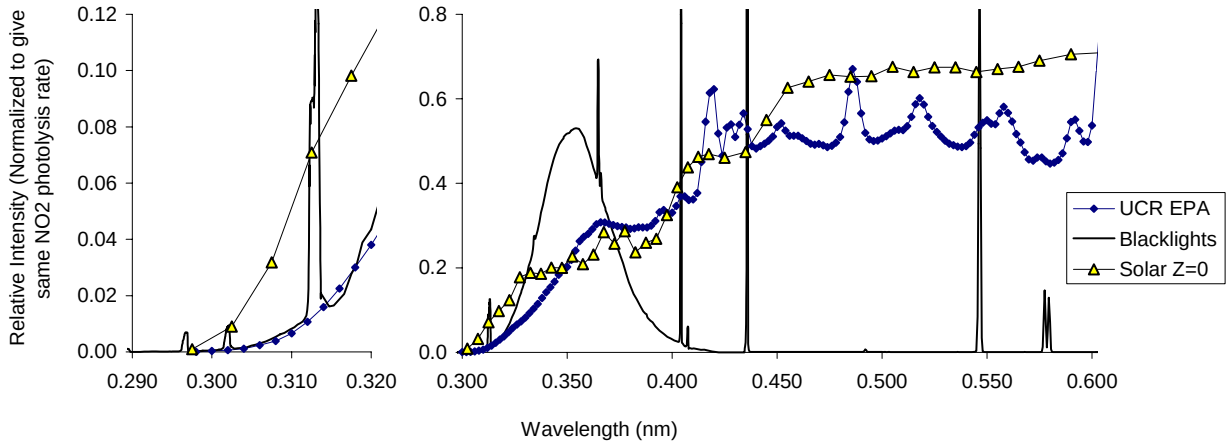

Figure 11. Spectrum of the argon arc light source used in the UCR EPA chamber. Blacklight and representative solar spectra, with relative intensities normalized to give the same NO_2 photolysis rate as that for the UCR EPA spectrum, are also shown.

The dual reactors are constructed of flexible 2 mil Teflon® film, which is the same material used in the other UCR Teflon chambers used for mechanism evaluation (e.g., Carter et al, 1995b; Carter, 2000a, and references therein). A semi-flexible framework design was developed to minimize leakage and simplify the management of large volume reactors. The Teflon film is heat-sealed into separate sheets for the top, bottom, and sides (the latter sealed into a cylindrical shape) that are held together and in place using bottom frames attached to the floor and moveable top frames. The moveable top frame is held to the ceiling by cables that are controlled by motors that raise the top to allow the reactors to expand when filled or lower the top to allow the volume to contract when the reactors are being emptied or flushed. These motors are in turn controlled by pressure sensors that raise or lower the reactors as needed to maintain slight positive pressure. During experiments the top frames are slowly lowered to maintain continuous positive pressure as the reactor volumes decrease due to sampling or leaks. The experiment is terminated once the volume of one of the reactor reaches about 1/3 the maximum value, which varied depending on the amount of leaks in the reactor, but the time involved was greater than the ≥6-hour duration of most of the experiments discussed in this report. Since at least some leaks are unavoidable in large Teflon film reactors, the constant positive pressure is important to minimize the introduction of enclosure air into the reactor that may otherwise result.

As indicated on Figure 10, the floor of the reactors has openings for a high volume mixing system for mixing reactants within a reactor and also for exchanging reactants between the reactors to achieve equal concentrations in each. This utilizes four 10” Teflon pipes with Teflon-coated blowers and flanges to either blow air from one side of a reactor to the other, or to move air between each of the two reactors. Teflon-coated air-driven metal valves are used to close off the openings to the mixing system when not in use, and during the irradiation experiments.

An AADCO air purification system that provides dry purified air at flow rates up to 1500 liters min^{-1} is used to supply the air to flush the enclosure and to flush and fill the reactors between experiments. The air is further purified by passing it through cartridges filled with Purafil® and heated Carulite 300® which is a Hopcalite® type catalyst and also through a filter to remove particulate matter. The measured NO_x, CO, and non-methane organic concentrations in the purified air were found to be less than the detection limits of the instrumentation employed (see Analytical Equipment, below).

The chamber enclosure is located on the second floor of a two-floor laboratory building that was designed and constructed specifically to house this facility (Carter et al, 2002a). Most of the analytical instrumentation is located on the ground floor beneath the chamber, with sampling lines leading down as indicated on Figure 10.

Analytical Instrumentation

Table 9 gives a listing of the analytical and characterization instrumentation whose data were utilized for this project. Other instrumentation was available and used for some of these experiments, as discussed by Carter 2002a, but the data obtained were not characterized for modeling and thus not used in the mechanism evaluations for this project. The table includes a brief description of the equipment, species monitored, and their approximate sensitivities, where applicable. These are discussed further in the following sections.

Ozone, CO, NO, and NO_y were monitored using commercially available instruments as indicated in Table 9. A second ozone analyzer, based on the chemiluminescence method, was utilized in some experiments, and its data were consistent with the UV absorption instrument listed on Table 9. The instruments were spanned for NO, NO_2, and CO and zeroed prior to most experiments using the gas

Table 9. List of analytical and characterization instrumentation for the UCR EPA chamber.

Type	Model or Description	Species	Sensitivity	Comments
Ozone Analyzer	Dasibi Model 1003-AH. UV absorption analysis. Also, a Monitor Labs Chemiluminescence Ozone Analyzer Model 8410 was used as a backup.	O3	2 ppb	Standard monitoring instrument.
NO - NO_y Analyzer	Teco Model 42 C with external converter. Chemiluminescent analysis for NO, NOy by catalytic conversion.	NO	1 ppb	Useful for NO and initial NO_2 monitoring. Converter close-coupled to the reactors so the "NO_y" channel should include HNO_3 as well as NO_2, PANs, organic nitrates, and other species converted to NO by the catalyst.
		NOy	1 ppb	
CO Analyzer	Dasibi Model 48C. Gas correlation IR analysis.	CO	50 ppb	Standard monitoring instrument
TDLAS #1	Purchased from Unisearch Inc. in 1995, but upgraded for this chamber. See Carter (2002a). Data transmitted to DAC system using RS-232.	NO2	0.5 ppb	NO_2 data from this instrument are considered to be interference-free.
		HNO3	~ 1 ppb	HNO_3 data not available for most of the experiments modeled in this report and were not used for this project.
TDLAS #2	Purchased from Unisearch Inc. for this project. See Carter (2002a). Data transmitted to DAC system using RS-232.	HCHO	~ 1 ppb	Formaldehyde data from this instrument are considered to be interference-free.
		H_2O_2	~2 ppb	H_2O_2 data not taken during the experiments discussed in this report
GC-FID #1	HP 5890 Series II GC with dual columns, loop injectors and FID detectorsControlled by computer interfaced to network.	VOCs	~10 ppbC	30 m x 0.53 mm GS-Alumina column used for the analysis of light hydrocarbons such as ethylene, propylene, n-butane and trans-2-butene and 30 m x 0.53 mm DB-5 column used for the analysis of C_{5+} alkanes and aromatics, such as toluene m-xylene and several components of the Aromatic 100 solvent. Loop injection suitable for low to medium volatility VOCs that are not too "sticky" to pass through valves.
GC-FID #2	HP 5890 Series II GC with dual columns and FID detectors, one with loop sampling and one set up for Tenax cartridge sampling. (Only the Tenax cartridge system used for this project.) Controlled by computer interfaced to network.	VOCs	1 ppbC	Tenax cartridge sampling used for low volatility or moderately "sticky" VOCs that cannot go through GC valves but can go through GC columns. 30 m x 0.53 mm DB-1701 column

Table 9 (continued)

Type	Model or Description	Species	Sensitivity	Comments
Total Hydrocarbon analyzer, FID	Ratfisch Instruments, Model RS 55CA	VOCs	50 ppb	Standard commercial instrument, based on FID analysis. Used for injection tests only (see text)
Gas Calibrator	Model 146C Thermo Environmental Dynamic Gas Calibrator	N/A	N/A	Used for calibration of NO_x and other analyzers. Instrument acquired early in project and under continuous use.
Data Acquisition Sytem	Windows PC with custom LabView software, 16 analog input, 40 I/O, 16 thermo-couple, and 8 RS-232 channels.	N/A	N/A	Used to collect data from most monitoring instruments and control sampling solenoids. In-house LabView software was developed using software developed by Sonoma Technology for ARB for the Central California Air Quality Study as the starting point.
Temperature sensors	Various thermocouples, radiation shielded thermocouple housing	Tempera -ture	~0.1 ^{o}C	Primary measurement is thermocouples inside reactor. However, comparison with temperature measurements in the sample line suggest that irradiative heating may bias these data high by ~2.5^{o}C. See text.
Humidity Monitor	General Eastern HYGRO-M1 Dew Point Monitor	Humid-ity	Dew point range: -40 - 50°C	Instrument performing as expected, but dew point below the performance range for experiments discussed in this report.
Spectro-radiometer	LiCor LI-1800 Spectroradiometer	300-850 nm Light Spect-rum	Adequate	Resolution relatively low but adequate for this project. Used to obtain relative spectrum. Also gives an absolute intensity measurement on surface useful for assessing relative trends.
Spherical Irradiance Sensors	Biospherical QSL-2100 PAR Irradiance Sensor or related product. Responds to 400-700 nm light. Spectral response curve included.	Spherical Broad-band Light Intensity	Adequate	Provides a measure of absolute intensity and light uniformity that is more directly related to photolysis rates than light intensity on surface. Gives more precise measurement of light intensity trends than NO_2 actinometry, but is relatively sensitive to small changes in position.
Scanning Electrical Mobility Spectrometer (SEMS)	Similar to that described in Cocker et al. (2001)	Aerosol number and size distribut-ions	Adequate	Provides information on size distribution of aerosols in the 28-730 nm size range, which accounts for most of the aerosol mass formed in our experiments. Data can be used to assess effects of VOCs on secondary PM formation.

calibration system indicated on Table 9, and a prepared calibration gas cylinder with known amounts of NO and CO. O_3 and NO_2 spans were conducted by gas phase titration using the calibrator during this period. Span and zero corrections were made to the NO, NO_2, and CO data as appropriate based on the results of these span measurements, and the O_3 spans indicated that the UV absorption instrument was performing within its specifications.

As discussed by Carter (2002a), two Tunable Diode Laser Absorption Spectroscopy (TDLAS) are available at our laboratories, with the potential for monitoring up to four different species, though only data for NO_2 and formaldehyde were used in this project. TDLAS analysis is described in detail elsewhere (Hastie et al., 1983; Schiff et al., 1994) and is based on measuring single rotational - vibrational lines of the target molecules in the near to mid infrared using laser diodes with very narrow line widths and tunability. The sample for analysis is flushed through closed absorption cells with multi-pass optics held at low pressure (~25 Torr) to minimize spectral broadening. Because of the narrow bandwidth of the diode lasers required to get the highly species-specific measurement, usually separate diode lasers are required for each compound being monitored. Both TDLAS systems have two lasers and detection systems, permitting analysis of up to four different species using this method. However, for most experiments discussed in this report, only one detector was operational for each instrument, one for monitoring NO_2 and the other for monitoring formaldehyde.

The TDLAS NO_2 measurements were calibrated as using the NO_2 span measurements made by gas phase titration with the gas calibrator at the same time the NO-NO_y analyzer was calibrated. Span data were taken in conjunction with most experiments, and these data were used to derive span factors for the entire data set. The TDLAS formaldehyde measurements were calibrated using a formaldehyde permeation source that in turn was calibrated based on Wet chemical calibration procedure using Purpald reagent (Jacobsen and Dickinson, 1974; Quesenberry and Lee, 1996; NIOSH, 1994).

Organic reactants other than formaldehyde were measured by gas chromatography with FID detection as described elsewhere (Carter et al, 1993, 1995a); see also Table 9. The surrogate gaseous compounds ethylene, propylene, n-butane and trans-2-butene were monitored by using 30 m megabore GS-Alumina column using the loop sampling system. The second signal of the same GC outfitted with FID and 30 m megabore DB-5 column was used to analyze liquid components toluene, n-octane and m-xylene. The sampling methods employed for injecting the sample with the test compound on the GC column depended on the volatility or “stickness” of this compound. For analyses of more volatile specie such as Aromatic 100 Type1 solvent the same loop method was suitable.

Low volatility, more “sticky” test compounds such as Texanol were monitored on a second GC-FID using the Tenax cartridge sampling system. During most of the experiments discussed in this report this GC was outfitted with a 30 m DB-1701 megabore column, which gave good results in the analysis of the Texanol® isomers.

Both the GC instruments were controlled and their data were analyzed using HPChem software installed on a dedicated PC. The GC's were spanned using the prepared calibration cylinder with known amounts of ethylene, propane, propylene, n-butane, n-hexane, toluene, n-octane and m-xylene in ultrapure nitrogen. Analyses of the span mixture were conducted approximately every day an experiment was run, and the results were tracked for consistency.

As indicated on Table 9, aerosol number and size distributions were also measured in conjunction with our experiments. The instrumentation employed is to that described by Cocker et al. (2001). Particle size distributions are obtained using a scanning electrical mobility spectrometer (SEMS) (Wang and Flagan, 1990) equipped with a 3077 ^{85}Kr charger, a 3081L cylindrical long column, and a 3760A condensation particle counter (CPC). Flow rates of 2.5 LPM and 0.25 LPM for sheath and aerosol flow,

respectively, are maintained using Labview 6.0-assisted PID control of MKS proportional solenoid control valves and relating flow rate to pressure drop monitored by Honeywell pressure transmitters. Both the sheath and aerosol flow are obtained from the reactor enclosure. The data inversion algorithm described by Collins et al converts CPC counts versus time to number distribution. The tandem differential mobility analyzer (TDMA) measures physical changes to aerosol withdrawn from the chamber due to chemical or physical (temperature) changes in its environment. The results of the aerosol measurements will be described in a subsequent report, which is in preparation.

Most of the instruments other than the GCs and aerosol instrument were interfaced to a PC-based computer data acquisition system under the control of a LabView program written for this purpose. The TDLAS instruments were controlled by their own computers, but the data obtained were sent to the LabView data acquisition system during the course of the experiments using RS-232 connections. These data, and the GC data from the HP ChemStation computer, were collected over the CE-CERT computer network and merged into Excel files that are used for applying span, zero, and other corrections, and preparation of the data for modeling (Carter, 2002b).

Sampling methods

Samples for analysis by the continuous monitoring instrument were withdrawn alternately from the two reactors, zero air, or (for the earlier experiments) the enclosure, under the control of solenoid valves that were in turn controlled by the data acquisition system discussed above. Sampling from the enclosure was discontinued after experiment EPA133 (conducted on July 2, 2003) because of it caused problems with the O_3 analysis in the subsequent sample mode, apparently due to a humidity effect on the O_3 analysis (the enclosure had some humidity due to exchange with outside air, while the air in the reactors were dry). (This problem did not affect the data used for mechanism evaluation because data points at the end of the sampling cycles were not affected the affected points at the beginning of the sampling cycles were deleted from the dataset. In any case is not applicable for most experiments for this project.) For most experiments the sampling cycle was about 5 minutes for each reactor, the zero air, or (when applicable) the enclosure. The program controlling the sampling sent data to the data acquisition program to indicate which state was being sampled, so the data could be appropriately apportioned when being processed. Data taken less than 3-4 minutes after the sample switched were not used for subsequent data processing. The sampling system employed is described in more detail by Carter (2002a).

Samples for GC analysis in earlier experiments were taken at approximately 20-minute intervals from the sample line using 100 ml gas-tight glass syringes, which were then used to flush the sampling loop of the instrument with the air being sampled. After run EPA112 the samples for GC analyses were taken directly from each of the reactors through the separate sample lines attached to the bottom of the reactors. The GC sample loops were flushed for a desired time with the air from reactors using pump. In the analyses using the Tenax system the 100 ml sample was collected directly from the reactors onto Tenax-GC solid adsorbent cartridge and then placed in series with the GC column, thermally desorbed at 300 C and cryofocused on the column. The length of the sample lines was minimized to avoid possible losses.

Characterization Methods

Use of chamber data for mechanism evaluation requires that the conditions of the experiments be adequately characterized. This includes measurements of temperature, humidity, light and wall effects characterization. Wall effects characterization is discussed in detail by Carter (2004a) and most of that discussion is applicable to the experiments for this project. The instrumentation used for the other characterization measurements is summarized in Table 9, above, and these measurements are discussed further below.

Temperature was monitored during chamber experiments using calibrated thermocouples attached to thermocouple boards on our computer data acquisition system. The temperature in each of the reactors was continuously measured using relatively fine gauge thermocouples that were located ~1' above the floor of the reactors. These thermocouples were not shielded from the light, though it was hoped that irradiative heating would be minimized because of their small size. In order to obtain information about possible radiative heating effects, for a number of experiments the thermocouple for one of the reactors was relocated to inside the sample line. The results indicated that radiative heating is probably non-negligible, and that a correction needs to be made for this by subtracting ~2.5^{o}C from the readings of the thermocouples in the reactors. This is discussed by Carter (2004a).

Light Spectrum and Intensity. The spectrum of the light source in the 300-850 nm region was measured using a LiCor LI-1800 spectroradiometer, which is periodically calibrated at the factory. Spectroradiometer readings were taken several times during a typical experiment, though the relative spectra were found to have very little variation during the course of these experiments. Changes in light intensity over time were measured using a PAR spherical irradiance sensor that was located immediately in front of the reactors. In addition, NO_2 actinometry experiments were carried out periodically using the quartz tube method of Zafonte et al (1977) modified as discussed by Carter et al (1995b). In most cases the quartz tube was located in front of the reactors near where the PAR sensor was located. Since this location is closer to the light than the centers of the reactors, the measurement at this location is expected to be biased high, so the primary utility of these data are to assess potential variation of intensity over time. However, several special actinometry experiments were conducted where the quartz tube was located inside the reactors, to provide a direct measurement of the NO_2 photolysis rates inside the reactors. The light spectrum and actinometry results obtained for the experiments of interest are discussed later in this report.

Humidity. Humidity was measured using an EG&G model Hygro M1 chilled mirror dew point sensor. Its lower limit of -40°C is above the expected dew point of the purified air used in the experiments described in this report, but adequate for humidified experiments to be carried out for other projects.

Experimental Procedures

The reaction bags were collapsed to the minimum volume by lowering the top frames, and then emptying and refilling them at least six times after each experiment, and then filling them with dry purified air on the nights before experiments. Span measurements were generally made on the continuous instruments prior to injecting the reactants for the experiments. The reactants were then injected through Teflon injection lines (that are separate from the sampling lines) leading from the laboratory below to the reactors. The common reactants were injected in both reactors simultaneously (except for the first few runs), and were mixed by using the reactor-to-reactor exchange blowers and pipes for 10 minutes. The valves to the exchange system were then closed and the other reactants were injected to their respective sides and mixed using the in-reactor mixing blowers and pipes for 1 minute. The contents of the chamber were then monitored for at least 30 minutes prior to irradiation, and samples were taken from each reactor for GC analysis.

Once the initial reactants are injected, stabilized, and sampled, the argon light is then turned on to begin the irradiation. During the irradiation the contents of the reactors are kept at a constant positive pressure by lowering the top frames as needed, under positive pressure control. The reactor volumes therefore decrease during the course of the experiments, in part due to sample withdrawal and in part due to small leaks in the reactor. A typical irradiation experiment ended after about 6 hours, by which time the reactors are typically down to about half their fully filled volume. Larger leaks are manifested by more rapid decline of reactor volumes, and the run is aborted early if the volume declines to about 1/3 the

maximum. This was not the case for most of the experiments discussed in this report. After the irradiation the reactors were emptied and filled ten times as indicated above.

The procedures for injecting the various types of reactants were as follows. The NO and NO_2 were prepared for injection using a vacuum rack. Known pressures of NO, measured with MKS Baratron capacitance manometers, were expanded into Pyrex bulbs with known volumes, which were then filled with nitrogen (for NO) or oxygen (for NO_2). In order to maintain constant NO/NO_2 ratios the same two bulbs of specified volume were utilized in most of experiments. The contents of the bulbs were then flushed into the reactor(s) with nitrogen. Some of the gaseous reactants such as propylene and n-butane (other than for surrogate experiments) were prepared for injection using a high vacuum rack as well. For experiments with added CO, the CO was purified by passing it through an in-line activated charcoal trap and flushing it into the reactor at a known rate for the amount of time required to obtain the desired concentration. Measured volumes of volatile liquid reactants were injected, using a micro syringe, into a 2 ft long Pyrex injection tube surrounded with heat tape and equipped with one port for the injection of the liquid and other ports to attach bulbs with gas reactants. Then one end of the injection tube was attached to the "Y"-shape glass tube (equipped with stopcocks) that was connected to reactors and the other end of injection tube was connected to a nitrogen source. The test compound or solvent was injected into one of the reactors designated for each experiment. The optimal temperature of the glass injection tube and optimal duration of the injection were determined in preliminary tests as described below. The injection lines into the reactors were wrapped in heat tape and heated as well.

The procedures for injection of the hydrocarbon surrogate components were as follows. A cylinder containing n-butane, trans-2-butene, propylene and ethylene in nitrogen, was used for injecting the gaseous components of the surrogate. The cylinder was attached to the injection system and a gas stream was introduced into reactors at controlled flow for certain time to obtain desired concentrations. A prepared mixture with the appropriate ratios of toluene, n-octane and m-xylene was utilized for injection of these surrogate components, using the procedures as discussed above for pure liquid reactants. All the gas and liquid reactants intended to be the same in both reactors were injected at the same time. The injection consisted of opening the stopcocks and flushing the contents of the bulbs and the liquid reactants with nitrogen, with the liquid reactants being heated slightly using heat that surrounded the injection tube. The flushing continued for approximately 10 minutes.

Formaldehyde was a reactant and a component of the surrogate used in many of these experiments, and it was injected as follows. Because of the large volumes of the reactors it was impractical to use the method of formaldehyde preparation in a vacuum rack system by heating paraformaldehyde as employed in our previous chambers, and heating formaldehyde in a flow system tended to give irreproducible results. Formaldehyde was generated by catalytic decomposition of 1,3,5-trioxane, as described by Imada (1984). A diffusion tube at constant temperature was used as the source for a constant flow of 1,3,5-trioxane, which then is decomposed quantitatively to formaldehyde by a heated catalyst and injected in reactors for particular time depending of desired amount. This method was found to perform satisfactorily in reproducibly injecting the desired amounts of formaldehyde.

Injection Tests

Texanol®

Prior to conducting chamber experiments with Texanol®, tests were carried out to assure we could quantitatively inject this compound into the gas phase and to assess our analysis capabilities. These included injections into a total hydrocarbon analyzer at varying temperatures and injections into the chamber. The injections into the gas phase in the chamber experiments were carried out by placing desired quantity of the liquid (measured using a microsyringe) in a Pyrex injection tube, flushing the tube

with nitrogen heated to ~110°C at a flow rate of about 7 liters min^{-1}, and into the chamber through Teflon® tubes heated to ~125°C. The gas-phase material was analyzed by passing ~100 ml of air from the chamber trough a Tenax cartridge, then desorbing the contents of the cartridge onto a GC column. The GC was calibrated by preparing liquid solutions of Texanol® in methanol and placing them on the Tenax cartridge for analysis.

Both the gas-phase analysis and the methanol liquid solution analysis indicated two peaks for the Texanol® sample used. Based on communications with Rodney J. Boatman of Eastman Kodak the first peak attributed to 1-Hydroxy-2,2,4-Trimethylpentyl-3-Isobutyrate (the SAPRC-99 detailed model species TEXANOL2) and the second to 3-Hydroxy-2,2,4-Trimethylpentyl-1-Isobutyrate (SAPRC-99 model species TEXANOL1). The relative peak heights differed somewhat in the gas-phase samples than the liquid analysis, with the relative area of the second peak being 68% of the total in the liquid analysis, while it averaged 59±2% in the chamber injections. No effect of temperature on the isomer ratio was observed in injection tests where the temperature of the injection tube or injection line was varied. Although this phase difference in the isomeric ratios is not large, it is larger than the variability in the GC analysis, and probably should be taken into account when making reactivity estimates for the commercial Texanol® mixture from those calculated for its constituents. However, since the reactivities of the isomers differ by less than 5% in the SAPRC-99 MIR scale (see Table 11 later in this report), this change would have only an insignificant effect on the calculated reactivity of this mixture in this scale.

A Texanol® injection test experiment was carried out to evaluate our ability to quantitatively inject and analyze this in the gas phase, and to determine how much flushing time is required for quantitative injections. This consisted of continuously flushing the injection tube with a measured amount of Texanol® into one of the reactors over a 15 hour period, and monitoring the gas-phase materials over time by GC and the Ratfisch total hydrocarbon analyzer (see Table 9). CO was also injected and monitored over time to provide data to correct for effects of dilution caused by the continuous injection process. The results are shown on Figure 12, which gives plots of the Texanol carbon as calculated from

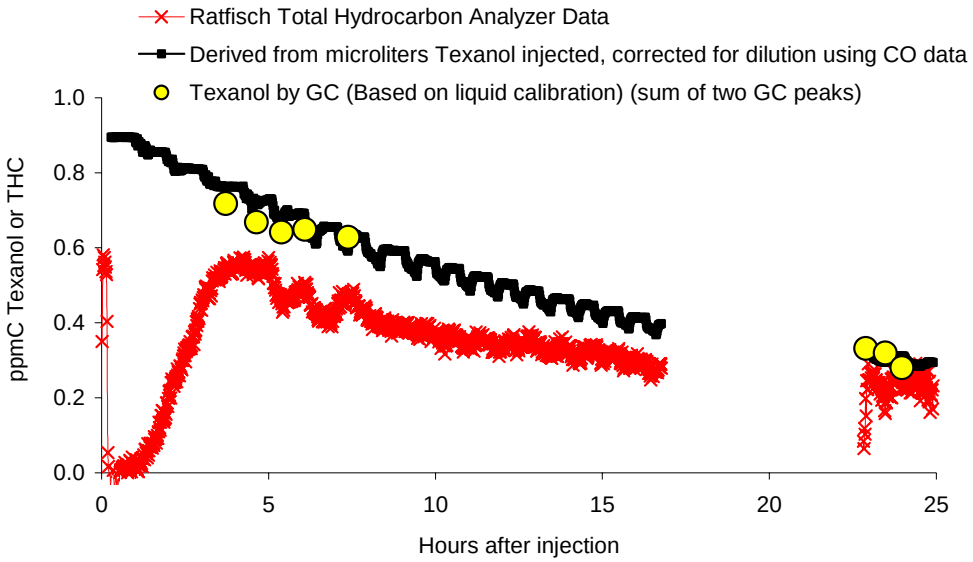

Figure 12. Experimental and calculated Texanol carbon levels in the Texanol injection test experiment.

the amount injected and corrected for dilution using the CO data, the Texanol analysis by GC, and the total carbon analysis (calibrated using propane). The total hydrocarbon data show the increase in Texanol over time during the injection process, and indicate that essentially all the Texanol is injected in less than 5 hours. The GC measurements (calibrated using the methanol solution) are in excellent agreement with the amount of Texanol® calculated from the volume injected and the dilution correction derived from the CO data, indicating that the GC analysis is quantitative and appropriately calibrated. The carbon as determined by the propane-calibrated FID-based Ratfisch total hydrocarbon analyzer was about 75% of the calculated or GC-determined value, suggesting that the propane calibration for the carbon response for this FID instrument is probably not quantitative[4]. A low response would be expected because of the oxygen content of the Texanol® isomers, though probably not this low. Note, however, that the total hydrocarbon data are used only for qualitative indications of how the Texanol® concentrations changed with time, not for determining the amounts of Texanol® injected into the chamber.

It was concluded that we were able to inject and analyze Texanol® quantitatively for the purpose of conducting reactivity chamber experiments. During the chamber experiments with Texanol®, the injection tube was heated to ~110°C and the injection lines were heated to ~125°C, as used in the experiment shown on Figure 12. The injections were carried out for at least 4 hours.

Hydrocarbon Solvents

Because the hydrocarbon solvents studied for this project are complex mixtures of many compounds that are not separate in our GC analyses, it is not practical to determine the amount injected into the gas-phase for our experiments by gas-phase analysis. Instead, it is necessary to calculate the amount injected based on the volume and density of liquid injected and the volume of the reactors. The reactor volumes were determined by comparing measured and injected amounts of NO_x, CO, and other reactants, and tended to be consistent from run to run when using pressure control to fill the reactors (see above). However, this method requires that all of the liquid solvent be completely injected into the gas phase in our injection procedures.

Tests were carried out to assure that the solvents were quantitatively injected into the gas phase using the procedures employed for this purpose as discussed above, and the required injector temperatures. The procedures were similar to those described above for Texanol®, except in this case we had to rely entirely on the Ratfisch total hydrocarbon analysis to determine when all the material was injected. In addition, experiments were conduced with the Ratfisch total hydrocarbon analyzer connected directly to the injection to determine how long it took to completely clear the injection line of hydrocarbon materials. These tests indicated that these solvents were completely injected using the procedures of our experiments. Based on this, for modeling purposes the amounts injected during the experiments were derived from the calculated amounts injected. Note that the Ratfisch total hydrocarbon analyzer was not used during most of the chamber experiments carried out for mechanism evaluation because its measurements were not considered to be sufficiently sensitive or quantitative for determining initial concentrations for modeling purposes.

---

[4] The total hydrocarbon analyzer used for the injection test experiments should not be confused with the total carbon analyzer used in the direct reactivity measurement experiments, which employed a totally different technique than the FID-based Ratfisch used in the injection test experiments.

Results

A chronological listing of the environmental chamber experiments carried out for this project is given in Table A-4 in Appendix A. These included experiments with the test compounds of interest for this study and appropriate characterization and control experiments needed for the data to be useful for mechanism evaluation. As indicated above, most of the experiments with the test compounds were incremental reactivity experiments that consisted of simultaneous irradiations of a standard base case ROG surrogate - NO_x mixture and the same mixture with the test compound added. In addition, an aromatic 100 - NO_x and aromatic 100 - CO - NO_x experiment was also carried out to provide additional mechanism evaluation data for that solvent. The relevant results of the characterization experiments are discussed first, followed by a summary of the results of the experiments with the test compounds. Additional discussions of the experimental results, including plots of significant data, are presented in the following section of this report, in conjunction with a discussion of the mechanism evaluation results using these data.

Characterization Results

The results of the individual characterization experiments that are relevant to the experiments for this project are summarized in the "Results" column of Table A-4 The initial characterization experiments relevant to the characterization of this chamber for are described in detail by Carter (2004a). The experiments carried out through August 2003 overlap those described by Carter (2004a), and thus need not be discussed further here.

The reactors were changed after August, 2003, and the results of the additional characterization runs are included in Table A-4. As with previous runs, there was some run-to-run variability in the characterization results, but the results of the new experiments were within the range of those observed previously. For example, Figure 13 shows the HONO offgasing parameters that best fit the radical or NO_x - sensitive characterization experiments discussed by Carter (2004a) and carried out during the period of this project. Since the results of the newer experiments were within the variability of the second set of

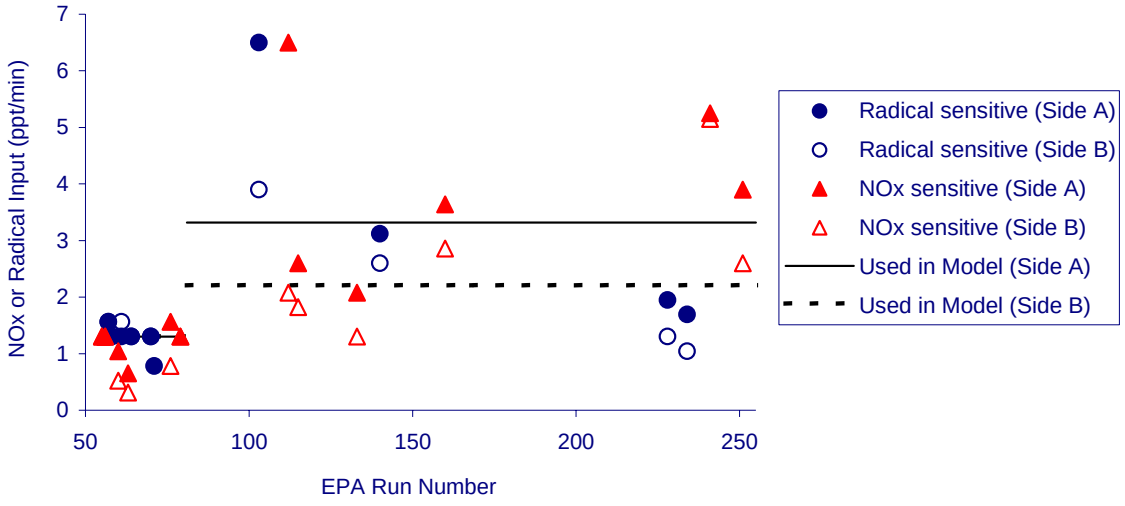

Figure 13. Plots of best fit HONO offgasing parameters against UCR EPA run number. (Data from Carter (2004a), with results of newer experiments for this project added.)

experiments discussed by Carter (2004a), we continued to use the same HONO offgasing parameter assignments when modeling these experiments as employed by Carter (2004a). (Note that the results of the incremental reactivity and hydrocarbon solvent - NO_x experiments are relatively insensitive to this parameter.)

The actinometry and other light characterization results discussed by Carter (2004a) are also applicable to the period of the later experiments discussed in this report. The results of the actinometry experiments carried out during this period indicate that the NO_2 photolysis rate of 0.260±0.004 min^{-1} is appropriate for modeling all the arc light irradiated experiments for this project. The spectral distribution measurements taken during this period also indicated no significant change in the arc light spectral distribution during this period.

The results of the side equivalency test experiments are shown on Table 10, where they can be compared with the results of the incremental reactivity experiments with added test compounds. These are discussed below in conjunction with the discussion of the incremental reactivity experiments with the added test compounds.

Mechanism Evaluation Experiments

Table 10 lists the initial concentrations and selected results for the incremental reactivity and the solvent - NO_x experiments with the coatings solvents carried out for this project and also for the n-octane and m-xylene incremental reactivity experiments carried out for comparison purposes. Concentration-time plots of selected data are given in the Mechanism Evaluation Results section, where they are compared with model predictions. In this section, we summarize briefly the data on Table 10 and the overall reactivity characteristics of these test compounds observed in these experiments. The implications of the results of these experiments for our ability to model the atmospheric impacts of these compounds or mixtures are discussed in the Mechanism Evaluation Results and Discussion sections.

The measures of gas-phase reactivity used for the added test compounds in the incremental reactivity experiments are the effects of the test compound or solvent on $\Delta([O_3]-[NO])$, or $([O_3]_t-[NO]_t)-([O_3]_0-[NO]_0)$, and IntOH, the integrated OH radical levels. As discussed elsewhere (e.g., Johnson, 1983; Carter and Atkinson, 1987; Carter and Lurmann, 1991, Carter et al, 1993), $\Delta([O_3]-[NO])$ gives a direct measure of the amount of conversion of NO to NO_2 by peroxy radicals formed in the photooxidation reactions, which is the process that is directly responsible for ozone formation in the atmosphere. This gives a useful measure of factors affecting O_3 reactivity even early in the experiments where O_3 formation is suppressed by the unreacted NO. Although this is the primary measure of the effect of the VOC on O_3 formation, the effect on radical levels is also a useful measure for mechanism evaluation, because radical levels affect how rapidly all VOCs present, including the base ROG components, react to form ozone.

The integrated OH radical levels are not measured directly, but can be derived from the amounts of consumption of reactive VOCs that react only with OH radical levels. In particular,

$$\mathrm{IntOH}_t = \frac{\ln([\mathrm{tracer}]_0/[\mathrm{tracer}]_t) - \mathrm{Dt}}{\mathrm{kOH}^{\mathrm{tracer}}} \qquad \text{(VII)}$$

where $[tracer]_0$ and $[tracer]_t$ are the initial and time t concentrations of the compound used as the OH tracer, kOH^{tracer} its OH rate constant, and D is the dilution rate in the experiments. The latter is small in our chamber and is neglected in our analysis. For most experiments, the base ROG surrogate component m-xylene is the most reactive compound in the experiment that reacts only with OH radicals, and was therefore used as the OH tracer to derive the IntOH data. However, in the Aromatic 100 - NO_x and

Table 10. Summary of initial concentrations and selected gas-phase results of the incremental reactivity and solvent - NO_x experiments.

Run	Test Type [a] Side		Added	Base Run Initial Concentrations NOx (ppb)	ROG (ppmC)	Hours	Final O_3 (ppb) Test	Base	$\Delta([O_3]-[NO])$ Change (ppb) 2 Hr	Final	IntOH Change (ppt-min)
				Side Equivalency Tests							
143	B	MIR		29	0.53	6	166	159	2	7	10
235	B	MIRa		32	0.55	5	164	160	4	4	3
159	B	MOIR/2		22	1.02	4	151	149	0	0	1
227	B	MOIR/2a		25	1.10	6	168	167	2	2	2
233	B	MOIR/2a		27	1.11	6	175	175	2	0	0
				n-Octane (measured ppm added)							
113	B	(C/N=14)	0.23	69	1.03	6	223	253	-29	-27	-30
114	B	MIR	0.11	31	0.57	4	110	133	-23	-21	-28
83	B	(C/N=20)	0.25	48	1.01	6	234	237	-20	0	-26
95	A	MOIR/2	0.20	25	0.80	5	146	152	-9	-3	-21
85	B	(C/N=100)	0.24	10	1.11	6	74	90	-8	-16	-10
				m-Xylene (measured ppm added)							
128	B	(C/N=10)	0.016	48	0.57	5	199	131	59	68	22
108	A	(C/N=14)	0.011	76	0.90	5	263	208	58	57	8
110	A	MIR	0.012	31	0.60	5	167	144	45	18	-3
84	A	(C/N=20)	0.028	51	1.16	6	255	258	41	-7	-3
123	B	MOIR/2	0.026	22	0.99	6	139	159	-7	-19	-8
100	B	(C/N=50)	0.014	5	0.33	6	58	67	-3	-10	-11
86	B	(C/N=100)	0.037	10	1.08	6	78	96	-12	-19	-4
				Texanol® (measured ppm added)							
229	A	MIRa	0.077	32	0.66	5	156	157	-7	-1	-20
230	B	MIRa	0.095	33	0.60	5	156	154	-5	1	-23
231	B	MOIR/2a	0.107	27	1.12	5	161	157	-2	1	-12
232	A	MOIR/2a	0.139	27	1.12	6	170	172	1	-1	-13
				VMP Naphtha solvent (calculated ppmC added)							
137	B	MIR	0.90	29	0.59	5	140	156	-26	-16	
238	A	MIRa	1.20	33	0.56	6	143	167	-56	-47	
126	B	MOIR/2	0.92	23	1.03	5	137	154	-13	-16	
243	B	MOIR/2a	0.90	27	1.17	6	156	171	-11	-14	-25
				ASTM-1C solvent (calculated ppmC added)							
168	A	MIR	0.90	28	0.55	6	132	171	-44	-41	-40
152	B	MOIR/2	0.91	25	0.93	6	141	161	-18	-20	-19
				ASTM-1B solvent (calculated ppmC added)							
151	A	MIR	0.90	30	0.56	6	153	175	-27	-24	-43
139	B	MOIR/2	0.90	20	0.90	6	133	147	-9	-14	-19
242	B	MOIR/2a	0.90	26	1.16	5	144	160	-13	-15	-16

Table 10 (continued)

Run	Test Side	Type [a]	Added	Base Run Initial Concentrations NOx (ppb)	ROG (ppmC)	Hours	Final O_3 (ppb) Test	Base	$\Delta([O_3]-[NO])$ Change (ppb) 2 Hr	Final	IntOH Change (ppt-min)
				ASTM-1A solvent (calculated ppmC added)							
167	B	MIR	0.90	30	0.56	6	168	168	13	1	-25
153	A	MOIR/2	0.97	24	1.02	6	146	170	-8	-23	-23
240	A	MOIR/2a	1.21	27	1.16	6	150	171	-13	-23	-21
				Aromatic 100 solvent (calculated ppmC added)							
127	A	MIR	0.52	29	0.56	5	157	147	52	7	-19
244	B	MIRa	0.31	32	0.63	6	179	175	48	4	-11
124	A	MOIR/2	0.52	23	1.07	5	132	147	-8	-17	-12
239	A	MOIR/2a	0.76	27	1.20	6	142	172	-13	-29	-14
136 [b]	A	Solvent - NO_x + CO	0.90	46	87 ppm CO	6	382		269 [c]	415 [c]	18 [c]
136 [b]	B	Solvent - NO_x	0.90	45	None	6	218		182 [c]	253 [c]	48 [c]
				ASTM-3C1 solvent (calculated ppmC added)							
163	A	MIR	0.89	24	0.53	6	137	158	-23	-24	-31
138	B	MOIR/2	0.90	22	1.05	6	159	144	2	15	-10
150	B	MOIR/2	0.84	23	1.03	5	155	159	1	-2	-11
237	B	MOIR/2a	1.20	26	1.13	6	168	174	-2	-6	-14

[a] Codes for types of base case experiments for the incremental reactivity experiments are as follows: "MIR": ~30 ppb NO_x, and ~0.5 ppmC 8-component ROG surrogate with formaldehyde; "MIRa": ~30 ppb NO_x and ~0.55 ppmC 7-component ROG surrogate without formaldehyde; "MOIR/2": ~25 ppb NO_x and ~1 ppmC 8-component ROG surrogate with formaldehyde; and "MOIR/2a": ~25 ppb NO_x and ~1.1 ppmC 7-component surrogate without formaldehyde. For reactivity experiments with other ROG or NO_x levels the ROG/NO_x ratio (C/N) is given.

[b] No base case ROG surrogate added; not an incremental reactivity experiment. Equal Aromatic-100 and NO_x injections in both sides, with CO added to Side A.

[c] Values shown are 2-hour and final $\Delta([O_3]-[NO])$ and final IntOH in the reactors.

Aromatic 100 - CO - NO_x experiments EPA136, the aromatic 100 constituent 1,2,4-trimethylbenzene was used as the OH tracer because it was present in relatively high levels and was well resolved by GC from the other reactants. The m-xylene and 1,2,4-trimethylbenzene OH radical rate constants used in this analysis were 2.36×10^{-11} and 3.25×10^{-11} cm^3 $molec^{-1}$ s^{-1}, respectively (Atkinson, 1989).

The side equivalency tests, where equal base ROG - NO_x mixtures are simultaneously irradiated without added test compounds, provide a measure of the sensitivity of the experiments to distinguish the effects of the added VOCs. Except for run 143, the side equivalency for the gas-phase measurements was excellent, with the O_3 and $\Delta([O_3]-[NO])$ differences being no greater than ~5 ppb and the IntOH differences being less than 5 ppt-min. The differences for run 143 were somewhat greater, but still less than the effects of the added VOCs for most of the other reactivity experiments listed on Table 10. The reason for the greater than usual non-equivalency for the side equivalency test run 143 is unknown.

Before discussing the results of the incremental reactivity experiments with the various compounds or mixtures, it is important to emphasize that incremental reactivities in the chamber are not necessarily those in the atmosphere. The purpose of the experiments is to test the predictive capabilities of the mechanisms, as discussed in the following section of this report. Although the experiments are designed to represent a range of *chemical* conditions applicable to the atmosphere, it is not practical to duplicate atmospheric conditions exactly, and different aspects of the mechanism have somewhat different relative importances in affecting the results of chamber experiments than in model simulations of the atmosphere. This is discussed further in the "Discussion and Conclusions" section of this report, where specific examples of the differences are presented.

The incremental reactivity experiments with n-octane were carried out at a variety of base case ROG and NO_x levels, with the ROG/NO_x ratios ranging from ~14 to 100. (The runs in Table 10 are listed in order of ascending ROG/NO_x ratios.) N-octane was found to have negative effects on both $\Delta([O_3]-[NO])$ and IntOH in all these experiments, though the magnitude of the effects tended to decrease somewhat as the ROG/NO_x ratio increased. The effects of n-octane on the initial NO oxidation and O_3 formation rates and the overall IntOH levels were uniformly negative, while the effects on the final O_3 levels were more variable, being relatively small for runs with ROG/NO_x ratios in the 20-30 range, but larger in the higher and lower ROG/NO_x runs.

The incremental reactivity experiments with m-xylene were also carried out at a variety of base case ROG and NO_x levels, with the ROG/NO_x ratio ranging from ~10 to 100. The effects of the m-xylene on the results were more strongly dependent on the ROG/NO_x ratios than was the case for n-octane. In the MIR and lower ROG/NO_x experiments the m-xylene had a uniformly positive effect on NO oxidation and O_3 formation, and it also had a slightly positive effect on IntOH in the lowest ROG/NO_x experiments. However, as the ROG/NO_x ratio increased above the MIR level the effect on the final O_3 level became small then negative and at sufficiently high ROG/NO_x the effect on the two-hour $\Delta([O_3]-[NO])$ also became negative. The effect of m-xylene on IntOH was also slightly negative at the higher ROG/NO_x ratios. This is consistent with results of previous incremental reactivity experiments with aromatics (Carter et al, 1995a).

The addition of Texanol® was found to have essentially no effect on NO oxidation or O_3 formation in either the MIR or MOIR/2 experiments, to within the uncertainty of the determination. On the other hand, the Texanol® was found to significantly reduce overall OH radical levels, with the effect being somewhat greater in the MIR runs than in the lower NO_x experiments. The negative effect on IntOH indicates that the added Texanol® is indeed affecting the chemistry of the system, even if the apparent O_3 is not changing. Apparently, the negative effect on O_3 caused by Texanol®'s radical inhibiting characteristics is almost exactly balanced by the positive effects of the O_3 formation caused by its direct reactions. It is surprising, however, that the balance would be nearly the same at the two ROG/NO_x ratios employed in our study.

The results of the incremental reactivity experiments with the primarily alkane petroleum distillates designated VMP Naphtha ASTM-1C, and ASTM-1B were very similar to those for n-octane, with uniformly negative effects on both $\Delta([O3]-[NO])$ and IntOH in all experiments, with the effects becoming somewhat less in the higher ROG/NO_x MOIR/2 experiments. The results with the 19% aromatic mixture ASTM-1A were between those for n-octane and m-xylene, having a uniformly negative effect on IntOH negative effects on $\Delta([O_3]-[NO])$ at the high ROG/NO_x experiments, but tending to have more positive effects on $\Delta([O_3]-[NO])$ (especially initially) in the low ROG/NO_x "MIR" experiments. This intermediate behavior is is as expected based on its composition.

One would expect the synthetic primarily branched alkane mixture ASTM-1B to have similar reactivity characteristics as n-octane and the primarily alkane hydrocarbon solvents, and as expected it

had negative effects on IntOH in all the experiments and negative effects on $\Delta([O_3]-[NO])$ in the MIR experiments. However, the effects on $\Delta([O_3]-[NO])$ in the higher NO_x MOIR/2 experiments is much smaller than expected and even positive in some experiments. Apparently the chemical reactivity characteristics of the alkanes in this mixture are different than those of the alkanes in the petroleum distillate-derived mixtures.

The results of the incremental reactivity experiments with Aromatic 100 were similar to those with m-xylene in that the effect on NO oxidation and O_3 formation was positive in the low ROG/NO_x experiments, but became negative in the higher ROG/NO_x MOIR/2 experiments. It was also similar to comparable experiments with m-xylene and toluene (Carter, 2004a) in that the addition of CO to the aromatic - NO_x irradiations caused both an increase in O_3 and a decrease in overall OH radicals. On the other hand, unlike the case for the m-xylene reactivity runs, the Aromatic 100 caused a decrease of IntOH in all experiments, not just those with high ROG/NO_x ratios. Therefore, the reactivity characteristics of the Aromatic 100 mixture, which contains higher molecular weight aromatics, are similar to, but not exactly the same, as that for the lighter aromatics such as m-xylene

It is important to recognize that although these experiments are designed to approximate the chemical environments in which the VOCs react, the actual magnitudes, and in some cases signs, of the impacts of the compounds or solvents in real atmospheres may be different than in any particular experiment. The ability of the current mechanism's to simulate the results of these experiments, and the implications concerning the atmospheric impacts of these solvents, are discussed in the "Mechanism Evaluation" section, below.

OH Radical Rate Constant Determination for the Texanol® isomers

Texanol® is a mixture of two isomers, 3-hydroxy-2,2,4-trimethylpentyl-1-isobutyrate and 1-hydroxy-2,2,4-trimethylpentyl-3-isobutyrate, that are referred to as "Texanol 1" and "Texanol 2" in the subsequent discussion. Their structures are shown on Table 11. There are no known experimental data concerning the rate constant for the reaction rate constant for the reaction with OH radicals despite the fact that this is an important factor affecting the compounds' reactivity. The current SAPRC-99 mechanism uses rate constants for these isomers that were derived by structure-reactivity estimates of Kwok and Atkinson (1995), applied as discussed by Carter (2000a). These are also given in Table 11.

Although measuring OH radical rate was not in the scope of this project, we found that the GC analysis employed in our laboratory using the Tenax cartridge method gave sufficiently precise measurements of these isomers in the gas phase to make a relative rate constant determination feasible. The two isomers were found to be well separated in our GC analyses, with the retention times and relative amounts (assuming equal response for the isomers on the FID detector) being as shown in Table 11. Note that the relative amounts of the two isomers when injected to the gas phase were consistent from analysis to analysis and experiment to experiment, but were different from when analyzed in a liquid solution.

If it is assumed that the Texanol® isomers react in our experiments only with OH radicals, then the ratio of OH radical rate constants with other compounds present that also only react with OH can be determined from their relative rates of decay. In this case, the kinetic differential equations for the organics can be solved and rearranged to yield

$$\ln\left(\frac{[\text{Organic}]_{t0}}{[\text{Organic}]_t}\right) - D_t = \frac{k_{\text{Organic}}}{k_{\text{Reference}}} \ln\left[\left(\frac{[\text{Reference}]_{t0}}{[\text{Reference}]_t}\right) - D_t\right] \qquad \text{(VIII)}$$

where $[\text{Organic}]_{t0}$ and $[\text{Organic}]_t$, $[\text{Reference}]_{t0}$, and $[\text{Reference}]_t$ are the initial and time=t concentrations of the test and reference compounds, respectively, k_{Organic} and $k_{\text{Reference}}$ are the test and reference

Table 11. Information on the Texanol® isomers relevant to this project.

Isomer [a]	3-Hydroxy-2,2,4-Trimethylpentyl-1-Isobutyrate	1-Hydroxy-2,2,4-Trimethylpentyl-3-Isobutyrate
Structure	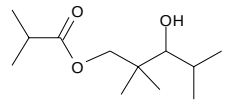	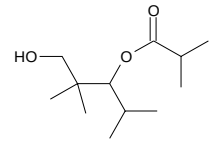
SAPRC-99 Model Species	TEXANOL1	TEXANOL2
GC Retention Time on 30 m x 0.53 mm DB-1701 column (min)	15.0	14.8
Fraction in mixture		
Liquid analysis [b]	68%	32%
Gas phase analysis [c]	58%	42%
OH Radical Rate constants (cm^3 $molec^{-1}$ s^{-1})		
SAPRC-99 estimation (Carter, 2000a)	1.62×10^{-11}	1.29×10^{-11}
Derived from chamber data (this work) [d]	1.68×10^{-11}	1.30×10^{-11}
MIR (gm O_3 /gm Isomer) [e]	0.86	0.91

[a] Assignments of GC peaks to individual isomers were made based on results of discussions with Rodney J. Boatman of Eastman Kodak Company.

[b] In methanol solution.

[c] Average of initial concentrations in the incremental reactivity experiments.

[d] Derived relative to m-xylene from relative rates of decay in the incremental reactivity experiments as discussed in the text. Relative to the OH rate constant for m-xylene of 2.36×10^{-11} cm^3 $molec^{-1}$ s^{-1} (Atkinson, 1989).

[e] Maximum Incremental Reactivity as predicted by current SAPRC-99 mechanism (Carter, 2000a), calculated using estimated OH rate constants.

compound's OH rate constant, and D_t is a factor added to account for dilution, which is assumed to be zero in our experiments. Therefore plots of $\ln([Organic]_{t0}/[Organic]_t)$ against $\ln([Reference]_{t0}/[Reference]_t)$ should yield a straight line with intercept of approximately zero and a slope that is the ratio of rate constants. Given the known value of $k_{Reference}$, then $k_{Organic}$ can then be derived.

m-Xylene is chosen as the reference compound because it is the most rapidly reacting compound in our experiments that reacts significantly only with OH radicals, and its OH radical rate constant is well known. The m-xylene and Texanol® isomer data taken during our Texanol® incremental reactivity experiments are given in Table 12, and plots of Equation (VIII) derived from these data are given on Figure 14. The slopes of these plots for the individual experiments, and those derived from fits to all the data (as shown on the figure) are also given on Table 12

Except for one point for isomer 2, all the data are well fit by Equation (VIII) assuming no dilution, with relatively little scatter and no discernable curvature, and no significant differences between

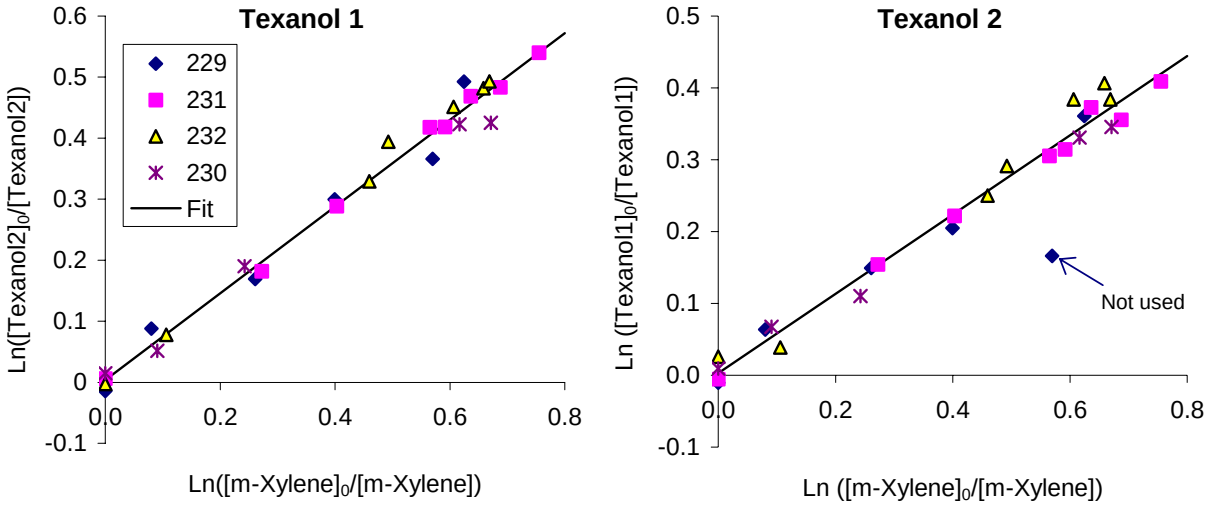

Figure 14. Plots of Equation (VIII) for the data from the Texanol® reactivity experiments.

the experiments. The OH radical rate constants derived from the fits to all the data, assuming an m-xylene OH rate constant of 2.36 x 10^{-11} cm^3 $molec^{-1}$ s^{-1} (Atkinson, 1989), are given on Table 11, above. It can be seen that the agreement with the estimated values is remarkable. Because the estimated values already incorporated in the SAPRC-99 mechanism agree with these experimental measurements to within the experimental uncertainty, no change was made to the SAPRC-99 mechanisms for these isomers as a result of these data.

Table 12. Data used for OH radical rate constant determinations for the Texanol® isomers.

Time (min)	GC Analyses (ppb)			Rate Constant Ratio Relative to m-Xylene	
	m-Xylene	Texanol 1	Texanol 2	Texanol 1	Texanol 2
		Run EPA229A			
Initial [a]	8.9	37.9	29.5		
103	8.9	38.4	29.8		
141	8.2	34.7	27.7		
179	6.9	32.0	25.4	0.72	0.56
220	6.0	28.1	24.0		
275	5.0	26.2	25.0 [b]		
318	4.8	23.1	20.5		
357	3.2	14.5	19.8		
		Run EPA231B			
Initial	24.7	64.7	44.4		
-21	24.7	64.3	44.7		
55	18.8	53.9	38.1		
90	16.5	48.5	35.6		
168	14.1	42.6	32.8	0.72	0.54
208	13.7	42.6	32.5		
235	13.1	40.5	30.6		
266	12.4	39.9	31.1		
338	11.6	37.7	29.5		
		Run EPA232A			
Initial	24.2	83.0	57.4		
-4	24.2	83.2	56.0		
42	21.7	76.7	55.3		
179	15.3	59.7	44.7	0.74	0.60
219	14.8	55.9	42.9		
299	13.2	52.8	39.1		
339	12.5	51.2	38.2		
362	12.4	50.7	39.1		
		Run EPA230B			
Initial	13.0	55.1	40.7		
-8	13.0	54.3	40.3		
45	11.8	52.3	38.0		
92	10.2	45.6	36.4	0.70	0.54
182	7.0	36.1	29.2		
217	6.6	36.0	28.8		
299	5.1	29.4	24.8		
340	4.4	24.9	22.1		
		Fits to All Data			
				0.71	0.55

[a] The initial concentration Equation (VIII) for each experiment was set to force a zero intercept for plots of Equation (VIII) for the experiment.

[b] This measurement is believed to be anomalous and was not used when computing the slopes or intercepts.

MECHANISM EVALUATION

Modeling methods

Standard Chemical Mechanism

The chemical mechanism evaluated in this work is the SAPRC-99 mechanism as documented by Carter (2000a). A complete listing of this mechanism is given by Carter (2000a) and in subsequent reports from our laboratory where this mechanism was used, all of which are available either as previous reports to the CARB or on our web site[5]. Files and software implementing this chemical mechanism are also available at our web site[6], with the chemical mechanism simulation computer programs available there being essentially the same as those employed in this work. Although changes have been made to the mechanisms of some individual VOCs due to subsequent experimental studies and reactivity assessment projects (Carter, 2003a), the affected VOCs do not include the Texanol® constituents or the hydrocarbon constituents of the complex hydrocarbon solvents studied for this project. Some changes were made to portions of the mechanism as part of the evaluation for this work, and these are discussed where applicable below.

As discussed previously (Carter, 2000a,b), the SAPRC-99 mechanism consists of a "base mechanism" that represents the reactions of the inorganic species and common organic products and lumped organic radical model species and "operators", and separate mechanisms for the initial reactions of the many types other organic compounds that are not in the base mechanism. The compounds, or groups of compounds, that are not included in the base mechanism but for which mechanism assignments have been made, are referred to as detailed model species. The latter include all the base ROG surrogate constituents and components of the solvents whose reactivities were evaluated in this work. These compounds can either be represented explicitly, with separate model species with individual reactions or sets of reactions for each, or using lumped model species similar to those employed in the "fixed parameter" version of SAPRC-99 (Carter, 2000b). The latter approach is useful when modeling complex mixtures in ambient simulations or simulations of experiments with complex mixtures, but the other approach, representing each compound explicitly, is more appropriate when evaluating mechanisms for individual compounds or simple mixtures. This is because the purpose of mechanism evaluations against chamber data is to assess the performance of the mechanism itself, not to assess the performance lumping approaches. The latter is most appropriately assessed by comparing simulations of explicit and condensed versions of the same mechanism in ambient simulations.

In view of this, all of the organic constituents of the base ROG surrogate were represented explicitly using separate model species for each compound. In addition, the two Texanol® isomers were also represented explicitly using separate model species in the model simulations of the experiments with this solvent. This gives the most explicit representation of the atmospheric reactions of these compounds within the framework of the SAPRC-99 mechanism.

However, this approach is not practical when modeling experiments with the petroleum distillates or synthetic hydrocarbon mixtures, which are mixtures represented by many detailed model species (see

---

[5] These reports can be downloaded from http://www.cert.ucr.edu/~carter/bycarter.htm.

[6] Files and software implementing the SAPRC-99 mechanism are available at http://www.cert.ucr.edu/~carter/SAPRC99.htm.

Table A-1 through Table A-3 in Appendix A for the detailed model species assignments for the hydrocarbon mixtures modeled for this project). Therefore, when modeling experiments with those mixtures the components that are not represented explicitly are lumped together in the same way that they would be if represented in ambient simulations using the "adjustable parameter" of the SAPRC-99 condensed mechanism (Carter, 2000b). This lumping approach, as applicable to the mixtures used in this study, is based on grouping compounds of the same type within given ranges of OH radical rate constants as indicated in Table 13. The kinetic and mechanistic parameters for the model species used to represent these mixture components, referred to as "lumped groups" in Table 13, are the weighed averages of those for the mixture of compounds they represent. Note that this is the same as the approach as used in this work, and by Carter (2000a), when calculating when calculating the atmospheric reactivities of these mixtures in the MIR and other reactivity scales.

Many of the components of the hydrocarbon mixtures were not identified as specific compounds, but as generic types such as "branched C8 alkanes". In those cases, it is necessary to assign mixtures of actual compounds that are assumed to be representative of the generic group in order to represent them in the mechanism. Other compounds (generally relatively minor constituents or high molecular weight compounds) are not represented explicitly, but are represented by another compound that is assumed to have approximately the same mechanism, using the "lumped molecule" approach. Assignments of individual compounds to mixtures or lumped molecule assignments that are applicable to the hydrocarbon mixtures studied in this report are given in Table 14.

Adjusted Mechanisms

As discussed by Carter (2004a), and also in the following section, the SAPRC-99 mechanism has a consistent bias to underpredict O_3 formation in the surrogate - NO_x irradiations at the lower ROG/NO_x ratios. This bias showed up in a consistent underprediction of O_3 in the base case of the standard MIR incremental reactivity experiment for this project. This bias should to some extent cancel out when

Table 13. Lumping method used when representing complex hydrocarbon mixtures in the model simulations for this project.

Hydrocarbon type	Lumped group [a]	OH Radical Rate Constant Range (cm^3 $molec^{-1}$ s^{-1}) Minimum	Maximum
Alkanes	ALK3	1.70e-12	3.41e-12
	ALK4	3.41e-12	6.81e-12
	ALK5	6.81e-12	-
Aromatics	ARO1	-	1.36e-11
	ARO2	1.36e-11	
Alkenes (excluding ethene)	OLE1	-	4.77e-11
	OLE2	4.77e-11	-

[a] The kinetic and mechanistic parameters for these model species were adjusted based on weighted averages of those for the compounds they represented in the simulation. Only groups applicable to the hydrocarbon mixtures studied in this work are shown.

Table 14. Lumped molecule representations used when representing the complex mixture hydrocarbon solvents.

Compound or Mixture	Representation in Mechanism			
	Fac	Compound	Fac	Compound
		Generic Mixture Assignments - Standard Representation (Used in all calculations unless noted otherwise. All representations made on a per-molecule basis)		
Branched C8 Alkanes	0.5	2,4-Dimethyl Hexane	0.25	4-Methyl Heptane
	0.25	2-Methyl Heptane		
Branched C9 Alkanes	0.5	2,4-Dimethyl Heptane	0.25	4-Methyl Octane
	0.25	2-Methyl Octane		
Branched C10 Alkanes	0.5	2,6-Dimethyl Octane	0.25	4-Methyl Nonane
	0.25	2-Methyl Nonane		
Branched C11 alkanes	0.5	2,6-Dimethyl Nonane	0.25	4-Methyl Decane
	0.25	3-Methyl Decane		
Branched C12 Alkanes	0.5	3,6-Dimethyl Decane	0.25	5-Methyl Undecane
	0.25	3-Methyl Undecane		
Branched C13 Alkanes	0.5	3,6-Dimethyl Undecane	0.25	5-Methyl Dodecane
	0.25	3-Methyl Dodecane		
Branched C14 Alkanes	0.5	3,7-Dimethyl Dodecane	0.25	6-Methyl Tridecane
	0.25	3-Methyl Tridecane		
C7 Cycloalkanes	1	Methylcyclohexane		
C8 Bicycloalkanes	1	Methylcyclohexane		
C8 Cycloalkanes	1	Ethylcyclohexane		
C9 Bicycloalkanes	0.5	Propyl Cyclohexane	0.5	1-Ethyl-4-Methyl Cyclohexane
C9 Cycloalkanes	0.5	Propyl Cyclohexane	0.5	1-Ethyl-4-Methyl Cyclohexane
C10 Bicycloalkanes	0.34	Butyl Cyclohexane	0.33	1-Methyl-3-Isopropyl Cyclohexane
	0.33	1,4-Diethyl-Cyclohexane		
C10 Cycloalkanes	0.34	Butyl Cyclohexane	0.33	1-Methyl-3-Isopropyl Cyclohexane
	0.33	1,4-Diethyl-Cyclohexane		
C11 Bicycloalkanes	0.34	Pentyl Cyclohexane	0.33	1,3-Diethyl-5-Methyl Cyclohexane
	0.33	1-Ethyl-2-Propyl Cyclohexane		
C11 Cycloalkanes	0.34	Pentyl Cyclohexane	0.33	1,3-Diethyl-5-Methyl Cyclohexane
	0.33	1-Ethyl-2-Propyl Cyclohexane		
C10 Monosubstituted Benzenes	1	n-Propyl Benzene		
C11 Monosubstituted Benzenes	1	n-Propyl Benzene		
C12 Monosubstituted Benzenes	1	n-Propyl Benzene		
C10 Disubstituted Benzenes	0.34	m-Xylene	0.33	o-Xylene
	0.33	p-Xylene		
C11 Disubstituted Benzenes	0.34	m-Xylene	0.33	o-Xylene
	0.33	p-Xylene		
C12 Disubstituted Benzenes	0.34	m-Xylene	0.33	o-Xylene
	0.33	p-Xylene		
C10 Tetrasubstituted Benzenes	0.34	1,3,5-Trimethyl Benzene	0.33	1,2,3-Trimethyl Benzene
	0.33	1,2,4-Trimethyl Benzene		
C10 Trisubstituted Benzenes	0.34	1,3,5-Trimethyl Benzene	0.33	1,2,3-Trimethyl Benzene

Table 14 (continued)

Compound or Mixture	Representation in Mechanism			
	Fac	Compound	Fac	Compound
	0.33	1,2,4-Trimethyl Benzene		
C11 Pentasubstituted Benzenes	0.34	1,3,5-Trimethyl Benzene	0.33	1,2,3-Trimethyl Benzene
	0.33	1,2,4-Trimethyl Benzene		
C11 Tetrasubstituted Benzenes	0.34	1,3,5-Trimethyl Benzene	0.33	1,2,3-Trimethyl Benzene
	0.33	1,2,4-Trimethyl Benzene		
C11 Trisubstituted Benzenes	0.34	1,3,5-Trimethyl Benzene	0.33	1,2,3-Trimethyl Benzene
	0.33	1,2,4-Trimethyl Benzene		
C12 Trisubstituted Benzenes	0.34	1,3,5-Trimethyl Benzene	0.33	1,2,3-Trimethyl Benzene
	0.33	1,2,4-Trimethyl Benzene		
C11 Tetralin or Indane	1	Tetralin		
C9 Terminal Alkenes	1	1-Nonene		
C10 Terminal Alkenes	1	1-Decene		
C10 Styrenes	1	Styrene		
Highly Branched Representation of Generic Branched Alkanes (Used in test calculations for ASTM-3C1 only)				
Branched C10 Alkanes	1	2,4,6,-Trimethyl Heptane		
Branched C11 Alkanes	1	2,3,4,6-Tetramethyl Heptane		
Branched C12 Alkanes	1	2,3,5,7-Tetramethyl Octane		
Lumped molecule assignments (Used for compounds not explicitly represented in mechanism)				
m-Ethyl Toluene	1	m-Xylene		
p-Ethyl Toluene	1	p-Xylene		
o-Ethyl Toluene	1	o-Xylene		
o-Diethyl Benzene	1	o-Xylene		
m-Diethyl Benzene	1	m-Xylene		
p-Diethyl Benzene	1	p-Xylene		
n-Butyl Benzene	1	n-Propyl Benzene		
1,2,3,5 Tetramethyl Benzene	0.5	1,2,3-Trimethyl Benzene	0.5	1,2,4-Trimethyl Benzene
Indan	1	Tetralin		
Methyl Indans	1	Tetralin		
1-Methyl Naphthalene	1	Methyl Naphthalenes		
2-Methyl Naphthalene	1	Methyl Naphthalenes		

simulating incremental reactivities because incremental reactivities are differences, and a similar bias would also occur to some extent in the added VOC test experiment. However, the addition of the test compound would change the effective ROG/NO_x ratio, and therefore the magnitude of the underprediction bias may be different than in the base case. Also, the bias means that the model is not correctly simulating the chemical environment in which the VOC is reacting, and could result in inaccurate predictions of the impacts of the reactions of the test compounds, even if their mechanisms are correct. Worse, the possibility of errors in the base case simulation compensating for errors in the mechanism of the test compounds can not necessarily be ruled out.

To assess this, it is useful to provide an alternative approach for evaluating the model performance for the test compounds where the biases in the simulations of the base case is removed or at least modified. Therefore, for this purpose we developed an adjusted version of the base mechanism where the bias is removed, and show the results of the model simulations of the incremental reactivity experiments using this mechanism as well as the standard base mechanism. These modifications are discussed below.

As discussed by Carter (2004a), we suspect that the bias in the model simulations of the ROG surrogate - NO_x experiments at low ROG/NO_x ratios is due to problems with the aromatic mechanisms. Although data were not available at the time to assess this hypothesis, since then we have conducted ROG surrogate - NO_x experiments where the aromatic constituents were removed at a variety of ROG/NO_x ratios, and preliminary results indicates that removal of the aromatics from the mixture tends to remove the bias. The most likely cause is the aromatics mechanisms not having sufficient radical input. This is apparently compensated for by other errors in the mechanism when the mechanism parameters related to radical input were adjusted when the SAPRC-99 mechanism was developed to optimize model fits to results of aromatic - NO_x experiments (Carter, 2000a).

The major adjusted parameter in the SAPRC-99 aromatics mechanisms that affect radical input are the yields of the model species AFG2 and AFG3 that are used to represent the highly photoreactive aromatic ring fragmentation products[7]. As discussed in the following section, it was found that increasing the yields of these two products in the toluene and m-xylene photooxidation mechanisms by a factor of 1.75 resulted in considerably better simulations of the ROG surrogate - NO_x experiments than the standard mechanism.

However, it is important to recognize that these adjusted toluene and m-xylene mechanisms are not necessarily "better" for these compounds, since their use will result in significant overpredictions of rates of O_3 formation in the toluene - NO_x and m-xylene - NO_x experiments used when SAPRC-99 was developed. However, their biases and errors would be different, and results of evaluations using both versions provide useful information on effects of the base mechanism biases on results of incremental reactivity simulations for the test compounds of interest.

It should be noted that some of the hydrocarbon solvents used as test compounds in the chamber experiments contained aromatics, and that m-xylene was used as a test compound in some of the incremental reactivity experiments discussed in this report. Since the purpose of this work is to evaluate the current mechanism for these compounds, most of the evaluations for the aromatic-containing solvents were carried out using the standard SAPRC-99 mechanisms for the aromatics constituents, including toluene and m-xylene[8]. However, simulations of the incremental reactivity experiments for m-xylene and the aromatic-containing solvents using the adjusted toluene and m-xylene mechanisms for both the base case and the added m-xylene were also carried out for comparison. These are discussed below.

---

[7] These two species have similar mechanisms, being different primarily in the action spectrum for their photodecomposition, with their yield ratios adjusted to obtain consistent results in simulations of blacklight and arc light experiments (Carter, 2000a).

[8] The toluene and m-xylene in the ROG surrogate were represented by separate model species than those used for toluene and m-xylene in the hydrocarbon solvents. The latter were represented by ARO1 or ARO2 as indicated in Table 13, with parameters adjusted using standard mechanisms for these compounds. The m-xylene in the m-xylene incremental reactivity test experiment was represented using two model species: the adjusted base mechanism m-xylene species with a concentration equal to that on the base case side, and the standard m-xylene mechanism model species to represent the additional m-xylene that was added.

Representation of Chamber Conditions

The procedures used in the model simulations of the environmental chamber experiments for this project were the same as discussed in detail by Carter (2004a) except as indicated below. As discussed in the previous section, many of the experiments overlapped in time with those modeled and reported by Carter (2004a), and the results of the characterization runs carried out subsequently for this project indicated no significant changes in chamber effects. Therefore the chamber effects model and parameters used in the simulations of the experiments for this project are the same as those used for the simulations of the later series of UCR EPA chamber experiments discussed by Carter (2004a). That report should be consulted for details of the characterization model and chamber effects parameters employed.

The conditions of the specific experiments were also determined as discussed by Carter (2004a), except as indicated. The temperatures used when modeling were the averages of the temperatures measured in the reactors, corrected as discussed by Carter (2004a). The light intensity and spectrum was assumed to be constant, and a constant photolysis rate of 0.260 min^{-1} was used, as indicated by the results of the actinometry measurements. The arc light spectral distribution used by Carter (2004a) was also used in this work because the spectral distribution measurements made during the experiments indicated no significant changes with time.

The initial reactant concentrations used in the model simulations were based on the measured values except for the experiments with the complex hydrocarbon mixtures. In some experiments there was initial concentration data for the base ROG constituents in only one of the two reactors; in those cases we assumed that the concentrations in the other reactor was the same. In the case of the experiments where a complex hydrocarbon mixture was added, the initial mixture component concentrations used for modeling purposes were calculated from the total amount of material injected into the gas phase, derived from the volume of liquid injected, its density and, and the calculated volume of the reactors, assuming complete injection of the material. The assumption of complete injection was supported by results of injection tests carried out with these hydrocarbon mixtures, as discussed above. The volumes of the reactors were determined in separate experiments where known amounts of materials were injected and analyzed in the gas-phase. Although the reactors are flexible, their initial volumes were very consistent from run to run because of the use of the pressure control system when filling the reactor to its maximum volume prior to the reactant injections (see Chamber Description section, above, and Carter, 2004a). The procedures used for representing the VOC constituents in the model were discussed in the previous section.

Atmospheric Reactivity Simulations

Although conducting atmospheric reactivity model simulations was not a major component of this project, a few such calculations were carried out for discussion purposes. In those cases the scenarios and methods used were the same as those used when calculating the MIR and other atmospheric ozone reactivity scales as described previously (Carter, 1994a,b 2000a). The base ROG constituents were represented using the lumping procedures incorporated in the condensed version of the SAPRC-99 mechanism (Carter, 2000b), and individual compounds whose reactivities were being assessed were represented explicitly. Complex hydrocarbon mixtures were represented in the ambient simulations using the same lumping procedures as employed when simulating the chamber experiments with these mixtures, as described above.

Simulations of Base Case Experiments

Effect of Mechanism Adjustments

In order to be able to use results of incremental reactivity experiments to evaluate mechanisms for the added test VOCs, it is necessary that the mechanism adequately simulate the results of the base case experiment, otherwise the environment where the test compounds react would not be appropriately represented in the model, and the evaluation may yield misleading results. As reported previously (Carter, 2004a) we have previously carried out a large number of experiments in the UCR EPA chamber using the same or similar ROG surrogate but at varying initial ROG and NO_x levels to provide a comprehensive test for the mechanism for this simulated ambient mixture. Although the results of the experiments at high ROG/NO_x ratios were reasonably well simulated, the model had a consistent bias towards underpredicting reactivity at lower ROG/NO_x ratios. This is shown on Figure 15, which gives plots of model underprediction bias for $\Delta([O_3]-[NO])$ for the ambient ROG surrogate experiments reported by Carter (2004a), and also for the base case experiments used in this study. The ranges of ROG/NO_x ratios for most of the base case experiments for this project are also shown.

It can be seen from Figure 15 that the standard SAPRC-99 mechanism gives reasonably good simulations of the final $\Delta([O_3]-[NO])$ in the MOIR/2 experiments, but has a consistent underprediction bias in the simulations of the MIR experiments. This can also be seen in Figure 16, which gives experimental and calculated $\Delta([O_3]-[NO])$ for representative base case experiments carried out for this project. (Plots for all the experiments are shown on in Figure 22 through Figure 30 in the next section.) This presents a potential problem in using the results of these MIR experiments when evaluating mechanisms for the test compounds.

As indicated in the previous section, the mechanisms for the toluene and the m-xylene in the base ROG surrogate can be adjusted to reduce this underprediction bias. The effect of this adjustment on the dependence of the model underprediction bias on the initial ROG/NO_x ratios for these ambient surrogate runs is also shown on Figure 15 and Figure 16. It can be seen that this adjustment removes the underprediction bias for the MIR experiments without significantly affecting the model performance in simulating the MOIR/2 experiments, with the mechanism overall having a slight *overprediction* bias in the simulations of both sets of experiments. The model still has a tendency to underpredict rates of O_3 formation and NO oxidation in the experiments at ROG/NO_x ratios lower than MIR, but simulations of those very low ROG/NO_x experiments are very sensitive to uncertainties in initial reactant concentrations and variable chamber effects, and the model simulation results are consequently much more variable.

The data from these experiments are also being used to assess model performance in simulations of the effects of the test compounds on overall radical levels, which is measured by the IntOH quantity described from the rates of decay of m-xylene in the experiments. Therefore, Figure 15 also shows how the dependence of the model underprediction bias on IntOH depends on the initial ROG/NO_x ratio, and experimental and calculated time series plots for IntOH are also shown on Figure 16 for selected experiments.

It can be seen that the standard mechanism also consistently underpredicts OH levels in the base case experiments, though the dependence on the ROG/NO_x ratio is different. In this case, the underprediction bias is approximately independent of the initial ROG/NO_x at MIR and higher ROG/NO_x ratios, and, contrary to the trend for $\Delta([O_3]-[NO])$, the bias tends to become less as the ROG/NO_x ratio decreases below MIR levels. Perhaps surprisingly, adjusting the aromatics mechanism to increase radical input has relatively little effect on the final IntOH predictions at the low and moderate to high ROG/NO_x ratios, with the effect being greatest under MIR conditions. Adjusting the mechanism to improve fits to fits to $\Delta([O_3]-[NO])$ MIR base case experiments improves the fits only slightly for INTOH in those

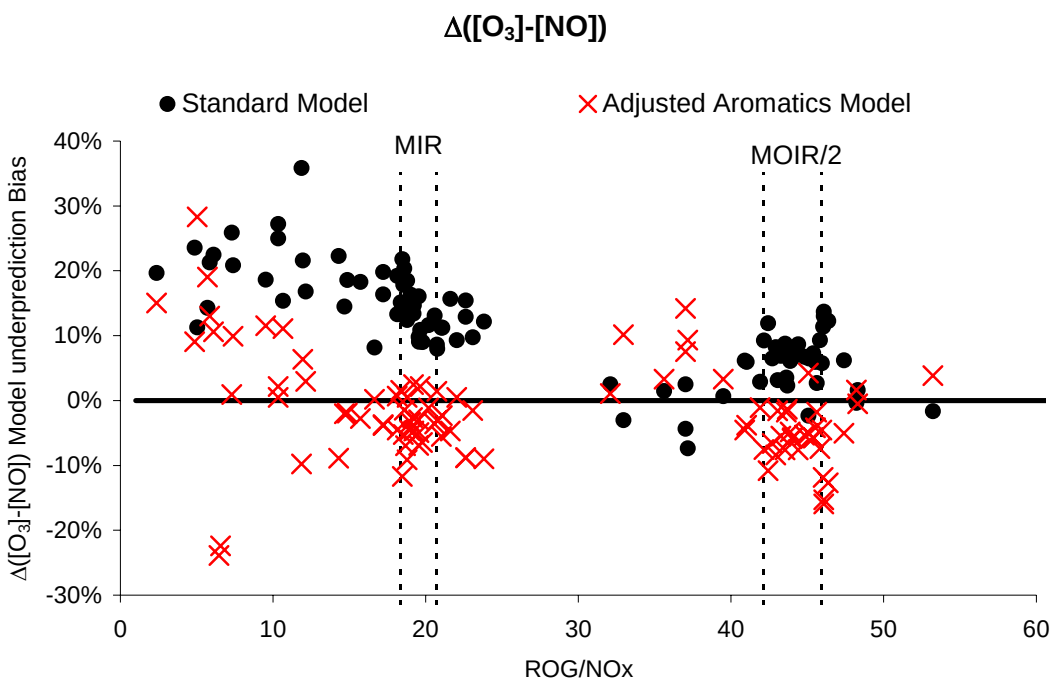

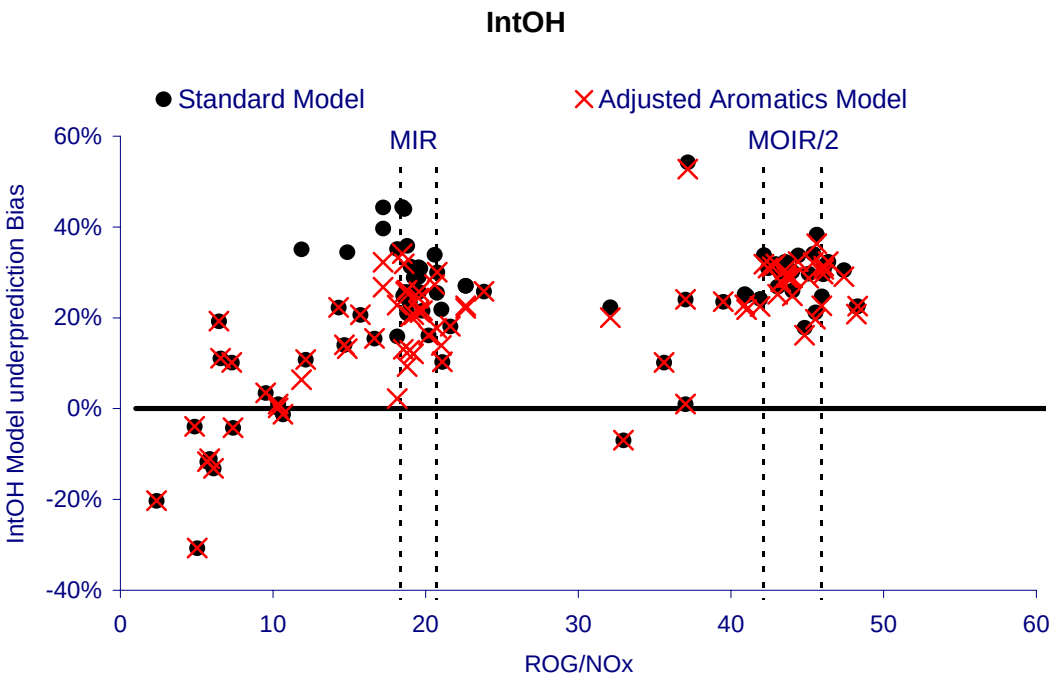

Figure 15. Dependence of the Δ([O3]-[NO]) and IntOH model underprediction bias on initial ROG/NO_x ratio in the surrogate - NO_x experiments for the SAPRC-99 model calculations using the standard and adjusted aromatics mechanisms.

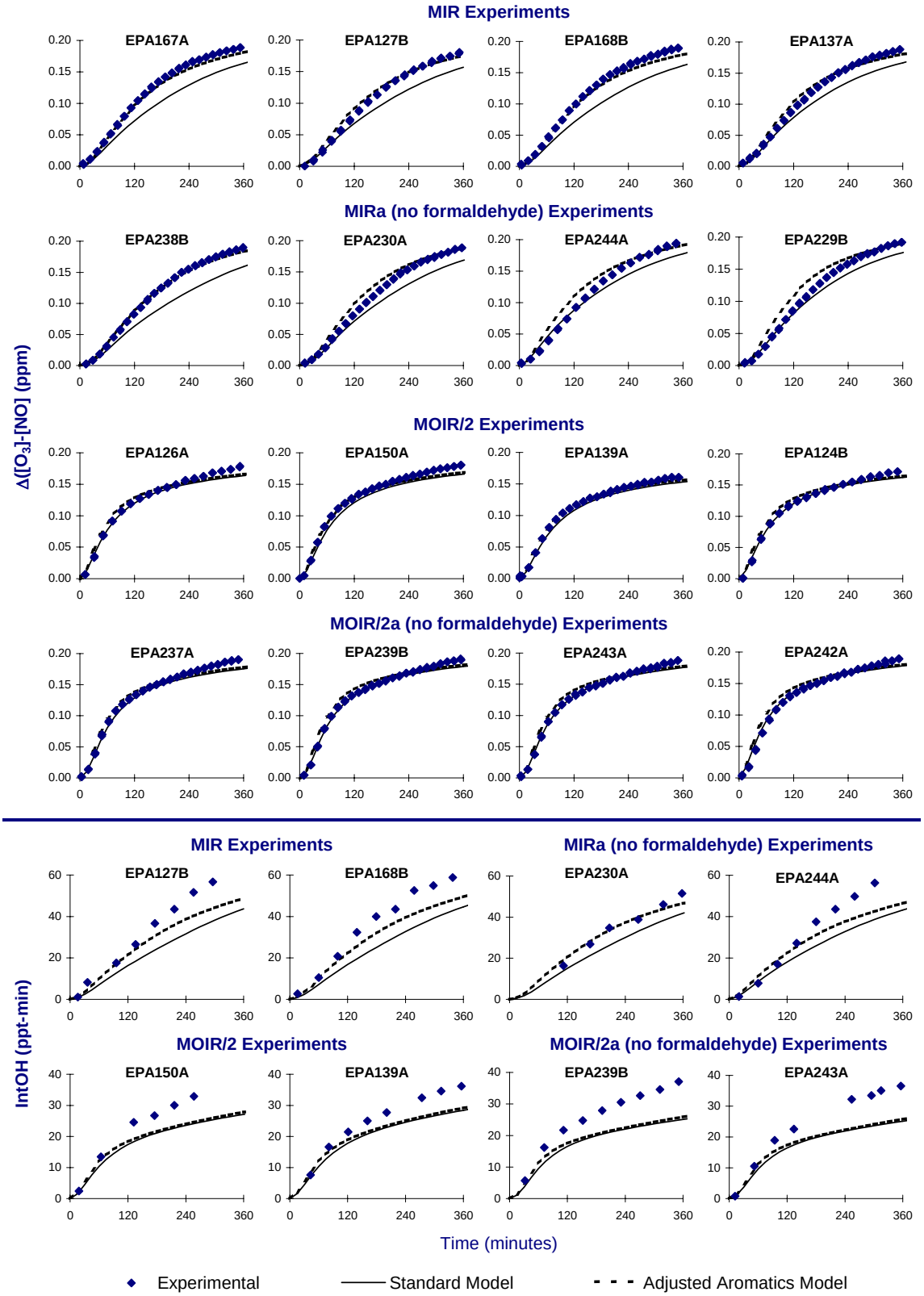

Figure 16. Experimental and calculated $\Delta([O_3]-[NO])$ and IntOH for selected base case experiments carried out for this project.

experiments, and does not improve the fits for other runs. Therefore, even with the increased radical inputs from the aromatics the SAPRC-99 mechanism consistently underpredicts OH levels in the experiments. This may have implications in the evaluation results, as discussed further below.

Predicted Effects of Removing Formaldehyde Base ROG Surrogate

During the period of this project we experienced recurring problems with our formaldehyde analysis system, which was frequently not operational. Because of occasional problems with the formaldehyde injection process, we felt it was necessary to have formaldehyde measurements in experiments where formaldehyde was injected for the experiments to be sufficiently well characterized for modeling. The formaldehyde injection process and maintaining the formaldehyde analysis system also increased the workload for the chamber experiments. Because formaldehyde data were not used as a primary means of for mechanism evaluation other than to establish initial concentrations, it would not be necessary to use the formaldehyde analysis system in our experiments if it were not a reactant in the base ROG surrogate. Therefore, to simplify our experimental procedures and improve productivity, and to permit more experiments to be conducted for this project within the available resources, we investigated whether removing formaldehyde from the base ROG surrogate would significantly affect the results.

Figure 17 shows concentration time plots for $\Delta([O_3]-[NO])$ and IntOH in model simulations of the two base case surrogate experiments with the standard and the modified base ROG surrogate. It can be seen that the removal of formaldehyde does affect the results, though the effect on IntOH is relatively small. It can also be seen that the effect of the formaldehyde removal can be compensated for by increasing the concentrations of the remaining base ROG constituents by 10%. With these two changes, the model predicts the $\Delta([O_3]-[NO])$ and IntOH data should be well within the run to run variability of the experiments.

Of course, getting the same O_3, NO, and OH radical simulations does not necessarily mean that other aspects of the chemical environment are sufficiently similar that incremental reactivity results would be unaffected. To investigate this, we conducted model simulations of hypothetical incremental reactivity experiments for all the VOC species that are separately represented in the current SAPRC-99 mechanism. To simulate realistic experiments where the amounts added would be adjusted based on the reactivity to obtain a measurable, but not overwhelming, effect on the results, the amount of added test compound was determined such that the estimated amounts reacted[9] would be approximately 10% of the initial base ROG concentrations. The results are shown on Figure 18, where the mechanistic reactivities calculated for the simulated incremental reactivity experiments with the modified base ROG surrogate are plotted against those calculated for the standard incremental reactivity experiments. The comparison is made on the basis of mechanistic reactivities (change in O_3 relative to the amount reacted) because that is the most uncertain component of the mechanisms that incremental reactivity experiments are designed to assess.

The results show that removing the formaldehyde from the base ROG surrogate has essentially no effects on predicted mechanistic reactivities in the MOIR/2 experiments for essentially all the model species, and the effects on the MIR experiments are small. The largest effect is that the inhibiting compounds are predicted to be about 25% more effective as inhibitors in the MIR experiments with the formaldehyde removed than when the formaldehyde is present. However, the trend is consistent so if the

[9] The estimated amounts reacted were calculated from the OH radical rate constant of the test compound and the calculated integrated OH levels in the base case experiments. Alkanes and highly photoreactive compounds were assumed to be 100% reacted for the purpose of these estimates.

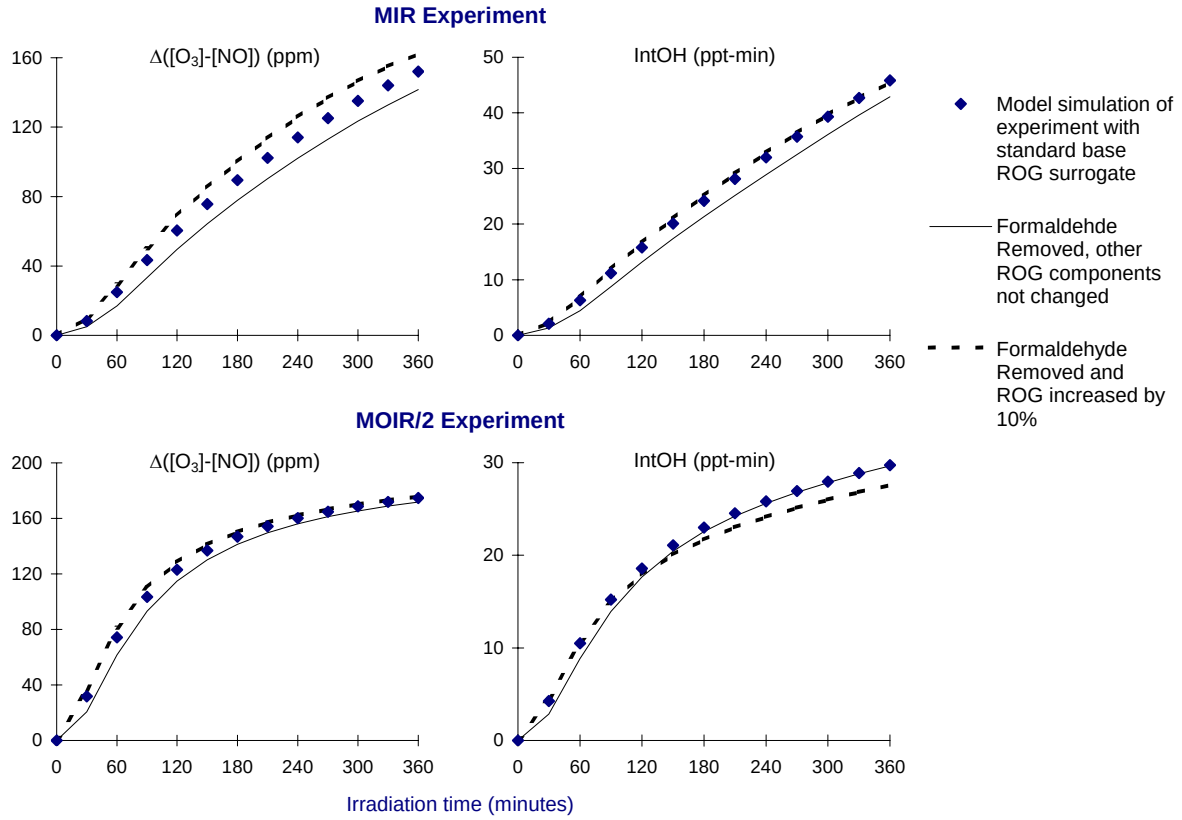

Figure 17. Effects of removing formaldehyde and increasing the base ROG concentrations by 10% on model simulations of the standard incremental reactivity base case experiments.

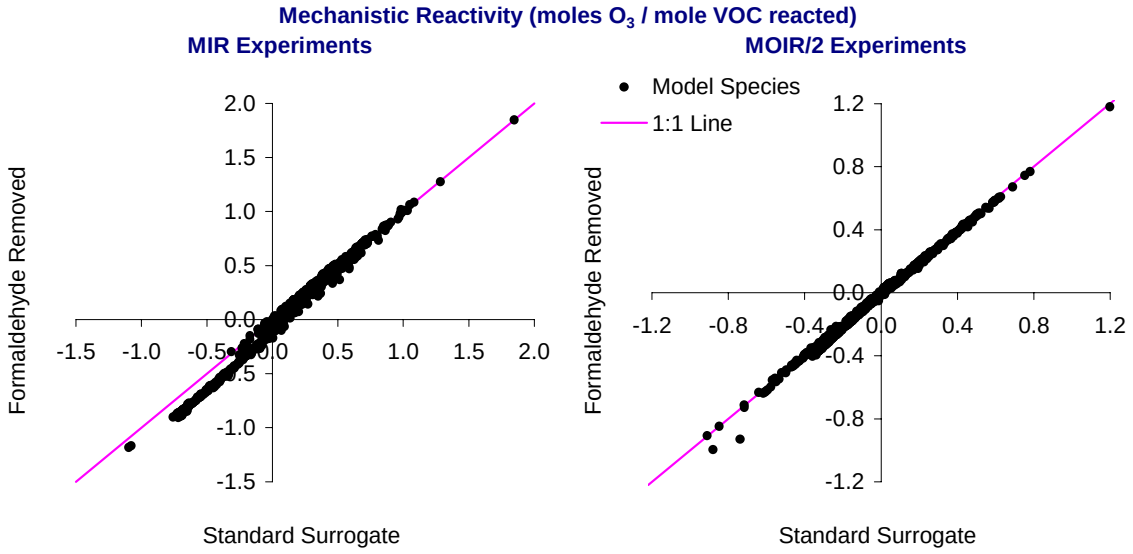

Figure 18. Comparisons of mechanistic reactivities calculated for all the SAPRC-99 detailed model species for simulated MIR or MOIR/2 incremental reactivity experiments using the standard ROG surrogate with those for the ROG surrogate with formaldehyde removed.

model could not correctly predict the inhibiting effect of a VOC in the standard surrogate experiment it would not predict it in the no-formaldehyde surrogate experiment, and vise-versa. Also, the ~25% effect is near the borderline of the ability of our experiments to distinguish mechanistic reactivity differences in any case.

Based on these results we conclude that removing the formaldehyde from the base ROG surrogate will have only small and usually indistinguishable results on the incremental reactivity measurements and should not affect conclusions concerning model performance in simulating incremental reactivity results. Since making this modification was expected to increase our productivity and potentially increase the number of experiments that could be carried out, we decided that overall this is beneficial to this program and this change was implemented approximately midway through the program (see Table A-4 in Appendix A.) The results of the simulations of the incremental reactivity experiments, discussed in the following section, showed no discernable differences that could be attributed to this change in the base case experiment.

Although this modification was not expected to significantly affect the results of the mechanisms evaluations using these data, for future studies it would probably be better to use more representative base ROG mixtures in reactivity experiments. For this purpose, it would be appropriate to update the base ROG surrogate employed, which would require input from the CARB and others on the most appropriate composition to use as a basis for deriving such a surrogate. This could not be done within the scope of the present project.

Simulations of Reactivity Results

m-Xylene

Incremental reactivity experiments for m-xylene were carried out as part of our initial evaluation of the use of this chamber for reactivity studies, and to evaluate the effects of varying base case surrogate and NO_x levels on reactivity measurements, using a compound that has been well studied previously (e.g., Carter et al, 1995a). The results are relevant to this project for this reason and also because m-xylene is representative of the aromatics present in many types of hydrocarbon solvents. As indicated on Table 10, above, experiments for this compound were carried out at a variety of ROG and NO_x levels in addition to those of the standard MIR and MOIR/2 experiments..

Figure 19 and Figure 20 show experimental and calculated concentration time plots for $\Delta([O_3]-[NO])$ and IntOH for the m-xylene incremental reactivity experiments. The experimental and calculated effects of the changes in $\Delta([O_3]-[NO])$ and IntOH caused by the m-xylene addition is also shown. The effects of adjusting the base mechanism to improve the fits to the MIR base case experiments are also shown. Because the base mechanism adjustment involved modifying the mechanism for m-xylene itself, two versions of the adjusted model calculations are shown. In the first, designated "Adjusted Aromatics Base Model," only the mechanism for the m-xylene in the base ROG was adjusted, and the standard m-xylene mechanism was used for the additional m-xylene in the added m-xylene test experiment. In the second, designated "Adjusted Aromatics Base and Test Model," the adjusted m-xylene mechanism was used for all the m-xylene in both experiments.

As discussed above, Figure 19 shows that the adjusted base mechanism gives better fits to the $\Delta([O3]-[NO])$ data in the base case experiments at the lower ROG/NO_x ratios, while the fits for the higher ROG/NO_x experiments, shown on Figure 20, are relatively unaffected. When the mechanisms for the aromatics in the base ROG are adjusted to better fit the base case data, the model gives a better prediction of the shapes of the time profile for the incremental reactivity for m-xylene (i.e., the change in

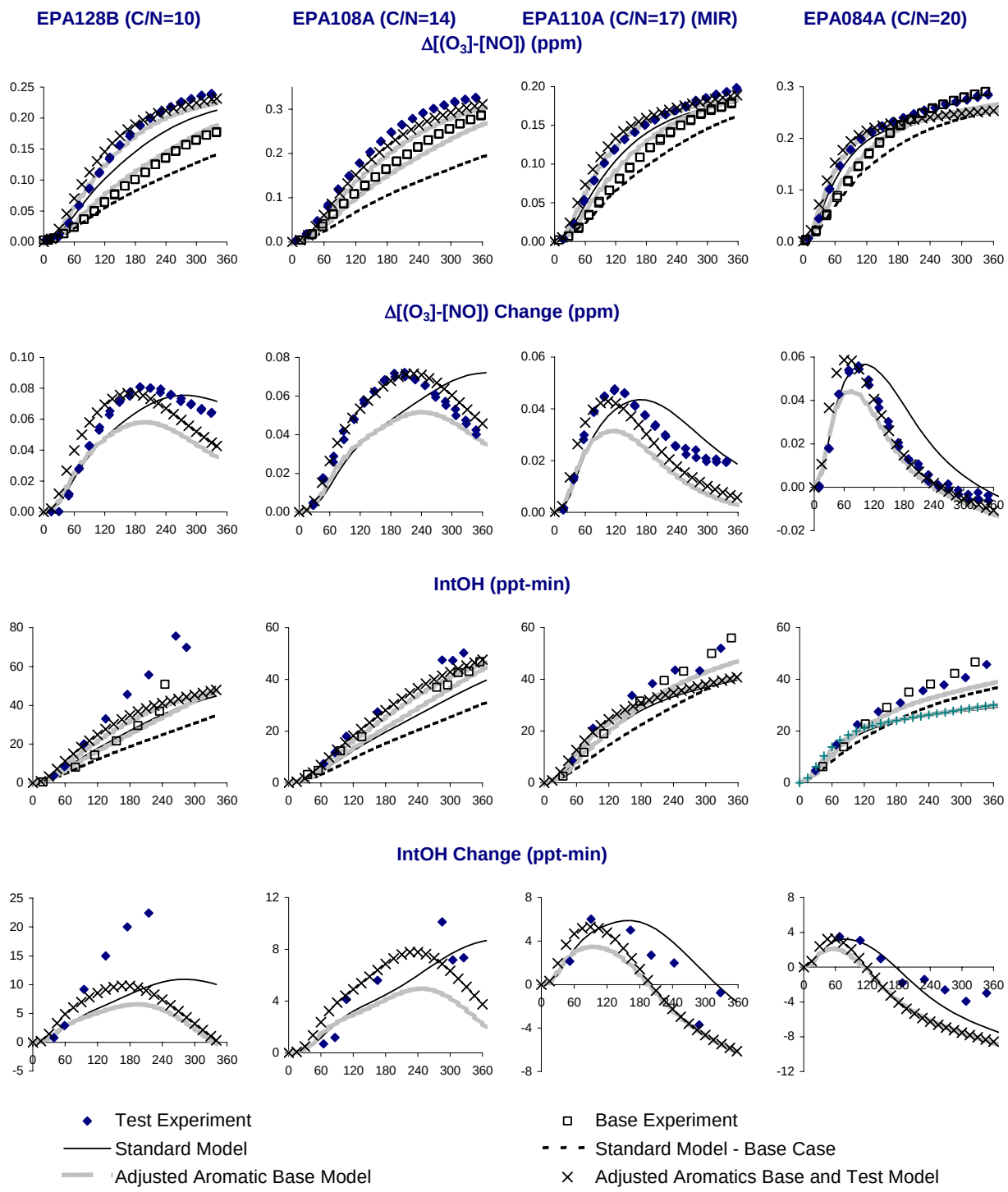

Figure 19. Experimental and calculated concentration-time plots for the m-xylene incremental reactivity experiments at the lower ROG/NO_x ratios. The mechanism for the added m-xylene was not adjusted for test case calculations.

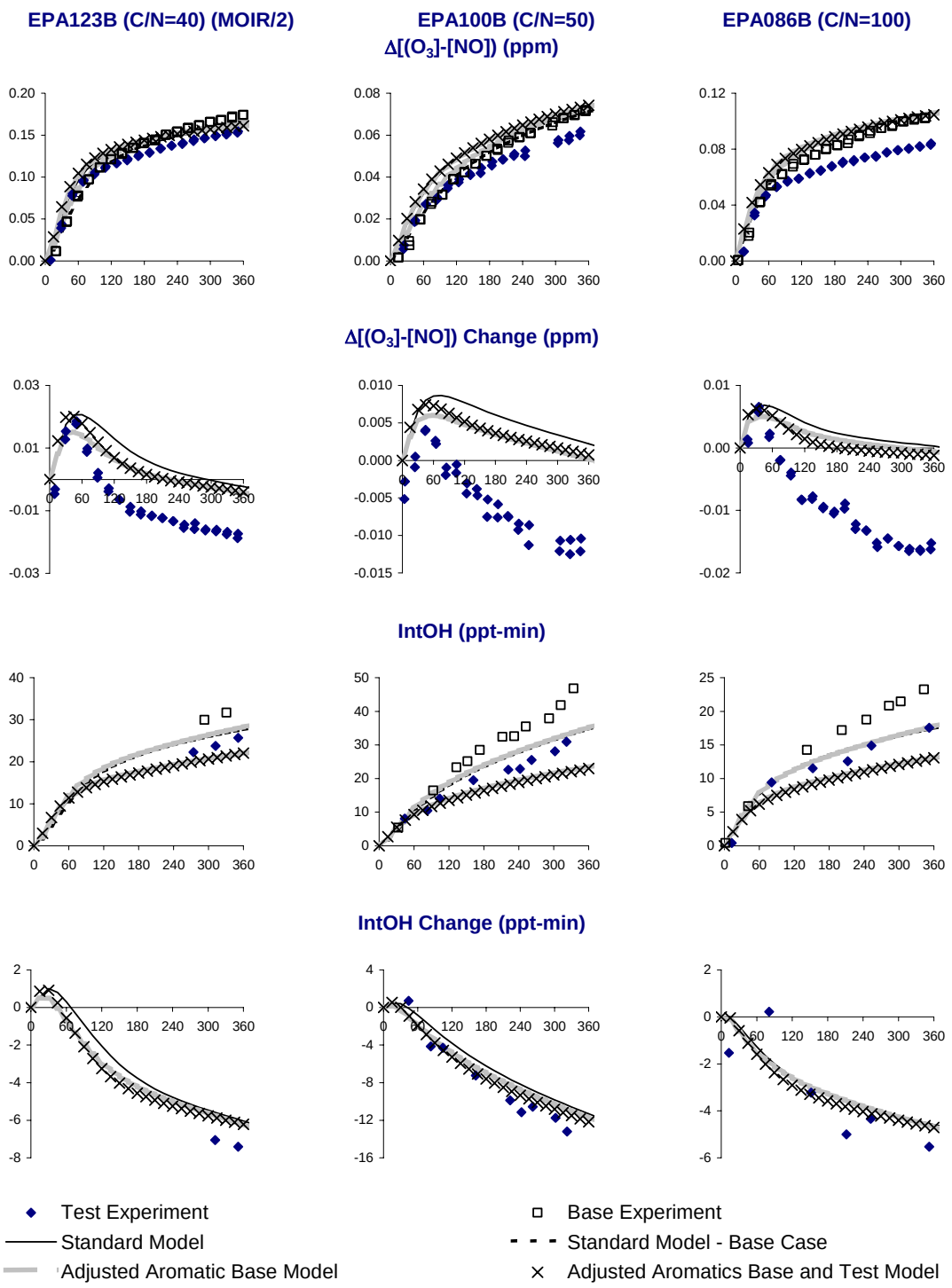

Figure 20. Experimental and calculated concentration-time plots for the m-xylene incremental reactivity experiments at the higher ROG/NO_x ratios. The mechanism for the added m-xylene was not adjusted for test case calculations.

Δ([O3]-[NO]) caused by its addition) in the lower ROG/NO_x experiments. This can be attributed to the better simulation of the overall conditions of the chemical background. The effects of the base mechanism adjustments on the Δ([O_3]-[NO]) incremental reactivities at the higher ROG/NO_x ratios is less, but still discernable.

If the mechanism for the added m-xylene in the test experiments is not adjusted, the adjustments to the base aromatics mechanism results in a decrease in calculated Δ([O_3]-[NO]) incremental reactivity in all experiments, with the effect being greatest in the lowest ROG/NO_x experiments. Although this adjustment improves the shapes of the incremental reactivity curves, it also results in a consistent tendency for the model to underpredict the Δ([O_3]-[NO]) incremental reactivity in the lower ROG/NO_x experiments, which it did not have when the base mechanism was not adjusted. This is despite the fact that the mechanism for the test compound is the same in both cases. This can be attributed to the higher radical sources in the base mechanism making the system overall slightly less sensitive to radical sources from the added test compound. Adjusting the mechanism for the added m-xylene in the test experiment to be consistent with that used for the m-xylene in the base ROG surrogate results in the best fits to the Δ([O_3]-[NO]) data in the lower ROG/NO_x experiments shown on Figure 19, with the fits being essentially to within experimental uncertainty in most cases.

On the other hand, both the adjusted and unadjusted aromatics mechanisms do not correctly predict the tendency of the added m-xylene to inhibit the final ozone levels in the NO_x -limited experiments, as shown on Figure 20. The model predicts that the final O_3 in these experiments is relatively unaffected by the addition of the m-xylene, while the experimental data indicate a small but measurable reduction in the final O_3, with the extent of reduction increasing as the ROG/NO_x increases (i.e., as the relative NO_x levels decreases). The adjustments to the base mechanism result in a very slight improvement in this regard, but the reduction in the final O_3 is still not predicted. The adjustments to the mechanism for the added m-xylene have essentially no effect on the incremental reactivity predictions in the latter stages of the high ROG/NO_x experiments.

Although as discussed above the model has a consistent tendency to underpredict OH radical levels in these surrogate - NO_x experiments, it gives reasonably good simulations of the effects of the added m-xylene on the overall radical levels as measured by IntOH, except for the experiment at the lowest ROG/NO_x ratio. As with Δ([O_3]-[NO]), the adjustments to the mechanism affect the predictions of the IntOH incremental reactivities at the lower ROG/NO_x ratios, but the predictions at the higher ratios are relatively insensitive to these adjustments. The precision of the IntOH data is such that one cannot make conclusions about which version of the mechanism is the most consistent with these data.

n-Octane

Incremental reactivity experiments with for n-octane were also carried out as part of our initial evaluation of the use of this chamber for reactivity measurements and of the effects of varying base case surrogate and NO_x levels on reactivity measurements modified base case surrogate and NO_x levels for incremental reactivity studies using compounds that have well studied previously. The experiments with n-octane are relevant to this project because the higher alkanes are major constituents of all the hydrocarbon solvents studied in this work except for Aromatic 100, and mechanisms for higher molecular weight esters such as Texanol® isomers are in many ways similar to those for higher alkanes. The ROG and NO_x levels used for these experiments are indicated on Table 10, and they include those for the standard MIR and MOIR/2 used for the other compounds in this study.

Experimental and calculated Δ([O_3]-[NO]) and IntOH data for the incremental reactivity experiments with n-octane are shown on Figure 21 and Figure 22. As with m-xylene discussed above and the other test compounds discussed below, results are shown with both the standard and the adjusted

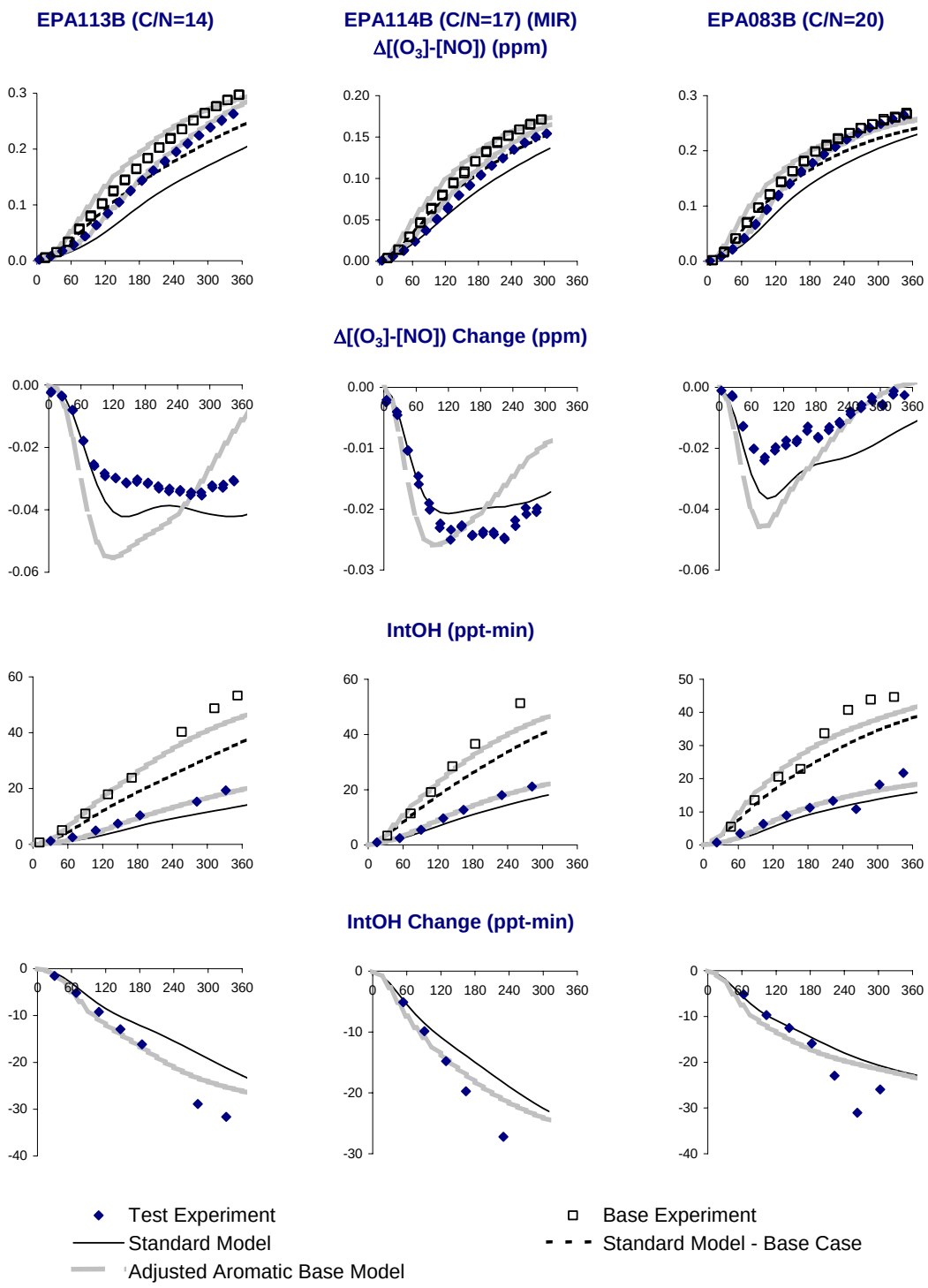

Figure 21. Experimental and calculated concentration-time plots for the n-octane incremental reactivity experiments at the lower ROG/NO_x ratios.

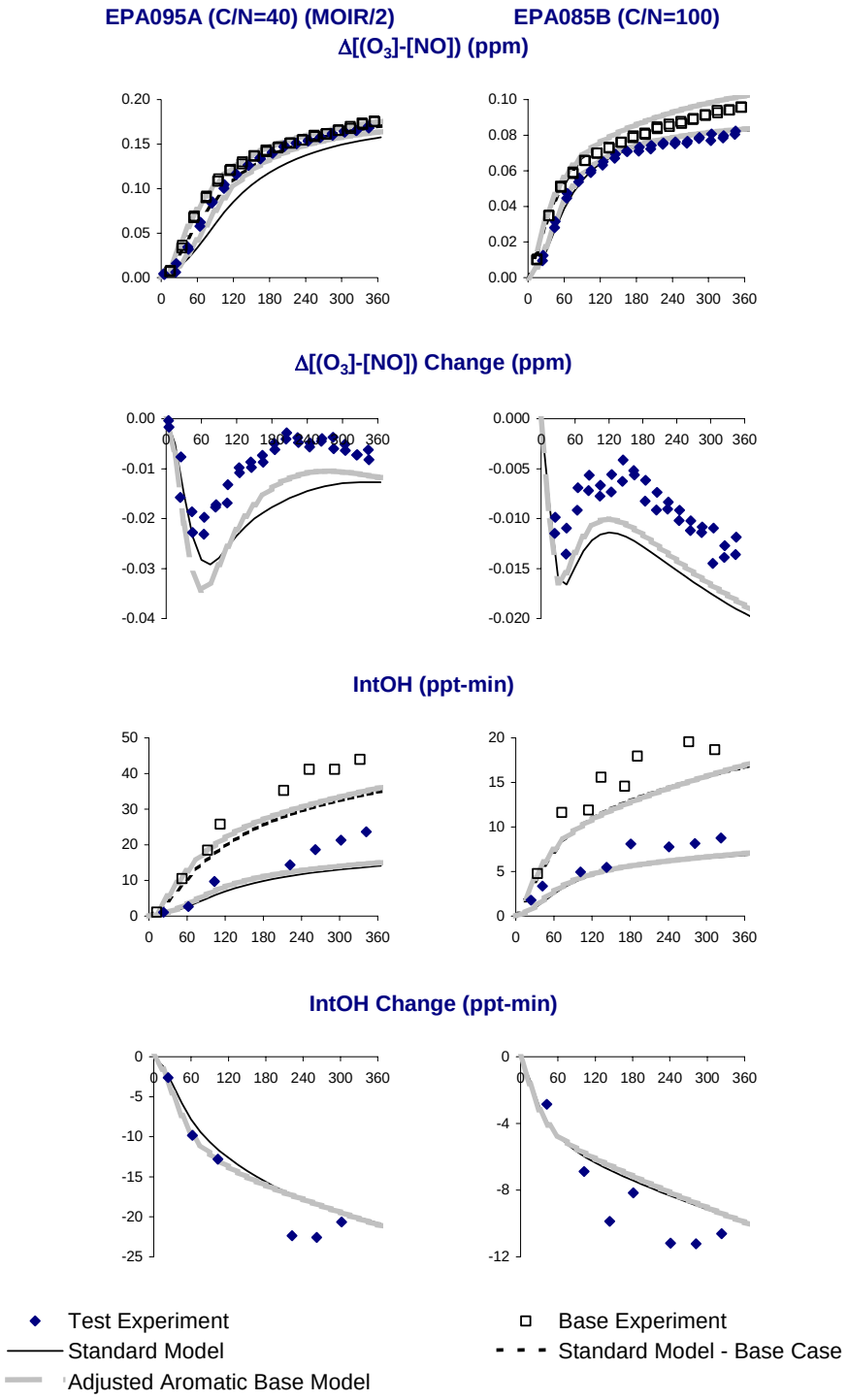

Figure 22. Experimental and calculated concentration-time plots for the n-octane incremental reactivity experiments at the higher ROG/NO_x ratios.

mechanisms for the aromatics in the base ROG. In this case, although the adjustments to the base mechanism improved the fits to the Δ([O3]-[NO]) results of the base case experiments, it did not result in significantly improved fits to the Δ([O_3]-[NO]) incremental reactivity data for these experiments. However, the effects of the added m-xylene on Δ([O_3]-[NO]) were relatively small in all experiments, and both the adjusted and unadjusted models fit the data to within their uncertainties.

Although the effects of the added n-octane on the Δ([O3]-[NO]) data were relatively small, the n-octane addition did have a large effect on inhibiting overall radical levels. The models gave reasonably good fits to the effects of the n-octane on IntOH, though there was a slight but consistent tendency to underpredict the IntOH reactivity at the end of the experiments, regardless of ROG/NO_x ratio. However, this bias is not large and may not necessarily indicate a problem with the n-octane mechanism given that the model tends to underpredict IntOH in the base case experiments.

Texanol®

The highest priority compound for study for this project was Texanol®, because it is extensively used as a solvent in water-based coatings and its reactivity has not previously been experimentally assessed. Although the OH radical rate constants for its constituent isomers were measured as part of this project, as discussed above the results indicated no need to modify the rate constants already in the SAPRC-99 mechanism.

The experimental and calculated Δ([O_3]-[NO]) and IntOH results for the incremental reactivity experiments with Texanol® are shown on Figure 23. Two MIR and two MOIR/2 experiments were carried out with this compound, and the experiments were well duplicated. The added Texanol® resulted in almost no measurable change in Δ([O_3]-[NO]) but a relatively large inhibition of OH radicals as measured by IntOH. This is very similar to the results discussed above for n-octane, though in this case the overall effects in Δ([O3]-[NO]) and (to a lesser extent) IntOH was somewhat smaller.

The results of the Texanol® experiments were well duplicated by the model simulations, and the adjustments to the base mechanism having relatively little effects on the predictions of the effects of the Texanol® addition. There was a slight tendency for the model to predict more Δ([O_3]-[NO]) inhibition than observed experimentally, but the results are well within the experimental uncertainty. There was a slightly greater tendency for the model to underpredict the IntOH inhibition caused by the Texanol® addition, similar to the results observed for n-octane. However, given the relatively small magnitude of the bias compared to the experimental variability and the fact that the model underpredicts IntOH in the base case experiment, it is judged that the discrepancy is not sufficient to merit adjustment of uncertain portions of the Texanol® isomers' mechanisms to improve the fits.

Hydrocarbon Solvent ASTM-1C

The results of the incremental reactivity experiments with the petroleum distillate hydrocarbon solvents will be discussed in order of increasing aromatic content[10]. Of the petroleum distillates studied, the solvent with the lowest alkane content, and the lowest predicted reactivity, is the solvent designated ASTM-1C. One MIR and one MOIR/2 incremental reactivity experiment was carried out with this solvent, and the experimental and calculated Δ([O_3]-[NO]) and IntOH results are shown on Figure 24.

[10] The synthetic hydrocarbon solvent designated ASTM-3C1 will be discussed last because it appears to have different reactivity characteristics than the alkane petroleum distillate solvents.

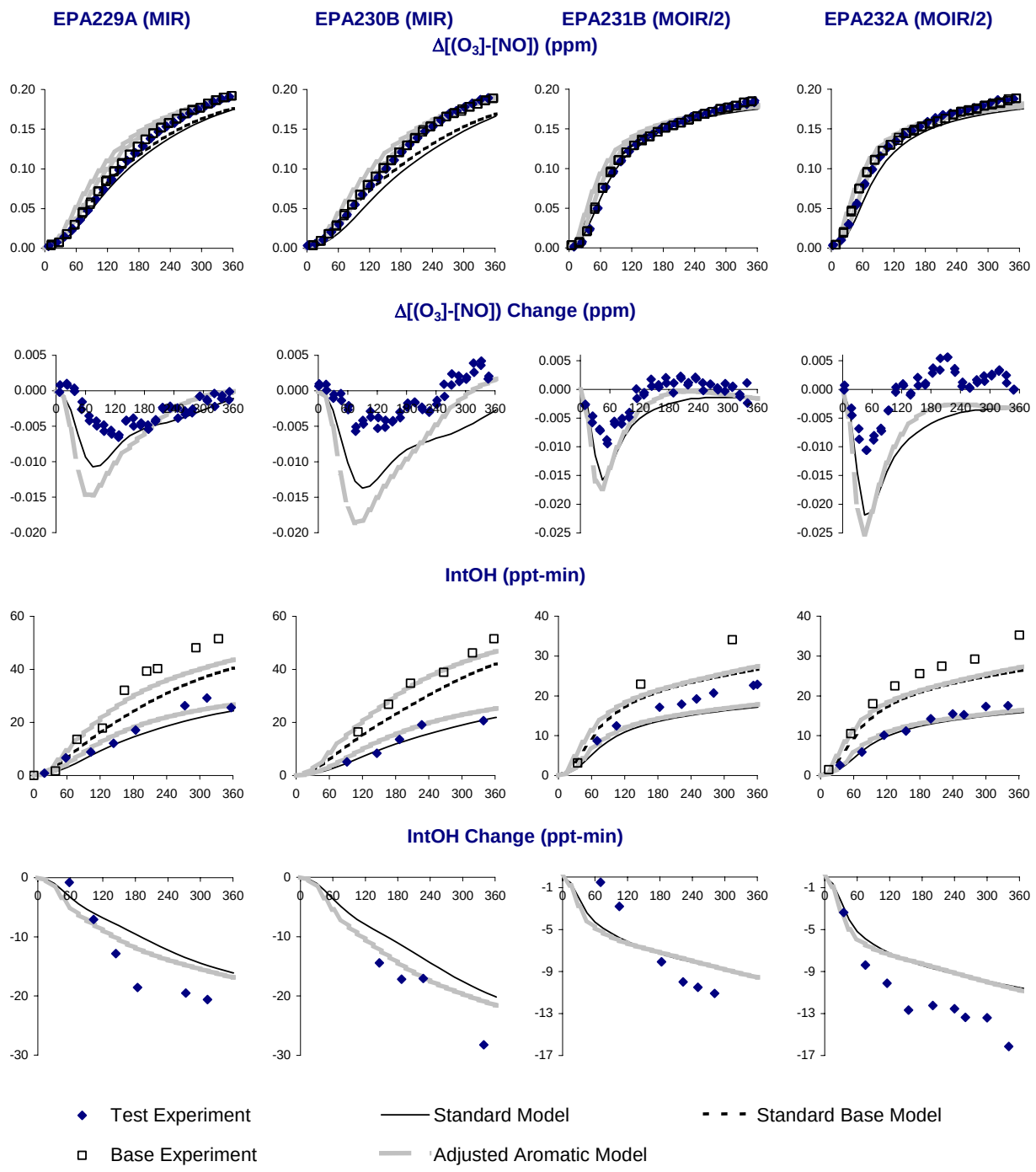

Figure 23. Experimental and calculated concentration-time plots for the Texanol® incremental reactivity experiments.

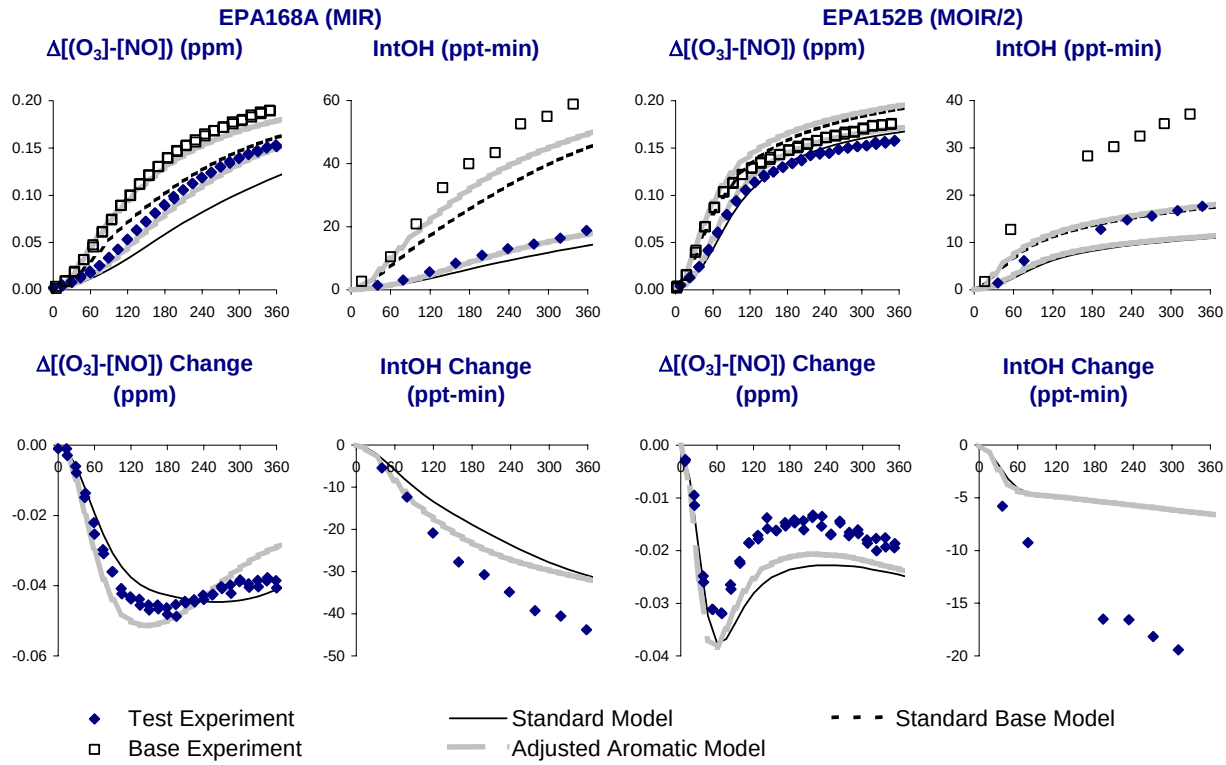

Figure 24. Experimental and calculated concentration-time plots for the ASTM-1C incremental reactivity experiments.

The addition of this solvent caused inhibition in both Δ([O_3]-[NO]) and IntOH in both experiments, though the effect on Δ([O3]-[NO])was much greater in the MIR than the MOIR/2 run.

The model gave good simulations to the effect of this solvent on Δ([O_3]-[NO]) in both experiments. Adjusting the mechanism for the base ROG had relatively small effects on the predictions of the solvent addition and the quality of the incremental reactivity fits to the data. The model slightly underpredicted the IntOH inhibition in the MIR experiment, but the discrepancy was not great considering the tendency of the model to underpredict IntOH in general. The model gave a very poor prediction of the IntOH effect in the low NO_x experiment, but the IntOH data for the base case experiment appear to be anomalously high relative to the model, compared to the results of the other MOIR/2 experiments. It would have been useful had another MOIR/2 experiment been conducted for this compound. As it is, the uncertainty in the data do not lead us to conclude that there is necessarily a problem with the model for this solvent.

VMP Naphaha Solvent

The VMP Naphtha solvent studied for this project had essentially negligible aromatic content but is expected to have higher overall reactivity (or less inhibition characteristics) than the ASTM-1C sample because of its lower carbon number (average carbon number of 8.7, compared to 10.8 for the ASTM-1C solvent.) One each MIR and MOIR/2 experiment was carried out with this solvent, in both cases one with formaldehyde in the base ROG surrogate and one without. The Δ([O_3]-[NO]) results for the incremental reactivity experiments with this solvent are shown on Figure 25. No IntOH data could be obtained

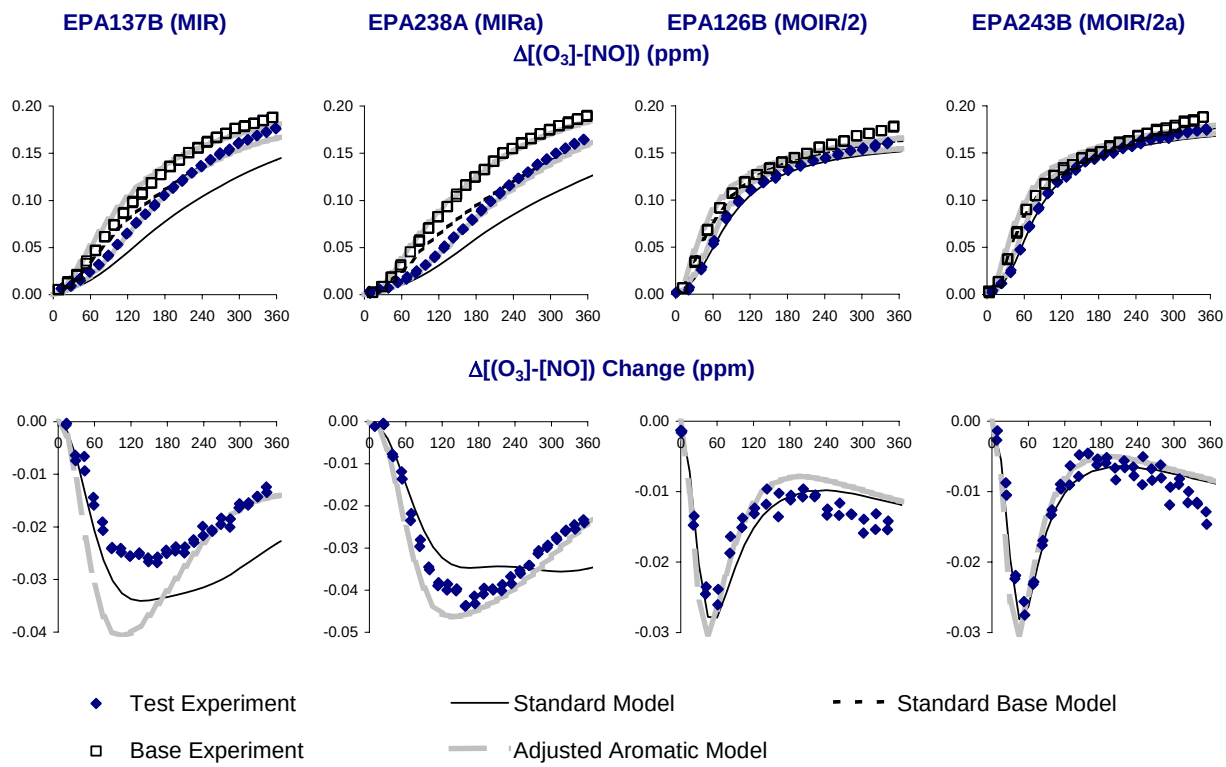

Figure 25. Experimental and calculated concentration-time plots for the VMP-Naphtha incremental reactivity experiments. Note that the effect of the naphtha on IntOH could not be determined because of interferences on the GC analysis for the tracer compounds.

because the Naphtha constituents caused GC interferences in the analysis of the potential OH radical tracer base ROG surrogate constituents.

As was the case with the ASTM-1C sample, the addition of the VMP Naphtha sample caused a decrease in $\Delta([O_3]\text{-}[NO])$ in all the experiments, with the decrease being much more in the case of the MIR run. However, the magnitude of the inhibition was somewhat less, as expected given the lower carbon number (and therefore lower inhibiting characteristics) for the constituents. The model gave very good simulations to the effects of the solvent on $\Delta([O_3]\text{-}[NO])$ three of the experiments, and fair simulations of the results of the MIR experiment EPA137. Its performance in simulating IntOH could not be evaluated, but it is reasonable to expect it would be similar to the ASTM-1A solvent, given the similarity of the solvents and the model performance in simulating their effects on $\Delta([O_3]\text{-}[NO])$.

Note that the results of the VMP Naphtha experiments with the formaldehyde removed from the base ROG surrogate were very similar to the corresponding experiment with the formaldehyde present. The experimental and calculated effect of the solvent on $\Delta([O_3]\text{-}[NO])$ in the MIR experiment was somewhat greater in the experiment with the formaldehyde removed, with the difference being somewhat grater in the experiment than the model predictions. This difference could be due at least in part to experimental variability.

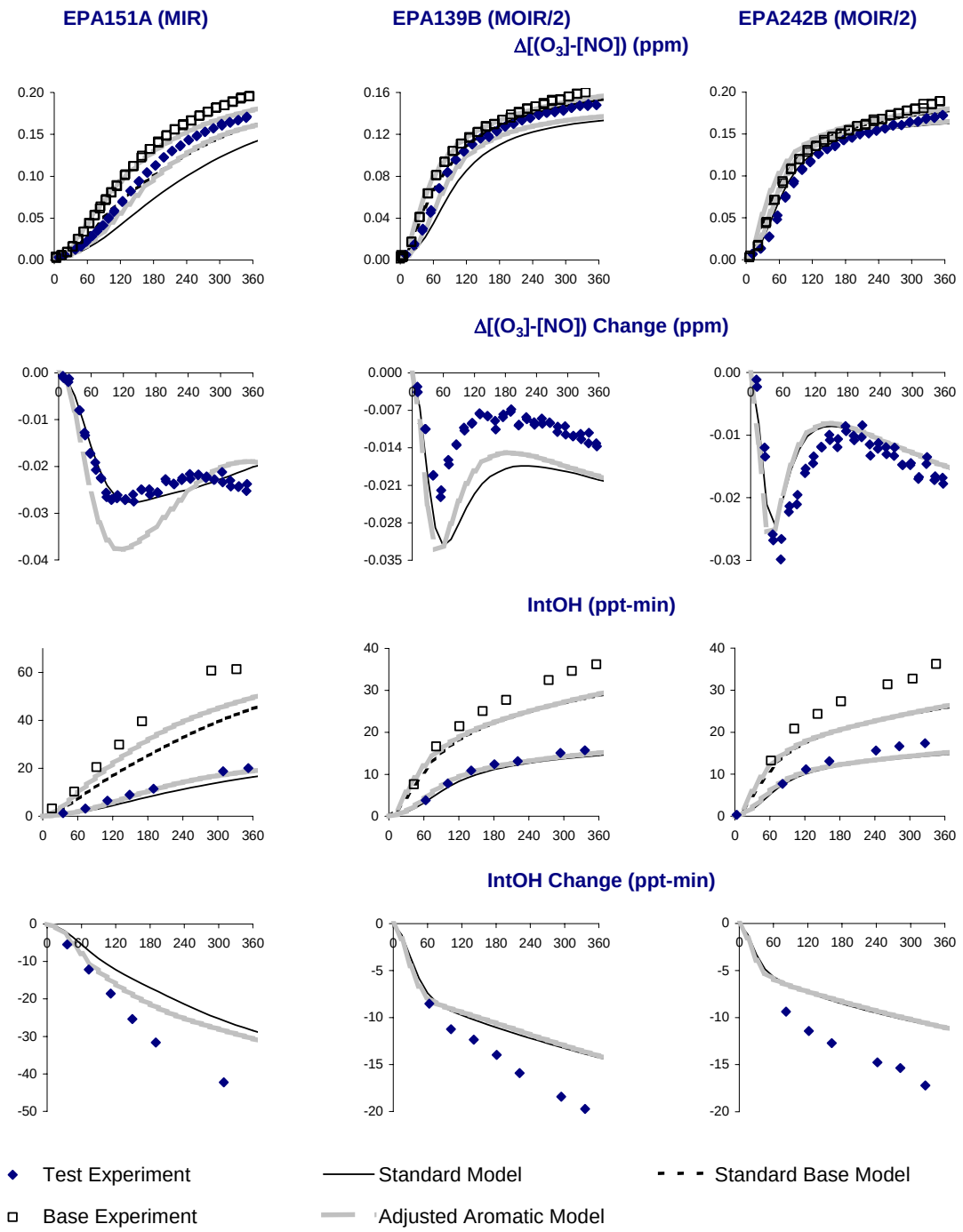

Figure 26. Experimental and calculated concentration-time plots for the ASTM-1B incremental reactivity experiments.

Hydrocarbon Solvent ASTM-1B

The sample of ASTM-1B solvent studied for this project had 6% aromatics content, which is enough to affect its predicted reactivity. Three experiments were carried out with this solvent, one MIR and two MOIR/2, and the $\Delta([O_3]-[NO])$ and IntOH results are shown on Figure 26. As with the non-aromatic petroleum distillates, the addition of this solvent caused reductions in both $\Delta([O_3]-[NO])$ and IntOH, though the effect on $\Delta([O_3]-[NO])$ in the MOIR/2 experiments was relatively small.

The ability of the model to simulate the experiments with this solvent was comparable to that for the low aromatic petroleum distillates discussed above. The model gave reasonably good simulations of the effects of the solvent on $\Delta([O_3]-[NO])$, and although is somewhat underpredicted the effect on IntOH, the underprediction was not greatly different than that observed for the other compounds and solvents discussed above.

Hydrocarbon Solvent ASTM-1A

The ASTM-1A sample studied for this project had almost 20% aromatic content, which is expected to significantly affect its reactivity. As with ASTM-1B, three incremental reactivity experiments were carried out with this solvent, one MIR and two MIOR/2. The $\Delta([O_3]-[NO])$ and IntOH results of these experiments are shown on Figure 27. Unlike the lower aromatic petroleum distillates discussed above, this solvent had positive effect on $\Delta([O_3]-[NO])$ in the MIR experiment, though the effect was very small and decreased to zero at the end of the run. It generally had a small negative effect on $\Delta([O_3]-[NO])$ in the MOIR/2 experiments and, as with the other solvents, inhibited IntOH levels.

The model gave reasonably good fits to the effects of the solvent addition on $\Delta([O_3]-[NO])$ and its simulations of the effects on IntOH were mostly comparable to the results observed for the other solvents. The simulations using the adjusted mechanism for the base ROG constituents predicted that the solvent slightly inhibited, rather than enhanced $\Delta([O_3]-[NO])$, but the magnitude of the effect either way is so small that this discrepancy is not considered to be significant. The model actually simulated the effect of the solvent on IntOH in the MIR experiment almost without bias, which is somewhat different than observed for the other solvents. However, the difference is not large and may be due in part to run to run variability.

The ASTM-1A sample had a small amount of m-xylene, and the model calculations shown on Figure 27 were carried out using the adjusted mechanism for this compound in the solvent as well as the base case. However, the weight fraction of m-xylene in the sample was less than 1%, so using an adjusted mechanism for this compound would have no effect on the simulation. The same is true for ASTM-1B, which has even lower aromatic and m-xylene content than ASTM-1A. This was verified by test calculations using ASTM-1A.

Aromatic 100 Solvent

The Aromatic-100 solvent consists of 100% aromatics, almost all in the C_9-C_{10} range. Over 60% of the mass consists of compounds, such as m-ethyl toluene, whose mechanisms had to be estimated based on analogy with similar aromatics (e.g., m-xylene) because of lack of data to develop a mechanism for the specific compound. Because important aspects of aromatics mechanisms have to be adjusted to fit chamber data and because different aromatic isomers have different reactivities, the ability of the model to simulate the reactivity of this solvent was considered to be quite uncertain. Therefore, studies of Aromatic 100 were included as a priority for this project.

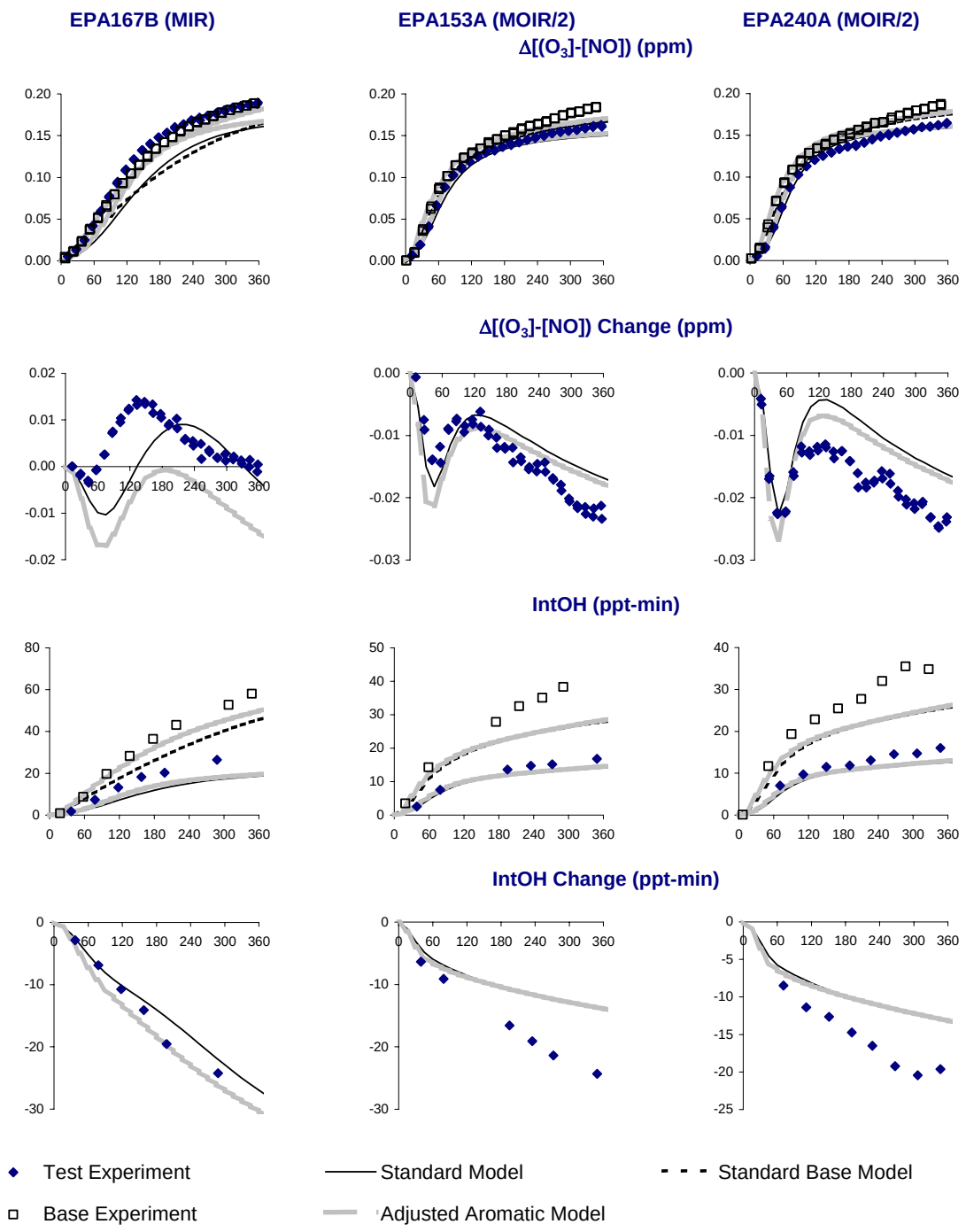

Figure 27. Experimental and calculated concentration-time plots for the ASTM-1A incremental reactivity experiments.

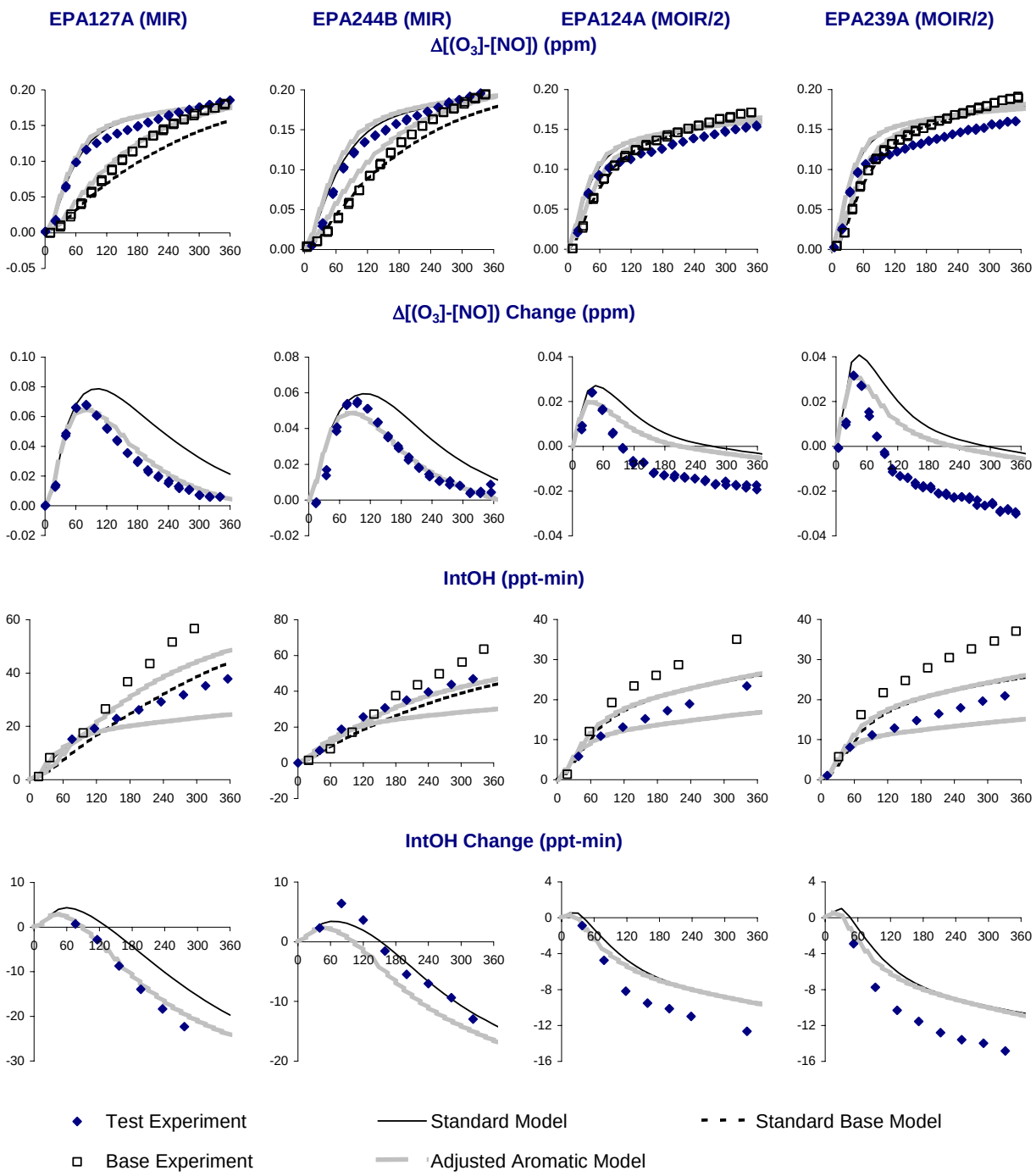

Figure 28. Experimental and calculated concentration-time plots for the Aromatic-100 incremental reactivity experiments.

A total of four incremental reactivity experiments with Aromatic 100 solvent were carried out for this project, two MIR and two MOIR/2. The results of these experiments are shown on Figure 28. The effects of this solvent on $\Delta([O_3]-[NO])$ were very similar to that observed for m-xylene. The addition of the solvent had a relatively large positive effect on $\Delta([O_3]-[NO])$ in the MIR experiments, with the effects decreasing with irradiation time, and small positive effects at the beginning of the MOIR/2 experiments, followed by an inhibition of O_3 by the time the irradiation ended. However, the effect of Aromatic 100 on IntOH was more negative than the case for m-xylene, tending to inhibit IntOH for most of the experiments except for the very start of the MIR runs.

Considering the uncertainties in the mechanisms for many of it is constituents, the model gave surprisingly good simulations of the incremental reactivity results, though the same discrepancies were observed as were observed in the simulations of the m-xylene experiments, discussed above. The model with the adjusted base ROG mechanisms gave very good simulations of both the $\Delta([O_3]-[NO])$ and IntOH data in the MIR experiments, good simulations on the effects on $\Delta([O_3]-[NO])$ in the initial stages of the MOIR/2 experiments, and fair simulations of the IntOH data in the MOIR/2 runs. However, as was the case with m-xylene, the model did not predict the inhibition of O_3 caused by the solvent addition at the end of the MOIR/2 experiments; instead it predicted that the effect on the final O_3 in these NO_x -limited experiments would approach zero. Note that the adjustments to the toluene and m-xylene mechanisms in the base ROG surrogate has no effect on the mechanisms for Aromatic 100 itself because the amounts of these compounds in this solvent was negligible.

In order to provide additional mechanism evaluation data for Aromatic 100, a separate experiment was carried out with only Aromatic 100 and NO_x injected into both reactors, and 90 ppm CO added to one of the reactors to determine its effect on the results. (See Table 10 for the initial concentrations used.) This is analogous to aromatics - NO_x + CO experiments carried out previously with toluene and m-xylene, where the model gave good simulations of O_3 formed in the aromatics - NO_x experiment but significantly underpredicted the amount of additional O_3 formation caused by the addition of NO (Carter, 2004a). It was interest to see if similar results would be obtained with Aromatic 100 as was observed with toluene and m-xylene. The results of this experiment are shown on Figure 29.

The results of this experiment are quite similar to the results of the analogous experiments with toluene and m-xylene as reported previously (Carter, 2004a). The model gives reasonably good simulations of O_3 in the aromatics - NO_x experiment, but underpredicts O_3 in the experiment with added CO and underpredicts, by about a factor of 2, the increase in O_3 caused by the addition of CO. This is attributed to the model not having sufficient radical sources in the mechanism, with this being compensated for by other aspects of the mechanism, such as direct NO to NO_2 conversions. The fact that the model consistently underpredicts IntOH is consistent with this explanation.

Synthetic Hydrocarbon Solvent ASTM-3C1

The ASTM-3C1 solvent sample differs from the other hydrocarbon samples studied for this project in that it a synthetic mixture and not a petroleum distillate. It consists primarily of branched alkanes and some cycloalkanes and essentially no normal alkanes and no aromatics. The reactivity results were also somewhat different from those for the petroleum distillate derived samples, as is evident below. A total of four incremental reactivity experiments were carried out with this solvent, one MIR and three MOIR/2 experiments. The $\Delta([O_3]-[NO])$ and IntOH results for those experiments are shown on Figure 30.

It can be seen that the model performance in simulating the $\Delta([O3]-[NO])$ data in the experiments with this synthetic solvent is not nearly as good as is obtained when simulating the results of the alkane-derived solvents. The model underpredicts, by approximately a factor of two, the inhibition in

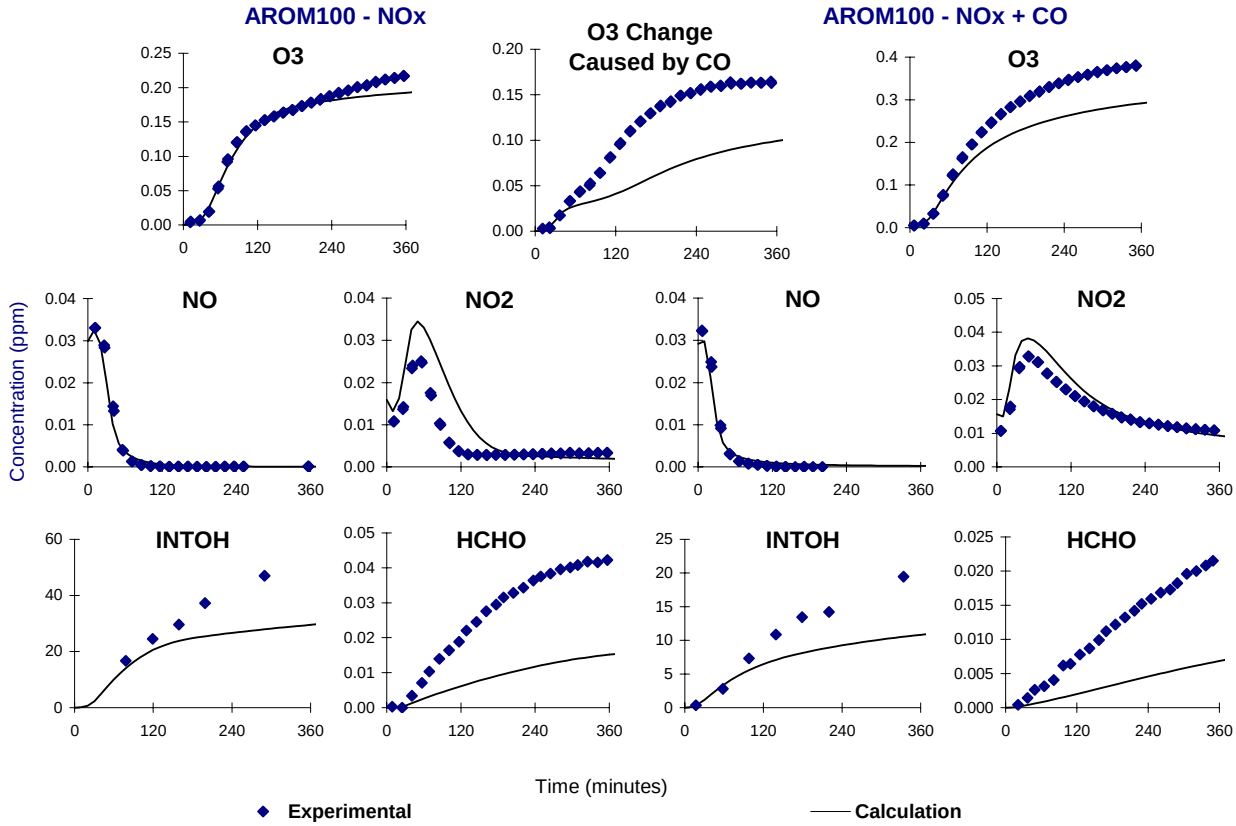

Figure 29. Experimental and calculated concentration-time plots for selected species for the Aromatic-100 - NO_x and Aromatic-100 - NO_x + CO experiments.

$\Delta([O_3]-[NO])$ caused by the addition of the solvent in the MIR experiment, and predicts that it consistently underpredicts $\Delta([O_3]-[NO])$ throughout the MOIR/2 runs, while the data indicate show the solvent having very little effect on $\Delta([O_3]-[NO])$ throughout the run. On the other hand, the model gives reasonably good predictions of the effect of the solvent on IntOH, but even in this regard it differs from the results for the petroleum distillates, where the model is generally biases low in simulating the IntOH reactivity. As discussed above, one might expect a general tendency to underpredict IntOH reactivity because the model consistently underpredicts IntOH in the base case experiment. Because of this, we place greater weight in the discrepancies in the $\Delta([O_3]-[NO])$ simulations, and consider the model performance for this solvent to be unsatisfactory.

The synthetic hydrocarbon ASTM-3C1 sample studied for this project may be similar in derivation as the Isopar-M®[11] samples we studied previously (Carter et al, 2000), though the sample studied in this project is a lighter hydrocarbon mixture (average carbon number of 11, compared to 13.6 for Isopar-M®). The SAPRC-99 mechanism was found to give generally good simulations of the results of incremental reactivity experiments with Isopar-M® that were carried out previously (Carter et al, 2000), though those experiments employed much higher base case ROG and NO_x levels than the

[11] Isopar is a registered trademark of ExxonMobil Chemical Company.

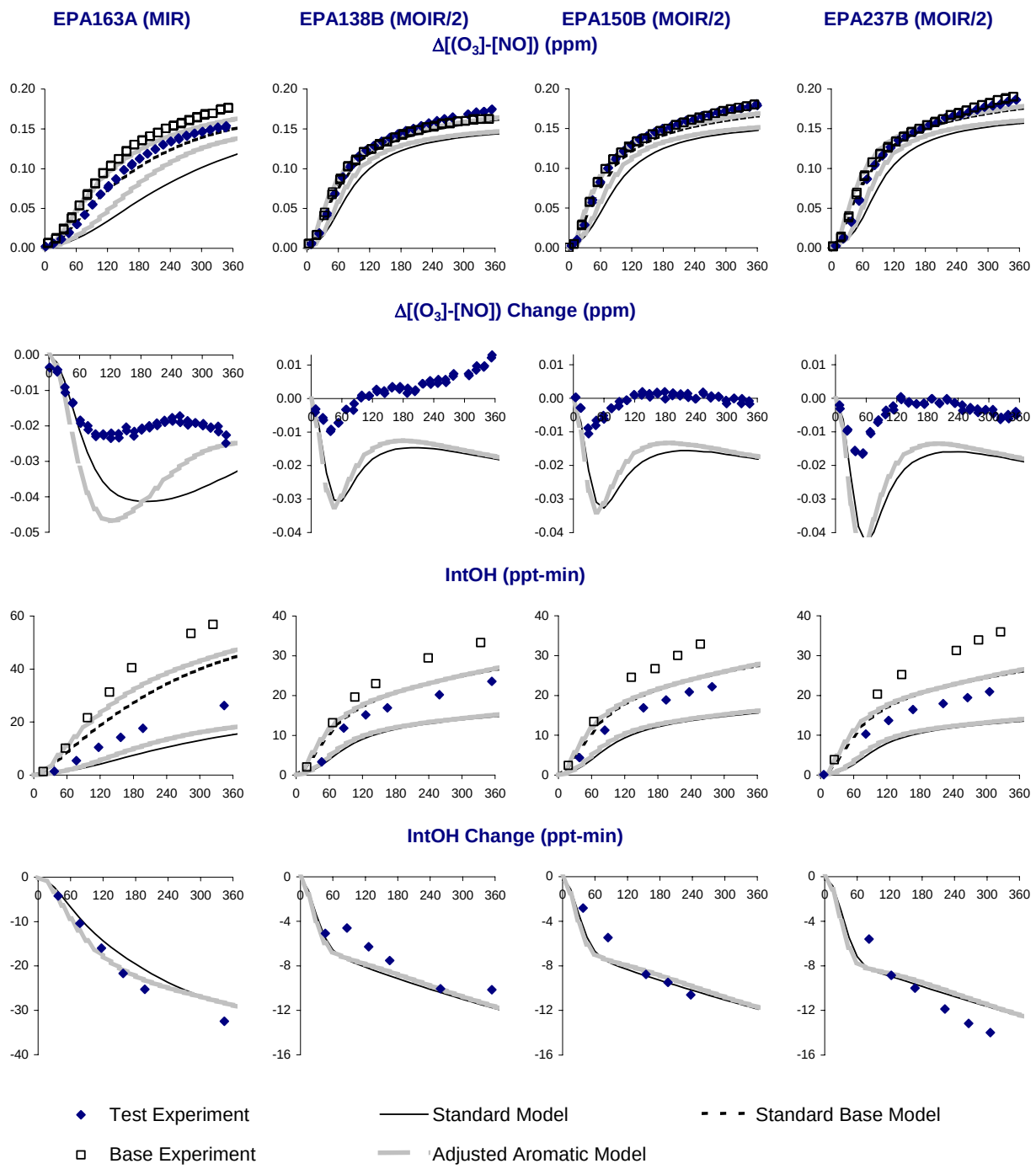

Figure 30. Experimental and calculated concentration-time plots for the ASTM-3C1 incremental reactivity experiments.

experiments for this project. However, a version of the mechanism representing the Isopar® components with much more branched alkanes was found to give better model predictions of measurements of acetone.

In order to assess whether using more branched alkanes to represent the unspeciated branched alkanes in this ASTM-3C1 sample would give better fits to these chamber data, the experiments were simulated using the "highly branched" alkane representation used by Carter et al (2000) when modeling the Isopar-M® mixture. This representation is shown on Table 14, above.

The effects of using this alternative "highly branched" representation of the generic branched alkanes is the ASTM-3C1 sample predictions of effects on $\Delta([O_3]-[NO])$ and IntOH are shown in Figure 31. (All calculations on this figure use the adjusted mechanism for the aromatics in the base ROG to give the best fits to the base case data.) It can be seen that using this alternative representation results in only very minor improvements to the fits for $\Delta([O_3]-[NO])$, and has essentially no effects on the predictions of IntOH reactivity.

In order to assess the effects of the mechanism uncertainties and biases indicated by these data on predictions of atmospheric reactivity, adjustments were made to the mechanism used to represent the ASTM-3C1 constituents in order to improve the fits to the data. As indicated in Table 13, above, these complex hydrocarbon mixtures are represented in the simulations of the chamber experiments (and the atmosphere) by lumping together alkanes with similar OH rate constants into various ALKn lumped model species, whose parameters are derived based on the mixtures compounds they represent. In the case of this ASTM-3C1 sample, all the model species used to represent the C_{10}-C_{12} branched and cyclic alkanes have OH radical rate constant in the range that causes them to be lumped with ALK5, which means that this solvent is represented in the model by a single lumped model species. Modifications to the mechanisms for this model species can then be used as a basis for deriving adjusted mechanisms that may give better fits to the data. The mechanistic parameters for this lumped model species used when modeling the ASTM-3C1 experiments are shown on Table 15.

The major mechanistic parameters that affect predictions of an alkane's reactivity in environmental chamber experiments are its OH radical rate constant, its overall organic nitrate yield, and the number of NO to NO_2 conversions involved in its overall reactions. These affect how fast the compound reacts, its tendency to inhibit radicals, and its direct reactivity, respectively. The reactivities of the products they form will also affect their reactivities, but in the case of alkanes their effects on simulations of chamber experiments are generally secondary to the effects on the other parameters.

Table 15 shows that the main difference between the standard and the highly branched representation of the unspeciated branched alkanes is that the latter has about 0.4 more NO to NO_2 conversions. It also has a somewhat more reactive product distribution, which could have an impact in atmospheric reactivity predictions. However, as shown on Figure 31, the differences between these two representations do not result in large differences in the simulations of the chamber data.

In order for the lumped mechanism for ASTM-3C1 to fit the chamber data, it is necessary to either significantly decrease the overall organic nitrate yield or significantly increase the number of NO to NO_2 conversions. Table 15 shows two adjusted versions of the mechanism that were necessary to yield satisfactory fits to the $\Delta([O_3]-[NO])$ reactivity data, one where only the nitrate yield was adjusted and the other where the NO to NO_2 conversions were adjusted and the nitrate yield held fixed, and Figure 31 shows the fits that were obtained with these adjusted mechanisms.

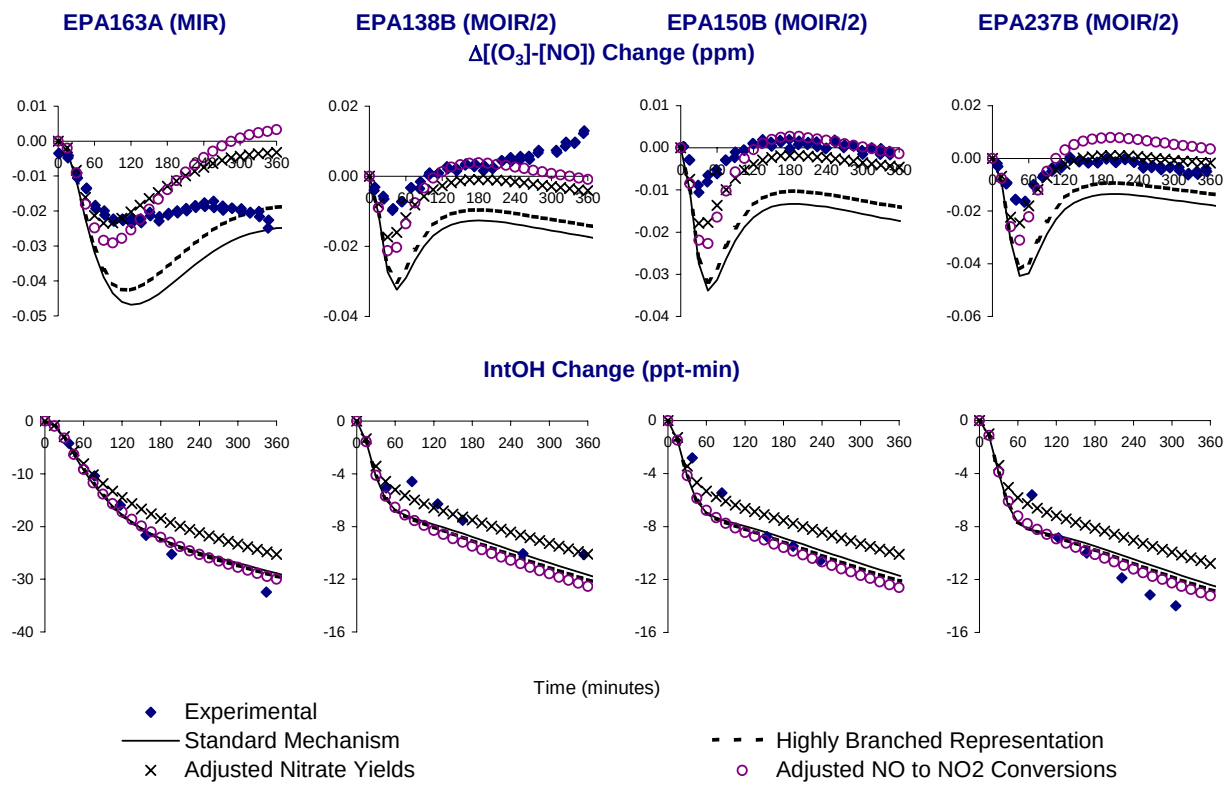

Figure 31. Effects of alternative representations and mechanisms on calculated effects of ASTM-3C1 addition on $\Delta([O_3]-[NO])$ and IntOH. All calculations used the adjusted aromatics mechanism for the base ROG simulation.

Table 15. Selected mechanistic parameters for the lumped ALK5 model species used to represent the ASTM-3C1 in the chamber and atmospheric reactivity simulations.

Parameter	Standard	Highly Branched	Adjusted Nitrate	Adjusted Conversions
OH Rate Constant (cm^3 $molec^{-1}$ s^{-1})	1.30×10^{-11}	1.31×10^{-11}	Same as Standard	
Nitrate Yield	47%	47%	30%	47%
NO to NO_2 Conversions	2.51	2.92	2.68 [a]	4.53
Product Yields				
Formaldehyde	0.00	0.05	Same as Standard	
Acetaldehyde	0.02	0.21		
Lumped Higher Aldehydes	0.15	0.14		
Acetone	0.06	0.39		
MEK	0.01	0.12		
PROD2 (Higher ketones, etc.)	0.43	0.46		

[a] This was not adjusted. Reducing the nitrate yield results in a corresponding increase in the NO to NO_2 conversion because of the reactions of the radicals that otherwise form the nitrate.

It can be seen that the fits to $\Delta([O_3]-[NO])$ are not greatly different regardless of whether the nitrate yield or the NO to NO_2 conversions were adjusted, while adjusting the nitrate yield causes a slight reduction in IntOH reactivity. The precision of the IntOH measurement is such that the data do not clearly indicate which adjustment (or a combination of the two) is more appropriate. The fits to IntOH are actually slightly better with the adjustment of the NO to NO_2 conversions, but the fits with the adjusted nitrate yield mechanism are more consistent with what was observed for n-octane and the petroleum distillate solvents, where the inhibition of IntOH was generally underpredicted.

DISCUSSION AND CONCLUSIONS

This project partly achieved its objective of reducing uncertainties in ozone reactivity estimates for architectural coatings VOCs. The evaluation of procedures for estimating reactivities of complex hydrocarbon mixtures indicated that, the bin assignments incorporated in the CARB's aerosol coatings regulation are reasonably consistent with reactivity estimates based on available compositional information, with the possible exception of the lowest boiling point bins that contain cycloalkanes. A new procedure was derived to estimate reactivities of complex hydrocarbon mixtures with limited compositional information that may serve as a basis for updating hydrocarbon bin assignments when the regulatory reactivity scale is updated or modified. Environmental chamber data were obtained that generally validate the current estimated mechanisms for the Texanol® isomers and the current compositional estimates and mechanisms used to estimate reactivities of petroleum distillate hydrocarbon solvents, at least for MIR conditions. These were the successes for this project, and their implications are discussed further below.

However, this project did not achieve all of its objectives and indicated potentially significant problems and uncertainties in current reactivity estimates for petroleum distillate VOCs that need to be resolved. Model simulations of the environmental chamber experiments with the synthetic hydrocarbon mixture that was studied indicated that the current compositional assumptions or mechanisms for at least some synthetic mixtures of branched alkanes tend to somewhat underestimate their ozone impacts, and no clear resolution of this problem was found. There is also a problem with the current mechanisms for aromatics that affects atmospheric simulations of MIR conditions (Carter, 2004a) that may introduce biases into relative reactivity estimates for architectural coatings and other VOCs, though the nature, significance, and magnitude of these biases are unknown. The incremental reactivity data obtained in this and previous studies also suggest that current mechanism may underestimate the tendency of aromatics to inhibit O_3 formation under NO_x -limited conditions. While this probably will not affect MIR calculations (since MIR represents relatively high NO_x conditions), it does reflect on the models' ability to predict ozone impacts of aromatics in general, and may affect more regionally based reactivity scales (e.g., see Carter et al, 2003) should they be adopted in the future. These issues regarding aromatic mechanisms and reactivity probably cannot be resolved without completely overhauling the aromatics mechanisms, which is a very major undertaking that could not be accomplished during the period covered by this report. Finally, although progress was made in improving the utility of the direct reactivity measurement method for reactivity screening and reducing uncertainty in reactivity estimates, we were unable to complete this task with the time and resources allocated for it in this program.

These areas of success and problems, and their implications concerning uncertainties in current reactivity estimates for architectural coatings VOCs and research needs, are discussed further below.

Estimation of Hydrocarbon Solvent Compositions and Reactivity

We believe that this project provides an independent peer review of the CARB's hydrocarbon bin MIR assignments that are incorporated in its current regulations, which we felt was needed. The Kwok et al (2000) approach is based on relating estimated carbon numbers and compositional categories directly to MIRs, but we feel a more appropriate and general approach is to relate these to estimated distributions of chemical compounds, and then use the reactivities for those compounds to derive the reactivities for the mixtures. This would permit a consistent approach to be used for other reactivity scales besides the SAPRC-99 MIR, and provides a separation of compositional and reactivity estimates, which could be useful for uncertainty analyses.

The results of our analysis indicate that, with the exceptions of bins 1 and 3-5, and possibly bins 13, 18-20 and 24, the hydrocarbon bin assignments derived by Kwok et al (2000) and adopted in the CARB aerosol coatings regulation perform reasonably well in predicting MIRs for hydrocarbon solvents for which detailed compositional data are available. However, the values for bins 1 and 3-5 appear to be biased high by about 25-50%. This is because the method derived by Kwok et al (2000) assumed that substantial amounts of relatively reactive cyclopentanes may be in some of the solvents in these bins. Although this was not the case for the limited number of solvents in these bins used in our evaluation, this may not be applicable to other solvents currently in use. This issue of possible cyclopentane content is not applicable for the other bins, and in those cases for which solvents with compositional data are available, the CARB assignments agree with the MIRs for the analyzed solvents to within ±25% in most cases.

Data concerning cyclopentane content should be examined carefully when the regulatory reactivity scale is updated because it has a non-negligible impact on reactivity assignments for the low boiling point hydrocarbon bins. This is less of an issue for the heavier hydrocarbon solvents, since there is generally less variability in the reactivities of the possible constituents within the same hydrocarbon type categories.

This project also achieved its objective in providing a general procedure for estimating compositions of hydrocarbon solvents with limited compositional data that is not tied to any single reactivity scale. The information it requires is the same as that required to make CARB bin assignments, though the more precise the information (e.g., specific boiling points or aromatic contents, rather than general ranges) the more precise the estimate. It predicts reactivities derived from detailed compositional data for the individual hydrocarbons to better than ±15% in most cases, given only their boiling point ranges and their hydrocarbon type analysis results. It can be used to derive bin assignments that perform at least as well as the CARB assignments for the hydrocarbon solvents used in this evaluation, predicting the reactivities derived from the detailed compositional data to within ±25% for all the bins, including the low boiling point bins 1 and 3-5.

Therefore, this new “spreadsheet” method for deriving hydrocarbon composition and reactivity estimates could be used as a basis for updating the bin reactivity assignments when reactivity scales are updated, or if use of a different reactivity scale is adopted. However, before it is used in a regulatory application it needs to be evaluated using the full distribution of solvents in use, including solvents in bins 1 or 3-5 that might possibly have higher cyclopentane content than predicted by this method. The method for making bin calculations proposed in this work is based on the objective of estimating the composition of a solvent that represents the average or mid-point in reactivity in the range of solvents in any given bin. The method would need to be modified if the policy objective is to base the bin reactivity assignments on the most reactive of the solvents in a given bin, as may have been the policy when the CARB adopted the present regulation. This will need to be discussed and assessed at the time the regulatory reactivity scale is updated.

There are no data available to us to evaluate the performance of the CARB MIR assignments for bins 13, 18-20 and 24. However, given the performance of the spreadsheet method developed in this work in predicting reactivities derived from detailed compositional data for the other bins, it is reasonable to expect that its performance in predicting the reactivities of these other bins is also satisfactory.

These results suggest that uncertainty in reactivity assignments due to compositional uncertainty is approximately ±25% if unbiased bin assignments are used, and better than ±15% if the specific type distribution and boiling point data are taken into account. It is important to recognize that this does not take into account chemical mechanism uncertainty, which might be significantly greater, particularly for solvents high in aromatics or branched alkanes. The environmental chamber experiments, discussed below, provide the appropriate basis for assessing chemical mechanism uncertainty. For example, the

results suggest that it might be appropriate to put synthetic hydrocarbon mixtures of branched alkanes in separate bins with higher reactivity estimates than currently used for them.

Progress in Developing a Direct Reactivity Measurement Method

This program was not successful in achieving its objective of adapting the direct reactivity measurement method developed by Carter and Malkina (2002) to obtain data of utility for assessing architectural coatings VOC reactivity. However, some progress was made, and the objective may eventually be obtainable. The addition of the total carbon analyzer based on a combustion catalyst and CO_2 monitoring was found to solve the problem of analyzing the amount of test compound added, and provided a useful method for monitoring how changes in the amount of added VOC affected the $\Delta([O_3]-[NO])$ measurements. Although this introduced a source of uncharacterized variability in the data that cannot be determined, if the direct reactivity results for a standard compound with a well characterized mechanism, such as propane, are used to normalize the data, then the results are consistent with model predictions for compounds with as low a volatility as n-dodecane. It may be possible to obtain equally consistent measures of direct reactivity for materials with even lower volatility, but this has not been assessed. In any case, the results to date suggest that the method could be useful as a screening method for assessing direct reactivities of hydrocarbon solvents, especially in the volatility range used in architectural coatings.

Unfortunately, the time and resources allocated to this task were expended before we could investigate or improve it further and apply it more widely to other compounds and hydrocarbon solvents. This is because of the amount of time and testing required before the total carbon analyzer to yielded satisfactory results, and the time expended in the unsuccessful attempts to elucidate the differences between experimental results and model predictions. Although normalizing the direct reactivity results to those for a known compound appear to yield satisfactory results, it obviously would be better if the conditions of the experiments that affect the results were better characterized and the sources of uncharacterized variability were removed. In any case, additional funding would be required to develop and apply this method further.

It is particularly unfortunate that we ran out of resources for this task before we could at least apply it to the specific hydrocarbon solvents chosen for study for this project. The results of the experiments we did carry out with the n-alkanes and the Safety-Kleen mineral spirits sample (Carter et al, 1997) suggested that useful mechanism evaluation results could have been obtained, at least in a relative sense. Direct reactivity measurements for the synthetic branched alkanes solvent ASTM-3C1, compared to those for the other all-alkane solvents, could potentially have elucidated the source of the discrepancies between the model calculations and the environmental chamber data for this particular solvent. For example, if it gave approximately the same direct reactivity results as, for example, the ASTM-1C petroleum distillate, then it would rule out the source of the discrepancy being due to inappropriate OH rate constants or NO to NO_2 conversions in the mechanism, and suggest that the problem is more likely due to inappropriate overall nitrate yields. As discussed below, this would have impacts on estimates of its calculated atmospheric reactivity.

Environmental Chamber Reactivity Evaluations

The major task in this project was to conduct environmental chamber experiments to evaluate estimates of atmospheric ozone impacts of the water-based coatings solvent Texanol® and representatives of different types of hydrocarbon solvents used in coatings. This project was successful in conducting experiments useful for mechanism evaluation with all of these solvents, and the results are useful not only for evaluating the current SAPRC-99 mechanism as discussed in this report, but also for evaluating

updated mechanisms once they become developed. This is important, because as discussed below there is a need to update the mechanisms current used for at least some of the solvents that have been studied.

Use of Chamber Data for Mechanism Evaluation

Before discussing the implications of the results for the specific solvents, it is important to reiterate that the primary objective of these experiments was not to directly measure their atmospheric reactivity, but to provide data to test the ability of chemical mechanisms used in models to predict their impacts in the atmosphere. This is because atmospheric conditions that affect VOC reactivity are highly variable, and it is not practical to duplicate in an environmental chamber all of the physical conditions that will affect quantitative measures of atmospheric reactivity. This is important to consider in the context of this project because the environmental chamber results, taken by themselves, indicate that all the solvents studied for this project except for Aromatic 100 either inhibit the formation of O_3 or have negligible impacts on its formations under the conditions of the experiments. However, this, by itself, does not necessarily indicate that these solvents will always inhibit ozone formation in the atmosphere.

For example, Figure 32 shows the results of model simulations of adding equal relative amounts of Texanol® and the dearomatized C_{10}-C_{12} alkane solvent ASTM-1C to the "MIR" environmental chamber incremental reactivity experiment and to an airshed box model scenario representing those used to derive the MIR scale. The same mechanisms for the compounds were used in the airshed as in the chamber simulation, and as discussed above the MIR experiment was designed to approximate the chemical conditions of the atmospheric simulations used to derive the MIR scale. Although the model predicts, as is observed in our experiments, that Texanol® has no measurable effect on O_3 in the chamber simulation, an equal relative amount is calculated to have a positive impact on O_3 in the atmospheric simulation. Likewise, the same representation and mechanism for the ASTM-1C solvent that correctly predicts that it has negative impacts on our experiments in the chamber predicts that it has a positive effect on O_3 in the atmosphere. This illustrates that using environmental data by itself may lead to misleading results for these types of compounds, and that modeling is necessary to extrapolate, in effect, from conditions of the chamber to conditions of the atmosphere.

The reasons for the differences between the chamber and ambient reactivity simulations illustrated in Figure 32 can be readily explained. As discussed previously (e.g., Carter and Atkinson, 1989), there are a number of different aspects of a mechanism that can affect its overall ozone impact, and the relative importance of these aspects can vary with environmental conditions. Compounds such as the Texanol® isomers or the C_{8+} alkanes present are highly reactive in two senses, one negatively and one positively. They are negatively reactive in the sense that their reactions significantly inhibit overall radical levels, due to the relatively high levels of organic nitrate formation predicted in their mechanisms (Carter, 2000a). If this were the only factor of importance, these compounds would inhibit O_3 formation under all conditions, because the radical inhibition reduces the amounts of base ROG components that react to form ozone. However, these compounds are also positively reactive in the sense that they react relatively rapidly and cause a relatively large number of NO to NO_2 conversions when they react. Thus there is a relatively large amount of ozone that is formed in their direct reactions. These large reactivity impacts work against each other in both the chamber and the atmospheric simulations, and small differences in the relative importances of these two types of impacts can have large effects on predictions of reactivity. Generally, environmental chamber experiments tend to be somewhat more sensitive to radical inhibition effects than atmospheric simulations. In the case of Texanol® the negative and positive aspects almost exactly balance in the chamber experiments, while in the atmospheric its net reactivity is predicted to be positive because the negative effect of the radical inhibition is relatively less important. In the case of the ASTM-1C solvent (and many other alkanes, such as n-octane), the balance shifts from a net negative effect in the chamber experiments to a net positive effect in the atmosphere.

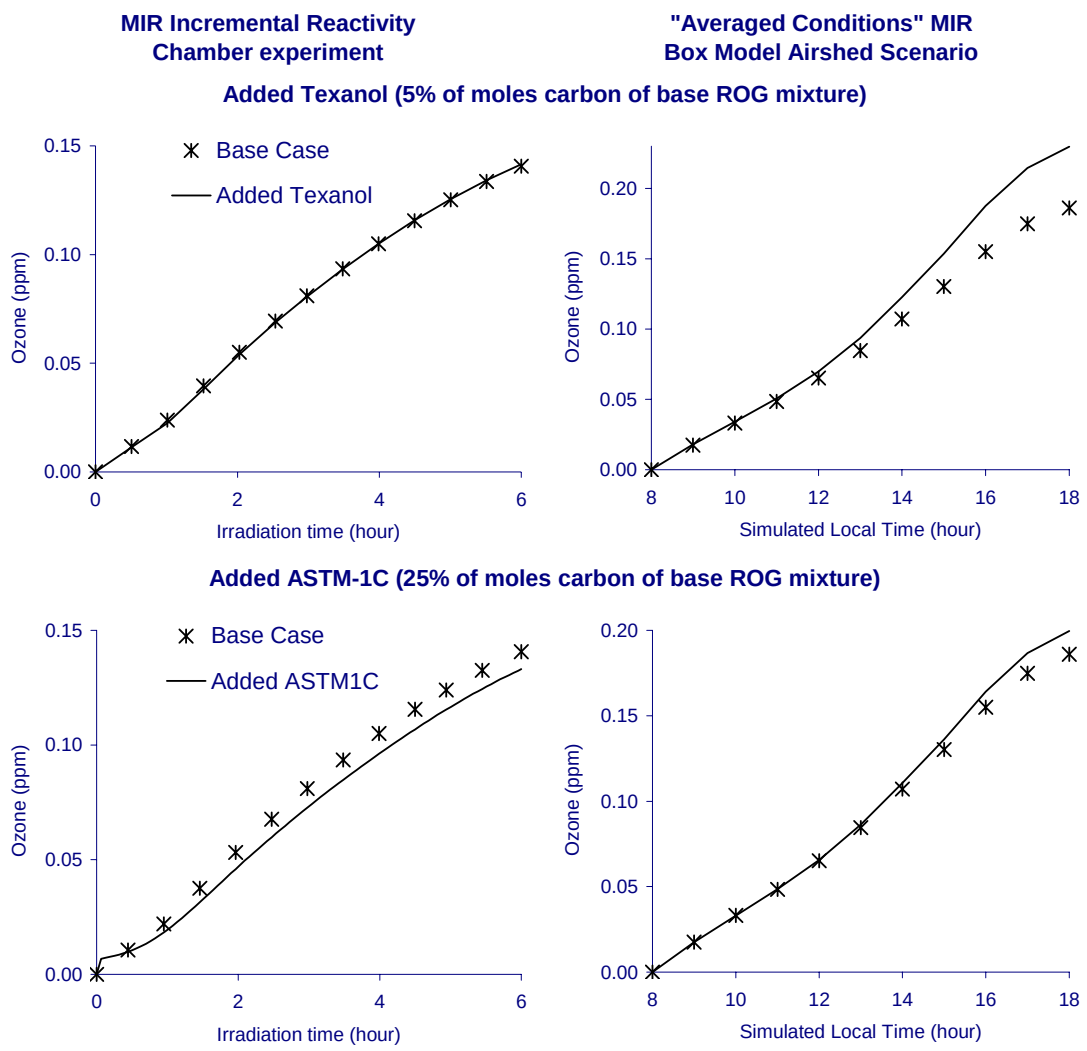

Figure 32. Comparisons of environmental chamber and atmospheric incremental reactivity simulations for equal relative additions of Texanol® or ASTM-1C solvent.

Therefore, in terms of its ability to predict the atmospheric impact of a particular VOC, what is important is whether the model correctly predicts the magnitudes of the different types of impacts under various conditions. The use of experiments with differing chemical conditions can provide a means to test different aspects of the mechanisms if they differ in their sensitivities of these aspects. This is why we conduct mechanism evaluation experiments at differing levels of NO_x availability, because it significantly affects the relative importance of the aspects of the mechanisms regarding NO_x sinks, which are important at affecting reactivities at low NO_x levels. This is also why it would be useful to have an ability to measure direct reactivities of VOCs in an experiment that is much less sensitive to radical inhibition effects than is the case for environmental chamber experiments. In any case, if the model cannot correctly predict the *net* impact of a VOC on O_3 formation in an environmental chamber experiment, it cannot be expected to accurately predict the net impact of the VOC on O_3 formation in the atmosphere, even if that net impact differs in magnitude or sign.

In this regard, it is also important that the model be able to correctly predict the relative importances of the various impacts of the VOC's mechanisms on net ozone formation. Otherwise it would not give correct predictions of the VOC's atmospheric impacts even if the VOC's mechanism is correct, and it may give misleading results when evaluating the mechanism using chamber data. This is why it is important that the model give a reasonably good simulation of the base case scenario if it is to reliably predict reactivities in the atmosphere, or if it is to give a reliable evaluation of the predictive capability of the mechanism in the chamber experiment.

Unfortunately, as discussed by Carter (2004a) there is a problem with the current mechanism in underpredicting rates of O_3 formation in the lower ROG/NO_x ratio experiments such as the MIR experiments carried out for this project. We were unable to correct this problem with a mechanism that is consistent with all the data within the time frame of this project. Therefore, for the purpose of providing at least a better approximation of the conditions of the base case experiments for evaluating the mechanisms of the test VOCs studied for this project, we developed a modification to the base case aromatics that did not have this bias in the simulations of the base case experiments. This is not a "better" aromatics mechanism because it significantly overpredicts their reactivities in the aromatics - NO_x experiments that were used when developing the existing mechanisms, and still does not correctly predict the effects of adding CO to aromatics - NO_x irradiations (Carter, 2004a). However, its use at least gives us some indication of how sensitive the evaluation results may be to this bias in the mechanism.

The results of this evaluation were actually somewhat encouraging in this regard. As expected, the use of the adjusted base mechanism improved the fits of the simulations to the base case experiments and also improved predictions of the time profiles for the incremental reactivity results in the MIR experiments. However, in general the use of the adjusted base mechanism did not change the conclusions one would draw from the experiments as to the overall performance of the mechanisms of the test compounds in predicting effects on ozone formation or overall radical levels. This suggests that the uncertainties in the base case mechanism may not necessarily be affecting evaluation results using incremental reactivity chamber data. However, this does not rule out the possibility that other modifications of the base case mechanisms, which may be more chemically accurate, may affect incremental reactivity predictions to a greater extent than the adjustment examined in this study.

One area where there is likely to be a problem in this regard is the predictions of the effects of the test compounds on overall OH radical levels. The current mechanism for the base case experiment consistently underpredicts integrated OH radical levels throughout the ROG/NO_x range that is relevant to the experiments for this project. The mechanism also underpredicts the magnitudes of the OH radical impacts of essentially all test VOCs on integrated OH levels whose mechanisms give good simulations of their effects on NO oxidation and O_3 formation, including those whose mechanism are considered to be reasonably well established (Carter, 2000a). It is likely that the tendency of the mechanism to underpredict integrated OH (IntOH) impacts for VOCs whose other impacts tend to be correctly simulated may be due to the tendency of the base case mechanism to underpredict IntOH. This tends to reduce the utility of IntOH incremental reactivity data for mechanism evaluation, unless the results are significantly out of line with the results for other VOCs.

Therefore, the uncertainties in current base mechanism result in greater uncertainty and lower precision in use of these chamber data for evaluating the mechanisms for the test compounds or solvents that were studied than would be the case if the problems with the present base mechanism did not exist. However, these data will be available for an updated evaluation of the mechanisms for these solvents should a future mechanism be developed that hopefully will not have the problems and biases of the present base case mechanisms. With less uncertainty in the base case mechanism, and better simulations of the base case O_3 and integrated OH data, a more precise evaluation of the predictive capabilities of the mechanisms for these solvents can be carried out using the chamber data from this project. In any case,

until the base mechanism is updated and the problems discussed above are resolved, the current version of the SAPRC-99 mechanism still provides "best estimates" of atmospheric reactivities that are presently available.

Evaluation Results for Texnaol®

Perhaps the greatest success for this project was the experiments with Texanol®. Overall, the results of the experiments with this solvent tended to validate the existing mechanism assignments that were made for its constituents that were based on applications of various estimation methods (Carter, 2000a). Despite our concerns about being able to obtain quality data for such a low volatility material, tests indicated that our ability to quantitatively inject and analyze the Texanol® isomers in the gas phase was entirely satisfactory. Indeed, the gas-phase analysis of the isomers was sufficiently precise that we were able to use relative rate technique to measure their OH radical rate constants, relative to that for m-xylene, which is present in the experiments as a base ROG component. The results indicate that the OH radical rate constants for 3-hydroxy-2,2,4-trimethylpentyl-1-isobutyrate and 1-hydroxy-2,2,4-trimethylpentyl-3-isobutyrate were 1.68 and 1.30 x 10^{-11} cm^3 $molec^{-1}$ s^{-1}, respectively, in excellent agreement with the estimated values of respectively 1.62 and 1.29 x 10^{-11} cm^3 $molec^{-1}$ s^{-1} that are incorporated in the existing mechanism.

The results of the Texanol® experiments were well duplicated by the model simulations, with the adjustments to the base mechanism having relatively little effects on the incremental reactivity predictions. As indicated above the Texanol® addition had no measurable effect on NO oxidation and O_3 formation, but it did have a large effect on the integrated OH values, indicating that it was indeed perturbing the conditions. Apparently the model correctly predicted that under the conditions of these experiments the positive effect of the O_3 formed from the direct reactions of the Texanol® isomers almost exactly balances out the relatively large negative effects on OH levels.

These results, together with the results of the OH radical rate constant measurements, indicate that there is no need to revise the current mechanisms used for the Texanol® isomers, or revise the current estimates for their atmospheric reactivities. This tends to validate the general estimation methods used to estimate mechanisms in SAPRC-99 for such compounds (Carter, 2000a), though with such a large and complex molecule the good agreement (especially for the OH rate constants) may be due to a coincidental cancellation of errors. Although as discussed above this will need to be revisited if the base mechanism undergoes significant modifications in the future, but we suspect that the results and conclusion will probably be similar.

The one unexpected results of this study, that does have implications on reactivity estimates for Texanol® as used in coatings, concerned the relative importances of the two isomeric esters. The isomers apparently readily interconvert, and the distribution of the isomers appears to be different when measured in the gas phase than in the liquid phase. In the liquid phase the dominant isomer, the 1-ester, is ~68% of the total, while in our gas-phase analysis the relative amount of the 1-ester was reduced to about ~28% and was independent of the temperature used in the injection system. Unpublished results from Corsi and co-workers (R. Corsi, University of Texas, personal communication, 2005) also indicate that the isomers have different distributions in the gas phase than in liquid samples, so our results have been seen in other laboratories. This affects atmospheric reactivity estimates because the two isomers have somewhat different mechanisms and reactivities.

The current MIR estimate (Carter, 2000a, 2002a) the Texanol® is based on a liquid-phase-derived ratio of 67% 1-ester and 33% 3-ester. Since the MIR values for the two esters are 0.865 and

0.911, respectively[12,13], this yields an MIR value of 0.880 for the solvent itself. However, for atmospheric reactivity estimates the gas-phase ratio is probably more appropriate, since this is the phase where the compounds react to affect O_3 formation. Based on our results, we recommend deriving the atmospheric reactivity for the whole Texanol® mixture based on assuming 58% and 42% of the 1- and 3-esters, respectively, which would yield a revised SAPRC-99 MIR of 0.884. Although the change in the estimated mixture MIR is insignificant and certainly does not indicate a need to revise the current regulatory MIR for this solvent, the assumed composition should be updated when the reactivity scales are revised.

Evaluation Results for Petroleum Distillate Hydrocarbon Samples

This project was also successful in obtaining environmental chamber data useful for evaluating mechanisms for representative petroleum-derived hydrocarbon solvents with varying degrees of aromatic content from all (or essentially all) alkane VMP naphtha and ASTM-1C to all-aromatic Aromatic 100. Although more precise evaluation results can be obtained if the base mechanism is improved, in general the results of the evaluations with the adjusted and unadjusted base mechanisms were comparable, suggesting that updated evaluation may not give significantly different results.

The results of the chamber experiments petroleum-distillate-derived primarily alkane hydrocarbon solvents were generally consistent with model predictions, and generally were comparable to the evaluation results for n-octane, whose mechanism is considered to be reasonably well established, and whose reactivity characteristics are similar. The performance of the mechanism in simulating the results of the experiments with aromatic contents up to ~20% was similar to its performance in simulating the all-alkane mixtures, and the model appropriately predicted the reactivity trends caused by the increasing aromatic contents. Therefore, although there are uncertainties due to problems with the base mechanism, the data obtained tend to validate our existing estimates for the reactivities of these types of solvents, and do not indicate a need to change the atmospheric reactivity estimates for them at the present time. However, this will need to be reevaluated when the base mechanisms are updated, as is the case for the other solvents studied for this project.

Of the compounds and samples studied for this project, the Aromatic 100 is expected to have the greatest degree of uncertainty in the mechanism. This is because the uncertainties in aromatic mechanisms are such that their mechanisms cannot be completely predicted or estimated *a-priori*, but have to have important aspects adjusted to fit chamber data. Chamber data are available for the di- and tri-methylbenzene isomers and ethyl benzene and adjusted mechanisms have been developed for those compounds, but these constitute less than 40% by weight of this solvent, according to the analysis data we obtained. Thus, over 60% by weight of this solvent contain compounds for which no chamber data are available to develop mechanisms, and whose mechanisms are estimated by analogy with other compounds. Our studies with the alkylbenzenes show that the mechanistic parameters and reactivities can vary significantly from isomer to isomer even after differences in OH radical rate constants are taken into account, and that ethylbenzene has much lower reactivity than expected based on analogy to toluene

---

[12] All atmospheric reactivity values given in this discussion are in units of grams O_3 per gram VOC.

[13] Note that the more reactive of the two isomers is in fact the one with the lower OH rate constant. This is because a lower total number of NO to NO_2 conversions is calculated for the 1-ester, due to the fact that the alcohol group is at a secondary carbon, where there is a greater chance for OH radicals to react at an α position. This reaction results in the direct formation of HO_2, resulting in fewer NO to NO_2 conversions than is the case for reactions at other positions in the molecule.

(Carter, 2000a). For this reason, estimating aromatic mechanisms by analogy is highly uncertain and subject to error.

In view of this, it is of interest that the ability of the model to simulate the results of the experiments with Aromatics-100 is of comparable quality of the ability of the model to simulate comparable experiments with m-xylene. As with m-xylene, the model gives reasonably good simulations of the impacts of Aromatic 100 on the results of the higher NO_x MIR experiments and during the first period of the lower NO_x incremental reactivity runs, and also gives reasonably good simulations of O_3 formation in aromatics - NO_x experiments without the added base ROG surrogate. These are the chemical conditions used to derive the MIR scale. Therefore, the mechanistic estimates and lumped-molecule assignments made when deriving mechanisms for the Aromatic 100 constituents for which no data are available appear to be validated at least to some extent, at least for purposes of deriving a MIR scale. However, it is possible (indeed likely) that assignments that underestimate the reactivities of some of the components in the complex mixture are being cancelled out by assignments that overestimate reactivities of other constituents.

The results of the evaluation for Aromatic 100 are also similar to those for m-xylene in indicating problems with the mechanisms for aromatics in general. The model consistently underpredicted the effect of adding CO to the Aromatic 100 - NO_x irradiations, and did not correctly predict the extent to which the added solvent inhibited final O_3 levels in the higher ROG/NO_x incremental reactivity experiments. This is essentially the same as the results obtained in the incremental reactivity experiments for m-xylene and the experiments examining the effects of added CO on toluene - NO_x and m-xylene - NO_x irradiations (Carter, 20004). Therefore, all the aromatic mechanism problems that apply to m-xylene and the other aromatics are also applicable to Aromatic 100. Better model performance in simulating Aromatic 100 reactivity would be expected if the base mechanism is improved, but this would need to be evaluated.

It would be of interest to see if the results obtained with this Aromatic 100 sample are also applicable to petroleum distillates with higher molecular aromatics, such as Aromatic 150 or Aromatic 200. Here, the extrapolations are being made to even larger molecules relative to the molecules that have been studied, and the molecular structures are more variable. For example, the contributions of naphthalenes and alkylbenzenes with four or more substituents, which are not well represented by compounds that have been studied, become more important in these solvents. Therefore, the extrapolated mechanisms for these heavier aromatic mixtures must be considered to be even more uncertain than those for the Aromatic 100 sample studied in this work.

Evaluation Results for the Synthetic Branched Alkane Hydrocarbon Sample

This project also obtained useful mechanism evaluation results for a synthetic hydrocarbon mixture high in branched alkenes. Although this particular sample is referred to as “ASTM-3C1” in the discussion in this report based on its designation in the D 235-02 specification (ASTM, 2003), the specification only refers to its physical properties and bromine number, and solvents with this designation could well include petroleum-distillate-derived solvents. Although this probably should be verified by experiments with petroleum-distillate derived ASTM-3C1 solvents, we assume that the results obtained with this sample are only applicable to synthetic hydrocarbon mixtures made using similar processes as used to make this sample. Information concerning the specific process used to make this sample was not provided, but that should be included as part of any more comprehensive reactivity evaluations of synthetic hydrocarbons of this type.

The reason we distinguish this sample from the other all-alkane hydrocarbon mixtures, and suggest that the process used to synthesize the solvent may be important, is that different reactivity and mechanism evaluation results were obtained in the experiments with this sample compared to the results

with the other alkane mixtures. In particular, less inhibition of ozone was observed in the experiments when this solvent was added in the incremental reactivity experiments compared to the other alkane mixtures and compared to the model predictions. This is the only hydrocarbon solvent sample studied to date where the SAPRC-99 mechanism could not simulate the experimental reactivity data within the uncertainty of the determination for all the experimental conditions that were examined (see, for example, Carter et al, 2000, 2002 as well as the experiments for this project). Since the model underpredicts the inhibiting effects of this solvent, we can conclude that it is likely to underpredict its impact on ozone formation in atmospheric simulations.

The actual branched alkane compounds in this and other hydrocarbon solvents in this carbon number range are difficult to determine because of the very large number of isomers that are possible. The set of compounds used in the standard model calculations to represent the unspeciated branched alkanes in hydrocarbon solvents is based on analyses for petroleum distillate samples, for which available analyses indicate relatively low degrees of branching. However, the process used to make this sample may result in more highly branched alkanes, which in general are predicted to have higher reactivity because of increased NO to NO_2 conversions and lower molecular weight, and generally more reactive, products because of the increased importance of decomposition vs. isomerization processes for the alkoxy radical intermediates (Carter, 2000a). To investigate if this could account for the results, we used an alternative representation for the unspeciated C_{10}-C_{12} alkanes in this sample where they were represented by compounds with a much higher degree of branching (i.e., using a tetramethyl heptane to represent branched C_{11} alkanes instead of mixture of methyl decanes and dimethyl nonanes). Although this resulted in a slight improvement in model predictions of the experiments, the change was relatively small and not sufficient to account for the discrepancies. In order to fit the data, it was necessary to assume either much lower overall nitrate yields or much more NO to NO_2 conversions than currently estimated by any of the C_{10}-C_{12} branched alkanes in the current mechanism.

The cause of this discrepancy affects predictions of atmospheric reactivities of this solvent. This is shown on Table 16, which gives calculated atmospheric MIR values for this solvent using the various mechanisms that were evaluated. It can be seen that the adjusted mechanisms that fit the data give atmospheric MIR estimates that are ~25% to ~75% higher than predicted using the current mechanism and compositional assignments. It can also be seen that the change in the calculated MIR is affected by the extent to which the discrepancy is due to overestimation of the total nitrate yields or underestimation of the number of NO to NO_2 conversions, i.e. the direct reactivity, of the constituents in the solvent. Better compositional and mechanistic information, or, lacking that, measurements of direct reactivities or total nitrate yields for the solvents are needed to distinguish between these two alternatives, since the chamber data obtained in this study is clearly not adequate to distinguish between these two alternatives.

This solvent falls into CARB bin 12, and the CARB MIR assignment for that bin is also shown on Table 16 for comparison. It can be seen that although this bin assignment gives an appropriate reactivity estimate for this solvent if the standard composition and mechanism is assumed, it is low, by about a factor of 1.5 to 2, if the mechanism is adjusted to fit the chamber data. Note that of the solvents in Bin 12 used to evaluate the bin assignments for this project, six are like this solvent in being predominantly branched alkanes, and two are predominantly normal alkanes (see Table 3, above). It appears likely that at least some, but not all, of the other bin 12 solvents that are high in branched alkanes are like this one, though the derivation of these solvents was not given. If this is the case, revised bin assignments for these solvents is probably appropriate. On the other hand, it is likely that the current mechanisms for the normal alkanes are reasonably satisfactory (e.g., see Carter, 2000a, Carter et al, 1996), and, as indicated on Table 3, the bin MIR assigned to these solvents may if anything overestimate their reactivities. Thus, it appears that these types of solvents need to be treated separately when the bin assignments are updated.

Table 16. Atmospheric MIR values calculated for the ASTM-3C1 sample using various assumed compositions and adjusted mechanisms.

Mechanism or Assignment	Consistent with Chamber Data?	Atmos. MIR [a] (gm O_3/gm VOC)
CARB Bin 12 assignment (applicable to this solvent)		0.81
Standard composition assignment and standard mechanism	No	0.87
Highly branched compositional assignment, standard mechanism.	No	1.3
Adjusted mechanism - total nitrate yield reduced	Yes	1.1
Adjusted mechanism - total NO to NO_2 conversions increased	Yes	1.5

[a] Calculated using the standard methodology used to derive the MIR scales as given by Carter (2000a, 2003b)

It should be noted that this is not the only synthetic solvent high in branched alkanes that has been studied in environmental chamber experiments. Carter et al (2000) obtained environmental chamber data for "ISOPAR-M®[14], a synthetic material consisting primarily of C_{11}-C_{16} branched and cyclic alkanes, of which ~84% is branched. This is a heavier material than the ASTM-3C1 solvent studied for this project, though it would still fall into CARB Bin 12 (albeit at the extreme high end of the range). Experimental and calculated reactivity results for selected experiments carried out with this solvent are shown on Figure 33, with the experiments shown being the examples of each type of run where the model gave the best fits to the base case experiment. The figure also indicates the base case concentrations used for those experiments, which are considerably higher than used in this study. It can be seen that for this solvent the model gives reasonably good fits to the effects of the solvent on $\Delta([O_3]-[NO])$ in the "mini-surrogate" and the lower NO_x full surrogate experiment, but overpredicts the $\Delta([O_3]-[NO])$ inhibition in the higher NO_x full surrogate run. Thus, the results with this heavier ISOPAR-M® solvent are similar to those for the ASTM-3C1 solvent in one example of the three types of experiments used in the Carter (2000) study but not on the other examples. The use of the "highly branched" representation for the unspeciated branched alkanes gives essentially the same fits to the data as shown on Figure 33, though it calculates a ~40% higher MIR for this solvent.

The differences between the results of Carter et al (2000) with ISOPAR-M® and the results of this study with the ASTM-3C1 solvent could be due either to the differences of the base case experiments or to differences in the molecular weight range of the material, or to differences in the way the materials were synthesized. Additional information and experiments with these materials and experiments with other types of synthetic branched alkane materials would be needed to fully assess this.

Implications of Chamber Results on Maximum Incremental Reactivities

Since the California Air Resources Board currently uses the Maximum Incremental Reactivity (MIR) scale in its reactivity-based regulations, the implications of the results of the chamber experiments on the MIR's of the solvents studied is of particular interest. As discussed above, although there were problems with some aspects of the mechanism evaluation, the results indicated that the MIRs calculated

[14] ISOPAR-M is a registered trademark of the ExxonMobil Chemical Company.

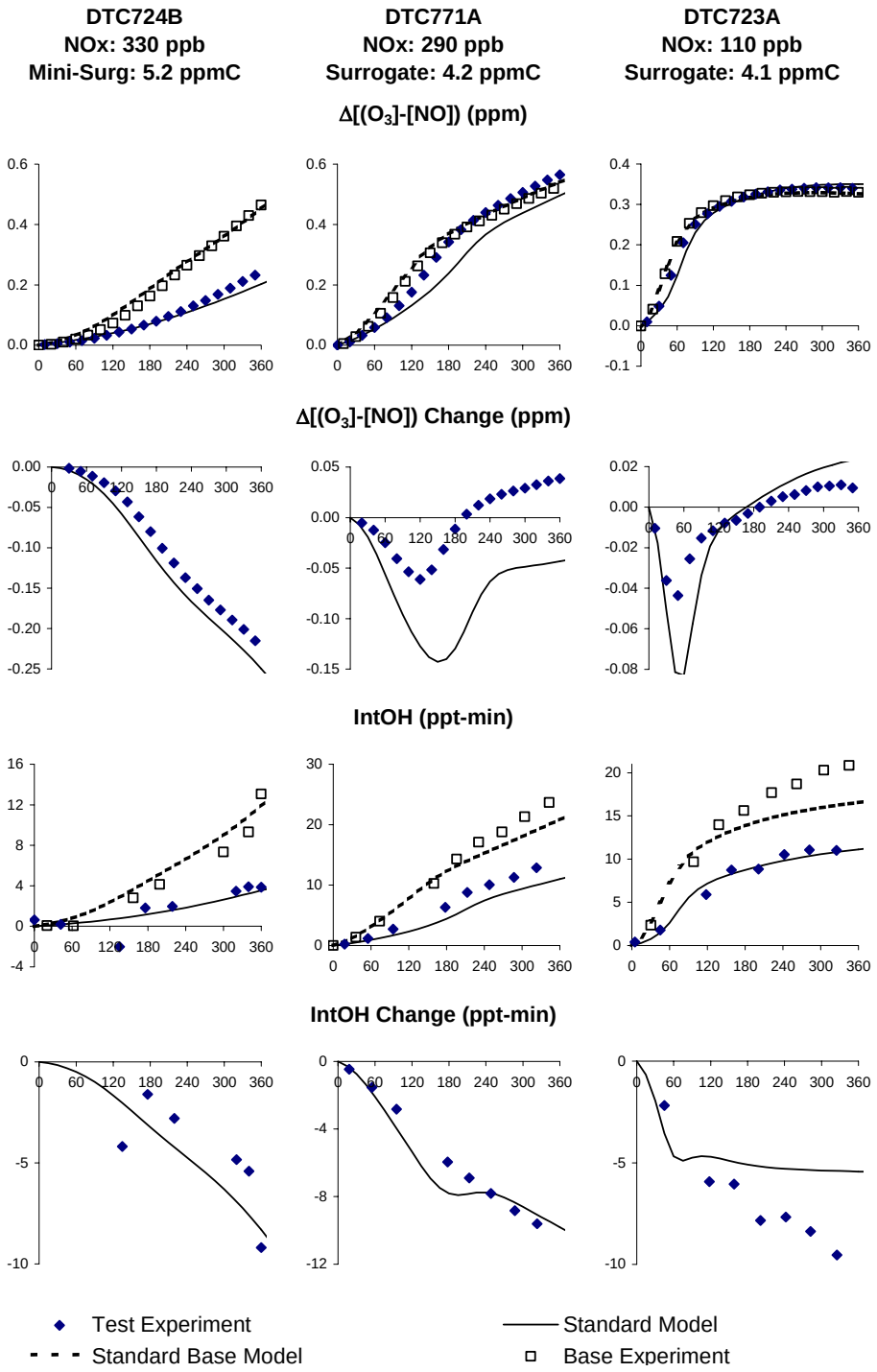

Figure 33. Experimental and calculated concentration-time plots for selected incremental reactivity experiments with ISOPAR-M®, carried out by Carter et al (2000).

using the current SAPRC mechanism continue to be the current best estimates for all the solvents studied except the synthetic isoparaffinic solvent ASTM-3C1. The results of the chamber experiments with the latter indicate that the current assignments and mechanisms for its components would underestimate its MIR, though the extent of its underestimation is uncertain. The current best estimate MIRs (or range of MIRs) for the studied solvents are summarized on Table 17. The uncertainty classification code as used with the existing MIR tabulations (Carter, 2000a, 3003a) is also given in the table.

Although the MIRs on Table 17 represent our current best estimates, it is clear from the results of this and our previous mechanism evaluation study (Carter, 2004a) that the SAPRC-99 mechanism needs to be updated. The mechanism for the aromatics is particularly problematical, and is probably the reason for the tendency for the model to underpredict O_3 at the lower ROG/NO_x ratios and its tendency to underpredict OH levels under most conditions. The effect a mechanism update that solves this problem on calculated MIRs for the compounds or solvents studied, or any other compounds or mixtures for that matter, cannot be determined until the updated mechanism is developed and the MIRs are recalculated. Until then, the magnitude and even direction of the changes in the MIRs is unknown. The chamber simulations of reactivities with the adjusted aromatics mechanism suggests that the change might not be large, but this cannot be assured.

Also, the reactivities of the Texanol® and the higher alkanes present in the hydrocarbon solvents may be sensitive to changes in the base mechanism because their net reactivities are determined by the differences between their relatively large and opposing direct and indirect reactivities. Changes in the balances between these two effects is the reason that the net reactivities are different in chamber experiments than in the atmosphere, and changes in the base mechanism may also affect this balance. Again, the magnitude and sign of this change cannot be determined until the mechanism is updated.

Recommendations

The first priority in reducing uncertainties in ozone impact estimates, and also increasing the value and utility of the mechanism evaluation data obtained for this project, is to improve the base mechanism, particularly for the aromatics, so that all the available data can be accurately simulated. The ability of the aromatics mechanism to predict effects of added aromatics on O_3 levels in low NO_x experiments also needs to be improved. We are attempting to address this priority in our current project to develop an updated and improved SAPRC mechanism (Carter, 2003b), but progress to date is slow and success is not assured. Additional resources and time may be required before this objective can be achieved. Once this is accomplished, the data obtained in this project can be used for a more precise evaluation of the mechanisms of the compounds and solvents of interest.

Information is needed concerning why the reactivity and mechanism evaluation results for at least some of the synthetic branched alkanes mixtures are different than those for the petroleum-distillate-based hydrocarbon solvents. This will require a more comprehensive compositional analysis of such mixtures and probably mechanistic and chamber studies of the types of compounds involved. Additional solvents of this type need to be studied to see if the results obtained with the sample studied in this work is typical or anomalous, and to elucidate the differences between the results of the experiments discussed here and the experiments of Carter et al (2000) with ISOPAR-M®. Direct reactivity measurements of these types of solvents and their representative constituents would also be useful in this regard. It is likely that the general estimation methods for branched alkanes that are incorporate in the SAPRC-99 mechanism may need to be updated to improve predictions of mechanisms for highly branched alkanes.

Although the results of the experiments with the Aromatic 100 sample were consistent with our expectations based on data for the more well studied aromatics, the uncertainties in estimating reactivities

Table 17. Current best estimate MIRs and uncertainty classification codes for the compounds or solvents studied for this project.

Name	Description	MIR [a]	Uncertainty Classification [b] and discussion
N-C8	n-Octane	1.09	2a - MIR not expected to change by more than a factor of 2 (more likely less than ~50%) when the mechanism is updated, primarily because of an expected sensitivity of the net reactivity to changes in the base mechanism.
TEXANOL	Isobutyrate monoesters of 2,2,4-trimethyl-1,3-pentanediol	0.88	
VMP-NAPH	VMP Naphtha, Primarily C_7-C_9 mixed alkanes	1.35	
ASTM-1C	Dearomatized Mixed Alkanes, Primarily C_{10}-C_{12}	0.96	
ASTM-1B	Reduced Aromatics Mineral Spirits, Primarily C_{10}-C_{12} mixed alkanes with 6% aromatics	1.26	
ASTM-1A	Regular mineral spirits, Primarily C_{10}-C_{12} mixed alkanes with 19% aromatics	1.97	2a - Comments above are also applicable to this solvent, but uncertainty slightly higher because of uncertainties in aromatics mechanisms.
M-XYLENE	m-Xylene	10.61	2c - Change in MIR when aromatics mechanisms are updated is uncertain but probably less than ~50%. Reactivities in MOIR and other lower NO_x scales are much more uncertain and probably are overestimated.
AROM100	Primarily C_9-C_{10} alkylbenzenes	7.70	
ASTM3C1	Synthetic isoparaffinic alkanes, primarily C_{10}-C_{12} branched alkanes	1.1 - 1.5	4 - The current assignments and mechanism for this mixture underestimates its reactivity. MIRs given are ranges of values using mechanisms adjusted to fit the data.

[a] SAPRC-99 Maximum Incremental Reactivity in units of gm O_3 /gm VOC

[b] Uncertainty classification code as used in tabulation by Carter (2003a)

for complex aromatic mixtures will increase as the boiling point ranges of the mixtures increase. This is because the estimated mechanisms for the components are based on extrapolations from a limited number relatively low molecular weight analogues, and the extrapolations become more uncertain as the differences in the sizes and structures of the molecules increases. Environmental chamber reactivity data are needed for higher molecular weight aromatics compounds more representative of those in the heavier solvents, to give better estimates of the reactivities of their constituents and hopefully better methods for estimating mechanisms for high molecular weight aromatics in general. In the short run, experiments with the heavier aromatics solvents, such as Aromatics 150 or Aromatics 200, could serve to reduce the

uncertainties of the present estimates, and to indicate the priority for additional research in this area. Note that this need will probably not go away even if the mechanisms for aromatics in general are improved.

The incremental reactivity experiments for this project were carried out using a highly simplified mixture to represent the "base case" reactive organic gas species present in the simulated atmospheres, and the mixture employed may not be representative of current atmospheres. Although the detailed composition of the base ROG surrogate may not have a large effect on evaluations if they are appropriately represented in the model, use of a more updated and less simplified mixture in future incremental reactivity chamber experiments would reduce concerns about the representativeness of the data obtained. We recommend that the CARB or appropriate experts in ambient air analysis and/or emissions provide recommendations on a representative ambient mixture to be used in future reactivity studies, and an appropriate base ROG mixture for chamber experiments be derived based on this.

We recommend that additional limited funding be made available so that the direct measurement method as it presently exists be applied to hydrocarbon solvents of interest, including synthetic branched alkane mixtures where there appear to be problems with the current mechanism. Attempts should be made to improve the method and improve its characterization and variability, but the near-term priority should be to obtain useful data with the existing method that at least can be used in the relative sense.

The results of this project do not indicate a compelling need to change the hydrocarbon bin assignments for regulations already in place, but revisions will be needed when the regulatory reactivity scale is updated or if a new regulatory reactivity scale is adopted. Before this is done, a protocol needs to be established for deriving bin reactivity estimates based on relationships between solvent properties and compositions. The "spreadsheet" method derived in this work gives an example of how this can be done, but this should be peer reviewed before it is adopted in regulations. If regulatory mandates require use of upper (or lower) limit estimates, separate protocols should be derived for obtaining for upper, lower, and "best estimate" reactivities of solvents in a bin, so that the effects of compositional uncertainties and the magnitudes of the regulatory biases are known. The method developed for this work are based on "best estimate" bin reactivity estimates, but could be modified for lower or upper limit analysis for this purpose. Even if the regulation requires that only best estimate values be used, an evaluation of the compositional uncertainty range would still be beneficial.

The results of this project indicate that it is probably necessary that separate bins be used for synthetic hydrocarbon solvents that are high in branched alkanes than are used for petroleum distillate derived solvents. It may be that the process that us used to synthesize these mixtures may also affect their reactivities; this needs to be evaluated. Hopefully there will be additional data for solvents of this type and better mechanistic estimates for the types of compounds they contain so better reactivity estimates for solvents in these bins can be made at the time the hydrocarbon bin reactivities need to be updated.

The discrepancy between current CARB bin assignments for lower boiling point hydrocarbon solvents and evaluation results using analyzed solvents is due to assumptions on cyclopentane contents of solvents in these bins that were not included in the evaluation dataset. Since the presence of cyclopentanes have non-negligible impacts on reactivity estimates for solvents of this type, a more comprehensive survey and analysis of the compositions of solvents in this category may be appropriate before the bin assignments are updated. Fortunately, distinguishing the C_5-C_7 isomers of relevance to these bins should be feasible if an appropriate GC analysis is employed.

Impacts on ground level ozone formation are not the only potential areas of concern for architectural coatings VOCs. The reactions of higher molecular weight solvents may affect formation of secondary particulate matter (PM), which is another area of regulatory concern. Some funding for making PM measurements during the experiments for this project was included in budget for this project, and we

obtained funding from the South Coast Air Quality Management District to make more extensive PM measurements of during the course of these experiments, and the results will be discussed in a subsequent report which is in preparation. However, the data obtained to date represent only a beginning in the work needed to develop and evaluate predictive models for the effects of VOCs on secondary PM formation, and considerably more work in this area is required before we can have any confidence in model predictions of impacts of VOCs on secondary PM formation.

REFERENCES

ASTM (2003): "Standard Specification for Mineral Spirits (Petroleum Spirits) (Hydrocarbon Dry Cleaning Solvent)," ASTM Committee D01 on Paints and Related Coatings, Materials, and Applications, and Subcommittee D01.35 on Solvents, Plasticizers, and Chemical Intermediates. Approved Dec. 10, 2002 and published February 2003.

Atkinson, R. (1989): "Kinetics and Mechanisms of the Gas-Phase Reactions of the Hydroxyl Radical with Organic Compounds," J. Phys. Chem. Ref. Data, Monograph no 1.

CARB (1993): "Proposed Regulations for Low-Emission Vehicles and Clean Fuels -- Staff Report and Technical Support Document," California Air Resources Board, Sacramento, CA, August 13, 1990. See also Appendix VIII of "California Exhaust Emission Standards and Test Procedures for 1988 and Subsequent Model Passenger Cars, Light Duty Trucks and Medium Duty Vehicles," as last amended September 22, 1993. Incorporated by reference in Section 1960.

CARB (2000): "Initial Statement of Reasons for the Proposed Amendments to the Regulation for Reducing Volatile Organic Compound Emissions from Aerosol Coating Products and Proposed Tables of Maximum Incremental Reactivity (MIR) Values, and Proposed Amendments to Method 310, 'Determination of Volatile Organic Compounds in Consumer Products'," California Air Resources Board, Sacramento, CA, May 5.

Carter, W. P. L. (1994a): "Development of Ozone Reactivity Scales for Volatile Organic Compounds," J. Air & Waste Manage. Assoc., 44, 881-899.

Carter, W. P. L. (1994b): "Calculation of Reactivity Scales Using an Updated Carbon Bond IV Mechanism," Report Prepared for Systems Applications International Under Funding from the Auto/Oil Air Quality Improvement Research Program, April 12.

Carter, W. P. L. (2000a): "Documentation of the SAPRC-99 Chemical Mechanism for VOC Reactivity Assessment," Report to the California Air Resources Board, Contracts 92-329 and 95-308, May 8. Available at http://cert.ucr.edu/~carter/absts.htm#saprc99 and http://www.cert.ucr.edu/~carter/reactdat.htm.

Carter, W. P. L. (2000b): "Implementation of the SAPRC-99 Chemical Mechanism into the Models-3 Framework," Report to the United States Environmental Protection Agency, January 29. Available at http://www.cert.ucr.edu/~carter/absts.htm#s99mod3.

Carter, W. P. L. (2002a): "Development of a Next Generation Environmental Chamber Facility for Chemical Mechanism and VOC Reactivity Research," Summary of Progress and Current Status, October 20. Available at http://www.cert.ucr.edu/~carter/epacham.

Carter, W. P. L. (2002b): "Data Processing Procedures for UCR EPA Environmental Chamber Experiments, Appendix B To Quality Assurance Project Plan." Prepared for the United States Environmental Protection Agency Cooperative Agreement CR 827331-01-0, April 25. Available at http://www.cert.ucr.edu/~carter/epacham.

Carter, W. P. L. (2003a): "The SAPRC-99 Chemical Mechanism and Updated VOC Reactivity Scales," http://www.cert.ucr.edu/~carter/reactdat.htm. Last modified February 5.

Carter, W. P. L. (2003b): "Updated Chemical Mechanism for Airshed Model Applications," Research Proposal to the California Air Resources Board, October.

Carter, W. P. L. (2004a): "Evaluation of a Gas-Phase Atmospheric Reaction Mechanism for Low NO_x Conditions," Final Report to California Air Resources Board Contract No. 01-305, May 5. Available at http://www.cert.ucr.edu/~carter/absts.htm#lnoxrpt.

Carter, W. P. L. (2004b): "Development of an Improved Chemical Speciation Database for Processing Emissions of Volatile Organic Compounds for Air Quality Models," Current project information page, http://www.cert.ucr.edu/~carter/emitdb.

Carter, W. P. L. and I. L. Malkina (2005): "Evaluation of Atmospheric Impacts of Selected Coatings VOC Emissions," Final report to the California Air Resources Board Contract No. 00-333, March 15. Available at http://www.cert.ucr.edu/~carter/absts.htm#coatrpt.

Carter, W. P. L., R. Atkinson, A. M. Winer, and J. N. Pitts, Jr. (1982): "Experimental Investigation of Chamber-Dependent Radical Sources," Int. J. Chem. Kinet., 14, 1071.

Carter, W. P. L. and R. Atkinson (1987): "An Experimental Study of Incremental Hydrocarbon Reactivity," Environ. Sci. Technol., 21, 670-679

Carter, W. P. L. and R. Atkinson (1989): "A Computer Modeling Study of Incremental Hydrocarbon Reactivity", Environ. Sci. Technol., 23, 864.

Carter, W. P .L., and Lurmann, F. W. (1991) Evaluation of a detailed gas-phase atmospheric reaction mechanism using environmental chamber data. Atmos. Environ. 25A:2771-2806.

Carter, W. P. L., J. A. Pierce, I. L. Malkina, D. Luo and W. D. Long (1993): "Environmental Chamber Studies of Maximum Incremental Reactivities of Volatile Organic Compounds," Report to Coordinating Research Council, Project No. ME-9, California Air Resources Board Contract No. A032-0692; South Coast Air Quality Management District Contract No. C91323, United States Environmental Protection Agency Cooperative Agreement No. CR-814396-01-0, University Corporation for Atmospheric Research Contract No. 59166, and Dow Corning Corporation. April 1.

Carter, W. P. L., D. Luo, I. L. Malkina, and J. A. Pierce (1995a): "Environmental Chamber Studies of Atmospheric Reactivities of Volatile Organic Compounds. Effects of Varying ROG Surrogate and NO_x," Final report to Coordinating Research Council, Inc., Project ME-9, California Air Resources Board, Contract A032-0692, and South Coast Air Quality Management District, Contract C91323. March 24. Available at http://www.cert.ucr.edu/~carter/absts.htm#rct2rept.

Carter, W. P. L., D. Luo, I. L. Malkina, and D. Fitz (1995b): "The University of California, Riverside Environmental Chamber Data Base for Evaluating Oxidant Mechanism. Indoor Chamber Experiments through 1993," Report submitted to the U. S. Environmental Protection Agency, EPA/AREAL, Research Triangle Park, NC., March 20..

Carter, W. P. L., D. Luo, and I. L. Malkina (1996): "Investigation of Atmospheric Ozone Formation Potentials of C12 - C16 n-Alkanes," Report to the Aluminum Association, October 28.

Carter, W. P. L., D. Luo, and I. L. Malkina (1997): "Investigation of the Atmospheric Ozone Formation Potentials of Selected Mineral Spirits Mixtures," Report to Safety-Kleen Corporation, July 25. Available at http://cert.ucr.edu/~carter/absts.htm#msrept.

Carter, W. P. L., J. H. Seinfeld, D. R. Fitz, and G. S. Tonnesen (1999): "Development of a Next-Generation Environmental Chamber Facility for Chemical Mechanism and VOC Reactivity Evaluation," Proposal to the U. S. Environmental Protection Agency, February 22. Available at http://www.cert.ucr.edu/~carter/epacham.

Carter, W. P. L., D. Luo, and I. L. Malkina (2000): "Investigation of the Ozone Formation Potentials of Exxsol® D95, Isopar-M®, and the Exxate® Fluids," Report to ExxonMobil Chemical Company, October 31, 2000. Available at http://www.cert.ucr.edu/~carter/absts.htm#exxprods.

Carter, W. P. L., D. Luo, and I. L. Malkina (2002): "Investigation of the Atmospheric Ozone Formation Potentials of Selected Branched Alkanes and Mineral Spirits Samples," Report to Safety-Kleen Corporation, July 11. Available at http://www.cert.ucr.edu/~carter/absts.htm#msrpt2.

Carter, W. P. L. and I. L. Malkina (2002): "Development and Application of Improved Methods for Measurement of Ozone Formation Potentials of Volatile Organic Compounds," Final report to California Air Resources Board Contract 97-314, May 22. Available at http://www.cert.ucr.edu/~carter/absts.htm#rmethrpt.

Carter, W. P. L., G. S. Tonnesen and G. Yarwood (2003): "Investigation of VOC Reactivity Effects Using Existing RegionalAir Quality Models," Final report to American Chemistry Council Contract SC-20.0-UCR-VOC-RRWG, April. Available at http://www.cert.ucr.edu/~carter/bsts.htm#ddmrept1.

Censullo, A., C., D. R. Jones, and M. T. Wills (2002): "Investigation of Low Reactivity Solvents," Final Report for California Air Resources Board Contract 98-310, May 10.

Febo, A., C. Perrino, M. Gerardi and R. Sparapini (1995): "Evaluation of a High-Purity and High Stability Continuous Generation System for Nitrous Acid," Environ. Sci. Technol. 29, 2390-2395.

Hastie, D. R, Mackay, G. I., Iguchi, T., Ridley, B. A.; and Schiff, H. I. (1983): "Tunable diode laser systems for measuring trace gases in tropospheric air," Environ. Sci. Technol. 17, 352A-364A.

Imada, M. R. (1984): "Formaldehyde Gas Generation System," Report #249, CA/DOH/AIHL/R-249, Air and Indusrial Hygiene Laboratory, Laboratory Services Branch, California Department of Health and Services, January,

Jacobsen, N. W. and R. G. Dickinson (1994): "Spectrometric Assay of Aldehydes as 6-Mercapto-3-substituted-s-triazolo(4,3-b)-s-tetrazines," Analytical Chemistry 46/2 (1974) 298–299.

Jaques, A. (2002): File "Aliphatic Bin Composition Data - HSP 4-02.xls", provided in an email from Andrew Jaques of the American Chemistry Council to Dongmin Luo of the California Air Resources Board, April 22.

Jaques, A. (2003): "Hydrocarbon Solvent Test Materials for Chamber Experiments," Letter provided by the Hydrocarbon Panel of the American Chemistry Council to W. P. L. Carter dated March 24, 2003.

Jaques, A (2004): “Sample Analysis for Products sent to Dr. W. Carter for CARB Architectural Coatings Research,” revised compositional information provided by the Hydrocarbon Panel of the American Chemistry Council on March 8, 2004.

Johnson, G. M. (1983): “Factors Affecting Oxidant Formation in Sydney Air,” in “The Urban Atmosphere -- Sydney, a Case Study.” Eds. J. N. Carras and G. M. Johnson (CSIRO, Melbourne), pp. 393-408.

Kwok, E. S. C., and R. Atkinson (1995): “Estimation of Hydroxyl Radical Reaction Rate Constants for Gas-Phase Organic Compounds Using a Structure-Reactivity Relationship: An Update,” Atmos. Environ 29, 1685-1695.

Kwok, E. S. C., C. Takemoto and A. Chew (2000): “Methods for Estimating Maximum Incremental Reactivity (MIR) of Hydrocarbon Solvents and their Classification,” Appendix C to “Initial Statement of Reasons for the Proposed Amendments to the Regulation for Reducing Volatile Organic Compound Emissions from Aerosol Coating Products and Proposed Tables of Maximum Incremental Reactivity (MIR) Values, and Proposed Amendments to Method 310, ‘Determination of Volatile Organic Compounds in Consumer Products’,” California Air Resources Board, Sacramento, CA, May 5.

Medeiros (2004): Arlean M. Medeiros, ExxonMobil Chemical Company, data provided to W. P. L. carter by email, October 29.

NIOSH (1994): “Sulfite titration of formaldehyde stock solution: modified Method 3500,” NIOSH Manual of Analytical Methods, NMAM, fourth edition, August 15.

Quesenberry, M. S. and Y. C. Lee (1996): “A Rapid Formaldehyde Assay Using Puprald Reagent: Application under Periodation Conditions,” Analytical Biochemistry. 234, 50–55.

Schiff, H.. I., Mackay, G. I. and Bechara, J. (1994): “The Use of Tunable Diode Laser Absorption Spectroscopy for Atmospheric Measurements”, Res. Chem. Intermed. 20, 1994, pp 525-556.

Wang SC and Flagan RC (1990): “Scanning Electrical Mobility Spectrometer,” Aerosol Science and Technology. 13(2): 230-240 1990

Zafonte, L., P. L. Rieger, and J. R. Holmes (1977): “Nitrogen Dioxide Photolysis in the Los Angeles Atmosphere,” Environ. Sci. Technol. 11, 483-487.

APPENDIX A. LISTINGS AND TABULATIONS

Hydrocarbon Solvent Composition Data

Table A-1. SAPRC-99 detailed model species compositional assignments for the hydrocarbon solvents studied in environmental chamber experiments for this project.

Description	Model Species	Composition (weight percent)					
		VMP-NAPH	AROM-100	ASTM-1A	ASTM-1B	ASTM-1C	ASTM-3C1
n-Octane	N-C8	9.6%	-	0.5%	0.1%	0.1%	-
n-Nonane	N-C9	3.6%	-	1.2%	1.1%	1.1%	-
n-Decane	N-C10	-	-	4.4%	3.9%	3.9%	-
n-Undecane	N-C11	-	-	5.9%	5.6%	5.6%	-
n-Dodecane	N-C12	-	-	2.7%	2.8%	2.7%	-
n-Tridecane	N-C13	-	-	0.5%	0.4%	0.6%	-
Branched C8 Alkanes	BR-C8	1.0%	-	1.0%	0.3%	0.3%	-
Branched C9 Alkanes	BR-C9	43.0%	-	2.6%	2.5%	2.4%	-
Branched C10 Alkanes	BR-C10	0.1%	-	9.3%	8.7%	8.4%	11.5%
Branched C11 alkanes	BR-C11	-	-	12.5%	12.4%	12.0%	77.8%
Branched C12 Alkanes	BR-C12	-	-	5.8%	6.2%	5.7%	6.7%
Branched C13 Alkanes	BR-C13	-	-	1.0%	0.9%	1.2%	-
C7 Cycloalkanes	CYC-C7	0.1%	-	-	-	-	-
C8 Bicycloalkanes	BCYC-C8	-	-	0.2%	0.1%	0.1%	-
C8 Cycloalkanes	CYC-C8	17.7%	-	0.8%	0.4%	0.5%	-
C9 Bicycloalkanes	BCYC-C9	-	-	0.6%	0.8%	0.9%	-
C9 Cycloalkanes	CYC-C9	24.5%	-	2.1%	3.1%	3.6%	-
C10 Bicycloalkanes	BCYC-C10	-	-	2.3%	2.8%	3.1%	-
C10 Cycloalkanes	CYC-C10	0.0%	-	7.5%	10.9%	12.6%	0.5%
C11 Bicycloalkanes	BCYC-C11	-	-	3.1%	4.0%	4.4%	-
C11 Cycloalkanes	CYC-C11	-	-	10.1%	15.6%	18.0%	3.2%
C12 Bicycloalkanes	BCYC-C12	-	-	1.4%	2.0%	2.1%	-
C12 Cycloalkanes	CYC-C12	-	-	4.7%	7.8%	8.6%	0.3%
C13 Bicycloalkanes	BCYC-C13	-	-	0.2%	0.3%	0.4%	-
C13 Cycloalkanes	CYC-C13	-	-	0.8%	1.2%	1.8%	-
Toluene	TOLUENE	-	-	0.1%	0.0%	-	-
Ethyl Benzene	C2-BENZ	-	0.0%	0.1%	0.0%	-	-
Isopropyl Benzene (cumene)	I-C3-BEN	0.0%	2.4%	0.1%	0.0%	-	-
n-Propyl Benzene	N-C3-BEN	-	7.1%	0.7%	0.2%	-	-
s-Butyl Benzene	S-C4-BEN	-	0.2%	-	-	-	-
C10 Monosubstituted Benzenes	C10-BEN1	-	0.1%	0.3%	0.1%	-	-
n-Butyl Benzene	N-C4-BEN	-	1.0%	-	-	-	-
C11 Monosubstituted Benzenes	C11-BEN1	-	-	0.3%	0.1%	-	-
m-Xylene	M-XYLENE	0.0%	0.0%	0.3%	0.1%	-	-
o-Xylene	O-XYLENE	-	0.8%	0.4%	0.1%	-	-
p-Xylene	P-XYLENE	0.1%	0.0%	0.1%	0.0%	-	-
m-Ethyl Toluene	M-ET-TOL	-	24.0%	0.5%	0.2%	-	-
p-Ethyl Toluene	P-ET-TOL	-	10.7%	0.5%	0.2%	-	-
o-Ethyl Toluene	O-ET-TOL	-	9.4%	2.1%	0.7%	-	-
o-Diethyl Benzene	O-DE-BEN	-	0.1%	-	-	-	-
m-Diethyl Benzene	M-DE-BEN	-	0.7%	0.5%	0.1%	-	-
p-Diethyl Benzene	P-DE-BEN	-	1.0%	-	-	-	-

Table A-1 (continued)

Description	Model Species	Composition (weight percent)					
		VMP-NAPH	AROM-100	ASTM-1A	ASTM-1B	ASTM-1C	ASTM-3C1
C10 Disubstituted Benzenes	C10-BEN2	-	3.2%	2.4%	0.8%	-	-
C11 Disubstituted Benzenes	C11-BEN2	-	-	0.7%	0.2%	-	-
1,2,3-Trimethyl Benzene	123-TMB	-	6.2%	0.6%	0.2%	-	-
1,2,4-Trimethyl Benzene	124-TMB	-	18.7%	-	-	-	-
1,3,5-Trimethyl Benzene	135-TMB	-	12.2%	0.7%	0.2%	-	-
C10 Tetrasubstituted Benzenes	C10-BEN4	-	0.0%	1.1%	0.4%	-	-
C10 Trisubstituted Benzenes	C10-BEN3	-	2.0%	2.9%	0.9%	-	-
Isomers of Butylbenzene	C10-BEN	-	0.1%	-	-	-	-
Isomers of Pentylbenzene	C11-BEN	-	-	2.1%	0.7%	-	-
C12 Trisubstituted Benzenes	C12-BEN3	-	-	0.3%	0.1%	-	-
Isomers of Hexylbenzene	C12-BEN	-	-	0.2%	0.1%	-	-
Naphthalene	NAPHTHAL	-	-	0.2%	0.1%	-	-
Methyl Indans	ME-INDAN	-	-	0.4%	0.1%	-	-
Methyl Naphthalenes	ME-NAPH	-	-	0.8%	0.2%	-	-
C12 Monosubstituted Naphthalene	C12-NAP1	-	-	0.6%	0.2%	-	-
C9 Internal Alkenes	C9-OLE2	0.1%	-	-	-	-	-

[a] Derived from compositional information supplied by Jaques (2003) for VMP-NAPH and AROM-100 and by Jaques (2004) for the other solvents. The composition of the aromatics in ASTM-1A was provided separately by Medeiros (2004). The aromatics in ASTM-1B is asssumed to have the same relative distribution as provided for ASTM-1A Medeiros (2004).

Table A-2. SAPRC-99 detailed model species compositional assignments for the hydrocarbon solvents analyzed by Censullo et al (2002).

Description	Model Species	Composition (weight percent)										
		CP01	CP02	CP03	CP04	CP05	CP06	CP07	CP08	CP10	CP11	CP12
n-Hexane	N-C6	-	-	-	-	0.9%	-	-	-	-	-	-
n-Heptane	N-C7	1.5%	-	-	-	7.2%	-	-	-	-	-	-
n-Octane	N-C8	11.9%	-	-	18.4%	0.1%	0.1%	-	-	-	-	0.1%
n-Nonane	N-C9	10.6%	5.7%	-	1.0%	-	2.2%	-	-	2.0%	7.9%	5.9%
n-Decane	N-C10	0.4%	12.9%	0.1%	-	-	4.4%	-	-	4.1%	10.6%	15.8%
n-Undecane	N-C11	-	2.0%	2.3%	-	-	2.4%	-	-	1.9%	1.0%	2.1%
n-Dodecane	N-C12	-	0.1%	1.2%	-	-	0.7%	-	-	0.9%	-	-
n-Tridecane	N-C13	-	-	-	-	-	-	-	-	-	-	-
2-Methyl Pentane	2-ME-C5	-	-	-	-	0.1%	-	-	-	-	-	-
3-Methylpentane	3-ME-C5	-	-	-	-	0.1%	-	-	-	-	-	-
2,2-Dimethyl Pentane	22-DM-C5	-	-	-	-	0.1%	-	-	-	-	-	-
2,3-Dimethyl Pentane	23-DM-C5	-	-	-	-	1.8%	-	-	-	-	-	-
2,4-Dimethyl Pentane	24-DM-C5	-	-	-	-	0.3%	-	-	-	-	-	-
2-Methyl Hexane	2-ME-C6	-	-	-	-	2.2%	-	-	-	-	-	-
3,3-Dimethyl Pentane	33-DM-C5	-	-	-	-	0.1%	-	-	-	-	-	-
3-Methyl Hexane	3-ME-C6	0.4%	-	-	-	3.5%	-	-	-	-	-	-
2,2-Dimethyl Hexane	22-DM-C6	0.1%	-	-	-	16.9%	-	-	-	-	-	-
2,3,4-Trimethyl Pentane	234TM-C5	-	-	-	0.2%	0.3%	-	-	-	-	-	-
2,3-Dimethyl Hexane	23-DM-C6	0.5%	-	-	1.1%	1.3%	-	-	-	-	-	-
2,5-Dimethyl Hexane	25-DM-C6	0.5%	-	-	0.4%	-	-	-	-	-	-	-
2-Methyl Heptane	2-ME-C7	3.8%	-	-	8.0%	0.6%	-	-	-	-	-	-
3-Methyl Heptane	3-ME-C7	3.4%	-	-	5.5%	0.1%	-	-	-	-	-	-
Branched C8 Alkanes	BR-C8	1.4%	-	-	2.3%	1.7%	-	-	-	-	-	-
2,3,5-Trimethyl Hexane	235TM-C6	-	-	-	-	-	-	-	-	-	-	-
2,4-Dimethyl Heptane	24-DM-C7	1.2%	-	-	2.0%	-	-	-	-	-	-	-
2-Methyl Octane	2-ME-C8	4.7%	0.1%	-	1.8%	-	0.2%	-	-	0.2%	-	-
3,3-Diethyl Pentane	33-DE-C5	-	0.1%	-	-	-	0.5%	-	-	0.4%	-	-
3,5-Dimethyl Heptane	35-DM-C7	1.2%	-	-	-	-	-	-	-	0.6%	0.1%	-
4-Ethyl Heptane	4-ET-C7	1.8%	-	-	2.7%	-	-	-	-	-	-	-
4-Methyl Octane	4-ME-C8	3.5%	0.6%	-	1.4%	-	0.1%	-	-	0.1%	0.5%	0.9%
Branched C9 Alkanes	BR-C9	11.3%	0.8%	-	7.6%	-	0.6%	-	-	0.7%	0.6%	1.3%
2,4-Dimethyl Octane	24-DM-C8	-	-	-	-	-	-	-	-	-	-	-
2,6-Dimethyl Octane	26DM-C8	0.2%	1.7%	3.5%	0.3%	0.0%	3.8%	-	-	3.5%	4.2%	2.2%
2-Methyl Nonane	2-ME-C9	0.6%	4.1%	3.5%	0.3%	0.0%	4.4%	-	-	3.9%	4.0%	5.0%
3-Methyl Nonane	3-ME-C9	0.2%	2.3%	-	-	-	1.0%	-	-	1.8%	2.2%	2.3%
4-Methyl Nonane	4-ME-C9	0.3%	3.2%	-	-	-	0.7%	-	-	0.9%	4.0%	0.7%
Branched C10 Alkanes	BR-C10	1.7%	15.3%	10.6%	0.8%	0.1%	17.6%	-	-	14.8%	9.0%	12.7%
2,6-Dimethyl Nonane	26DM-C9	-	2.8%	1.0%	-	-	2.0%	-	-	2.3%	2.5%	3.3%
3-Methyl Decane	3-ME-C10	-	0.2%	2.8%	-	-	0.4%	-	-	0.4%	1.3%	1.3%

Table A-2 (continued)

Description	Model Species	Composition (weight percent)										
		CP01	CP02	CP03	CP04	CP05	CP06	CP07	CP08	CP10	CP11	CP12
4-Methyl Decane	4-ME-C10	-	0.2%	-	-	-	1.4%	-	-	1.5%	1.6%	1.7%
Branched C11 alkanes	BR-C11	-	3.3%	6.1%	-	-	1.5%	-	-	1.3%	2.6%	4.7%
3,6-Dimethyl Decane	36DM-C10	-	-	0.8%	-	-	0.5%	-	-	0.3%	-	-
3-Methyl Undecane	3-ME-C11	-	-	2.7%	-	-	0.2%	-	-	0.1%	-	-
5-Methyl Undecane	5-ME-C11	-	0.1%	0.6%	-	-	0.2%	-	-	0.2%	-	-
Branched C12 Alkanes	BR-C12	-	0.5%	27.6%	-	-	4.8%	-	-	3.6%	-	-
3-Methyl Dodecane	3-ME-C12	-	-	0.1%	-	-	-	-	-	-	-	-
5-Methyl Dodecane	5-ME-C12	-	-	0.1%	-	-	-	-	-	-	-	-
Branched C13 Alkanes	BR-C13	-	-	1.7%	-	-	0.3%	-	-	0.4%	-	-
Branched C14 Alkanes	BR-C14	-	-	0.1%	-	-	-	-	-	-	-	-
Methylcyclopentane	ME-CYCC5	-	-	-	-	3.8%	-	-	-	-	-	-
1,3-Dimethyl Cyclopentane	13DMCYC5	-	-	-	-	11.8%	-	-	-	-	-	-
Ethyl Cyclopentane	ET-CYCC5	-	-	-	-	4.6%	-	-	-	-	-	-
Methylcyclohexane	ME-CYCC6	2.4%	-	-	0.9%	3.1%	-	-	-	-	-	-
C7 Cycloalkanes	CYC-C7	-	-	-	-	14.1%	-	-	-	-	-	-
C8 Bicycloalkanes	BCYC-C8	-	-	-	-	-	-	-	-	-	-	-
1,3-Dimethyl Cyclohexane	13DMCYC6	2.4%	-	-	9.8%	0.1%	-	-	-	-	-	-
Ethylcyclohexane	ET-CYCC6	2.8%	0.1%	-	-	-	0.3%	-	-	-	-	-
Propyl Cyclopentane	PR-CYCC5	-	-	-	-	-	-	-	-	0.1%	-	0.3%
C8 Cycloalkanes	CYC-C8	3.9%	1.2%	0.6%	11.2%	18.0%	4.9%	-	-	5.4%	2.4%	2.2%
C9 Bicycloalkanes	BCYC-C9	-	0.7%	-	-	-	2.3%	-	-	2.4%	0.5%	0.5%
1,1,3-Trimethyl Cyclohexane	113MCYC6	-	0.2%	-	2.2%	-	0.0%	-	-	0.0%	0.1%	0.1%
Propyl Cyclohexane	C3-CYCC6	0.6%	2.7%	-	-	-	2.0%	-	-	2.1%	1.1%	1.5%
C9 Cycloalkanes	CYC-C9	3.9%	6.7%	-	22.2%	-	12.0%	-	-	12.3%	15.3%	10.5%
C10 Bicycloalkanes	BCYC-C10	-	0.1%	3.4%	-	-	-	-	-	-	-	-
1,4-Diethyl-Cyclohexane	14DECYC6	-	0.7%	0.0%	-	-	0.7%	-	-	0.8%	1.9%	1.6%
1-Methyl-3-Isopropyl Cyclohexane	1M3IPCY6	-	2.3%	0.0%	-	-	2.4%	-	-	2.8%	4.5%	3.0%
Butyl Cyclohexane	C4-CYCC6	-	2.2%	0.9%	-	-	2.0%	-	-	2.7%	3.8%	3.4%
C10 Cycloalkanes	CYC-C10	-	9.3%	0.7%	-	-	11.9%	-	-	13.4%	11.7%	11.5%
C11 Bicycloalkanes	BCYC-C11	-	-	0.8%	-	-	-	-	-	-	0.1%	-
1,3-Diethyl-5-Methyl Cyclohexane	13E5MCC6	-	0.1%	3.0%	-	-	0.1%	-	-	0.1%	0.7%	0.4%
Pentyl Cyclohexane	C5-CYCC6	-	-	2.7%	-	-	-	-	-	-	-	-
C11 Cycloalkanes	CYC-C11	-	0.4%	11.9%	-	-	0.4%	-	-	0.5%	2.6%	1.7%
1,3,5-Triethyl Cyclohexane	135ECYC6	-	-	2.9%	-	-	0.2%	-	-	0.1%	-	-
1-Methyl-4-Pentyl Cyclohexane	1M4C5CY6	-	-	2.9%	-	-	0.2%	-	-	0.1%	-	-
Hexyl Cyclohexane	C6-CYCC6	-	-	2.9%	-	-	0.2%	-	-	0.1%	-	-
Benzene	BENZENE	-	-	-	-	0.3%	-	-	-	-	-	-
Toluene	TOLUENE	0.6%	-	-	-	6.5%	-	-	-	-	-	-
Ethyl Benzene	C2-BENZ	2.9%	0.1%	-	-	-	-	-	-	-	-	-
Isopropyl Benzene (cumene)	I-C3-BEN	0.3%	0.4%	-	-	-	0.3%	1.6%	-	0.3%	-	0.1%

Table A-2 (continued)

Description	Model Species	Composition (weight percent)										
		CP01	CP02	CP03	CP04	CP05	CP06	CP07	CP08	CP10	CP11	CP12
n-Propyl Benzene	N-C3-BEN	0.1%	0.5%	-	-	-	0.2%	4.4%	0.1%	0.2%	0.0%	-
s-Butyl Benzene	S-C4-BEN	-	-	-	-	-	-	0.1%	-	-	-	-
C10 Monosubstituted Benzenes	C10-BEN1	-	0.3%	-	-	-	0.3%	0.2%	0.2%	0.2%	0.3%	-
n-Butyl Benzene	N-C4-BEN	-	-	-	-	-	0.2%	0.0%	3.0%	0.2%	-	-
C11 Monosubstituted Benzenes	C11-BEN1	-	-	-	-	-	-	0.1%	0.4%	-	-	-
C12 Monosubstituted Benzenes	C12-BEN1	-	-	-	-	-	-	-	-	-	-	-
m-Xylene	M-XYLENE	10.1%	0.3%	-	-	-	0.2%	-	-	0.2%	-	-
o-Xylene	O-XYLENE	4.1%	-	-	-	-	-	1.7%	-	-	-	-
p-Xylene	P-XYLENE	3.8%	-	-	-	-	0.2%	-	-	0.1%	-	-
m-Ethyl Toluene	M-ET-TOL	0.4%	1.5%	-	-	-	0.6%	18.1%	0.3%	0.5%	0.1%	0.1%
p-Ethyl Toluene	P-ET-TOL	0.1%	0.6%	-	-	-	0.6%	8.2%	0.2%	0.3%	0.0%	0.3%
o-Ethyl Toluene	O-ET-TOL	0.1%	0.7%	-	-	-	0.2%	6.4%	0.3%	0.3%	-	-
o-Diethyl Benzene	O-DE-BEN	-	0.1%	-	-	-	0.2%	0.1%	0.2%	0.1%	-	-
m-Diethyl Benzene	M-DE-BEN	-	0.3%	-	-	-	0.1%	0.4%	1.2%	0.2%	-	-
p-Diethyl Benzene	P-DE-BEN	-	0.3%	-	-	-	0.1%	0.2%	1.3%	0.1%	-	-
C10 Disubstituted Benzenes	C10-BEN2	-	2.7%	-	-	-	0.7%	1.8%	6.6%	1.8%	1.7%	0.2%
C11 Disubstituted Benzenes	C11-BEN2	-	-	-	-	-	-	-	1.0%	-	-	-
C12 Disubstituted Benzenes	C12-BEN2	-	-	-	-	-	-	0.1%	0.3%	-	-	-
1,2,3-Trimethyl Benzene	123-TMB	-	2.4%	-	-	-	0.1%	6.9%	5.2%	0.1%	0.1%	0.4%
1,2,4-Trimethyl Benzene	124-TMB	0.2%	3.7%	-	-	-	1.5%	33.2%	5.2%	1.5%	0.4%	1.0%
1,3,5-Trimethyl Benzene	135-TMB	0.2%	1.1%	-	-	-	0.5%	9.6%	0.4%	0.5%	0.1%	-
1,2,3,5 Tetramethyl Benzene	1235MBEN	-	0.1%	-	-	-	0.3%	0.7%	10.8%	0.1%	-	0.1%
C10 Tetrasubstituted Benzenes	C10-BEN4	-	0.2%	-	-	-	0.5%	0.6%	11.4%	0.6%	0.1%	0.1%
C10 Trisubstituted Benzenes	C10-BEN3	-	1.6%	-	-	-	1.7%	3.7%	23.3%	1.9%	0.3%	0.8%
C11 Pentasubstituted Benzenes	C11-BEN5	-	-	-	-	-	-	-	0.8%	-	-	-
C11 Tetrasubstituted Benzenes	C11-BEN4	-	0.1%	-	-	-	0.3%	0.1%	3.6%	0.3%	-	-
C11 Trisubstituted Benzenes	C11-BEN3	-	-	-	-	-	0.2%	0.3%	6.9%	0.6%	-	-
C12 Trisubstituted Benzenes	C12-BEN3	-	-	-	-	-	-	-	-	-	-	-
Indan	INDAN	-	-	-	-	-	0.2%	1.0%	1.2%	0.1%	-	-
Naphthalene	NAPHTHAL	-	-	-	-	-	0.2%	0.1%	6.6%	0.1%	-	-
Tetralin	TETRALIN	-	-	-	-	-	-	0.1%	0.6%	-	-	-
Methyl Indans	ME-INDAN	-	0.1%	2.2%	-	-	1.0%	0.2%	6.0%	0.7%	0.3%	0.1%
1-Methyl Naphthalene	1ME-NAPH	-	-	-	-	-	-	-	0.2%	-	-	-
2-Methyl Naphthalene	2ME-NAPH	-	-	-	-	-	-	0.0%	0.8%	-	-	-
C11 Tetralin or Indane	C11-TET	-	-	-	-	-	-	0.1%	1.7%	-	-	-
C9 Terminal Alkenes	C9-OLE1	-	-	-	-	-	-	-	-	-	-	-
C10 Terminal Alkenes	C10-OLE1	-	-	-	-	-	-	-	-	-	-	-
C10 Styrenes	C10-STYR	-	-	-	-	-	-	-	0.2%	-	-	-

Table A-2 (continued)

Model Species	Composition (weight percent)														
	CP13	CP14	CP15	CP16	CP17	CP18	CP19	CP20	CP21	CP22	CP23	CP24	CP25	CP26	CP27
N-C6	-	-	-	-	-	-	-	-	-	-	-	-	-	-	-
N-C7	-	-	-	-	-	-	-	-	-	-	-	-	-	-	-
N-C8	-	19.1%	-	-	-	-	-	0.1%	-	-	6.7%	6.8%	0.1%	-	-
N-C9	0.1%	1.1%	2.7%	-	-	-	-	2.2%	-	-	2.2%	2.2%	2.2%	2.2%	-
N-C10	-	-	7.0%	1.1%	-	1.4%	-	4.7%	-	-	-	-	5.0%	4.7%	-
N-C11	-	-	3.0%	25.7%	-	25.8%	-	2.4%	-	-	-	-	2.6%	2.3%	-
N-C12	-	-	0.7%	3.9%	-	3.1%	-	0.9%	-	-	-	-	1.0%	0.9%	-
N-C13	-	-	-	0.1%	-	-	-	-	-	-	-	-	-	-	-
234TM-C5	-	0.2%	-	-	-	-	-	-	-	-	0.2%	0.1%	-	-	-
23-DM-C6	-	1.2%	-	-	-	-	-	-	-	-	0.4%	0.4%	-	-	-
25-DM-C6	-	0.4%	-	-	-	-	-	-	-	-	-	-	-	-	-
2-ME-C7	-	8.2%	-	-	-	-	-	0.1%	-	-	4.1%	4.1%	-	-	-
3-ME-C7	-	5.6%	-	-	-	-	-	-	-	-	2.2%	2.2%	-	-	-
BR-C8	-	2.3%	-	-	-	-	-	-	-	-	0.9%	0.9%	-	-	-
235TM-C6	-	-	-	-	-	-	-	-	-	-	-	-	-	-	-
24-DM-C7	-	0.8%	-	-	-	-	-	-	-	-	0.5%	0.5%	-	-	-
2-ME-C8	-	2.0%	-	-	-	-	-	-	-	-	-	-	-	-	-
4-ET-C7	-	2.6%	-	-	-	-	-	-	-	-	1.5%	1.5%	-	-	-
4-ME-C8	-	1.5%	0.4%	-	-	-	-	0.4%	-	-	0.9%	0.9%	0.3%	0.3%	-
BR-C9	-	7.2%	0.5%	-	-	-	-	1.0%	-	-	8.2%	8.1%	0.9%	0.6%	-
24-DM-C8	-	-	-	-	-	-	-	-	-	-	-	-	-	0.6%	-
26DM-C8	-	0.2%	2.1%	3.0%	-	2.8%	-	3.7%	-	-	0.9%	1.0%	3.8%	3.5%	-
2-ME-C9	0.1%	0.2%	3.1%	3.0%	-	2.9%	-	4.3%	0.0%	-	0.9%	1.0%	4.4%	3.6%	-
3-ME-C9	0.1%	-	1.8%	-	-	-	-	1.6%	0.1%	-	-	-	0.7%	1.0%	-
4-ME-C9	0.0%	-	2.4%	-	-	-	-	-	-	-	-	0.1%	-	0.8%	-
BR-C10	-	0.5%	9.5%	8.9%	-	8.4%	-	15.5%	-	-	3.7%	3.5%	16.1%	16.1%	-
26DM-C9	-	-	2.2%	1.5%	-	1.7%	-	0.5%	-	-	-	-	2.6%	2.2%	-
3-ME-C10	-	-	1.2%	4.1%	-	4.2%	-	0.9%	-	-	-	-	0.6%	0.9%	-
4-ME-C10	-	-	1.7%	3.5%	-	3.8%	-	1.4%	-	-	-	-	1.4%	0.5%	-
BR-C11	-	-	1.0%	9.4%	-	10.4%	-	2.9%	-	-	-	-	2.5%	2.2%	-
36DM-C10	-	-	0.4%	-	-	-	-	0.2%	-	-	-	-	0.2%	0.3%	-
3-ME-C11	-	-	0.1%	0.9%	-	0.7%	-	0.2%	-	-	-	-	0.2%	-	-
5-ME-C11	-	-	0.1%	0.8%	-	0.7%	-	0.2%	-	-	-	-	0.3%	0.2%	-
BR-C12	-	-	3.7%	12.7%	-	11.7%	-	4.0%	-	-	-	-	4.1%	2.0%	-
3-ME-C12	-	-	-	-	-	-	-	-	-	-	-	-	-	-	-
5-ME-C12	-	-	-	-	-	-	-	-	-	-	-	-	-	-	-
BR-C13	-	-	0.2%	0.7%	-	0.6%	-	0.6%	-	-	-	-	0.8%	0.6%	-
BR-C14	-	-	-	-	-	-	-	0.1%	-	-	-	-	0.1%	-	-
ET-CYCC5	-	-	-	-	-	-	-	-	-	-	0.1%	0.1%	-	-	-
ME-CYCC6	-	0.9%	-	-	-	-	-	-	-	-	0.8%	0.8%	-	-	-

Table A-2 (continued)

Model Species	Composition (weight percent)														
	CP13	CP14	CP15	CP16	CP17	CP18	CP19	CP20	CP21	CP22	CP23	CP24	CP25	CP26	CP27
CYC-C7	-	0.1%	-	-	-	-	-	-	-	-	-	-	-	-	-
BCYC-C8	-	-	-	-	-	-	-	-	-	-	1.1%	1.2%	-	-	-
13DMCYC6	-	6.9%	-	-	-	-	-	-	-	-	0.5%	9.1%	-	-	-
ET-CYCC6	-	-	-	-	-	-	-	-	-	-	5.7%	5.7%	-	-	-
PR-CYCC5	-	7.4%	-	-	-	-	-	-	-	-	-	-	-	-	-
CYC-C8	-	13.2%	1.3%	0.4%	-	0.6%	-	3.8%	-	-	30.7%	24.0%	2.3%	1.1%	-
BCYC-C9	-	-	0.5%	-	-	-	-	4.7%	-	-	1.3%	1.4%	3.3%	2.4%	-
113MCYC6	-	1.3%	0.6%	-	-	-	-	0.6%	-	-	8.0%	7.6%	0.6%	0.7%	-
C3-CYCC6	-	0.1%	2.8%	-	-	-	-	0.4%	-	-	0.8%	0.6%	2.0%	2.2%	-
CYC-C9	-	16.2%	11.6%	-	-	-	-	12.1%	-	-	14.5%	13.1%	10.4%	11.7%	-
BCYC-C10	-	-	-	-	-	-	-	-	-	-	-	-	-	-	-
14DECYC6	-	-	1.8%	-	-	-	-	1.1%	-	-	-	-	1.1%	0.9%	-
1M3IPCY6	-	-	4.2%	-	-	-	-	3.8%	-	-	0.1%	-	3.3%	2.5%	-
C4-CYCC6	0.1%	-	2.4%	1.0%	-	1.5%	-	2.4%	-	-	-	-	2.6%	2.1%	-
CYC-C10	0.1%	-	10.6%	0.5%	0.1%	0.7%	-	12.5%	-	-	0.1%	0.1%	13.0%	14.9%	-
BCYC-C11	-	-	0.2%	0.7%	-	0.6%	-	-	-	-	-	-	-	0.3%	-
13E5MCC6	-	-	0.7%	3.2%	-	3.3%	-	0.1%	-	-	-	-	0.1%	0.1%	-
C5-CYCC6	-	-	-	1.4%	-	1.4%	-	-	-	-	-	-	-	-	-
CYC-C11	-	-	2.8%	12.9%	-	13.1%	-	0.3%	-	-	-	-	0.3%	0.3%	-
135ECYC6	-	-	0.6%	0.2%	-	0.2%	-	-	-	-	-	-	-	0.2%	-
1M4C5CY6	-	-	0.6%	0.2%	-	0.2%	-	-	-	-	-	-	-	0.2%	-
C6-CYCC6	-	-	0.6%	0.2%	-	0.2%	-	-	-	-	-	-	-	0.2%	-
TOLUENE	-	0.0%	-	-	-	-	0.2%	-	-	-	-	-	-	-	0.0%
C2-BENZ	-	0.1%	0.2%	-	-	-	15.4%	-	0.0%	-	-	0.4%	-	-	15.8%
I-C3-BEN	1.6%	-	0.4%	-	-	-	0.1%	0.2%	1.0%	-	-	-	0.1%	0.3%	0.0%
N-C3-BEN	4.4%	-	0.7%	-	-	-	0.1%	0.2%	5.2%	0.1%	0.1%	0.1%	0.2%	0.6%	0.0%
S-C4-BEN	-	-	-	-	-	-	-	-	-	-	-	-	-	-	-
C10-BEN1	0.7%	-	0.2%	-	0.0%	-	-	0.1%	1.0%	0.2%	-	-	0.1%	0.3%	-
N-C4-BEN	0.1%	-	0.2%	-	0.5%	-	-	0.2%	0.0%	0.5%	-	-	0.2%	0.3%	-
C11-BEN1	-	-	-	-	0.1%	-	-	-	-	0.2%	-	-	-	-	-
C12-BEN1	-	-	0.2%	-	-	-	-	-	-	-	-	-	-	0.1%	-
M-XYLENE	-	0.2%	0.2%	-	-	-	44.6%	0.2%	0.2%	-	0.0%	0.2%	0.1%	0.3%	43.2%
O-XYLENE	1.7%	-	0.5%	-	-	-	19.8%	0.6%	1.4%	-	0.1%	0.1%	0.2%	0.6%	21.7%
P-XYLENE	-	0.1%	0.0%	-	-	-	19.3%	0.1%	0.1%	-	0.1%	0.1%	-	-	18.8%
M-ET-TOL	17.4%	-	0.7%	-	-	-	0.2%	0.4%	18.5%	0.2%	0.1%	0.0%	0.8%	0.8%	0.1%
P-ET-TOL	7.8%	-	0.6%	-	-	-	0.0%	0.5%	8.6%	0.1%	0.1%	0.0%	0.1%	0.6%	0.0%
O-ET-TOL	6.4%	-	0.1%	-	-	-	0.0%	0.3%	7.7%	0.1%	-	0.0%	0.3%	0.3%	0.0%
O-DE-BEN	0.1%	-	0.8%	-	0.2%	-	-	0.1%	0.1%	0.2%	-	-	0.1%	0.1%	-
M-DE-BEN	0.5%	-	0.4%	-	1.0%	-	-	0.1%	0.9%	0.9%	-	-	0.1%	0.2%	-
P-DE-BEN	-	-	0.5%	-	1.5%	-	-	-	-	1.2%	-	-	-	0.6%	-

Table A-2 (continued)

Model Species	Composition (weight percent)														
	CP13	CP14	CP15	CP16	CP17	CP18	CP19	CP20	CP21	CP22	CP23	CP24	CP25	CP26	CP27
C10-BEN2	2.6%	-	2.3%	-	7.0%	-	-	0.7%	3.2%	5.9%	-	-	0.9%	2.4%	-
C11-BEN2	0.3%	-	-	-	0.6%	-	-	-	-	0.5%	-	-	-	-	-
C12-BEN2	0.1%	-	0.5%	-	0.1%	-	-	-	-	0.2%	-	-	-	0.2%	-
123-TMB	6.7%	-	0.6%	-	1.3%	-	-	0.9%	6.4%	3.8%	-	0.0%	1.0%	1.5%	-
124-TMB	31.7%	-	0.8%	-	0.1%	-	0.1%	1.3%	31.1%	2.2%	0.1%	0.1%	1.4%	0.8%	0.1%
135-TMB	9.0%	0.2%	1.2%	-	-	-	0.0%	0.5%	9.1%	0.2%	0.0%	0.0%	0.6%	0.3%	0.1%
1235MBEN	0.8%	-	0.1%	-	15.2%	-	-	0.3%	0.2%	15.5%	-	-	0.3%	0.2%	-
C10-BEN4	0.7%	-	0.4%	-	13.0%	-	-	0.5%	0.2%	14.1%	-	-	0.6%	0.4%	-
C10-BEN3	5.1%	-	1.5%	-	41.7%	-	-	1.3%	3.5%	33.1%	-	-	1.3%	2.2%	-
C11-BEN5	-	-	-	-	0.1%	-	-	-	-	0.5%	-	-	-	-	-
C11-BEN4	0.2%	-	0.0%	-	1.6%	-	-	0.3%	-	2.2%	-	-	0.3%	0.2%	-
C11-BEN3	0.4%	-	0.3%	-	3.7%	-	-	0.3%	0.0%	4.2%	-	-	0.5%	0.2%	-
C12-BEN3	-	-	0.2%	-	-	-	-	-	-	-	-	-	-	0.1%	-
INDAN	1.0%	-	0.3%	-	0.7%	-	-	0.9%	1.4%	1.2%	-	-	0.9%	0.3%	-
NAPHTHAL	0.1%	-	0.2%	-	3.5%	-	-	0.0%	0.0%	4.9%	-	-	0.1%	-	-
TETRALIN	-	-	-	-	0.4%	-	-	-	-	0.4%	-	-	-	-	-
ME-INDAN	0.4%	-	1.0%	-	6.5%	-	-	0.4%	0.1%	5.7%	-	-	0.7%	1.1%	-
1ME-NAPH	-	-	-	-	0.1%	-	-	-	-	0.1%	-	-	-	-	-
2ME-NAPH	-	-	-	-	0.3%	-	-	-	-	0.5%	-	-	-	-	-
C11-TET	-	-	-	-	0.3%	-	-	-	-	1.0%	-	-	-	-	-
C9-OLE1	-	-	-	-	-	-	-	-	-	-	2.6%	1.9%	-	-	-
C10-OLE1	-	-	-	-	-	-	-	-	-	-	0.1%	-	-	-	-
C10-STYR	0.1%	-	-	-	0.3%	-	-	-	-	0.2%	-	-	-	-	-

Table A-2 (continued)

Model Species	Composition (weight percent)														
	CP28	CP29	CP30	CP31	CP32	CP33	CP34	CP35	CP36	CP37	CP39	CP40	CP41	CP42	CP43
N-C6	-	-	-	-	-	-	-	-	-	-	-	-	-	-	-
N-C7	13.8%	-	0.7%	-	-	-	-	-	-	-	-	-	-	-	-
N-C8	9.0%	1.6%	13.7%	-	-	-	-	16.0%	-	-	0.1%	-	-	-	0.5%
N-C9	0.1%	13.4%	7.8%	-	-	1.1%	-	1.0%	-	-	5.4%	-	-	-	8.8%
N-C10	-	3.3%	0.2%	-	-	13.7%	-	-	-	-	13.2%	-	-	-	13.9%
N-C11	-	0.1%	-	-	-	6.8%	-	-	-	-	2.2%	-	-	-	3.7%
N-C12	-	-	-	-	-	2.0%	-	-	-	-	0.1%	-	-	-	0.1%
23-DM-C5	1.1%	-	0.1%	-	-	-	-	-	-	-	-	-	-	-	-
24-DM-C5	-	-	-	-	-	-	-	-	-	-	-	-	-	-	-

Table A-2 (continued)

Model Species	Composition (weight percent)														
	CP28	CP29	CP30	CP31	CP32	CP33	CP34	CP35	CP36	CP37	CP39	CP40	CP41	CP42	CP43
2-ME-C6	3.3%	-	0.2%	-	-	-	-	-	-	-	-	-	-	-	-
33-DM-C5	0.2%	-	-	-	-	-	-	-	-	-	-	-	-	-	-
3-ME-C6	4.3%	-	0.2%	-	-	-	-	-	-	-	-	-	-	-	-
22-DM-C6	0.5%	-	-	-	-	-	-	-	-	-	-	-	-	-	-
234TM-C5	0.1%	-	-	-	-	-	-	0.2%	-	-	-	-	-	-	-
23-DM-C6	1.4%	-	0.6%	-	-	-	-	0.8%	-	-	-	-	-	-	-
25-DM-C6	3.0%	-	0.1%	-	-	-	-	0.1%	-	-	-	-	-	-	-
2-ME-C7	9.3%	0.2%	4.1%	-	-	-	-	5.6%	-	-	-	-	-	-	0.1%
3-ME-C7	7.1%	0.2%	3.9%	-	-	-	-	4.1%	-	-	-	-	-	-	0.1%
BR-C8	5.7%	-	1.7%	-	-	-	-	1.5%	-	-	-	-	-	-	-
235TM-C6	0.1%	0.1%	0.3%	-	-	-	-	0.2%	-	-	-	-	-	-	-
24-DM-C7	0.2%	0.3%	1.5%	-	-	-	-	0.7%	-	-	-	-	-	-	-
2-ME-C8	0.1%	2.2%	0.3%	-	-	-	-	-	-	-	-	-	-	-	1.4%
33-DE-C5	-	-	0.5%	-	-	-	-	-	-	-	-	-	-	-	-
35-DM-C7	0.1%	0.1%	2.8%	-	-	-	-	2.3%	-	-	-	-	-	-	-
4-ET-C7	3.1%	0.3%	2.0%	-	-	-	-	1.9%	-	-	-	-	-	-	0.1%
4-ME-C8	0.1%	1.7%	8.6%	-	-	0.2%	-	4.5%	-	-	0.6%	-	-	-	0.9%
BR-C9	0.7%	6.9%	12.7%	-	0.1%	0.7%	-	5.8%	-	-	0.7%	-	-	-	3.1%
24-DM-C8	-	0.8%	-	-	-	-	-	-	-	-	-	-	-	-	0.2%
26DM-C8	0.0%	4.3%	0.8%	-	-	4.8%	-	0.4%	-	-	3.3%	-	-	-	2.2%
2-ME-C9	0.0%	3.4%	0.6%	-	-	7.5%	-	0.4%	-	-	4.9%	-	-	-	6.3%
3-ME-C9	-	1.8%	0.2%	-	-	0.4%	-	-	-	-	-	-	-	-	3.5%
4-ME-C9	-	2.1%	0.2%	-	-	1.4%	-	-	-	-	2.7%	-	-	-	3.7%
BR-C10	0.1%	12.7%	2.6%	-	-	22.4%	-	1.1%	-	-	16.4%	-	-	-	17.4%
26DM-C9	-	-	-	-	-	2.3%	-	-	-	-	2.8%	-	-	-	2.2%
3-ME-C10	-	-	-	-	-	1.4%	-	-	-	-	0.6%	-	-	-	1.3%
4-ME-C10	-	-	-	-	-	1.7%	-	-	-	-	0.9%	-	-	-	1.7%
BR-C11	-	-	-	-	-	4.1%	-	-	-	-	1.6%	-	-	-	4.5%
36DM-C10	-	-	-	-	-	0.2%	-	-	-	-	0.1%	-	-	-	-
3-ME-C11	-	-	-	-	-	0.4%	-	-	-	-	-	-	-	-	-
5-ME-C11	-	-	-	-	-	0.3%	-	-	-	-	-	-	-	-	-
BR-C12	-	-	-	-	-	4.7%	-	-	-	-	0.5%	-	-	-	0.8%
BR-C13	-	-	-	-	-	0.2%	-	-	-	-	-	-	-	-	-
13DMCYC5	1.2%	-	-	-	-	-	-	-	-	-	-	-	-	-	-
ET-CYCC5	0.1%	-	0.0%	-	-	-	-	-	-	-	-	-	-	-	-
ME-CYCC6	21.7%	-	1.2%	-	-	-	-	0.2%	-	-	-	-	-	-	-
CYC-C7	1.2%	-	0.1%	-	-	-	-	-	-	-	-	-	-	-	-
13DMCYC6	3.8%	0.9%	5.1%	-	-	-	-	6.1%	-	-	-	-	-	-	-
ET-CYCC6	0.6%	3.1%	4.6%	-	-	-	-	-	-	-	-	-	-	-	0.5%
PR-CYCC5	-	0.2%	0.3%	-	-	-	-	0.5%	-	-	0.1%	-	-	-	-
CYC-C8	5.8%	1.8%	5.4%	-	-	2.5%	-	14.6%	-	-	1.4%	-	-	-	1.4%

Table A-2 (continued)

Model Species	Composition (weight percent)														
	CP28	CP29	CP30	CP31	CP32	CP33	CP34	CP35	CP36	CP37	CP39	CP40	CP41	CP42	CP43
BCYC-C9	-	0.3%	0.1%	-	-	1.6%	-	-	-	-	2.7%	-	-	-	0.1%
113MCYC6	-	1.5%	3.1%	-	-	-	-	1.3%	-	-	0.2%	-	-	-	0.2%
C3-CYCC6	-	3.2%	0.2%	-	-	0.2%	-	-	-	-	0.2%	-	-	-	1.7%
CYC-C9	-	26.8%	7.6%	-	-	3.9%	-	21.1%	-	-	6.5%	-	-	-	6.2%
BCYC-C10	-	-	-	-	-	-	-	-	-	-	-	-	-	-	-
14DECYC6	-	-	-	-	-	-	-	-	-	-	0.6%	-	-	-	0.7%
1M3IPCY6	-	1.5%	-	-	-	3.6%	-	-	-	-	1.3%	-	-	-	2.9%
C4-CYCC6	-	0.1%	-	-	-	1.5%	-	-	-	-	2.1%	-	-	-	1.9%
CYC-C10	-	4.7%	-	-	-	9.3%	-	-	-	-	11.1%	-	-	-	7.6%
BCYC-C11	-	-	-	-	-	-	-	-	-	-	-	-	-	-	-
13E5MCC6	-	-	-	-	-	-	-	-	-	-	0.0%	-	-	-	0.0%
C5-CYCC6	-	-	-	-	-	0.5%	-	-	-	-	-	-	-	-	-
CYC-C11	-	-	-	-	-	-	-	-	-	-	0.2%	-	-	-	0.2%
TOLUENE	2.2%	0.1%	0.4%	-	-	-	0.0%	-	-	-	-	0.1%	0.4%	-	-
C2-BENZ	-	-	0.4%	0.1%	0.1%	-	13.9%	1.3%	0.0%	-	0.1%	19.5%	17.6%	0.2%	-
I-C3-BEN	-	-	0.1%	1.8%	0.0%	-	0.0%	0.1%	1.5%	-	0.2%	0.1%	0.1%	1.0%	-
N-C3-BEN	-	-	-	4.4%	0.1%	-	-	0.0%	5.3%	0.1%	0.6%	0.0%	0.1%	3.4%	-
S-C4-BEN	-	-	-	-	-	-	-	-	-	-	-	-	-	-	-
C10-BEN1	-	-	-	0.3%	0.2%	-	-	-	0.4%	0.2%	0.4%	-	-	0.3%	-
N-C4-BEN	-	-	-	0.6%	0.5%	-	-	-	0.2%	0.6%	0.1%	-	-	0.1%	-
C11-BEN1	-	-	-	-	0.4%	-	-	-	-	0.5%	-	-	-	0.0%	-
C12-BEN1	-	-	-	-	-	-	-	-	-	-	-	-	-	-	-
M-XYLENE	-	-	3.1%	0.2%	0.1%	-	43.5%	4.4%	0.1%	-	0.3%	48.8%	42.6%	1.2%	-
O-XYLENE	-	-	1.0%	9.3%	0.1%	-	23.0%	2.2%	3.2%	-	0.2%	13.4%	19.5%	3.5%	-
P-XYLENE	-	-	0.6%	0.1%	0.0%	-	19.5%	1.7%	0.0%	-	0.1%	17.9%	19.3%	0.5%	-
M-ET-TOL	-	-	0.1%	17.8%	0.6%	-	0.0%	0.0%	20.0%	0.3%	1.6%	0.1%	0.2%	16.4%	-
P-ET-TOL	-	-	-	7.8%	0.3%	-	-	-	9.0%	0.2%	0.7%	0.0%	0.1%	7.5%	-
O-ET-TOL	-	0.4%	-	6.1%	0.4%	-	-	-	7.3%	0.3%	0.8%	0.0%	0.0%	5.3%	-
O-DE-BEN	-	-	-	0.1%	0.3%	-	-	-	0.1%	0.2%	0.1%	-	-	0.1%	-
M-DE-BEN	-	-	-	0.4%	1.2%	0.3%	-	-	0.6%	1.2%	0.3%	-	-	1.9%	-
P-DE-BEN	-	-	-	0.3%	1.2%	-	-	-	-	1.3%	0.4%	-	-	-	-
C10-BEN2	-	-	-	1.7%	6.5%	0.4%	-	-	2.4%	6.5%	2.2%	-	-	3.0%	-
C11-BEN2	-	-	-	0.0%	1.0%	-	-	-	-	1.4%	-	-	-	0.0%	-
C12-BEN2	-	-	-	0.0%	0.3%	-	-	-	-	0.3%	-	-	-	0.0%	-
123-TMB	-	-	-	5.4%	3.4%	-	-	-	7.8%	5.1%	1.5%	-	-	5.9%	-
124-TMB	-	-	0.1%	29.0%	4.4%	-	0.0%	-	25.4%	5.0%	3.9%	0.0%	0.0%	30.3%	-
135-TMB	-	-	0.1%	9.4%	0.6%	-	-	-	10.1%	0.4%	1.3%	0.0%	0.0%	9.7%	-
1235MBEN	-	-	-	0.6%	10.9%	-	-	-	0.4%	10.9%	0.2%	-	-	0.9%	-
C10-BEN4	-	-	-	0.6%	11.0%	-	-	-	0.4%	11.4%	0.2%	-	-	0.9%	-
C10-BEN3	-	-	-	3.1%	26.1%	-	-	-	4.1%	25.2%	1.8%	-	-	5.7%	-

Table A-2 (continued)

Model Species	Composition (weight percent)														
	CP28	CP29	CP30	CP31	CP32	CP33	CP34	CP35	CP36	CP37	CP39	CP40	CP41	CP42	CP43
C11-BEN5	-	-	-	-	0.3%	-	-	-	-	0.7%	-	-	-	-	-
C11-BEN4	-	-	-	0.0%	3.7%	-	-	-	-	3.9%	-	-	-	-	-
C11-BEN3	-	-	-	0.1%	6.8%	-	-	-	0.0%	7.6%	0.1%	-	-	0.3%	-
C12-BEN3	-	-	-	-	-	-	-	-	-	-	-	-	-	-	-
INDAN	-	-	-	0.9%	0.9%	-	-	-	1.6%	1.1%	0.1%	-	-	1.3%	-
NAPHTHAL	-	-	-	0.0%	8.4%	-	-	-	0.0%	6.6%	-	-	-	0.1%	-
TETRALIN	-	-	-	0.0%	0.7%	-	-	-	-	0.6%	-	-	-	0.0%	-
ME-INDAN	-	-	-	0.2%	7.2%	-	-	-	0.2%	5.3%	0.4%	-	-	0.5%	-
1ME-NAPH	-	-	-	-	0.1%	-	-	-	-	0.2%	-	-	-	-	-
2ME-NAPH	-	-	-	-	0.4%	-	-	-	-	0.8%	-	-	-	-	-
C11-TET	-	-	-	-	1.4%	-	-	-	-	2.0%	-	-	-	-	-
C10-STYR	-	-	-	-	0.1%	-	-	-	-	0.1%	-	-	-	-	-

Table A-3. SAPRC-99 detailed model species compositional assignments for the hydrocarbon solvents whose analysis was provided by the ACC (Jaques, 2002).

Model Species	Description	Composition (weight percent)											
		1-A	1-B	1-C	2-A	2-B	2-C	2-D	2-E	2-F	2-G	2-H	2-I
N-C5	n-Pentane	-	0.6%	-	-	-	0.4%	-	80.0%	55.5%	0.0%	-	-
N-C6	n-Hexane	64.0%	23.7%	9.2%	49.0%	-	24.2%	0.1%	-	17.5%	1.0%	83.0%	45.0%
N-C7	n-Heptane	-	7.7%	14.8%	1.0%	28.5%	4.4%	18.4%	-	-	-	-	-
N-C8	n-Octane	-	-	-	-	1.5%	-	0.3%	-	-	-	-	-
N-C9	n-Nonane	-	-	-	-	-	-	-	-	-	-	-	-
N-C10	n-Decane	-	-	-	-	-	-	-	-	-	-	-	-
N-C11	n-Undecane	-	-	-	-	-	-	-	-	-	-	-	-
N-C12	n-Dodecane	-	-	-	-	-	-	-	-	-	-	-	-
N-C13	n-Tridecane	-	-	-	-	-	-	-	-	-	-	-	-
N-C14	n-Tetradecane	-	-	-	-	-	-	-	-	-	-	-	-
N-C15	n-Pentadecane	-	-	-	-	-	-	-	-	-	-	-	-
N-C16	n-C16	-	-	-	-	-	-	-	-	-	-	-	-
N-C17	n-C17	-	-	-	-	-	-	-	-	-	-	-	-
N-C18	n-C18	-	-	-	-	-	-	-	-	-	-	-	-
BR-C5	Branched C5 Alkanes	-	1.0%	-	-	-	0.8%	-	20.0%	19.8%	1.0%	-	-
BR-C6	Branched C6 Alkanes	23.0%	36.3%	10.7%	48.0%	-	52.2%	0.5%	-	6.2%	98.0%	8.0%	55.0%
BR-C7	Branched C7 Alkanes	-	11.8%	17.3%	1.0%	59.9%	9.4%	71.5%	-	-	-	-	-
BR-C8	Branched C8 Alkanes	-	-	-	-	3.2%	-	1.1%	-	-	-	-	-
BR-C9	Branched C9 Alkanes	-	-	-	-	-	-	-	-	-	-	-	-
BR-C10	Branched C10 Alkanes	-	-	-	-	-	-	-	-	-	-	-	-
BR-C11	Branched C11 alkanes	-	-	-	-	-	-	-	-	-	-	-	-
BR-C12	Branched C12 Alkanes	-	-	-	-	-	-	-	-	-	-	-	-
BR-C13	Branched C13 Alkanes	-	-	-	-	-	-	-	-	-	-	-	-
BR-C14	Branched C14 Alkanes	-	-	-	-	-	-	-	-	-	-	-	-
BR-C15	Branched C15 Alkanes	-	-	-	-	-	-	-	-	-	-	-	-
BR-C16	Branched C16 Alkanes	-	-	-	-	-	-	-	-	-	-	-	-
BR-C17	Branched C17 Alkanes	-	-	-	-	-	-	-	-	-	-	-	-
BR-C18	Branched C18 Alkanes	-	-	-	-	-	-	-	-	-	-	-	-
CYCC5	Cyclopentane	-	0.4%	-	-	-	0.1%	-	-	0.8%	-	-	-
CYC-C6	C6 Cycloalkanes	13.0%	14.1%	18.4%	1.0%	-	7.2%	0.1%	-	0.2%	-	9.0%	-
CYC-C7	C7 Cycloalkanes	-	4.6%	29.6%	0.0%	6.7%	1.3%	7.9%	-	-	-	-	-
CYC-C8	C8 Cycloalkanes	-	-	-	-	0.4%	-	0.1%	-	-	-	-	-
CYC-C9	C9 Cycloalkanes	-	-	-	-	-	-	-	-	-	-	-	-
CYC-C10	C10 Cycloalkanes	-	-	-	-	-	-	-	-	-	-	-	-
CYC-C11	C11 Cycloalkanes	-	-	-	-	-	-	-	-	-	-	-	-
CYC-C12	C12 Cycloalkanes	-	-	-	-	-	-	-	-	-	-	-	-

Table A-3 (continued)

Model Species	Description	Composition (weight percent)											
		1-A	1-B	1-C	2-A	2-B	2-C	2-D	2-E	2-F	2-G	2-H	2-I
CYC-C13	C13 Cycloalkanes	-	-	-	-	-	-	-	-	-	-	-	-
CYC-C14	C14 Cycloalkanes	-	-	-	-	-	-	-	-	-	-	-	-
CYC-C15	C15 Cycloalkanes	-	-	-	-	-	-	-	-	-	-	-	-
CYC-C16	C16 Cycloalkanes	-	-	-	-	-	-	-	-	-	-	-	-
CYC-C17	C17 Cycloalkanes [a]	-	-	-	-	-	-	-	-	-	-	-	-
CYC-C18	C18 Cycloalkanes [a]	-	-	-	-	-	-	-	-	-	-	-	-
BENZENE	Benzene	-	-	-	-	-	-	-	-	-	-	-	-
BENZENE	Benzene	-	-	-	-	-	-	0.0%	-	-	-	-	-
TOLUENE	Toluene	-	-	-	-	-	-	0.0%	-	-	-	-	-
C2-BENZ	Ethyl Benzene	-	-	-	-	-	-	0.0%	-	-	-	-	-
C9-BEN1	C9 Monosubstituted Benzenes	-	-	-	-	-	-	-	-	-	-	-	-
C10-BEN1	C10 Monosubstituted Benzenes	-	-	-	-	-	-	-	-	-	-	-	-
C11-BEN1	C11 Monosubstituted Benzenes	-	-	-	-	-	-	-	-	-	-	-	-
C12-BEN1	C12 Monosubstituted Benzenes	-	-	-	-	-	-	-	-	-	-	-	-
C8-BEN2	C8 Disubstituted Benzenes	-	-	-	-	-	-	-	-	-	-	-	-
C8-BEN2	C8 Disubstituted Benzenes	-	-	-	-	-	-	-	-	-	-	-	-
C9-BEN2	C9 Disubstituted Benzenes	-	-	-	-	-	-	-	-	-	-	-	-
C10-BEN2	C10 Disubstituted Benzenes	-	-	-	-	-	-	-	-	-	-	-	-
C11-BEN2	C11 Disubstituted Benzenes	-	-	-	-	-	-	-	-	-	-	-	-
C12-BEN2	C12 Disubstituted Benzenes	-	-	-	-	-	-	-	-	-	-	-	-
C9-BEN3	C9 Trisubstituted Benzenes	-	-	-	-	-	-	-	-	-	-	-	-
C9-BEN3	C9 Trisubstituted Benzenes	-	-	-	-	-	-	-	-	-	-	-	-
C9-BEN3	C9 Trisubstituted Benzenes	-	-	-	-	-	-	-	-	-	-	-	-
C10-BEN3	C10 Trisubstituted Benzenes	-	-	-	-	-	-	-	-	-	-	-	-
C11-BEN3	C11 Trisubstituted Benzenes	-	-	-	-	-	-	-	-	-	-	-	-
C12-BEN3	C12 Trisubstituted Benzenes	-	-	-	-	-	-	-	-	-	-	-	-
C13-BEN3	C13 Trisubstituted Benzenes	-	-	-	-	-	-	-	-	-	-	-	-
C14-BEN3	C14 Trisubstituted Benzenes [a]	-	-	-	-	-	-	-	-	-	-	-	-
C15-BEN3	C15 Trisubstituted Benzenes [a]	-	-	-	-	-	-	-	-	-	-	-	-
C16-BEN3	C16 Trisubstituted Benzenes [a]	-	-	-	-	-	-	-	-	-	-	-	-
C17-BEN3	C17 Trisubstituted Benzenes [a]	-	-	-	-	-	-	-	-	-	-	-	-

[a] There is no model species of this type for this carbon number. The reactivity is calculated based on assuming the same per-molecule reactivity of the highest carbon number model species of this type that is defined (e.g., CYC-C16 or C13-BEN3).

Table A-3 (continued)

Model Species	Composition (weight percent)															
	2-J	2-K	2-L	2-M	2-N	2-O	3-A	3-B	4-A	5-A	6-A	6-B	6-C	6-D	6-E	6-F
N-C5	-	-	-	-	-	-	-	-	-	-	-	-	-	-	-	-
N-C6	-	-	4.0%	45.2%	47.5%	17.3%	-	0.0%	-	-	-	-	-	-	-	0.0%
N-C7	7.0%	-	-	6.8%	0.5%	7.8%	-	5.0%	26.0%	-	-	-	-	1.4%	-	14.5%
N-C8	-	-	-	-	-	-	-	0.1%	-	-	-	-	8.2%	11.0%	-	5.4%
N-C9	-	-	-	-	-	-	-	-	-	-	-	6.0%	10.8%	5.4%	2.5%	-
N-C10	-	-	-	-	-	-	-	-	-	-	-	8.7%	-	0.2%	8.7%	-
N-C11	-	-	-	-	-	-	-	-	-	-	-	2.4%	-	-	7.6%	-
N-C12	-	-	-	-	-	-	-	-	-	-	-	-	-	-	0.2%	-
BR-C5	-	-	-	-	-	-	-	-	-	0.9%	-	-	-	-	-	-
BR-C6	-	-	95.0%	40.9%	44.6%	46.9%	11.3%	0.0%	-	43.1%	-	-	-	-	-	0.0%
BR-C7	91.0%	28.0%	-	6.1%	0.5%	21.1%	1.4%	1.9%	69.0%	44.0%	-	-	-	2.2%	-	11.9%
BR-C8	-	72.0%	-	-	-	-	0.3%	0.0%	-	-	-	-	7.7%	16.5%	-	4.4%
BR-C9	-	-	-	-	-	-	-	-	-	-	4.3%	8.8%	10.3%	8.1%	3.9%	-
BR-C10	-	-	-	-	-	-	-	-	-	-	32.5%	12.8%	-	0.3%	13.8%	-
BR-C11	-	-	-	-	-	-	-	-	-	-	9.8%	3.5%	-	-	12.0%	-
BR-C12	-	-	-	-	-	-	-	-	-	-	0.1%	-	-	-	0.3%	-
CYCC5	-	-	-	-	-	-	-	-	-	0.0%	-	-	-	-	-	-
CYC-C6	-	-	1.0%	0.9%	6.9%	4.1%	75.7%	0.0%	-	1.0%	-	-	-	-	-	0.1%
CYC-C7	2.0%	-	-	0.1%	0.1%	1.9%	9.6%	91.0%	2.0%	1.0%	-	-	-	4.4%	-	46.3%
CYC-C8	-	-	-	-	-	-	1.7%	1.8%	-	-	-	-	27.1%	33.6%	-	17.2%
CYC-C9	-	-	-	-	-	-	-	-	-	-	4.9%	20.3%	35.9%	16.5%	6.6%	-
CYC-C10	-	-	-	-	-	-	-	-	-	-	37.0%	29.6%	-	0.6%	23.5%	-
CYC-C11	-	-	-	-	-	-	-	-	-	-	11.1%	8.1%	-	-	20.4%	-
CYC-C12	-	-	-	-	-	-	-	-	-	-	0.2%	-	-	-	0.5%	-
BENZENE	-	-	-	-	-	-	-	-	-	0.1%	-	-	-	-	-	-
BENZENE	-	-	-	-	-	0.7%	-	0.0%	-	4.9%	-	-	-	-	-	0.0%
TOLUENE	-	-	-	-	-	0.3%	-	0.1%	3.0%	5.0%	-	-	-	-	-	0.1%
C2-BENZ	-	-	-	-	-	-	-	0.0%	-	-	-	-	-	-	-	0.1%
C9-BEN3	-	-	-	-	-	-	-	-	-	-	0.0%	-	-	-	-	-
C10-BEN3	-	-	-	-	-	-	-	-	-	-	0.1%	-	-	-	-	-
C11-BEN3	-	-	-	-	-	-	-	-	-	-	0.0%	-	-	-	-	-
C12-BEN3	-	-	-	-	-	-	-	-	-	-	0.0%	-	-	-	-	-

Table A-3 (continued)

Model Species	Composition (weight percent)															
	6-G	7-A	7-B	7-C	7-D	7-E	8-A	9-A	9-B	10-A	10-B	10-C	11-A	11-B	11-C	11-D
N-C5	-	-	-	-	-	-	-	-	0.3%	-	-	-	-	-	-	-
N-C6	-	-	-	-	-	-	-	-	13.9%	0.2%	0.2%	-	-	-	-	-
N-C7	0.1%	31.2%	-	-	-	-	-	1.1%	10.4%	16.8%	11.0%	-	-	-	-	-
N-C8	9.1%	3.9%	-	-	-	-	-	25.7%	2.0%	3.0%	5.9%	-	-	-	-	0.1%
N-C9	4.9%	-	-	-	-	-	-	0.3%	1.4%	-	-	12.1%	1.4%	-	6.3%	1.1%
N-C10	0.1%	-	-	-	-	-	-	-	-	-	-	5.7%	6.0%	1.9%	9.2%	3.8%
N-C11	-	-	-	-	-	-	-	-	-	-	-	0.2%	9.1%	9.4%	1.4%	5.6%
N-C12	-	-	-	-	-	-	-	-	-	-	-	-	7.4%	8.4%	1.1%	2.8%
N-C13	-	-	-	-	-	-	-	-	-	-	-	-	-	2.6%	-	0.6%
BR-C5	-	-	-	-	-	-	-	-	0.4%	-	-	-	-	-	-	-
BR-C6	-	-	-	-	-	-	-	-	20.3%	0.3%	0.3%	-	-	-	-	-
BR-C7	0.1%	55.2%	-	-	-	-	-	1.3%	15.2%	22.7%	18.0%	-	-	-	-	-
BR-C8	13.0%	6.8%	-	4.0%	3.0%	100.0%	-	31.4%	3.0%	4.1%	9.6%	-	-	-	-	0.3%
BR-C9	6.9%	-	8.7%	69.0%	14.1%	-	-	0.3%	2.1%	-	-	20.9%	0.7%	-	8.4%	2.3%
BR-C10	0.1%	-	60.1%	27.0%	62.6%	-	-	-	-	-	-	9.8%	3.0%	1.8%	12.2%	7.8%
BR-C11	-	-	28.1%	-	20.2%	-	-	-	-	-	-	0.3%	4.6%	8.7%	1.9%	11.6%
BR-C12	-	-	-	-	-	-	-	-	-	-	-	-	3.7%	7.7%	1.4%	5.8%
BR-C13	-	-	-	-	-	-	-	-	-	-	-	-	-	2.4%	-	1.2%
CYCC5	-	-	-	-	-	-	-	-	0.3%	-	-	-	-	-	-	-
CYC-C6	-	-	-	-	-	-	-	-	13.9%	0.4%	0.5%	-	-	-	-	-
CYC-C7	0.4%	2.7%	-	-	-	-	-	1.5%	10.4%	31.9%	30.3%	-	-	-	-	-
CYC-C8	42.1%	0.3%	-	-	-	-	1.0%	35.2%	2.0%	5.7%	16.2%	-	-	-	-	0.6%
CYC-C9	22.4%	-	0.3%	-	-	-	87.0%	0.4%	1.4%	-	-	22.2%	3.8%	-	20.3%	4.6%
CYC-C10	0.3%	-	1.9%	-	-	-	12.0%	-	-	-	-	10.4%	16.0%	4.9%	29.6%	15.4%
CYC-C11	-	-	0.9%	-	-	-	-	-	-	-	-	0.4%	24.3%	23.9%	4.6%	22.8%
CYC-C12	-	-	-	-	-	-	-	-	-	-	-	-	19.8%	21.4%	3.5%	11.4%
CYC-C13	-	-	-	-	-	-	-	-	-	-	-	-	-	6.7%	-	2.3%
BENZENE	-	-	-	-	-	-	-	-	0.0%	-	-	-	-	-	-	-
BENZENE	-	-	-	-	-	-	-	-	1.5%	0.2%	0.1%	-	-	-	-	-
TOLUENE	0.0%	-	-	-	-	-	-	0.1%	1.1%	12.6%	5.2%	-	-	-	-	-
C2-BENZ	0.2%	-	-	-	-	-	-	1.9%	0.2%	2.3%	2.8%	-	-	-	-	-
C9-BEN1	0.1%	-	-	-	-	-	-	0.0%	0.2%	-	-	-	-	-	-	-
C10-BEN1	0.0%	-	-	-	-	-	-	-	-	-	-	-	-	-	-	-
C8-BEN2	0.0%	-	-	-	-	-	-	0.0%	-	-	-	-	-	-	-	-
C8-BEN2	0.2%	-	-	-	-	-	-	1.0%	-	-	-	-	-	-	-	-
C9-BEN2	0.1%	-	-	-	-	-	-	0.0%	-	-	-	12.1%	-	-	-	-
C10-BEN2	0.0%	-	-	-	-	-	-	-	-	-	-	5.7%	-	-	-	-
C11-BEN2	-	-	-	-	-	-	-	-	-	-	-	0.2%	-	-	-	-
C12-BEN2	-	-	-	-	-	-	-	-	-	-	-	-	-	-	-	-

Table A-3 (continued)

Model Species	Composition (weight percent)															
	11-E	11-F	11-G	11-H	11-I	11-J	11-K	11-L	12-A	12-B	12-C	12-D	12-E	12-F	12-G	12-H
N-C9	-	-	-	-	0.0%	0.1%	0.0%	-	-	-	-	-	-	-	-	-
N-C10	0.6%	0.2%	-	-	0.3%	0.6%	0.3%	-	-	-	-	-	-	-	9.0%	-
N-C11	4.6%	5.7%	1.8%	-	0.5%	0.9%	0.5%	0.1%	-	-	-	-	-	-	44.0%	-
N-C12	10.6%	11.9%	7.0%	-	0.5%	0.4%	0.6%	0.8%	-	-	-	-	-	-	39.0%	13.9%
N-C13	4.2%	4.0%	9.5%	-	0.4%	0.1%	0.5%	1.0%	-	-	-	-	-	-	6.0%	49.5%
N-C14	-	0.2%	3.5%	-	0.2%	-	0.1%	0.2%	-	-	-	-	-	-	1.0%	35.6%
N-C15	-	-	0.2%	-	0.1%	-	-	-	-	-	-	-	-	-	-	-
N-C16	-	-	-	-	0.0%	-	-	-	-	-	-	-	-	-	-	-
BR-C9	-	-	-	-	0.9%	1.1%	0.9%	-	-	-	-	-	-	-	-	-
BR-C10	0.9%	0.2%	-	-	6.0%	8.7%	6.5%	-	2.0%	2.0%	-	0.4%	11.5%	6.8%	0.1%	-
BR-C11	6.7%	6.2%	2.6%	53.4%	10.8%	12.3%	10.3%	1.7%	52.0%	31.0%	-	41.6%	77.8%	42.7%	0.4%	-
BR-C12	15.4%	13.0%	10.2%	28.5%	10.3%	5.0%	12.0%	22.0%	42.0%	29.0%	11.0%	42.9%	6.7%	42.7%	0.4%	0.1%
BR-C13	6.1%	4.3%	13.8%	7.1%	7.7%	0.8%	11.2%	29.6%	4.0%	24.0%	53.0%	11.6%	-	4.9%	0.1%	0.5%
BR-C14	-	0.2%	5.1%	-	4.7%	-	2.2%	4.6%	-	12.0%	30.0%	3.5%	-	-	0.0%	0.4%
BR-C15	-	-	0.3%	-	2.2%	-	-	-	-	2.0%	6.0%	-	-	-	-	-
BR-C16	-	-	-	-	0.4%	-	-	-	-	-	-	-	-	-	-	-
CYC-C9	-	-	-	-	1.1%	2.8%	1.1%	-	-	-	-	-	-	-	-	-
CYC-C10	1.5%	0.5%	-	-	7.7%	21.7%	8.2%	-	-	-	-	-	0.5%	0.2%	-	-
CYC-C11	11.7%	14.0%	3.7%	6.6%	13.7%	30.8%	13.2%	1.2%	-	-	-	-	3.2%	1.3%	-	-
CYC-C12	27.0%	29.2%	14.7%	3.5%	13.2%	12.6%	15.4%	15.2%	-	-	-	-	0.3%	1.3%	-	-
CYC-C13	10.7%	9.7%	19.8%	0.9%	9.9%	2.1%	14.3%	20.3%	-	-	-	-	-	0.2%	-	-
CYC-C14	-	0.5%	7.4%	-	6.0%	-	2.7%	3.2%	-	-	-	-	-	-	-	-
CYC-C15	-	-	0.5%	-	2.7%	-	-	-	-	-	-	-	-	-	-	-
CYC-C16	-	-	-	-	0.5%	-	-	-	-	-	-	-	-	-	-	-

Table A-3 (continued)

Model Species	Composition (weight percent)																
	14-A	14-B	14-C	15-A	15-C	15-D	15-E	15-F	15-G	16-A	16-B	16-C	16-D	16-E	17-A	17-B	17-C
N-C7	-	0.4%	-	-	-	-	-	-	-	-	-	-	-	-	-	-	-
N-C8	-	2.0%	-	-	0.3%	0.2%	-	0.2%	-	-	-	-	-	-	-	-	-
N-C9	10.2%	8.0%	-	7.8%	1.3%	1.2%	-	2.5%	0.0%	-	-	-	-	-	-	-	-
N-C10	12.9%	7.6%	0.7%	9.3%	4.8%	4.2%	0.5%	7.8%	0.3%	-	-	-	-	-	-	-	-
N-C11	6.8%	2.0%	10.6%	9.3%	6.2%	6.0%	10.8%	6.8%	0.5%	-	-	-	-	-	-	-	-
N-C12	4.1%	-	10.1%	4.7%	2.9%	2.9%	10.1%	1.7%	0.5%	-	-	-	0.0%	0.2%	-	-	-
N-C13	-	-	1.6%	-	0.5%	0.6%	1.4%	-	0.4%	1.1%	-	-	0.3%	2.6%	-	-	-
N-C14	-	-	-	-	-	-	0.2%	-	0.2%	6.9%	-	-	0.8%	9.5%	-	32.7%	57.9%

Table A-3 (continued)

Model Species	Composition (weight percent)																
	14-A	14-B	14-C	15-A	15-C	15-D	15-E	15-F	15-G	16-A	16-B	16-C	16-D	16-E	17-A	17-B	17-C
N-C15	-	-	-	-	-	-	-	-	0.1%	8.8%	1.1%	-	0.7%	7.3%	-	45.5%	30.9%
N-C16	-	-	-	-	-	-	-	-	0.0%	3.8%	3.6%	-	0.2%	2.0%	-	17.8%	6.8%
N-C17	-	-	-	-	-	-	-	-	-	0.4%	5.8%	-	0.1%	0.4%	-	2.0%	1.0%
N-C18	-	-	-	-	-	-	-	-	-	-	7.6%	-	-	-	-	1.0%	-
BR-C7	-	0.6%	-	-	-	-	-	-	-	-	-	-	-	-	-	-	-
BR-C8	-	2.9%	-	-	0.6%	0.3%	-	0.3%	-	-	-	-	-	-	-	-	-
BR-C9	5.7%	11.6%	-	4.5%	2.5%	2.4%	-	3.9%	0.9%	-	-	-	-	-	-	-	-
BR-C10	7.2%	11.0%	0.8%	5.4%	9.3%	8.4%	0.5%	12.3%	6.0%	-	-	-	-	-	-	-	-
BR-C11	3.8%	2.9%	12.0%	5.4%	12.1%	12.0%	11.7%	10.8%	10.8%	-	-	-	-	-	-	-	-
BR-C12	2.3%	-	11.4%	2.7%	5.6%	5.7%	11.0%	2.7%	10.3%	-	-	-	0.6%	0.5%	-	-	-
BR-C13	-	-	1.8%	-	0.9%	1.2%	1.5%	-	7.7%	1.7%	-	-	9.5%	6.0%	35.0%	-	-
BR-C14	-	-	-	-	-	-	0.3%	-	4.7%	10.9%	-	0.5%	24.6%	21.5%	39.0%	0.3%	1.1%
BR-C15	-	-	-	-	-	-	-	-	2.2%	13.9%	1.3%	4.9%	20.8%	16.5%	22.0%	0.5%	0.6%
BR-C16	-	-	-	-	-	-	-	-	0.4%	5.9%	4.2%	17.3%	5.7%	4.5%	4.0%	0.2%	0.1%
BR-C17	-	-	-	-	-	-	-	-	-	0.7%	6.7%	16.2%	1.9%	1.0%	-	0.0%	0.0%
BR-C18	-	-	-	-	-	-	-	-	-	-	8.8%	15.1%	-	-	-	0.0%	-
CYC-C7	-	0.7%	-	-	-	-	-	-	-	-	-	-	-	-	-	-	-
CYC-C8	-	3.4%	-	-	0.7%	0.5%	-	0.5%	-	-	-	-	-	-	-	-	-
CYC-C9	12.0%	13.6%	-	8.8%	2.7%	3.9%	-	6.0%	0.8%	-	-	-	-	-	-	-	-
CYC-C10	15.2%	12.9%	1.4%	10.5%	10.2%	13.7%	0.7%	18.9%	5.9%	-	-	-	-	-	-	-	-
CYC-C11	8.0%	3.4%	21.2%	10.5%	13.3%	19.6%	16.9%	16.6%	10.5%	-	-	-	-	-	-	-	-
CYC-C12	4.8%	-	20.2%	5.3%	6.1%	9.3%	15.8%	4.1%	10.1%	-	-	-	0.3%	0.3%	-	-	-
CYC-C13	-	-	3.2%	-	1.0%	2.0%	2.2%	-	7.6%	2.3%	-	-	5.2%	3.3%	-	-	-
CYC-C14	-	-	-	-	-	-	0.4%	-	4.6%	14.9%	-	0.5%	13.5%	12.0%	-	-	1.0%
CYC-C15	-	-	-	-	-	-	-	-	2.1%	18.9%	3.7%	4.1%	11.5%	9.2%	-	-	0.5%
CYC-C16	-	-	-	-	-	-	-	-	0.4%	8.1%	12.2%	14.7%	3.1%	2.5%	-	-	0.1%
CYC-C17	-	-	-	-	-	-	-	-	-	0.9%	19.5%	13.8%	1.0%	0.6%	-	-	0.0%
CYC-C18	-	-	-	-	-	-	-	-	-	-	25.6%	12.9%	-	-	-	-	-
C9-BEN1	0.3%	-	-	0.5%	-	-	-	-	-	-	-	-	-	-	-	-	-
C10-BEN1	0.4%	-	-	0.6%	-	-	-	-	-	-	-	-	-	-	-	-	-
C11-BEN1	0.2%	-	-	0.6%	-	-	-	-	-	-	-	-	-	-	-	-	-
C12-BEN1	0.1%	-	-	0.3%	-	-	-	-	-	-	-	-	-	-	-	-	-
C9-BEN2	0.9%	-	-	1.8%	-	-	-	-	-	-	-	-	-	-	-	-	-
C10-BEN2	1.1%	-	-	2.1%	-	-	-	-	-	-	-	-	-	-	-	-	-
C11-BEN2	0.6%	-	-	2.1%	-	-	-	-	-	-	-	-	-	-	-	-	-
C12-BEN2	0.4%	-	-	1.1%	-	-	-	-	-	-	-	-	-	-	-	-	-
C9-BEN3	-	0.3%	-	-	-	-	-	-	-	-	-	-	-	-	-	-	-
C9-BEN3	-	1.7%	-	-	0.4%	0.1%	-	0.1%	-	-	-	-	-	-	-	-	-

Table A-3 (continued)

Model Species	Composition (weight percent)																
	14-A	14-B	14-C	15-A	15-C	15-D	15-E	15-F	15-G	16-A	16-B	16-C	16-D	16-E	17-A	17-B	17-C
C9-BEN3	0.9%	6.8%	-	1.8%	1.5%	0.5%	-	0.7%	0.3%	-	-	-	-	-	-	-	-
C10-BEN3	1.1%	6.5%	0.2%	2.1%	5.7%	1.7%	0.3%	2.1%	1.8%	-	-	-	-	-	-	-	-
C11-BEN3	0.6%	1.7%	2.3%	2.1%	7.4%	2.4%	7.5%	1.8%	3.3%	-	-	-	-	-	-	-	-
C12-BEN3	0.4%	-	2.2%	1.1%	3.4%	1.1%	7.0%	0.5%	3.1%	-	-	-	0.0%	0.0%	-	-	-
C13-BEN3	-	-	0.4%	-	0.6%	0.2%	1.0%	-	2.3%	0.1%	-	-	0.0%	0.0%	-	-	-
C14-BEN3	-	-	-	-	-	-	0.2%	-	1.4%	0.3%	-	-	0.1%	0.0%	-	-	-
C15-BEN3	-	-	-	-	-	-	-	-	0.7%	0.4%	-	-	0.1%	0.0%	-	-	-
C16-BEN3	-	-	-	-	-	-	-	-	0.1%	0.2%	-	-	0.0%	0.0%	-	-	-

Chamber Experiment Listing

Table A-4. Summary chamber experiments that are relevant to this project.

Run [a]	Date	Type [b]	Purpose and Applicable Conditions.	Results
83	3/20/03	ROG=1 ppmC, NO_x=50 ppb Surrogate + n-Octane	Incremental reactivity test experiment with a previously studied VOC as part of the variable ROG and NO_x surrogate evaluation. 250 ppb n-octane added to Side B.	Results shown on Table 10 and Figure 21.
84	3/21/03	ROG=1 ppmC, NO_x=50 ppb Surrogate + m-Xylene	Incremental reactivity test experiment for variable ROG and NO_x surrogate evaluation. 30 ppb m-xylene added to Side A.	Results shown on Table 10, and Figure 20.
85	3/25/03	ROG=1 ppmC, NO_x=10 ppb Surrogate + n-Octane	Low NO_x incremental reactivity test experiment for variable ROG and NO_x surrogate evaluation. 200 ppb n-octane added to Side B.	Results shown on Table 10 and Figure 22.
86	3/27/03	ROG=1 ppmC, NO_x=10 ppb Surrogate + m-Xylene	Low NO_x incremental reactivity test experiment for variable ROG and NO_x surrogate evaluation. 25 ppb m-xylene added to Side B.	Results shown on Table 10, and Figure 20.
95	4/15/03	Standard MOIR/2 surrogate [c] + n-Octane	Incremental reactivity test experiment for variable ROG and NO_x surrogate evaluation. 200 ppb n-octane added to Side A. Note that this base case will become the standard "MOIR/2" base case for the coatings reactivity study.	Results shown on Table 10 and Figure 22.
100	4/22/03	ROG=0.25 ppmC, NO_x=5 ppb Surrogate + m-Xylene	Low NO_x incremental reactivity test experiment for variable ROG and NO_x surrogate evaluation. 15 ppb m-xylene added to Side B.	Initial formaldehyde uncertain because of lack of formaldehyde data and possible problems with formaldehyde injection. Results shown on Table 10, and Figure 20.
103	4/25/03	CO - NO_x Irradiation	Characterization run to evaluate chamber radical source. 50 ppm CO and 25 ppb NO_x injected in both sides.	O_3 and apparent radical source higher on side A. Model simulations fit O_3 data with Apparent radical input relative to the NO_2 photolysis rates of 25 and 15 ppt for Sides A and B, respectively.

Run [a]	Date	Type [b]	Purpose and Applicable Conditions.	Results
105	4/29/03	Actinometry	The NO_2 photolysis rate was measured at various locations, including inside each reactor.	The measured NO_2 photolysis rates were 0.264 and 0.259 min^{-1} inside Sides A and B, respectively. These are the same to within the experimental uncertainty, and within the range observed in previous and subsequent in-reactor actinometry experiments. The data indicate no trend in light intensity during the period of these experiments.
108	5/7/03	ROG=1 ppmC, NO_x=70 ppb Surrogate + m-Xylene	Incremental reactivity test experiment with a previously studied VOC as part of the variable ROG and NO_x surrogate evaluation. 20 ppb m-xylene added to Side A.	Results shown on Table 10 and Figure 19.
110	5/9/03	Standard MIR Surrogate [c] + m-Xylene	Incremental reactivity test experiment for variable ROG and NO_x surrogate evaluation. 10 ppb m-xylene added to Side A. Note that this base case will become the standard "MIR" base case for the coatings reactivity study. PM data taken for both reactors.	Results shown on Table 10 and Figure 19.
112	5/12/03	CO - Air	Characterization run to evaluate apparent NO_x offgasing rates. 100 ppm CO added to both sides. No NO_x injected.	More O_3 formed in Side A than Side B. Model simulations fit using ratios of NO_x offgasing to NO_2 photolysis rates of 20 and 8 ppt for Sides A and B, respectively.
113	5/13/03	ROG=1 ppmC, NO_x=70 ppb Surrogate + n-Octane	Incremental reactivity test experiment with a previously studied VOC as part of the variable ROG and NO_x surrogate evaluation. 200 ppb n-octane added to Side B.	Results shown on Table 10 and Figure 21.
114	5/14/03	Standard MIR Surrogate + n-Octane	Incremental reactivity test experiment with previously studied VOC using the standard MIR base case. 100 ppb n-octane added to Side B.	Results shown on Table 10 and Figure 21.
115	5/15/03	CO - HCHO - Air	Characterization and control experiment that is sensitive to NO_x offgasing rates and is useful for actinometry because HCHO consumption is expected to be due only to photolysis. 80 ppm CO and 100 ppb formaldehyde injected into both sides. No NO_x injected.	The formaldehyde consumption rates were 9.2 and 7.1 x 10^{-4} min^{-1} on Sides A and B, respectively. These correspond to calculated NO_2 photolysis rates of respectively 0.25 and 0.19 min^{-1}, which are within the uncertainty range of the measurement. Somewhat more O_3 was formed in Side A. The data were fit with apparent NO_x offgasing rates, relative to the NO_2 photolysis rate, of 10 and 5 ppt, respectively.

Run [a]	Date	Type [b]	Purpose and Applicable Conditions.	Results
120	5/29/03	Actinometry	The NO_2 photolysis rate was measured at various locations, including inside each reactor.	The measured NO_2 photolysis rates were 0.262 and 0.251 min^{-1} inside Sides A and B, respectively. These are within the range observed in previous and subsequent in-reactor actinometry experiments, and indicate no trend in light intensity during the period of these experiments.
123	6/5/03	Standard MOIR/2 Surrogate + m-Xylene	Incremental reactivity test experiment with previously studied VOC using the standard MOIR/2 base case. 30 ppb m-xylene added to Side B.	Results shown on Table 10, and Figure 20.
124	6/6/03	Standard MOIR/2 Surrogate + Aromatic-100	Standard MOIR/2 incremental reactivity experiment for Aromatic-100. 500 ppbC Aromatic 100 injected Side B.	Results shown o Table 10 and Figure 28.
126	6/10/03	Standard MOIR/2 Surrogate + VMP Naphtha	Standard MOIR/2 incremental reactivity experiment for VMP Naphtha. 900 ppb VMP Naphtha injected into Side B.	Results shown on Table 10 and Figure 25. The effect of VMP naphtha on IntOH could not be determined because of GC interferences in the analysis of m-xylene and n-octane.
127	6/11/03	Standard MIR Surrogate + Aromatic-100	Standard MIR incremental reactivity experiment for Aromatic-100. 500 ppbC Aromatic 100 injected Side B.	Results shown o Table 10 and Figure 28.
128	6/16/03	ROG=0.5 ppmC, NO_x=50 ppb Surrogate + m-Xylene	Low ROG/NO_x Incremental reactivity test experiment with a previously studied VOC as part of the variable ROG and NO_x surrogate evaluation. 20 ppb m-xylene added to Side B.	Results shown on Table 10 and Figure 19.
133	7/2/03	CO - HCHO - Air	Characterization and control experiment that is sensitive to NO_x offgasing rates and is useful for actinometry because HCHO consumption is expected to be due only to photolysis. 80 ppm CO and 100 ppb formaldehyde injected into both sides. No NO_x injected.	The formaldehyde consumption rates were 1.2 x 10^{-3} on both sides, which was about 25% higher than in the previous such experiment and also higher than expected from the NO_2 actinometry data. Somewhat more O_3 was formed in Side A. The data were fit with apparent NO_x offgasing rates, relative to the NO_2 photolysis rate, of 10 and 5 ppt, respectively.
136	7/10/03	Aromatic-100 - NO_x + CO	Mechanism evaluation experiment for Aromatic-100 of the type found useful for other aromatics. 0.9 ppmC of Aromatic-100 and 50 ppb NO_x injected in both sides, and 90 ppm CO injected into Side A. No PM data.	Results shown on Table 10 and Figure 29.

Run [a]	Date	Type [b]	Purpose and Applicable Conditions.	Results
137	7/11/03	Standard MIR Surrogate + VMP Naphtha.	Standard MIR incremental reactivity experiment for VMP Naphtha, 900 ppmC VMP Naphtha injected Side B.	Results shown on Table 10 and Figure 25. The effect of VMP naphtha on IntOH could not be determined because of GC interferences.
138	7/14/03	Standard MOIR/2 Surrogate + ASTM-3C1	Standard MOIR/2 incremental reactivity experiment for ASTM-3C1. 900 ppb ASTM-3C1 injected into Side B.	Results shown on Table 10 and Figure 30
139	7/15/03	Standard MOIR/2 Surrogate + ASTM-1B	Standard MOIR/2 incremental reactivity experiment for ASTM-1B. 900 ppb ASTM-1B injected into Side B.	Results shown on Table 10 and Figure 26.
140	7/16/03	CO - NO_x Irradiation	Characterization run to evaluate chamber radical source. 50 ppm CO and 25 ppb NO_x injected in both sides.	O_3 and apparent radical source slightly higher on side A. Model simulations fit O_3 data with Apparent radical input relative to the NO_2 photolysis rates of 12 and 10 ppt, respectively.
143	7/22/03	Standard MIR Surrogate Side Equivalency Test	Assess side equivalence with standard MIR surrogate experiment. Standard MIR surrogate injected into both sides.	Slightly more O_3 and m-xylene consumption was observed on Side B. The differences were not great compared to the effects of test compounds, but were larger than observed in most side equivalency test runs.
150	8/5/03	Standard MOIR/2 Surrogate + ASTM-3C1	Standard MOIR/2 incremental reactivity experiment for ASTM-3C1. 900 ppb ASTM-3C1 injected into Side B.	Results shown on Table 10 and Figure 30
151	8/6/03	Standard MIR Surrogate + ASTM-1B	Standard MIR incremental reactivity experiment for ASTM-1B, 900 ppmC ASTM-1B injected Side B.	Results shown on Table 10 and Figure 26.
152	8/7/03	Standard MOIR/2 Surrogate + ASTM-1C	Standard MOIR/2 incremental reactivity experiment for ASTM-1C. 900 ppb ASTM-1C injected into Side B.	Results shown on Table 10 and Figure 24.
153	8/8/03	Standard MOIR/2 Surrogate + ASTM-1A	Standard MOIR/2 incremental reactivity experiment for ASTM-1A. 900 ppb ASTM-1A injected into Side B.	Results shown on Table 10 and Figure 27.
156	8/14/03	O_3 Decay	Ozone dark decay determination and control experiment for effect of dark O_3 on PM measurements. ~300 ppb O_3 injected in both sides and monitored for only 2 hours because of equipment problems.	O_3 dark decay rates were ~4 x 10^{-4} on both sides, which is higher than assumed in the chamber model, but the measurement is uncertain because of the short exposure time. Nucleation observed on Side A but not B. No measurable PM volume.

Run [a]	Date	Type [b]	Purpose and Applicable Conditions.	Results
158	8/16/03	O_3 Decay	Repeat of previous O_3 decay experiment but with longer exposure time. ~300 ppb O_3 injected in both sides and monitored for 2 hours.	O_3 dark decay rates were 0.8-1.2 x 10^{-4}, which is slightly lower than assumed in the chamber model. Nucleation occurred on both sides, but PM number was higher on Side A and Side A had small but measurable PM volume.
159	8/18/03	Standard MIR Surrogate Side Equivalency Test	Assess side equivalence with standard MIR surrogate experiment. Standard MIR surrogate injected into both sides.	Good side equivalency observed for O_3 and other gas-phase measurements. However, about two times more PM formed on Side A.
160	8/19/03	CO - Air	Characterization run to evaluate apparent NO_x offgasing rates. 100 ppm CO added to both sides. No NO_x injected.	Slightly more O_3 formed in Side A than Side B. Model simulations fit using ratios of NO_x offgasing to NO_2 photolysis rates of ~18 and 12 ppt for Sides A and B, respectively. No PM formation.
163	8/22/03	Standard MIR Surrogate + ASTM-3C1	Standard MIR incremental reactivity experiment for ASTM-3C1, 900 ppmC ASTM-3C1 injected Side A.	Results shown on Table 10 and Figure 30
167	8/28/03	Standard MIR Surrogate + ASTM-1A	Standard MIR incremental reactivity experiment for ASTM-1A, 900 ppmC ASTM-1A injected Side B.	Results shown on Table 10 and Figure 27.
168	8/29/03	Standard MIR Surrogate + ASTM-1C	Standard MIR incremental reactivity experiment for ASTM-1C, 900 ppmC ASTM-1B injected Side A.	Results shown on Table 10 and Figure 24.
	9/03 - 11/03	Chamber and Procedure Modifications	New reactors were installed then the chamber was used for experiments for the EPA OBM project. Several blacklight experiments for PM studies conduced in November.	
			From this point on, formaldehyde was removed from the standard ROG surrogate and the amounts of the other ROG constituents were increased by 10% to yield approximately the same reactivity.	
			Characterization runs carried out after this point are not discussed by Carter (2004).	
226	12/11/03	New Standard MIR Surrogate [d] Side Equivalency Test	Test side equivalency for O_3 and PM for the new standard "MIR" base case surrogate experiment. 30 ppb NO_x and 0.55 ppmC (nominal) ROG surrogate (without formaldehyde) injected into both reactors.	Good side equivalency for Ozone. Model underpredicted O_3 to about the same extent as with previous "MIR" base case experiments. PM data only obtained for last few hours of experiment. About 25% more PM volume on Side A than B. Higher PM on Side A is consistent with results of previous experiment.

Run [a]	Date	Type [b]	Purpose and Applicable Conditions.	Results
227	12/12/03	New Standard MOIR/2 Surrogate[d] Side Equivalency Test	Test side equivalency for O_3 and PM for the new standard "MOIR/2" base case surrogate experiment. 25 ppb NO_x and 1.1 ppmC (nominal) ROG surrogate (without formaldehyde) injected into both reactors.	Good side equivalency for Ozone. Results in good agreement with model prediction, as is the case with previous "MOIR/2" base case experiments. No valid PM data.
228	12/15/03	CO - NO_x	Control experiment to test chamber radical source. 25 ppb NO_x and 50 ppm CO added to both reactors.	Results reasonably consistent with standard chamber model. Somewhat more O_3 on Side A, consistent with previous such experiments. Data fit by HONO offgasing rates of 2.0 and 1.3 ppt min^{-1} for Sides A and B, respectively.
229	12/16/03	Standard MIR surrogate + Texanol	New standard MIR incremental reactivity experiment for Texanol. Estimated 90 ppb Texanol injected into Side A, but amount injected uncertain because of operator error. Texanol isomers measured by GC was ~70 ppb.	Results shown on Table 10 and Figure 23.
230	12/17/03	Standard MIR surrogate + Texanol (repeat)	Repeat previous experiment because of uncertainty in Texanol injection, except in this case the Texanol was injected into Side B. Calculated 95 ppb of Texanol injected, in reasonably good agreement with GC analysis of Texanol isomers.	Results shown on Table 10 and Figure 23.
231	12/18/03	Standard MOIR/2 Surrogate + Texanol	New standard MOIR/2 incremental reactivity experiment for Texanol. 90 ppb Texanol injected in Side B.	Results shown on Table 10 and Figure 23.
232	12/19/03	Standard MOIR/2 Surrogate + Texanol	MOIR/2 incremental reactivity experiment with Texanol with larger amount of injected Texanol. 140 ppb Texanol injected into Side B.	Results shown on Table 10 and Figure 23.
233	12/23/03	Standard MOIR/2 Surrogate side equivalency test	Assess side equivalency after Texanol experiments and obtain comparison and base case data for PM data in each reactor. MOIR/2 base case surrogate - NO_x mixture injected into both sides.	Good side equivalency for O_3 and other gas-phase species.
		Inactive	The chamber was inactive for the Christmas and new-years breaks.	

Run [a]	Date	Type [b]	Purpose and Applicable Conditions.	Results
234	1/7/04	CO - NO_x	Control experiment to test chamber radical source. 25 ppb NO_x and 50 ppm CO added to both reactors.	Somewhat more O_3 formed in Side A than B, consistent with previous runs. However NO oxidation and O_3 formation rates somewhat lower than predicted by standard chamber model. Data fit by HONO offgasing rates of 1.7 and 1.0 ppt min^{-1} for Sides A and B, respectively.
235	1/8/04	Standard MIR Surrogate side equivalency test	Assess side equivalency after break and obtain comparison and base case data for PM data in each reactor. MIR base case surrogate - NO_x mixture injected into both sides.	Good side equivalency for O_3. Approximately twice as much PM formed in Side A as B, which is a greater difference than previous runs.
236	1/9/04	NO_x - Air	Control experiment to test background effects. 25 ppb NO_x injected into both sides.	Slightly faster conversion of NO to NO_2 on Side A than B. In order for model to fit the NO to NO_2 conversion rates, it was necessary to assume the equivalent of 1 ppm CO on each side.
237	1/13/04	Standard MOIR/2 Surrogate + ASTM IIIC1	Additional reactivity experiment for ASTM IIIC1 petroleum distillate. 1.2 ppmC distillated added to Side B.	Results shown on Table 10 and Figure 30
238	1/14/04	Standard MIR Surrogate + VMP Naphtha.	Additional reactivity experiment for VMP Naphtha petroleum distillate. 1.2 ppmC distillated added to Side A.	Results shown on Table 10 and Figure 25. The effect of VMP naphtha on IntOH could not be determined because of GC interferences.
239	1/15/04	Standard MOIR/2 Surrogate + Aromatic-100	Additional reactivity experiment for Aromatic 100 petroleum distillate. 0.8 ppmC distillate added to Side A.	Results shown o Table 10 and Figure 28.
240	1/16/04	Standard MOIR/2 Surrogate + ASTM-1A	Additional reactivity experiment for ASTM 1A petroleum distillate. 1.2 ppmC distillate added to Side A.	Results shown on Table 10 and Figure 27.
241	1/21/04	Formaldehyde - CO irradiation	Control experiment to test for NO_x offgasing effects and also formaldehyde actinometry experiment.	The formaldehyde consumption rate was about 40% higher than expected based on the assigned NO_2 photolysis rate and calculated rate ratios. Essentially the same O_3 formation on each side. O_3 formation slightly greater than predicted by standard chamber model. Data fit by HONO offgasing rates of 5.2 ppt min^{-1} for both Sides A and B.
242	1/27/04	Standard MOIR/2 Surrogate + ASTM-1B	Additional reactivity experiment for ASTM 1B petroleum distillate. 0.9 ppmC distillate added to Side B.	Results shown on Table 10 and Figure 26.

Run [a]	Date	Type [b]	Purpose and Applicable Conditions.	Results
243	1/28/04	Standard MOIR/2 Surrogate + VMP Naphtha	Additional reactivity experiment for VMP Naphtha petroleum distillate. 0.9 ppmC distillate added to Side B.	Results shown on Table 10 and Figure 25. The effect of VMP naphtha on IntOH could not be determined because of GC interferences.
244	1/29/04	Standard MIR Surrogate + Aromatic-100	Additional reactivity experiment for Aromatic 100 petroleum distillate. 0.3 ppmC distillate added to Side B.	Results shown o Table 10 and Figure 28.
251	2/12/04	CO - Air	Control experiment to test for NO_x offgasing effects. 50 ppm CO injected in both sides.	Approximately the same amount of O_3 formed on both sides. Amount of O_3 formed somewhat higher than predicted by standard chamber effects model. Data fit by HONO offgasing rates of 3.9 and 2.6 ppt min^{-1} for Sides A and B, respectively.

[a] EPA Run number. Gaps in run numbers reflect experiments carried out for other projects, or experiments that were aborted because of equipment or instrumentation problems, and that are not expected to affect the characterization results.

[b] Unless indicated otherwise, "Surrogate" refers to the 8-component "Full Surrogate" as used in previous environmental chamber incremental reactivity studies in our laboratories. After November, 2003, formaldehyde was removed from the surrogate and the other ROG components were increased by 10% to yield approximately the same reactivity (see text).

[c] The designation "Standard MIR Surrogate" refers to experiments with 0.5 ppmC base case surrogate and 30 ppb NO_x, The designation "Standard MOIR/2 Surrogate" refers to experiments with 1 ppmC base case surrogate and 25 ppb NO_x. After formaldehyde was removed from the surrogate the target initial ROG levels for the standard MIR and MOIR/2 surrogate runs were increased to 0.55 and 1.1 ppmC, respectively.

[d] From this point on, the "Standard" MIR or MOIR/2 surrogates refer to the surrogates where formaldehyde was removed. These are designated as MIRa or MOIR/2a in Table 10. See footnote [c].